

Computational Design of Indoor Arenas (CDIA)

Integrating multi-functional spaces
and long-span roof structures

Wang Pan

Computational Design of Indoor Arenas (CDIA)

Integrating multi-functional spaces and
long-span roof structures

Wang Pan



20#10

Design | Sirene Ontwerpers, Véro Crickx

Keywords | indoor arena, computational design, multi-functional space, long-span roof structure.

ISBN 978-94-6366-423-3

ISSN 2212-3202

© 2021 Wang Pan

This dissertation is open access at <https://doi.org/10.7480/abe.2021.10>

Attribution 4.0 International (CC BY 4.0)

This is a human-readable summary of (and not a substitute for) the license that you'll find at: <https://creativecommons.org/licenses/by/4.0/>

You are free to:

Share — copy and redistribute the material in any medium or format

Adapt — remix, transform, and build upon the material

for any purpose, even commercially.

This license is acceptable for Free Cultural Works.

The licensor cannot revoke these freedoms as long as you follow the license terms.

Under the following terms:

Attribution — You must give appropriate credit, provide a link to the license, and indicate if changes were made. You may do so in any reasonable manner, but not in any way that suggests the licensor endorses you or your use.

Unless otherwise specified, all the photographs in this thesis were taken by the author. For the use of illustrations effort has been made to ask permission for the legal owners as far as possible. We apologize for those cases in which we did not succeed. These legal owners are kindly requested to contact the author.

Computational Design of Indoor Arenas (CDIA)

Integrating multi-functional
spaces and long-span
roof structures

Dissertation

for the purpose of obtaining the degree of doctor
at Delft University of Technology
by the authority of the Rector Magnificus, prof.dr.ir. T.H.J.J. van der Hagen
chair of the Board for Doctorates
to be defended publicly on
Wednesday, 19 May 2021 at 10:00 o'clock

by

Wang PAN
Master of Architecture, South China University of Technology, P.R. China
born in Wuhan, Hubei, P.R. China

This dissertation has been approved by the promotor.

Composition of the doctoral committee:

Rector Magnificus, Prof.dr.ir. I.S. Sariyildiz Prof.dr.ir. Y. Sun	chairperson Delft University of Technology, promotor South China University of Technology, P.R. China, promotor
Dr. M. Turrin	Delft University of Technology, copromoter

Independent members:

Prof.dr.ir. M. Overend	Delft University of Technology
Prof.dr. G. Vrachliotis	Delft University of Technology
Prof.dr. M. F. Tasgetiren	Yasar University, Turkey
Prof.dr.ir. B. Li	Southeast University, P.R. China

The doctoral research has been carried out in the context of an agreement on joint doctoral supervision between South China University of Technology, P.R. China and Delft University of Technology, the Netherlands.

This research was funded by the China Scholarship Council (CSC).

Preface

This PhD research project originally began at South China University of Technology (SCUT), as a part of the research project about sports building design in Prof. Yimin Sun's team in the School of Architecture, SCUT. The research project focuses on the integration of the multi-functional space and long-span roof structure of indoor arena during architectural conceptual design, which is crucial for the indoor arena designs and is always emphasized during the design practice in Prof. Sun's team. The author obtained related knowledge about long-span structure during his study in SCUT during 2004 to 2008 as a bachelor student majored in civil engineering, and obtained related knowledge and experience about the conceptual design of indoor arenas during his study in SCUT as a Master student majored in architectural design and in his design practice in Prof. Sun's team during 2009 to 2012.

From July 2015, funded by China Scholarships Committee (CSC, from July 2015 to June 2017) and SCUT (from July 2017 to June 2018) and based on the agreement on joint supervision and double degree of doctoral research signed by SCUT and TUD in 2014, this research project is continuous in the chair of TOI in the faculty of architecture and the built environment, Delft University of Technology (TUD), within the framework of USE (SCUT-TU Delft Joint Research Centre on Urban Systems & Environment). Based on the long-term research on computational design in TOI, the research project introduces various computational methods and techniques to support the integration of the multi-functional space and long-span roof structure of indoor arenas, and aims at proposing a design method to make substantive contributions both the fields of indoor arena designs and computational design.

Acknowledgement

After eight years (from September 2012), this research is finally done. The dissertation is a description and conclusion for the current work and also a milestone for my whole academic life, based on which, future work will be developed in different directions. Here, I would like to appreciate the generous help of many people, without which I cannot finish the research.

First, I would like to appreciate the generous help of my promotors, Prof. dr. ir. Yimin Sun and Prof. dr. ir. Sevil Sariyildiz. From 2009, I do my research as a master student and then a Ph.D. candidate under the guidance of Prof. Sun. During these years, I learnt various knowledge about the architectural design of indoor arenas from him, which provides the main foundation of this research. Besides, based on his support, I was involved in design projects of various large-scale public buildings and urban environments. In these practical projects, I gained adequate knowledge and experience about architectural and urban design, which are crucial for this research. In 2015, based on the recommendation of Prof. Sun and the funding provided by China Scholarship Committee (CSC), I had a chance to continue this research at Delft University of Technology (TUD). In TUD, Prof. Sariyildiz received me at the Chair of Design Informatics (TOI). Under her guidance, I began my research about computational design and combined it with the original research about the conceptual design of indoor sports arenas. Without her guidance and encouragement, I could not finish this research. I still clearly remember that around 2015 to 2016 when I cannot find a specific research direction and lost confidence, Sevil encouraged me and gave me confidence. She led me to think about the big picture and the whole storyline about the research work time and time again and guide me to finish the research proposal and go/ no go report. With her encouragement and guidance, I passed my go/ no go meeting and finished the research work.

I would also appreciate the generous help of my daily supervisors, Dr. Michela Turrin and Prof. dr. ir. Christian Louter. In 2014, with the introduction of Michela, I had the chance to apply for a Ph.D. position in TUD. During my research in TUD, Michela and Christian provided generous help and guided me to finish a series of research tasks and papers. Even though Christian cannot be listed as co-promotor finally, he had provided lots of supports and guided the research as a co-promotor. Besides, I would also appreciate the supports from Dr. Martin Tenpierik in the acoustic aspects of the research.

I would also like to appreciate the generous help of two Chinese ladies in TUD, Ms. Lily Li and Ms. Bo Song. Lily is my alumna in SCUT and also a staff in the Faculty of Technology, Policy and Management of TUD. She facilitated the collaboration between SCUT and TUD, based on which I have the chance to do my research between the two Universities. Besides, she also provides lots of suggestions and helps for my work and living, which supports me to finish my research work. Bo is our secretary in TOI. She supports our daily work in the faculty. Besides, she also provided generous help and valuable suggestions for my work and my communications with promoters and supervisors.

I would also thank my Chinese friends in TUD, Qingpeng Li (李清鹏), Yu Chen (陈宇), Yi Xia, Dadi Zhang (张达頔), Tiantian Du (杜甜甜), Yuting Tai (郜玉婷), Mei Liu (刘美), Yu-chou Chiang (姜遇洲), Emeline Lin (林宓), Nan Bai (白楠), Meng Meng (孟梦), Langzi Chang (常浪子), Biyue Wang (王碧月), Anxiao Zhang (张安晓), Xiaocou Zheng (郑响凑), Qin Qin (秦琴), Kaiyue Yang (杨凯越), Penglin Zhu (朱鹏霖), Yan Song (宋岩), Muxi Lei (雷慕曦), Liang Xiong (熊亮), Danhua Xu (徐丹华), Henran Yang (杨赫然), Xiaoyu Yuan (袁小雨), Xiaoyu Du (杜小宇) and my colleagues and friends in Faculty of Architecture and the Built Environment, Mikta Farid Alkadri, Berk Ekici, Cemre çubukçuoğlu, Pirouz Naurian, Paul de Ruiter, Henry Kiksen, Hans Hoogenboom, Daniëna, Tessa Vermeulen, Andrew Borgart, Peter Eigenraam, Nick ten Caat, Dr. Marcin, Prof. dr. ir. Andy van den Dobbelsteen, Michiel Fremouw. With the help and supports from all of you, I have a good and memorable time in Delft.

Thanks should also give to Prof. dr. ir. Jing Wang (王静老师), Dr. ir. Dongjin Qi (戚冬瑾老师), Ding Yang (杨定), Peng Gao (高鹏), Dejian Peng (彭德建), Wei Dai (戴伟), Xiao Guo (郭晓), Bowei Huang (黄博威), Weibin Lin (林伟斌). You are my colleagues in both SCUT and TUD. I still clearly remember how we support and help each other in both work and living during these years.

I would also thank my other colleagues and friends in SCUT, Prof. Chunyang Zhang (张春阳老师), Prof. Pin Su (苏平老师), Fenqiang Wang (汪奋强老师), Minzhi Li(李敏稚), Sheng Xia (夏晟), Tianxiang Leng (冷天翔), Lu Xiong (熊璐), Fang Deng (邓芳), Weikang Ye (叶伟康), Yonggang Shen (申永刚), Yiwei Lu (陆仪韦), Yeqin Huang(黄焯焯), Fan Peng (彭帆), Yanyan Liang (梁艳艳), Manjiao Huang (黄曼娇), Lin Zou (邹林), Dongbiao Xie (谢东彪), Qiantan Li (李倩覃), Xiaojing Zhu (朱晓静), Yizhi Zhu (祝艺芝), Yiqi Xu (徐亦奇), Chen Chen (陈琛), Wenyu Zhang (张文宇), Feng Zhou (周峰), Hao Huang (黄浩), Junhan Qin (覃俊翰), Haiquan Li (李海全), Hou Ye (侯叶), Shanglin Wu (邬尚霖), Yixin Zhang (章艺昕), Hao Yuan (袁浩), Pudao Huang (黄普涛), Le Luo (骆乐), Jun Guo (芮俊), Huizhen Chen (陈辉镇).

Finally, I would appreciate my family. I don't want to say too much here because I know no matter how many words cannot express my love and appreciation to all of you.

Contents

List of Tables	16
List of Figures	17
Summary	21
Samenvatting	25

1 Introduction 31

1.1	Research background	31
1.2	Research motivation and goals	34
1.3	Research questions	38
1.4	Research methodology	39
1.4.1	Literature review	41
1.4.2	Method development	41
1.4.3	Case studies	42
1.5	Significance	43
1.5.1	Societal relevance	43
1.5.2	Scientific relevance	43
1.5.3	Readers of this thesis	43

2 Literature review: Integrated design and the related design exploration of indoor multi-functional arenas 47

2.1	Introduction	47
2.2	Formulation process of indoor arenas	49
2.2.1	Pitch for various activities	50
2.2.2	Seating tiers (stands) for spectators	55
2.2.2.1	Formulation of a raw seating bowl	56
2.2.2.2	Formulation of the boundary curve of the seating bowl	65

2.2.3	Long-span roof and the structure	67
2.2.3.1	Geometry of the long-span roof	67
2.2.3.2	Typologies of long-span roof structure	70
2.2.3.3	Design parameters of long-span roof structure	77
2.2.4	Interrelationships between the multi-functional space and long-span roof structure	79
2.3	Design requirements and the related assessments of indoor arenas	79
2.3.1	Design requirements and the related assessments of multi-functionality	80
2.3.1.1	Events	81
2.3.1.2	Assemblies	86
2.3.1.3	Exhibitions and daily sports for the public	93
2.3.2	Design requirements and the related assessments of long-span roof structure	94
2.3.2.1	Load-carrying capacity	94
2.3.2.2	Safety	96
2.3.2.3	Efficiency, economy, and sustainability	98
2.3.3	Qualitative design requirements and the related assessments	99
2.3.3.1	Qualitative design requirements and the overall form/geometry of buildings	99
2.3.3.2	Assessments of qualitative aspects based on visual investigations in interactive designs	100
2.4	Basic demands of the conceptual design of indoor arenas	102
2.4.1	Generating numerous and diverse design alternatives for conceptual design exploration	102
2.4.2	Obtaining adequate information of design alternatives for the assessments of various design requirements	103
2.4.3	Adapting to different scenarios laying different emphases on quantitative and qualitative design requirements	104
2.5	Summary	104
3	Literature review: Computational design methods for architectural conceptual design	109

3.1	Introduction	109
3.2	Parametric modelling: a process to associate elements and generate design alternatives	112
3.2.1	Background	112
3.2.2	Applications of parametric modelling	114
3.2.3	Diversity of design alternatives: a further requirement of parametric modelling	116
3.2.4	Parametric design for sports buildings	117

3.3	Building Performance Simulations (BPSs) for indoor arenas	120
3.3.1	Simulations of spatial capacity and the view of spectators	122
3.3.2	Simulations of acoustics	122
3.3.2.1	Empirical methods	122
3.3.2.2	Geometrical acoustic methods	124
3.3.2.3	Wave-based methods	124
3.3.2.4	Simulation of acoustics for architectural conceptual design of indoor arenas	125
3.3.3	Structural analysis tools	125
3.3.3.1	Mechanics analysis for structure	126
3.3.3.2	Loading model	130
3.3.3.3	Structural simulations in architectural conceptual design	133
3.4	Optimization based on heuristic algorithm	134
3.4.1	Background	134
3.4.2	Simulation-based stochastic optimization	136
3.4.2.1	Black-box system	136
3.4.2.2	Algorithms for simulation-based stochastic optimization	137
3.4.2.3	Metaheuristic algorithms	138
3.4.3	Multi-Objective Optimization (MOO)	141
3.4.4	Multi-Disciplinary Optimization (MDO)	142
3.4.5	MOO-based conceptual design and its limitations	143
3.5	Surrogate models based on supervised learning	144
3.5.1	Surrogate models	144
3.5.2	Supervised learning methods for surrogate models	145
3.5.2.1	Multi-layer perceptron neural network	147
3.5.2.2	Poly-nominal regression and response surface method	153
3.5.2.3	Radial Basis Function (RBF) network	155
3.5.2.4	Local Linear Mapping (LLM) based on Self-Organizing Map (SOM)	157
3.5.2.5	Decision/regression tree	160
3.5.3	Limitations of surrogate models based on supervised learning	162
3.6	Unsupervised clustering based on Self-Organizing Map (SOM)	163
3.6.1	Clustering	163
3.6.2	Self-Organizing Map (SOM)	163
3.6.3	Design exploration of different types of geometries based on SOM	165
3.7	Assumption of a computation method for the conceptual design of indoor arenas	166
3.8	Summary	168

4 Method development: CDIA – Computational Design of Indoor Arenas 177

4.1 Introduction 177

4.2 Pre-processing components of CDIA: IAG and Framework-NAIA 180

4.2.1 Indoor Arena Generator (IAG): a versatile and flexible parametric model of indoor sports arenas 180

4.2.2 Framework for Numeric Assessments of Indoor Arenas (Framework-NAIA) 187

4.3 CDIA: a flexible method including three workflows 191

4.3.1 Defining promising designs among ‘well-performing’ designs by using MOO 191

4.3.1.1 Search for ‘well-performing’ designs based on heuristic algorithm 193

4.3.1.2 Result data process and visualization 193

4.3.1.3 Limitations 194

4.3.2 Defining ‘well-performing’ designs among preferred types of designs by using SOM clustering and MOO 194

4.3.2.1 Visual investigations of different types of design alternatives by using SOM clustering 195

4.3.2.2 Search for ‘well-performing’ designs among preferred types of designs according to quantitative requirements by using MOO 197

4.3.2.3 Limitations 197

4.3.3 Defining promising designs based on both numeric assessments and visual investigations by using SOM-MLPNN 197

4.3.3.1 Clustering and sampling the design alternatives by using SOM 199

4.3.3.2 Design of Experiments (DoEs) 199

4.3.3.3 Obtain multiple indicators related to quantitative requirements for each design alternatives in the design space 200

4.3.3.4 Data visualization to support the explorations of design alternatives according to both numeric data and visual investigations 200

4.3.3.5 Limitations 201

4.4 Summary 201

5 Case studies: applying CDIA in the designs of two typical arenas 205

5.1 Introduction 205

5.2	Two typical examples: Barclay Centre and O2 Arena	207
5.2.1	Barclay Centre: an arena mainly for sports events and sometimes for pop-music concerts	207
5.2.2	O2 Arena: an arena for both pop-music concerts and sports events	208
5.3	Pre-processing of CDIA based on IAG and Framework-NAIA	209
5.3.1	Defining design space based on IAG	209
5.3.2	Formulate numeric assessment criteria related to quantitative design requirements based on Framework-NAIA	213
5.4	Applying CDIA to support conceptual designs in different scenarios	216
5.4.1	Using MOO to support the design exploration emphasizing numeric assessments	217
5.4.1.1	Using MOO for the hypothetical design of Barclay Centre	218
5.4.1.2	Using MOO for the hypothetical design of O2 Arena	220
5.4.2	Using SOM clustering and MOO to support the design exploration emphasizing visual investigations	223
5.4.2.1	SOM clustering supporting the visual investigations and selections of design alternatives according to qualitative design requirements	225
5.4.2.2	Using MOOs to search for 'well performing' designs among selected types	228
5.4.3	Using SOM-MLPNN to support the design exploration equally emphasizing numeric assessments and visual investigations	233
5.4.3.1	SOM clustering, sampling, and Design of Experiments (DoEs)	233
5.4.3.2	Training, validations, and tests of MLPNN models	236
5.4.3.3	Design explorations based on data visualizations	243
5.5	Discussions and summary	247

6 Discussions, conclusions and recommendations 251

6.1	Discussions	251
6.1.1	Answers to the research questions	251
6.1.2	Practical guidelines of CDIA	255
6.2	Conclusions	256
6.3	Recommendations	257

Appendix 259

List of Tables

- 2.1 Requirements on the dimensions and the capacity of spectators for sports events 52
- 2.2 Classification of structural geometry (Engle, 2007) 69
- 2.3 Classification of structural types (Majowiecki, 2000) 70
- 2.4 Classification of structural types for long-span roofs according to the transfer of loads (Engel, 2007) 71
- 2.5 Classification of structural type according to the combinations of structural elements (Dong, 2012) 72
- 2.6 Premium Viewing Distance (PVD) and accepted viewing Distance for different sports 83
- 2.7 Premium Viewing Distance (PSV) for stage-performances 88
- 2.8 Factors of different loads for different states according to En-1990:2002 (CEN,2002a) 96
- 3.1 Exemplary simulation/analysis tools for different aspects 121
- 3.2 Exemplary absorption coefficients for different areas of indoor arenas (Bork, 2005) 123
- 3.3 Some activation functions and error functions for MLPNN 150
- 4.1 Process and parameters of the proposed parametric model (Pan et al. 2019) 183
- 4.2 Framework for Numeric Assessment of Indoor Arenas (Framework-NAIA) 188
- 5.1 The design parameters of the design example of Barclay Centre 211
- 5.2 Design parameters of the example of O2 arena 212
- 5.3 Input data of the optimization for the Barclay Centre (OPT-BC). 213
- 5.4 Input data of the optimizations for the O2 Arena (OPT-O2). 215
- 5.5 Loading combinations for the long-span roof structure 216
- 5.6 Parameters of the optimizations of the designs of Barclay Centre and O2 Arena 217
- 5.7 Inputs and parameters of SOM clustering 224
- 5.8 The parameters of the MLPNN models and the training process 237

List of Figures

- 1.1 The scheme of the conceptual design process for indoor arena with emphasis on the integration of the multi-functional space and long-span roof structure 35
- 1.2 The workflows of three computational design methods and their limitations in satisfying the demands of conceptual design of indoor arenas 36
- 1.3 The methodology of the thesis 40
- 2.1 The composition of the Colosseum of Rome (MApaPLAN.com) and a modern indoor aren 50
- 2.2 The composition of overall space (O/A) for sports competitions (Sport England, 2015) 51
- 2.3 A comparison of the overall space (O/A) sizes for different sports 52
- 2.4 Three types of stage-setting for stage performances (Left: end stage; middle: side stage; right: central stage) 53
- 2.5 The spatial requirements of exhibitions (IAEE, 2014) 53
- 2.6 The badminton-court-based modular layout approach for multiple sports courts (Sports England, 2012) 54
- 2.7 Seating tiers in a typical arena and a two-steps generation process (Pan et al., 2019) 55
- 2.8 The diagram of the regulations about seating tiers according to EN 13200-1:2012 (CEN, 2012) 56
- 2.9 Sightline for a spectator according to EN 13200-1:2012 (CEN, 2012) 57
- 2.10 Seating tiers with different slopes caused by different values of 'V' 58
- 2.11 The pitches with different sizes impact the shape of the seating tiers 60
- 2.12 Different heights of the first seating row impact the shape of the seating tiers 61
- 2.13 Seating tiers divided into different sections 62
- 2.14 Seating tiers with different number of rows for each section of the tiers 63
- 2.15 Overhanging or stepping back the upper tiers for two-section seating tiers 64
- 2.16 Seating tiers with different outlines 65
- 2.17 Seating tiers with different asymmetry ratios 66
- 2.18 Space frame structures of London aquatic centre (left: Detail, 2012) and Rio velodrome (right: theB1M, 2012 and Wikipedia, 2012) 73
- 2.19 Truss beam structures of the gymnasium of China Agricultural University (left: SCUTAD, 2008a) and the aquatic centre of Guangzhou (right: SCUTAD, 2010) 74
- 2.20 Grid shell structures of the Gymnasium of Beijing University of Technology (left: SCUTAD, 2008b) and Chang'an sports arena (right: SCUTAD, 2014) 75
- 2.21 Some basic structural tessellations (Engel, 2007) 76
- 2.22 Design parameters of the geometry of long-span roof 78

- 2.23 Definitions of viewing distance, horizontal viewing angle, and vertical viewing angle for sports events 81
- 2.24 Assessments of seating tiers for basketball according to the indicators related to viewing distance, horizontal viewing angle, and vertical viewing angle 85
- 2.25 Definitions of viewing distance, horizontal viewing angle, and vertical viewing angle for stage performance 87
- 2.26 Assessments of seating tiers for stage performance (side-stage) according to the indicators related to viewing distance, horizontal viewing angle, and vertical viewing angle 89
- 2.27 Assessments of seating tiers for stage performance (end-stage) according to the indicators related to viewing distance, horizontal viewing angle, and vertical viewing angle 90
- 2.28 Reverberation time for different activities (Soru, 2014) 92
- 2.29 Examples of sports buildings for which the overall form satisfying the requirements related to qualitative aspects (left: Philippine arena, picture sources: Populous, 2011; middle: Guangzhou aquatic centre, pictures sources: SCUTAD, 2010; right: Tokyo national stadium, picture sources: Tokyo 2020, 2019) 100
- 3.1 Two different parametric definitions (a) and (b) for a similar design concept (Harding, 2014) 113
- 3.2 Workflow of an architectural design concluding four parametric design strategies according to Hudson (2010) 115
- 3.3 Various design concepts proposed by Bjarke Ingels Group architects for Escher Tower project (left) and Various concepts with diverse types of geometries generated by 'Embryo' (right) (Harding, 2014) 117
- 3.4 The hierarchical structure of Seating Bowl Modeller (SBM) (Hudson, 2010) 118
- 3.5 Four typical seating bowls generated by SBM (Hudson, 2010) 118
- 3.6 A one-side grandstand generated by a changeable outer outline (Sun et al., 2013) 119
- 3.7 An example about the assembly and analysis of a structure model based on Karamba 3d 133
- 3.8 An exemplary workflow of genetic algorithm (left) and interactive genetic algorithm (right) (Mueller et al., 2015) 141
- 3.9 A typical workflow of a surrogate model supported by supervised learning in architectural design 147
- 3.10 An exemplary scheme of a Multi-Layer Perceptron Neural Network (MLPNN) 148
- 3.11 A typical radial basis function network 155
- 3.12 A regression tree (left) and the related predictors' space (right) (Torgo, 2017) 161
- 3.13 An example of using SOM clustering to group design alternatives to geometry features (Harding, 2016). 166
- 4.1 The scheme of CDIA 178
- 4.2 The generation of the roof structure (Pan et al. 2019) 185
- 4.3 Some design alternatives of indoor arenas generated by IAG (Pan et al. 2019) 186
- 4.4 The process of the first workflow by using MOO 192
- 4.5 The workflow defining 'well-performing' designs among preferred types of designs by using SOM clustering and MOO 195
- 4.6 The workflow of SOM-MLPNN to support the design exploration according to both quantitative and qualitative design requirements 198

- 5.1 The scheme of the cases studies (the picture sources of Barclay Arena: info-stade, 2013 and Advance Graphics, 2015; the picture sources of O2 Arena: Trip2london, 2014 and Wikipedia, 2016) [206](#)
- 5.2 Barclay Centre (left (left: Info-stade, 2013, and middle: Advance Graphics, 2015) and a similar configuration (right) generated by IAG [207](#)
- 5.3 O2 Arena (left: Trip2london, 2014, and middle: Wikipedia, 2016) and a similar configuration (right) generated by IAG [208](#)
- 5.4 The results of MOO for the design of Barclay Centre [219](#)
- 5.5 The results of the first MOO for the design of O2 Arena (the Picture source of the London Aquatics Centre: World Para Swimming, 2011) [221](#)
- 5.6 The results of the second MOO for the design of O2 Arena (the picture sources of Barcelona Arena: Architects+Artisans, 2017 and Amalgam, 2016) [222](#)
- 5.7 The trained SOM network of the design space for the design example of Barclay Centre [226](#)
- 5.8 The trained SOM network of the design space for the design example of O2 Arena [227](#)
- 5.9 The results of the MOO for the selected design alternatives in the design example of Barclay Centre [229](#)
- 5.10 The results of the first MOO for the selected design alternatives in the design example of O2 Arena [230](#)
- 5.11 The results of the second MOO for the selected design alternatives in the design example of O2 Arena [231](#)
- 5.12 The results of SOM clustering in the SOM-MLPNN for the design example of Barclay Centre [234](#)
- 5.13 The results of SOM clustering in the SOM-MLPNN for the design example of O2 Arena [235](#)
- 5.14 The training, validations, and tests data of the MLPNN models to approximate the indicators of spectator view and acoustics for the design example of Barclay Centre [238](#)
- 5.15 The training, validations, and tests data of the MLPNN models to approximate structural indicators for the design example of Barclay Centre [239](#)
- 5.16 The training, validations, and tests data of the MLPNN models to approximate the indicators of spectator view and acoustics for the design example of O2 Arena [240](#)
- 5.17 The training, validations, and tests data of the MLPNN models to approximate structural indicators for the design example of O2 Arena [241](#)
- 5.18 Exploring the output spaces related to various quantitative indicators according to the design alternatives with different geometry types (design example of Barclay Centre) [244](#)
- 5.19 Exploring the output spaces related to various quantitative indicators according to the design alternatives with different geometry types (design example of O2 Arena) [245](#)

Summary

This research project focuses on the conceptual design of indoor arenas by using computational techniques based on the emphasis on the integration of the multi-functional space and long-span roof structure.

Indoor arenas are important public buildings catering for various activities (e.g. sports events, stage performances, assemblies, exhibitions, and daily sports for the public) and serving as landmarks in urban contexts. In an arena, the multi-functional space and long-span roof structure are highly interrelated, which impact the multi-functionality (the spatial capacity, spectator view, and acoustics for various activities) and the structural performance and mainly defines the overall form of the building. Therefore, it is crucial to integrate the multi-functional space and long-span roof structure to formulate proper forms for indoor arenas, in order to satisfy various design requirements.

This integration is especially important for the architectural conceptual design phase, since this phase costs less in the whole design process but its outcomes mainly impact the performance of the building during its whole lifecycle. The main task for conceptual design is to explore diverse design alternatives according to the background of the project (which is the divergent step) in order to define promising alternative (s) according to the assessments related to various design requirements (which is the convergent step). The design requirements, which should be satisfied by the design alternatives, can be divided into quantitative ones and qualitative ones. The quantitative design requirements are usually related to architectural functionality and engineering aspects (e.g. structure, energy consumption, daylighting, ventilation), which can be assessed by numeric indicators. While the qualitative design requirements are usually related to some aspects related to humanity and social science (e.g. aesthetics, culture and history, politics, psychology, and philosophy), which are difficult to be effectively assessed based on numeric data and need to be evaluated by the visual investigations of designers according to their knowledge and experience.

Specifically, for the conceptual design of indoor arenas, the integration of the multi-functional space and long-span roof structure demands proper definition and association of various building elements based on further analyses about the complex interrelationships among them. Based on the integration, in the divergent

step of conceptual design, diverse design alternatives should be generated for the design exploration. The design exploration demands the information about the quantitative indicators and the overall geometries of the generated design alternatives, for the related numeric assessments and visual investigations. In the convergent step, based on the numeric assessments and visual investigations in the design exploration, the definition of promising design(s) demands challenging decision making. Moreover, different design scenarios of conceptual design in practice should also be considered, in which designers can prioritize the numeric assessments related to quantitative design requirements, or prioritize the visual investigations related to qualitative design requirements, or place equal emphasis on both of them. For the satisfaction of these demands, traditional design methods and tools are limited in dealing with mass information and in supporting the design exploration and decision making with high complexity. Nevertheless, some computational design techniques have the potential to satisfy these demands, therefore, to support the conceptual design of indoor arenas.

This thesis aims at formulating a computational design method to support the conceptual design of indoor arenas. The method emphasises on:

- the integration of the multi-functional space and long-span roof structure,
- the assessments according to both numeric data related to quantitative design requirements and visual investigation related to qualitative design requirements,
- different scenarios in which designers can place different emphases or priorities on numeric assessments and visual investigations.

It is worth noting that the design method, named CDIA (computationally integrated design of indoor arenas), does not intend to replace human designers. In contrast, it aims to provide more information of diverse design alternatives for designers to support them in making decisions efficiently based on full investigations of the information in a wide range.

Specifically, CDIA is formulated based on the computational techniques of parametric modelling, Building Performance Simulations (BPSs), Multi-Objective Optimizations (MOOs), surrogate models based on Multi-Layer Perceptron Neural Network (MLPNN), and clustering based on Self-Organizing Map (SOM clustering). These techniques have been used in the conceptual designs of various types of buildings. However, there are still limitations for each of them in supporting the conceptual design of indoor arenas, which should be overcome during the formulation of CDIA. These techniques are applied in five components in CDIA. The first two components, Indoor Arena Generator (IAG) based on parametric modelling and the framework of Numeric Assessments of Indoor Arenas (framework-NAIA) based on BPSs, are used for the

pre-processing step. While the MOOs, MLPNN, and SOM clustering are used for the three workflows corresponding to the three design scenarios (in which different emphases are placed on numeric assessments and visual investigations).

For the pre-processing step, IAG, a flexible and versatile parametric model for indoor arenas, is proposed, according to the composition and design parameters of indoor arenas. By setting and changing the values of the parameters, it can generate various types of building forms with three frequently-used structural types (grid-shell, space frame, and truss beam) based on the integration of the multi-functional space and long-span roof structure. Framework-NAIA, which is the other component of the pre-processing step, consists of the numeric indicators and related building performance simulation (BPS) tools about the multi-functionality (spatial capacity, view of spectators, acoustics for various activities) and structural performance. The framework also provides possible assessment criteria related to the indicators, based on which each of the indicators can be used as a design objective or a constraint to assess a design. Therefore, designers can rapidly customize specific criteria and combine the BPS tools with IAG to assess the generated design alternatives.

Based on the pre-process components, three workflows of CDIA are formulated for the three corresponding design scenarios. The first workflow is proposed for the design scenario in which designers are supposed to prioritize the numeric assessments related to quantitative design requirements for design alternatives. Multi-Objective Optimization (MOO) is used in this workflow, to search for 'well-performing' designs in a wide design space containing diverse design alternatives (generated by IAG), according to customized numeric assessment criteria (formulated based on the framework-NAIA) related to quantitative design requirements. Among the 'well-performing' designs selected by the MOO, designers can further select promising design(s) based on visual investigations related to qualitative design requirements.

The second workflow is proposed for the design scenario in which designers are supposed to prioritize the visual investigation related to qualitative design requirements for design alternatives. In this workflow, SOM clustering is used to cluster all the design alternatives (generated by IAG) into groups according to geometry features and to reflect the design space based on a two dimensional SOM network which organizes various typical designs. Based on the SOM network, designers can explore various types of designs and select promising types based on visual investigation related to qualitative design requirements. All the design alternatives within these types are selected out, among which MOO is used to search for 'well-performing' designs based on numeric assessment criteria (formulated based on the framework-NAIA) related to quantitative design requirements.

The third workflow is proposed for the design scenario in which designers are supposed to place equal emphases on numeric assessments related to quantitative design requirements and visual investigation related to qualitative design requirements. This workflow is achieved by using Multi-Layer Perceptron Neural Network based on SOM clustering (SOM-MLPNN). In SOM-MLPNN, the SOM clustering, being similar to that in the second workflow, is used to cluster designs into groups according to geometry features and generate a typical design for each cluster. Therefore, designers can visually inspect various types of designs. Moreover, the inputs vectors of the typical designs generated by SOM clustering are used as the sampled/labelled inputs for design of experiments (DoEs) and MLPNN to predict the values of numeric indicators related to quantitative design requirements for all the design alternatives (generated by IAG) in the design space. Based on data visualization, designers can explore designs and select promising ones, according to both numeric assessments and visual investigations.

The proposed method (with its three workflows) is applied to the hypothetical designs of two typical indoor arenas (Barclay Centre in New York and O2 Arena in London) in the case studies. According to the results, the effects of CDIA in satisfying the demands of the conceptual design of indoor arenas are verified. The three workflows are able to support designers to define promising design(s) in the corresponding design scenarios. Based on the results, guidelines of CDIA in practice are formulated, and the related limitations are discussed.

The main contribution of the thesis is the formulation of CDIA, which overcomes the limitations of the current computational techniques, therefore, to effectively support the conceptual design of indoor arenas focusing on the integration of the multi-functional space and long-span roof structure. Within the overall framework of CDIA, the proposed components and workflows also make contributions to both academic research and design practice. The IAG includes various types of geometries of multi-functional space and three types of long-span roof structures with various geometries, which can provide diverse types of design alternatives for both research and design work. The three workflows based on MOOs, MLPNNs, and SOM clustering provide different ways to support design explorations for architectural conceptual designs. Besides, CDIA can also be used as the platform to study the relationships between the overall building geometries and the quantitative indicators (related to multi-functionality and structural performance), which is crucial for academic research and integrated designs as well as the cooperation between architects and structural engineers. Moreover, the method of CDIA is developable, therefore, more quantitative aspects (e.g. thermal, energy, daylighting, ventilation) can be taken into account, and the method can also be developed to use for the designs of other building types.

Samenvatting

Dit onderzoeksproject richt zich op het conceptueel ontwerp van overdekte arena's door gebruik te maken van computationele technieken gebaseerd op de nadruk op de integratie van de multifunctionele ruimte en de structuur van het lange-dak.

Overdekte arena's zijn belangrijke openbare gebouwen die geschikt zijn voor verschillende activiteiten (bv. sportevenementen, theatervoorstellingen, bijeenkomsten, tentoonstellingen en dagelijkse sporten voor het publiek) en die dienen als herkenningspunten in een stedelijke context. In een arena zijn de multifunctionele ruimte en de lange overspanning van de dakstructuur sterk met elkaar verweven, wat een impact heeft op de multifunctionaliteit (de ruimtelijke capaciteit, het uitzicht voor de toeschouwers en de akoestiek voor de verschillende activiteiten) en de structurele prestaties en vooral de algemene vorm van het gebouw bepaalt. Daarom is het cruciaal om de multifunctionele ruimte en de lange overspanning te integreren om de juiste vormen voor overdekte arena's te formuleren, om zo te voldoen aan de verschillende ontwerpisen.

Deze integratie is vooral belangrijk voor de architecturale conceptuele ontwerpfase, aangezien deze fase minder kost in het hele ontwerpproces, maar de uitkomsten ervan vooral van invloed zijn op de prestaties van het gebouw gedurende de hele levenscyclus. De belangrijkste opgave voor het conceptueel ontwerp is het verkennen van diverse ontwerpalternatieven naar aanleiding van de achtergrond van het project (wat de divergerende stap is) om veelbelovende alternatief(en) te definiëren aan de hand van de beoordelingen met betrekking tot verschillende ontwerpisen (wat de convergerende stap is). De ontwerpisen, waaraan de ontwerpalternatieven moeten voldoen, kunnen worden onderverdeeld in kwantitatieve en kwalitatieve eisen. De kwantitatieve ontwerpisen zijn meestal gerelateerd aan architectonische functionaliteit en technische aspecten (bijv. structuur, energieverbruik, daglichttoetreding, ventilatie), die kunnen worden beoordeeld met behulp van numerieke indicatoren. Terwijl de kwalitatieve ontwerpisen meestal verband houden met bepaalde aspecten die verband houden met de mensheid en de sociale wetenschappen (bijvoorbeeld esthetiek, cultuur en geschiedenis, politiek, psychologie en filosofie), die moeilijk effectief kunnen worden beoordeeld op basis van numerieke gegevens en moeten worden geëvalueerd door de visuele onderzoeken van de ontwerpers op basis van hun kennis en ervaring.

Specifiek voor het conceptuele ontwerp van overdekte arena's vereist de integratie van de multifunctionele ruimte en de lange-dakconstructie een goede definitie en associatie van verschillende bouwelementen op basis van verdere analyses van de complexe onderlinge relaties. Op basis van de integratie, in de divergerende stap van het conceptuele ontwerp, moeten diverse ontwerpalternatieven worden gegenereerd voor de ontwerpverkenning. De ontwerpverkenning vraagt om informatie over de kwantitatieve indicatoren en de totale geometrie van de gegenereerde ontwerpalternatieven, voor de bijbehorende numerieke beoordelingen en visuele onderzoeken. In de convergente stap, gebaseerd op de numerieke beoordelingen en visuele onderzoeken in de ontwerpverkenning, vraagt de definitie van veelbelovende ontwerp(en) om uitdagende besluitvorming. Bovendien moeten ook verschillende ontwerpscenario's van conceptueel ontwerp in de praktijk worden overwogen, waarbij ontwerpers prioriteit kunnen geven aan de numerieke beoordelingen met betrekking tot kwantitatieve ontwerpeisen, of aan de visuele onderzoeken met betrekking tot kwalitatieve ontwerpeisen, of aan beide evenveel nadruk kunnen leggen. Om aan deze eisen te voldoen, zijn de traditionele ontwerpmethoden en -hulpmiddelen beperkt in het omgaan met massa-informatie en in het ondersteunen van de ontwerpverkenning en -beslissing met hoge complexiteit. Desalniettemin hebben sommige computationele ontwerptechnieken de potentie om aan deze eisen te voldoen, waardoor ze het conceptuele ontwerp van overdekte arena's ondersteunen.

Deze dissertatie heeft tot doel een computationele ontwerpmethode te formuleren ter ondersteuning van het conceptuele ontwerp van overdekte arena's. De methode legt de nadruk op:

- de integratie van de multifunctionele ruimte en de overspanning,
- de beoordelingen op basis van zowel numerieke gegevens met betrekking tot kwantitatieve ontwerpvereisten als visueel onderzoek met betrekking tot kwalitatieve ontwerpvereisten,
- verschillende scenario's waarin ontwerpers verschillende accenten of prioriteiten kunnen leggen op numerieke beoordelingen en visuele onderzoeken.

Het is het vermelden waard dat de ontwerpmethode, genaamd CDIA (computationeel geïntegreerd ontwerp van overdekte arena's), niet bedoeld is om menselijke ontwerpers te vervangen. Het is daarentegen wel de bedoeling om meer informatie te verschaffen over diverse ontwerpalternatieven voor ontwerpers om hen te ondersteunen bij het efficiënt nemen van beslissingen op basis van een volledig onderzoek van de informatie in een breed scala.

Specifiek is CDIA geformuleerd op basis van de computationele technieken van parametrische modellering, Building Performance Simulations (BPSs), Multi-Objective Optimizations (MOOs), surrogaatmodellen gebaseerd op Multi-Layer Perceptron Neural Network (MLPNN), en clustering op basis van Self-Organizing Map (SOM clustering). Deze technieken zijn gebruikt in de conceptuele ontwerpen van verschillende soorten gebouwen. Er zijn echter nog steeds beperkingen voor elk van hen in de ondersteuning van het conceptuele ontwerp van overdekte arena's, die moeten worden overwonnen tijdens de formulering van CDIA. Deze technieken worden in het CDIA in vijf componenten toegepast. De eerste twee componenten, Indoor Arena Generator (IAG) op basis van parametrische modellering en het framework van Numeric Assessments of Indoor Arenas (framework-NAIA) op basis van BPS's, worden gebruikt voor de voorbereiding. Terwijl de MOO's, MLPNN en SOM clustering worden gebruikt voor de drie workflows die overeenkomen met de drie ontwerpscenario's (waarin verschillende accenten worden gelegd op numerieke beoordelingen en visueel onderzoek).

Voor de voorbereidingsstap wordt IAG, een flexibel en veelzijdig parametrisch model voor overdekte arena's, voorgesteld, afhankelijk van de samenstelling en de ontwerpparameters van de overdekte arena's. Door de waarden van de parameters in te stellen en te wijzigen, kan het verschillende types van gebouwwormen genereren met drie veelgebruikte structurele types (rasterschaal, ruimtevakwerk en vakwerkligger) op basis van de integratie van de multifunctionele ruimte en de structuur van het lange-dak. Framework-NAIA, de andere component van de voorbereidingsstap, bestaat uit de numerieke indicatoren en gerelateerde gebouwprestatiesimulatie (BPS) tools over de multifunctionaliteit (ruimtelijke capaciteit, uitzicht van toeschouwers, akoestiek voor diverse activiteiten) en structurele prestaties. Het kader biedt ook mogelijke beoordelingscriteria met betrekking tot de indicatoren, op basis waarvan elk van de indicatoren kan worden gebruikt als een ontwerpdoel of een beperking om een ontwerp te beoordelen. Daarom kunnen ontwerpers snel specifieke criteria aanpassen en de BPS-tools combineren met IAG om de gegenereerde ontwerpalternatieven te beoordelen.

Op basis van de pre-proces componenten worden drie workflows van CDIA geformuleerd voor de drie bijbehorende ontwerpscenario's. De eerste workflow wordt voorgesteld voor het ontwerpscenario waarin ontwerpers de numerieke beoordelingen met betrekking tot kwantitatieve ontwerpseisen voor ontwerpalternatieven moeten prioriteren. Multi-Objective Optimization (MOO) wordt gebruikt in deze workflow, om te zoeken naar 'goed presterende' ontwerpen in een brede ontwerpruimte met diverse ontwerpalternatieven (gegenereerd door IAG), volgens aangepaste numerieke beoordelingscriteria (geformuleerd op basis van de kader-NAIA) met betrekking tot kwantitatieve ontwerpseisen. Onder de 'goed

presterende' ontwerpen die door het MOO worden geselecteerd, kunnen ontwerpers op basis van visuele onderzoeken naar kwalitatieve ontwerpeisen veelbelovende ontwerpen selecteren.

De tweede workflow wordt voorgesteld voor het ontwerpscenario waarin ontwerpers prioriteit moeten geven aan het visuele onderzoek met betrekking tot kwalitatieve ontwerpeisen voor ontwerpalternatieven. In deze workflow wordt SOM clustering gebruikt om alle ontwerpalternatieven (gegenereerd door IAG) te clusteren in groepen volgens geometriekenmerken en om de ontwerpruimte weer te geven op basis van een tweedimensionaal SOM-netwerk dat verschillende typische ontwerpen organiseert. Op basis van het SOM-netwerk kunnen ontwerpers verschillende typen ontwerpen verkennen en veelbelovende typen selecteren op basis van visueel onderzoek met betrekking tot kwalitatieve ontwerpeisen. Alle ontwerpalternatieven binnen deze typen worden geselecteerd, waarbij MOO wordt gebruikt om te zoeken naar 'goed presterende' ontwerpen op basis van numerieke beoordelingscriteria (geformuleerd op basis van de kader-NAIA) met betrekking tot kwantitatieve ontwerpeisen.

De derde workflow wordt voorgesteld voor het ontwerpscenario waarbij ontwerpers evenveel nadruk moeten leggen op numerieke beoordelingen met betrekking tot kwantitatieve ontwerpeisen en visueel onderzoek met betrekking tot kwalitatieve ontwerpeisen. Deze workflow wordt gerealiseerd door gebruik te maken van Multi-Layer Perceptron Neural Network op basis van SOM-MLPNN (SOM-MLPN). In SOM-MLPNN wordt de SOM-clustering, die vergelijkbaar is met die in de tweede workflow, gebruikt om ontwerpen te clusteren in groepen op basis van geometriekenmerken en een typisch ontwerp voor elk cluster te genereren. Hierdoor kunnen ontwerpers verschillende soorten ontwerpen visueel inspecteren. Bovendien worden de inputvectoren van de typische ontwerpen die door SOM-clustering worden gegenereerd, gebruikt als de bemonsterde/gelabelde input voor het ontwerp van experimenten (DoE's) en MLPNN om de waarden te voorspellen van numerieke indicatoren met betrekking tot de kwantitatieve ontwerpvereisten voor alle ontwerpalternatieven (gegenereerd door IAG) in de ontwerpruimte. Op basis van datavisualisatie kunnen ontwerpers ontwerpen verkennen en veelbelovende ontwerpen selecteren, op basis van zowel numerieke beoordelingen als visuele onderzoeken.

De voorgestelde methode (met zijn drie workflows) wordt toegepast op de hypothetische ontwerpen van twee typische overdekte arena's (Barclay Centre in New York en O2 Arena in Londen) in de casestudies. Volgens de resultaten worden de effecten van CDIA op het voldoen aan de eisen van het conceptuele ontwerp van overdekte arena's geverifieerd. De drie workflows zijn in staat om ontwerpers te

ondersteunen bij het definiëren van veelbelovende ontwerpen in de bijbehorende ontwerpscenario's. Op basis van de resultaten worden richtlijnen van CDIA in de praktijk geformuleerd en worden de bijbehorende beperkingen besproken.

De belangrijkste bijdrage van het proefschrift is de formulering van CDIA, die de beperkingen van de huidige rekentechnieken overwint, zodat het conceptuele ontwerp van overdekte arena's, gericht op de integratie van de multifunctionele ruimte en de structuur van het lange-dak, effectief kan worden ondersteund. Binnen het algemene kader van CDIA leveren de voorgestelde componenten en workflows ook bijdragen aan zowel academisch onderzoek als aan de ontwerppraktijk. Het IAG omvat verschillende soorten geometrieën van de multifunctionele ruimte en drie soorten lange-dakconstructies met verschillende geometrieën, die verschillende soorten ontwerpalternatieven kunnen bieden voor zowel onderzoeks- als ontwerpwerkzaamheden. De drie workflows gebaseerd op MOO's, MLPNN's en SOM-clustering bieden verschillende manieren om ontwerpverkenningen voor architectonische conceptuele ontwerpen te ondersteunen. Daarnaast kan CDIA ook gebruikt worden als platform om de relaties tussen de totale gebouwgeometrie en de kwantitatieve indicatoren (met betrekking tot multifunctionaliteit en structurele prestaties) te bestuderen, wat cruciaal is voor academisch onderzoek en geïntegreerde ontwerpen en voor de samenwerking tussen architecten en constructeurs. Bovendien is de methode van CDIA ontwikkelbaar, waardoor meer kwantitatieve aspecten (bijv. warmte, energie, daglicht, ventilatie) in aanmerking kunnen worden genomen en de methode ook kan worden ontwikkeld om te gebruiken voor de ontwerpen van andere bouwtypen.

1 Introduction

1.1 Research background

Indoor arenas, as a kind of large-scale public buildings, usually cater to important activities (sports events, concerts, assemblies, exhibitions, etc.) and serve as landmarks for cities. With the developments of professional sports as well as the industries of recreation and entertainment, more and more indoor arenas are built or renovated in both China and Europe. In China, according to the reports of the General Administration of Sports of China (Liu et al., 2015; Liu et al., 2018) there are 1.957 million sports fields or venues in China, and 62,000 sports venues (647,000,000 m² in total) are planned to be built during 2015 to 2025. In Europe, based on the emphasis on sports by the European Union for more than 30 years, and since the development of sporting equipment and venues is one of the four areas that included in the EC law (Garcia, 2006), a number of sports facilities are also needed for the future. Within this context, it is crucial to achieve successful indoor arenas, which satisfy various design requirements, for our society.

To achieve a successful indoor arena, one of the most important task is to integrate the multi-functional space and the long-span roof structure during the design process, since these two elements are highly interrelated and the integration mainly defines the overall form of the building and impacts the satisfaction of various design requirements (Pan, et al., 2019, 2020;). This integration should be achieved during conceptual design (the early stage of building design process), since it takes a relatively small part (5-8%) of the cost (Miller, 1993), but its outcomes mainly impact the performance of the building during the whole lifecycle (Ellis and Torcellini, 2008; Gane and Haymaker, 2010).

Nowadays, computational design has been widely used for building design processes. In computational design, computational tools, methods, and techniques are used to enable designers to encode the design requirements and rules into algorithms that generate alternative designs for buildings (Sariyildiz, 2012). It is

also considered as a study of how programmable computers can be integrated into the process of design by developing computer algorithms (Harding, 2014). Several computational design methods have been used to support architectural conceptual designs, including parametric modelling, building performance simulations (BPS), multi-objective optimisation (MOO), and machine learning (supervised and unsupervised learning). These methods are considered to be more efficient (Sariyildiz, 2012; Harding 2014; Turrin, 2014; Tseranidis et al., 2016), comparing to traditional design methods, in supporting the generation and assessments of numerous designs, based on which more aspects related to engineering can be integrated with architectural designs.

Specifically, multi-objective optimisation (MOO) has been widely applied to support integrated design which combines architectural and engineering aspects during the early design stage to improve the related quantitative performance of the building (Sariyildiz, 2012; Gerber et al., 2012; Turrin et al., 2012; von Buelow, 2012; Lin et al., 2014; Mueller et al., 2015; Brown et al., 2016; Yang et al., 2018). In these applications, MOOs search for 'well-performing' designs according to numeric assessment criteria provided by designers, and among them, designers can define final design(s). The process consists of form generation based on parametric modelling, performance evaluation based on building performance simulations, and multi-objective optimisation (MOO). The parametric modelling can associate different elements of a building to define a changeable geometry model based on parameters. This geometry model can generate numerous design alternatives by changing the values of the parameters, while guaranteeing predefined geometric relations (Turrin, et al., 2011). The values of various indicators related to different aspects (e.g. structure, HVAC, energy, acoustics, daylighting) of the design alternatives can be obtained by building performance simulations and assessed based on numeric criteria formulated by designers. Among the design alternatives included in the optimisation process, the ones which perform better can be found according to the numeric assessment criteria. However, in most cases, this process only focuses on the well-performing designs, which limits the design exploration in a small range.

Besides, machine learning methods, including supervised and unsupervised learning methods, have also been used in architectural conceptual design. Supervised learning methods, which can learn a mapping between inputs and outputs according to labelled data (Murphy, 2012), have been used to support surrogate models. A surrogate model, based on the mapping learnt by a certain supervised learning method, can replace the time-consuming simulations and rapidly predict the performance/output values of numerous design alternatives in the design space (Kozziel et al., 2011; Tseranidis et al., 2016). Therefore, surrogate model based on supervised learning has been used to support designers to explore numerous

designs according to indicators related multiple kinds of building performance, which overcomes the limitations of MOOs (Hajela et al., 1992; Wortmann et al., 2015; Tseranidis et al., 2016; Yang et al., 2016). However, for the predictions fulfilled by a supervised learning method, there can be uncertainties which can lead to unacceptable errors of these predictions. A series of methods are proposed to quantify the uncertainties (Kasiviswanathan et al., 2016) and to improve the performance of the supervised learning methods (Shanmuganathan, 2016; Samarasinghe, 2016). Moreover, although the performance data of numerous alternatives can be predicted by a surrogate model, it is difficult for designers to visually investigate the designs one by one.

Clustering (a subset of unsupervised learning methods), which can group data objects into clusters according to their features (Murphy, 2012), has been used to support the design exploration of geometries during architectural conceptual designs (Harding, 2016; Harding et al., 2018). Based on clustering, numerous designs can be grouped into clusters according to geometry features (indicated by the design inputs). Designs with similar geometries are in the same group. For each group, a representative design is generated, and all these representative designs are organised on a two-dimensional network to reflect the design space. Therefore, designers can have an overview of the whole design space and explore various design alternatives according to their geometry types. However, clustering is limited in supporting further design exploration based on numeric assessments related to quantitative design requirements.

However, despite their advantages, currently, these methods are still limited in supporting the conceptual design of indoor arenas with an emphasis on the integration of multi-functional space and long-span roof structure. The conceptual design of indoor arenas deals with complex interrelationships between various aspects of the building, challenging decision-makings related to multiple design requirements, as well as the different scenarios in which designers can lay different emphases on various design requirements (details are discussed in the next section). In this light, a specific computational design method is necessary to support such conceptual design processes, therefore, to achieve best-performing indoor arenas.

1.2 Research motivation and goals

Conceptual design is the early stage of the building design process, which aims to generate promising design(s) according to various design requirements (Turrin, 2014). These requirements can be divided into two sets, both of which are highly related to the overall form of the building:

- Quantitative design requirements related to architectural functionality and engineering aspects (e.g. structure, HVAC, climate and energy). For a design, its satisfaction of these requirements can be measured and evaluated based on numeric data.
- Qualitative design requirements related to humanity and social science (e.g. aesthetics, culture, psychology, and politics). So far, for a design, it is still difficult to efficiently assess its satisfaction of these requirements based on numeric data, and designers tend to assess the design based on visual investigations, according to their knowledge and experience.

To generate promising designs satisfying various design requirements, the process of conceptual design can be divided into two steps: a divergent step in which various designs are generated and a convergent steps in which the generated designs are assessed and selected (Okudan, 2008). To progress across the two steps, the information (related to both quantitative and qualitative design requirements) of the numerous design alternatives should be rapidly obtained and organised in an effective way, based on which designers can perform a design exploration to investigate and assess design alternatives according to numeric data and visual investigations. Specifically, for the conceptual design of indoor arenas, before the divergent step, the multi-functionality and the long-span roof structure should be integrated to define the overall form (figure 1.1, A). Based on the integration, numerous and diverse design alternatives should be provided in the divergent step (figure 1.1, B). Designers explore and investigate the design alternatives according to numeric assessments related quantitative design requirements and visual investigations related to qualitative design requirements (figure 1,1 C), based on which, in convergent step, designers can define promising design(s) for the following design stages (figure 1.1, D). In this light, to support the conceptual design of indoor arenas with an emphasis on the integration of the multi-functional space and long-span roof structure, three demands should be satisfied:

- Generating numerous and diverse design alternatives based on the integration of the multi-functional space and long-span roof structure.
- Obtaining adequate information to support the exploration of the generated designs based on both numeric data and visual investigations, therefore, to support designers in assessing the satisfaction of both quantitative and qualitative design requirements.
- Supporting designers to select proper designs according to the assessments, in which the designers' different emphases on quantitative or qualitative design requirements should be taken into account.

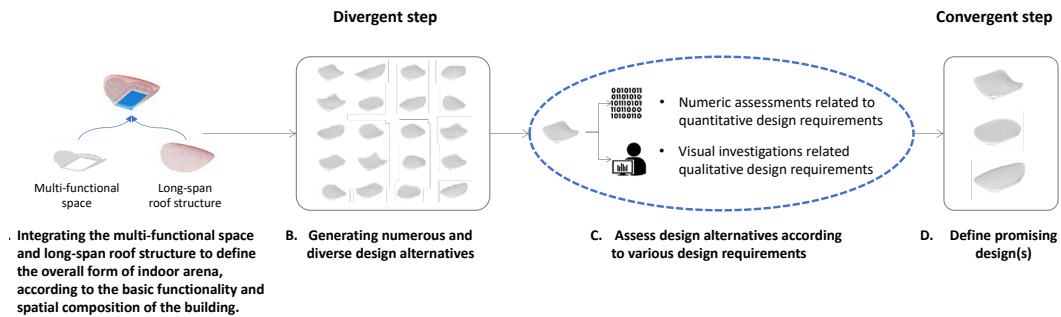


FIG. 1.1 The scheme of the conceptual design process for indoor arena with emphasis on the integration of the multi-functional space and long-span roof structure

However, the challenge is that the current computational design methods are still limited in satisfying these demands. Figure 1.2 illustrates the overall workflows of three methods which have been used in conceptual design (MOO, surrogate model based on supervised learning, and clustering based on self-organizing map).

In these methods, a parametric model should be firstly formulated based on the basic spatial composition of an indoor arena. In the parametric model, various elements of the building are associated and controlled by parameters. By changing the values of the parameters (design inputs), various designs can be generated, and the set of all the designs is design space. In practice, the current parametric modelling approaches focus on one or several specific types of alternatives in each design process. As a result, the generated alternatives can be similar in geometry. However, in the divergent step of conceptual design, it is crucial for designers to study design alternatives with diverse geometries, since different types of geometries

can perform differently in various aspects (related to both quantitative and qualitative design requirements). Therefore, a flexible parametric model is needed to generate a broader design space which includes diverse types of designs.

Building performance simulations (BPS) are then used to obtain the values of different indicators (related to quantitative design requirements) for the designs generated by the parametric model. However, since the simulations are usually time-consuming, it is impractical to use them to obtain the performance data of numerous designs.

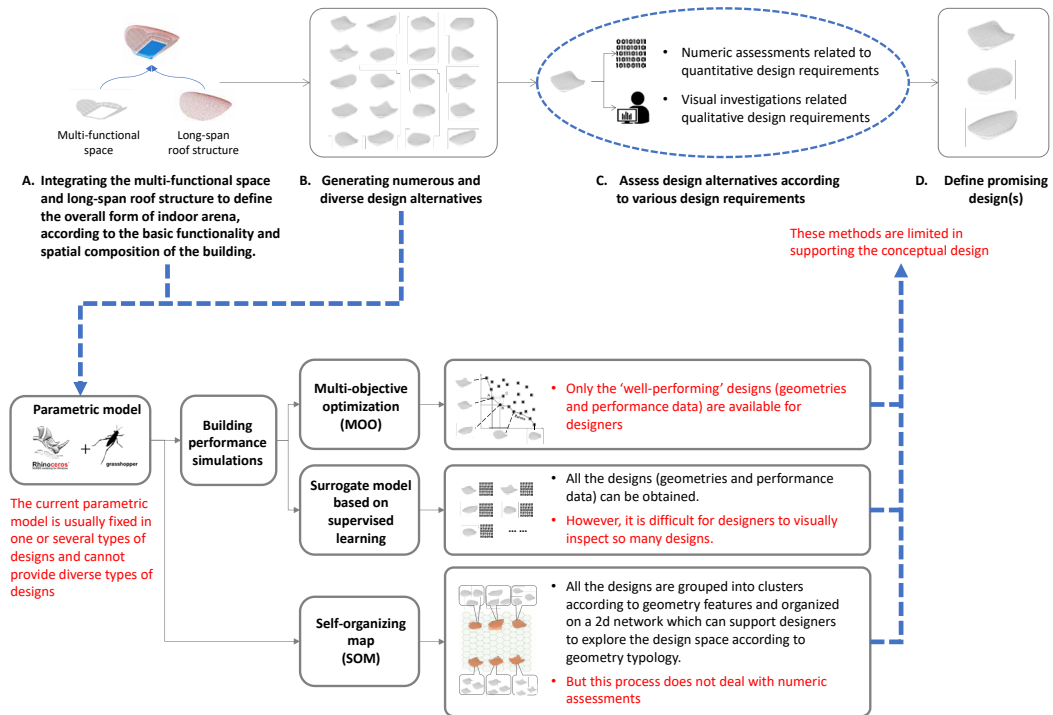


FIG. 1.2 The workflows of three computational design methods and their limitations in satisfying the demands of conceptual design of indoor arenas

Based on the parametric model and the simulations, these methods support design explorations in different ways:

- MOOs iteratively search for 'well-performing' designs within the design space according to specific criteria by using a certain heuristic algorithm (e.g. genetic algorithm). However, a standard MOO only provides the 'well-performing' designs to designers. Besides, in general, MOOs can efficiently deal with the problems in which the design objectives are not more than three, but when the objectives are more than three, it is difficult to find optimal solutions.
- Surrogate models based on supervised learning can learn the relationships between the design inputs and performance data. They are used to rapidly approximate the performance data for numerous designs. Therefore, based on several surrogate models and a parametric model, it is possible to obtain both the geometries and performance data of all the design alternatives within a discrete design space. However, it is impractical for designers to investigate so many designs. It is necessary to efficiently organise the information about the geometries and performance data (related to quantitative aspects) of the numerous designs and to demonstrate the relationships between them.
- SOMs are used in design exploration to group numerous design alternatives into clusters according to their geometry features (indicated by the parameters/ design inputs) and generated a node design for each cluster to represent all the designs within the cluster. Moreover, all the node designs are organised by a two-dimensional network and similar ones are close while different ones are far away, which can reflect the design space (but the effect of the reflection can become weak, as the dimensions of the design space increase, since the curse of dimensionality). Therefore, by using SOMs, designers can investigate various types of design alternatives according to geometry features. However, in this application of SOM, designers do not obtain any information about the numeric data related to quantitative design requirements.

To overcome the limitations of these methods and to satisfy the aforementioned demands of the conceptual design of indoor arenas, it is necessary to propose a design method. Such a method should also be flexible to adapt to different scenarios in which designers can lay different emphases or priorities on numeric assessments and visual investigations.

This thesis aims at formulating a design method for the conceptual design of indoor arenas, based on computational design.

The proposed method should:

- support the integration of the multi-functional space and long-span roof structure of an indoor arena and the generation of numerous design alternatives with diverse geometries.
- support the design exploration for the generated design alternatives based on:
 - numeric data of multiple indicators related to the quantitative design requirements (about the multi-functionality of indoor arenas and the performance of the long-span roof structures);
 - visual investigation according to designers' experience and knowledge related to the qualitative design requirements (about aesthetics, culture, psychology, etc.);
- be adapted to different scenarios in which designers can lay different emphases or priorities on numeric assessments and visual investigations.

It is worth noting that this thesis does not focus on formulating a total automatic design process which delegates human designers. Instead, it intends to support the conceptual design of indoor arenas in a scientific way.

1.3 Research questions

According to the motivation and goals of the research, the research question is formulated:

How can designers be supported to fulfil the conceptual design of indoor arenas?

Specifically, this research question can divide into the following sub-questions:

- How can the method support designers to formulate diverse design alternatives based on the integration of the multi-functional space and long-span roof structure and generate, by using the proposed method?
- How can the method support designers to obtain adequate information of the generated design alternatives, therefore, to fulfil numeric assessments related to quantitative design requirements (about the multi-functionality and the performance of the long-span roof structure) and visual investigations related to qualitative design requirements (about aesthetics, culture, psychology, etc.), based on the proposed method?
- How can the method support designers to lay different emphases or priorities on numeric assessments and visual investigation of the design alternatives, based on the proposed method?
- How can the method support designers to select the final design(s) as the outcome(s) of the conceptual design?

1.4 Research methodology

In this research project, the following methodology is used (Figure. 1.3).

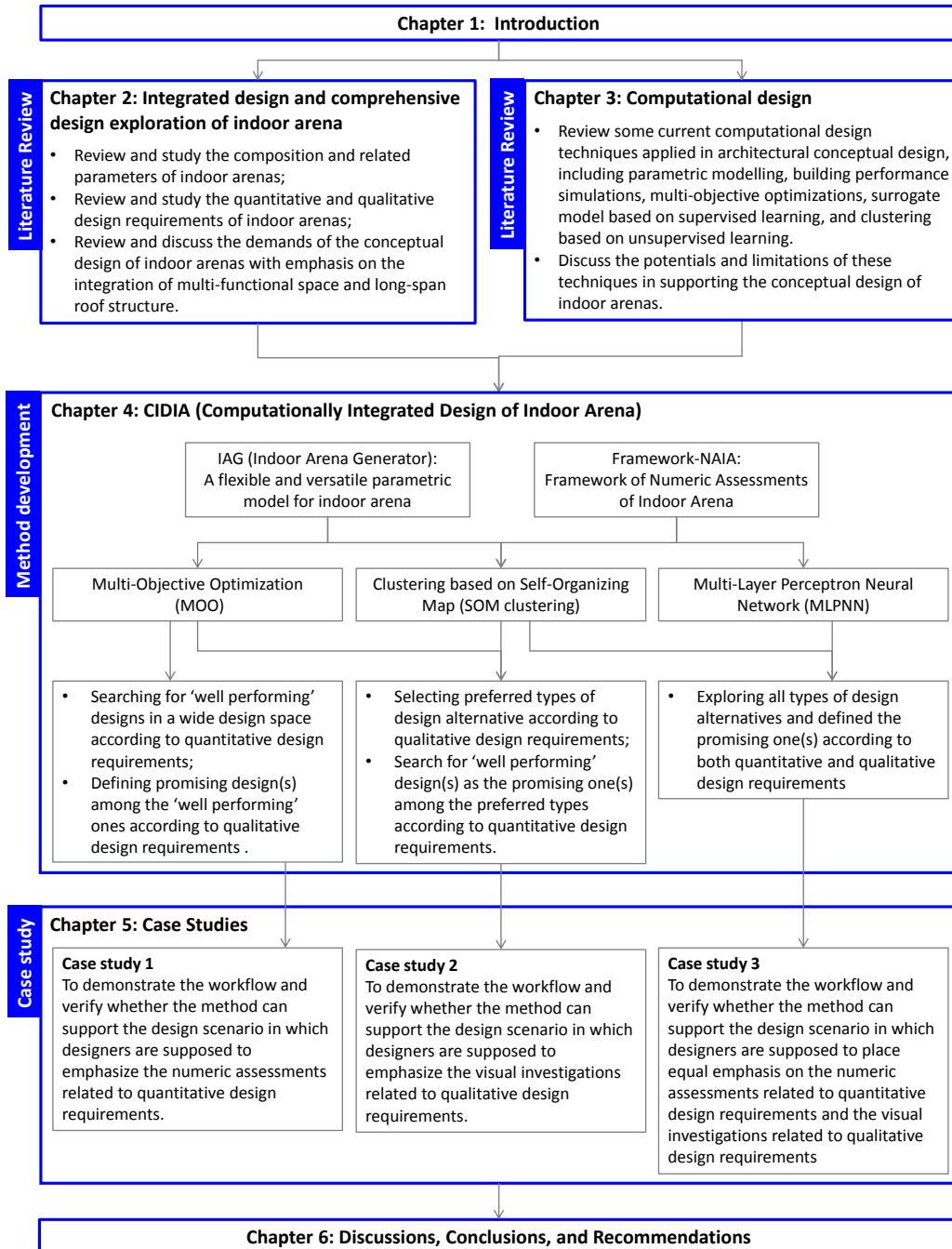


FIG. 1.3 The methodology of the thesis

1.4.1 Literature review

The literature review focuses on the conceptual design of indoor arenas (with an emphasis on the integration of structural and architecture) and the computational design methods which are currently used to support architectural conceptual designs.

- For the conceptual design of indoor arenas based on the integration of the multi-functionality and long-span roof structure, the literature review aims to study several aspects of indoor arenas and formulate basic demands of the conceptual design process. 1) Studying the basic functionality and spatial composition (including relationships between elements and the related parameters) of indoor arenas, with an emphasis on the integration of the multi-functional space and long-span roof structure. 2) Studying various design requirements and related assessments of indoor arenas, including quantitative design requirements (about the multi-functionality and structural performance) and qualitative design requirements. 3) Formulating the basic demands of the conceptual design of indoor arenas, which should be satisfied by the proposed method.
- Several computational design methods (parametric modelling, BPSs, MOOs, surrogate model based on supervised learning, and unsupervised clustering based on SOM), which have been used in architectural conceptual designs, are reviewed. The aim is to clarify their potentials and limitations in supporting the conceptual design of indoor arenas, according to the demands formulated in the last part. By taking advantage of the potentials and overcoming the limitations of these methods, a hypothesis of the proposed method (CDIA: computation-based integrated design of indoor arena) is formulated.

1.4.2 Method development

Based on the formulated hypothesis, the proposed method (CDIA), which satisfies the aforementioned demands of the conceptual design of indoor arenas, is developed and applied in case studies to verify the effects. In CDIA, three different workflows are proposed to adapt to the aforementioned different scenarios (in which the emphases or priorities on numeric assessments and visual investigations). The three workflows are based on the components of IAG (Indoor arena generator, a flexible and versatile parametric model for indoor arenas), Framework-NAIA (the framework of numeric assessment for indoor arenas), multi-objective optimisations (MOOs), multi-layer perceptron neural network (MLPNN) and self-organising map (SOM).

- IAG integrates the multi-functional space and long-span roof structure to formulate a parametric model of indoor arenas, according to the basic functionality and spatial composition of indoor arenas (which are reviewed and studied in the literature review part). By using IAG, various design alternatives with diverse types of geometries and three different types of long-span roof structures can be generated. It is used to overcome the limitation of the current parametric models which are usually fixed in one or several types of geometries, therefore, to extend the design space for design exploration.
- Framework-NAIA is developed to support the numeric assessments related to quantitative design requirements. It is a framework concluding various indicators and related BPSs corresponding to multiple quantitative requirements of indoor arenas. In this thesis, these indicators and related BPSs are corresponding to multi-functionality (the spatial capacity, the views of spectators, and the acoustics of multiple activities) and structural performance. Based on the framework, designers can select indicators to formulate different numeric assessment criteria for the exploration of design alternatives.
- Based on the IAG and framework-NAIA, CDIA is formulated by using the components of MOO, multi-layered MLPNN, and SOM. To adapt to different scenarios in practice (in which designers can lay different emphases on numeric assessments and visual investigations), CDIA is composed of three independent workflows based on different combinations of the components.

1.4.3 Case studies

A series of case studies are used to demonstrate and verify the three workflows of CDIA. Two hypothetical designs abstracted from real projects, representing two typical arena types, are selected as examples to test the effects and adaptability of CDIA in supporting the conceptual design of indoor arenas. The examples are: 1) an indoor arena mainly for sports events and also sometimes for pop-music concerts (with an end-stage), which is abstracted from the Barclay centre in New York, U.S. and 2) an indoor arena for both pop-music concerts (with an end-stage) and sports events which is abstracted from the O2 arena in London, U.K. These examples are applied to the three workflows of CDIA one by one. The results of the case studies for each workflow are discussed to summarise the effects and limitations, based on which guidelines of application of CDIA are formulated.

1.5 Significance

1.5.1 Societal relevance

For the general public, this research supports the achievement of best performing indoor arenas with high-quality multi-functional spaces, well-performing roof structures, and proper forms, which satisfies the societal demands. Specifically, the best performing indoor arenas, which require less cost in both construction and life-cycle maintenance, meet the demands of sustainability.

For the design community, this research proposes a design method to support designers in defining promising designs during the conceptual design of indoor arenas. It also provides an effective and efficient foundation for the collaboration of architects and structural engineers, therefore, improves the design work towards multidisciplinary integration.

1.5.2 Scientific relevance

The proposed method (CDIA), which integrates various aspects of different disciplines during architectural conceptual design, improves the design process in a scientific way. It enlarges the perspective of integrated design and also provides a way based on which further scientific research about the relationships between building geometries and multiple kinds of building performance can be fulfilled.

1.5.3 Readers of this thesis

The main readers of the thesis are the researchers who focus on integrated building designs, the conceptual design of indoor arenas, and computational design. The thesis is also suitable for architects and structural engineers focusing on the designs of sports buildings or other large-scale public buildings. Moreover, it is also useful for other stakeholders involving in the design, construction, and maintenance of indoor arenas.

References

- Brown, N.C., Mueller, C.T. (2016). Design for structural and energy performance of long span buildings using geometric multi-objective optimization, *Energy and Building*, 127, pp. 748–761, DOI: 10.1016/j.enbuild.2016.05.090.
- Ellis, P., Torcellini, P., Crawley, D., (2008). Energy Design Plugin: An EnergyPlus Plugin for SketchUp. In: *Proceedings of Simbuild 2008*, Berkeley, USA. <https://www.osti.gov/biblio/936191-energy-design-plugin-energyplus-plugin-sketchup-preprint> [Accessed: 7-April-2019]
- Gane, V., Haymaker, J., (2010). Design Scenarios: Enabling Requirements-Driven Parametric Design Spaces. In: *Stanford Center for Integrated Facility Engineering Technical Report # 194*
- García, B. (2006). The European Union and Sport, rescuing the nation-state? In: *ECPR Joint Sessions of Workshops*, Nicosia, Cyprus, 2006. <https://ecpr.eu/Filestore/PaperProposal/86bc8bfd-09f7-49a5-af23-991dc2e1a06c.pdf>
- Gerber, D., Lin, S., Pan, B., Solmaz, A. (2012). Design Optioneering: Multidisciplinary Design Optimization through Parameterization, Domain Integration and Automation of a Genetic Algorithm, in: *Symp. Simul. Archit. Urban Des.*, 2012: pp. 23–30.
- Hajela, H., Berke, L. (1992). Neural networks in structure analysis and design: an overview, *Computing Systems in Engineering*, 3 (1-4), pp.535-538. DOI: 10.1016/0956-0521(92)90138-9
- Harding, J. (2014) Meta-parametric design: Developing a computational approach for early stage collaborative practice. EngD. University of Bath.
- Harding, J. (2016). Dimensionality reduction for parametric design exploration. In: *Adriaenssens, S., Gramazio, F., Kohler, M., Menges, A., Pauly, M. eds., Advances in Architectural Geometry AAG 2016*. Zürich, Switzerland: vdf Hochschulverlag AG an der ETH Zürich, pp. 274–287. DOI: 10.3218/3778-4.
- Harding, J., Brandt-Olsen, C. (2018). Biomorpher: Interactive evolution for parametric design. *International Journal of Architectural Computing*, 16, pp. 144–163. DOI: 10.1177/1478077118778579.
- Kasiviswanathan, K.S., Sudheer, K.P., He, J. (2016). Quantification of Prediction Uncertainty in Artificial Neural Network Models. In: *S. Shanmuganathan, S. Samarasinghe (Eds.), Artificial Neural Network Modelling*, Vol. 628, Springer, Berlin, 2016, pp. 145–159. DOI: 10.1007/978-3-319-28495-8.
- Koziel, S., Ciaurri, D.E., Leifsson, L. (2011). Surrogate-based methods, In: *S., Koziel, X.S. Yang (Eds.), Computational Optimization, Methods and Algorithms. Studies in Computational Intelligence*, Vol. 356, Springer, Berlin, 2011, pp. 33–59. DOI: 10.1007/978-3-642-20859-1_3.
- Lin, S., Gerber, D. (2014). Designing-in performance: A framework for evolutionary energy performance feedback in early stage design, *Automation in Construction*, 38, pp.59–73. DOI: 10.1016/j.autcon.2013.10.007.
- Liu, G., Dai, J., Cao, K., Zheng, J. (2018) *Annual report on development of sport for all in China*, Social Science Academic Press, Beijing, China. ISBN: 978-7-5201-2795-0
- Miller, L., (1993), *Concurrent Engineering Design: integrating the best practices for process improvement*. In: *Society of Manufacturing Engineers*, Dearborn, Michigan. ISBN-13: 978-0872634336
- Mueller, C., Ochsendorf, J. (2015). Combining structural performance and designer preferences in evolutionary design space exploration, *Automation in Construction*, 52, pp. 70–82. DOI: 10.1016/j.autcon.2015.02.011.
- Murphy, K. P. (2012) *Machine Learning: A Probabilistic Perspective*. The MIT press, Cambridge, Massachusetts, 2012. <https://mitpress.mit.edu/books/machine-learning-1> [Accessed: 7-April-2019]
- Okudan, Gul E., Tauhid, S., (2008). Concept selection methods - a literature review from 1980 to 2008, *International Journal of Design Engineering* 1 (3), pp. 243–277. DOI: 10.1504/IJDE.2008.023764.
- Pan, W., Sun, Y., Turrin, M., Louter, C., Sariyildiz, S. (2020), Design exploration of quantitative performance and geometry typology for indoor arena based on self-organizing map and multi-layered perceptron neural network. *Automation in Construction*, 114, pp. DOI: 10.1016/j.autcon.2020.103163
- Pan, W., Turrin, M., Louter, C., Sariyildiz, S., Sun, Y. (2019). Integrating multi-functional space and long-span structure in the early design stage of indoor sports arenas by using parametric modelling and multi-objective optimization. *Journal of Building Engineering*, 22, pp. 464–485. DOI: 10.1016/j.jobe.2019.01.006.

- Samarasinghe, S. (2016) Order in the Black Box: Consistency and Robustness of Hidden Neuron Activation of Feed Forward Neural Networks and Its Use in Efficient Optimization of Network Structure, in: S. Shanmuganathan, S. Samarasinghe (Eds.), *Artificial Neural Network Modelling*, Vol. 628, Springer, Berlin, 2016, pp.15-43. DOI: 10.1007/978-3-319-28495-8_2
- Sariyildiz, S. (2012). Performative Computational Design. In: *International Congress of Architecture 2012*. Konya Turkey: Selcuk University, pp. 313-344.
- Shanmuganathan, S. (2016) Artificial Neural Network Modelling: An Introduction, in: S. Shanmuganathan, S. Samarasinghe (Eds.), *Artificial Neural Network Modelling*, Vol. 628, Springer, Berlin, 2016, pp. 1-14. DOI: doi.org/10.1007/978-3-319-28495-8_1
- Tseranidis, S., Brown, N.C., Mueller, C.T. (2016). Data-driven approximation algorithms for rapid performance evaluation and optimization of civil structures, *Automation in Construction*, 72, pp. 279-293. DOI: 10.1016/j.autcon.2016.02.002.
- Turrin, M. (2014), *Performance Assessment Strategy: a computational framework for conceptual design of large roofs*. PhD. Delft University of Technology.
- Turrin, M., von Buelow, P., Kilian, A., Stouffs, R. (2012). Performative skins for passive climatic comfort: A parametric design process, *Automation in Construction*, 22, pp. 36-50. DOI: 10.1016/j.autcon.2011.08.001.
- Turrin, M., von Buelow, P., Stouffs, R. (2011). Design explorations of performance driven geometry in architectural design using parametric modelling and genetic algorithms, *Advanced Engineering Informatics*, 25, pp. 656-675. DOI: 10.1016/j.aei.2011.07.009.
- von Buelow, P. (2012). Paragen-Performative Exploration of Generative Systems, *Journal of IASS*, 53, pp. 271-284.
- Wortmann, T., Costa, A., Nannicini, G., Schroepfer, T. (2015). Advantages of surrogate models for architectural design optimization. *Analysis and Intelligence for Engineering Design*, 29 (4), pp.471-481. DOI: 10.1017/S0890060415000451.
- Yang, D., Ren, S., Turrin, M., Sariyildiz, S., Sun, Y. (2018). Multi-disciplinary and multi-objective optimization problem re-formulation in computational design exploration: a case of conceptual sports building design, *Automation in Construction*, 92, pp.242-269. DOI: 10.1016/j.autcon.2018.03.023.
- Yang, D., Sun, Y., di Stefano, D., Turrin, M., Sariyildiz, S. (2016). Impacts of problem scale and sampling strategy on surrogate model accuracy. In: *IEEE Congress Evol. Comput. '16, IEEE, 2016*, pp. 4199-4207. DOI: 10.1109/CEC.2016.7744323.

2 Literature review: Integrated design and the related design exploration of indoor multi-functional arenas

2.1 Introduction

Based on literature reviews, this chapter aims at:

- 1 clarifying how to generate an indoor arena based on the elements of multi-functional space (the pitch and seating tiers) and long-span roof structure, according to the basic functions of indoor arenas;
- 2 clarifying how to assess the design of indoor arena according to various design requirements (including quantitative ones related multi-functionality and structural performance and quantitative ones related to aesthetics, culture, psychology, etc.);
- 3 clarifying the basic demands of the conceptual design of indoor arenas, which should be satisfied by the proposed method in this research.

For the first aim, in section 2.2, the basic function and the composition of indoor arenas are studied, based on which the integration of the multi-functional space (pitch and seating tiers) and long-span roof structure is emphasized. Further, for the elements (pitch, seating tiers, roof structure) of indoor arenas, the design parameters related to the geometries and the interrelationship between the elements are studied based on literature review and the examples of 129 selected indoor arenas all over the world (see Annex 1). Moreover, the diversity of the overall form/geometry of designs is also discussed. Based on these studies, a generation process of indoor arenas is formulated.

For the second aim, in section 2.3, the design requirements of indoor arenas are studied, which can be divided into two sets:

- Quantitative design requirements related to architectural functionality and multiple engineering aspects, which can be described and evaluated by a series of numeric indicators. Among various quantitative design requirements, the aspects of multi-functionality and structure are emphasized, since they are directly related to the integration of the multi-functional space and long-span roof structure of indoor arenas. Specifically, the multi-functionality is divided into the spatial capacity, viewing of spectators, and acoustics for various activities (sports events, stage-performances, exhibitions, and daily sports for the public). For both the multi-functionality and structural performance, the related numeric indicators are studied based on the review of related work and design codes.
- Qualitative design requirements related to humanity and social science (including aesthetics, psychology, politics, culture, urbanism, etc.), which are difficult to be efficiently assessed by numeric data so far but still evaluated by visual investigations of designers according to their knowledge and experience. It is a characteristic of architectural design, which makes it differ from other engineering designs.

For the third aim, in section 2.4, the research work related to architectural conceptual design is reviewed, in which the generation of various designs and the assessments of the generated designs according to multiple design requirements during conceptual design are highlighted. Based on these highlighted aspects and the studies in the previous sections, three basic demands are formulated for the conceptual design of indoor arenas with emphasis on the integration of multi-functional space and long-span roof structure. 1) Integrating the multi-functional space and long-span roof structure to generate numerous and diverse design alternatives. 2) Obtaining adequate information to support the exploration of the generated designs based on both numeric data and visual investigations, therefore, to support designers in assessing the satisfactions of the designs about both quantitative and qualitative

design requirements. 3) Supporting designers to select promising designs according to the assessments, in which different emphases of designers on quantitative or qualitative design requirements should be considered. The three demands should be satisfied by the proposed method, according to which, in the next chapter, several computational design methods are reviewed to clarify the potential and limitations.

2.2 Formulation process of indoor arenas

The basic function of an arena or stadium is to provide a space for competitions/matches of player (or other activities, e.g. concerts, assembly, exhibitions) and for spectators to watch the competitions/matches (or other activities). In an arena or a stadium, for the players and related staff, there should be courts or tracks for the match, spaces for activities before the match, and the rooms for changing, rest, management of the games, etc. For spectators, there should be seating tiers, lobbies for rest, etc.

The Colosseum of Rome is considered as the prototype of both outdoor stadia and indoor arenas (figure 2.1, left). It is composed of an oval pitch in the centre, oval seating tiers around the pitch, a retractable roof supported by cables, and affiliate spaces behind the seating tiers. Till today, this composition of sports arenas still remains (figure 2.1, right), but the design of these elements (the pitch, seating tiers, roof, and annex spaces) and the relationships between them are standardized gradually.

In general, an arena or stadium can be divided into a core space and annex spaces around or beside it (Culley and Pascoe, 2009; John et al. 2013; Ding and Mei, 2018). The core space is composed of a pitch in the centre for the competitions/matches or other activities (figure 2.1, A) and seating tiers around the pitch for spectators (figure 2.1, B). The combination of the pitch and seating tiers is defined as multi-functional space, since it determines the capacity of the arena in catering for various activities. For an indoor arena, there is an intact long-span roof covering the whole multi-functional space (figure 2.1, C), while for an outdoor or semi-outdoor stadium, the roof usually does not cover the pitch. There are some stadiums with retractable roofs which can cover the whole space, but basically, they are still considered as outdoor stadiums. Around or beside the core space, there are annex spaces which provide various rooms to serve the multi-functional space (e.g. lobbies, corridors, training halls, rooms as the backstage for events, etc.).

This research focuses on the multi-functional space (the pitch and seating tiers) and the long-span roof structure of indoor arenas, since they are highly interrelated, and their combination mainly defines the overall form of the building and impacts the satisfaction of various design requirements. The details of and the interrelationships between the pitch, seating tiers, and long-span roof structure are elaborated in section 2.2.1 to section 2.2.4.

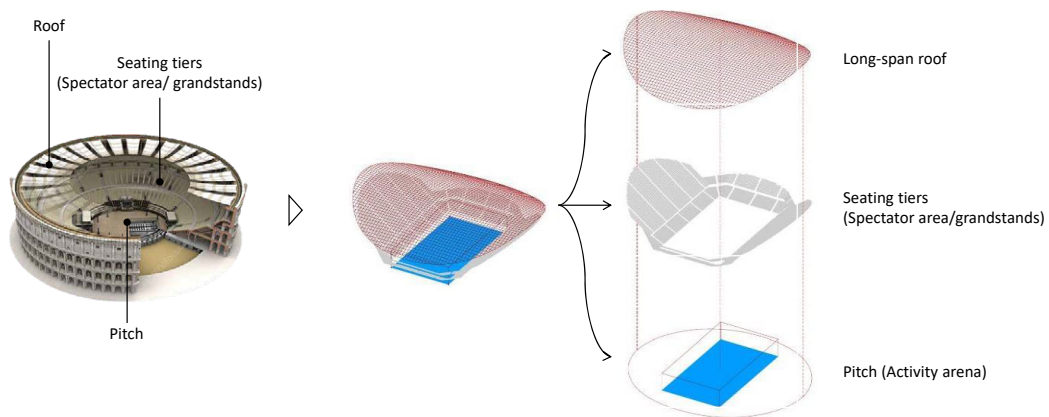


FIG. 2.1 The composition of the Colosseum of Rome (MApaPLAN.com) and a modern indoor arena

2.2.1 Pitch for various activities

A pitch (or an activity area) is the field for sports competitions, stage-performances, or other activities in an indoor arena. Its shape and size should be defined based on the spatial requirements of these activities. Among various activities, sports competitions/events, stage-performance and assemblies, exhibitions, and daily sports for the public.

Sports competitions are the most important activities for indoor arenas. According to the design guide of Sport England (2015), the overall space (O/A) for a sports competition pitch includes the principle play area (PPA) for the court, the run off area (R/O) for safety space, and the affiliate area for coach and team members (figure 2.2). The dimensions of the O/A vary for different sports are listed in table 2.1 and illustrated in figure 2.3.

In practice, developers and designers usually determine which sports competitions will be held in the arena, and then define a large enough pitch. If the O/A sizes of some sport competitions are smaller than the size of the pitch, the blank is usually filled with retractable tiers. According to the dimensions in table 2.1, conventionally, a 68m × 42m × 12m pitch (for gymnastics artistic) can accommodate most of the sports courts (figure 2.3), except indoor athletics, track cycling, speed skating, swimming, and diving (which are usually held in special venues).

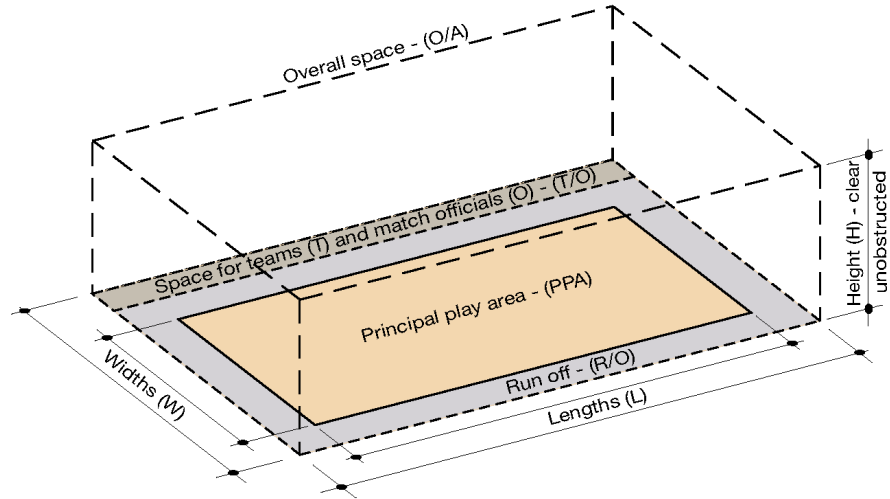


FIG. 2.2 The composition of overall space (O/A) for sports competitions (Sport England, 2015)

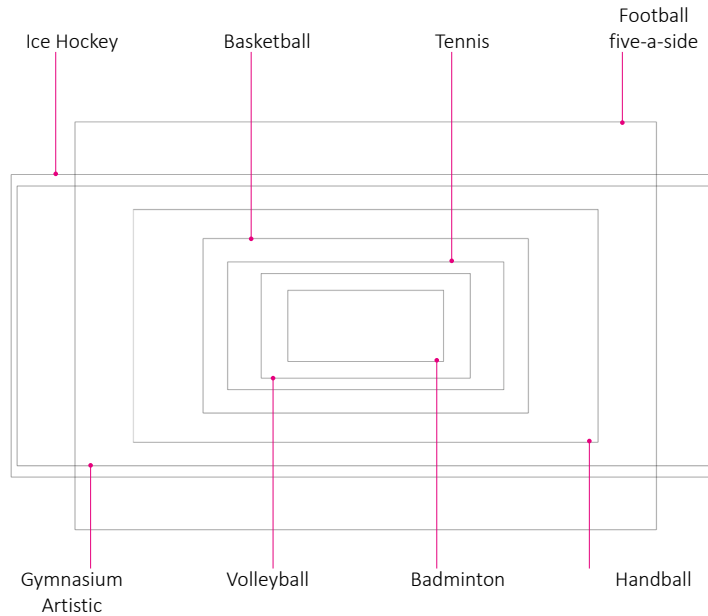


FIG. 2.3 A comparison of the overall space (O/A) sizes for different sports

TABLE 2.1 Requirements on the dimensions and the capacity of spectators for sports events

sports	Principle Play Area (PPA), m	Run off (R/O), m		Overall Area (O/A), m	Capacity of spectators (Olympic games)
		side	end		
Ice hockey	61 × 26 × 6	5	2	65 × 36 × 6	10,000
Gymnastics Artistic	60 × 34 × 10	4	4	68 × 42 × 10	12,000
Handball	40 × 20 × 12	2	2	50 × 28 × 12	10,000
Basketball	28 × 15 × 9	2.05	2.05	32.1 × 21.1 × 9	15,000
Football (five-a-side)	50 × 35 × 7.5	3	3	56 × 41 × 7.5	6,000
Volleyball	18 × 9 × 12.5	5	6.5	31 × 22 × 12.5	15,000
Tennis (indoor)	23.77 × 10.97 × 12	3.66	6.4	36.57 × 18.29 × 12	10,000
Gymnastics Rhythmic	13 × 13 × 12	4	4	21 × 21 × 12	6,000
Trampoline Jumping	28 × 12 × 12 Four beds	4	4	36 × 20 × 12	4,000
Judo	8 × 8 × 3.5	3	3	14 × 14 × 3.5	8,000
Badminton	13.4 × 6.1 × 12	2	2	17.4 × 10.1 × 12	5,000
Table Tennis	14 × 7 × 5	2	2	18 × 12 × 5	5,000
Short track speed skating	61 × 26 × 6	5	2	65 × 36 × 6	8,000
Figure skating / Ice sport artistic	61 × 26 × 6	5	2	65 × 36 × 6	8,000

Stage performances (e.g. concerts) and assemblies are another important kind of activities for indoor arenas. According to the statistics of a famous trade industry journal 'POLLSTAR' (2016), more and more famous indoor arenas cater for concerts. For stage-performances and assemblies, the stage is usually set inside the pitch, and the blank of the pitch is also filled with retractable seats. In general, the stage can be set in three different locations within a rectangular pitch: in the centre, along the side, and at the end (figure 2.4), which largely influences the view of spectators (details are elaborated in section 2.3.1.2).

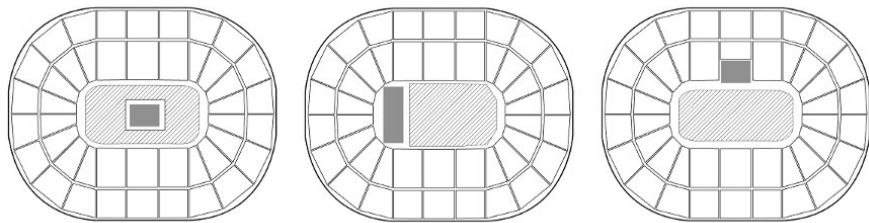


FIG. 2.4 Three types of stage-setting for stage performances (Left: end stage; middle: side stage; right: central stage)

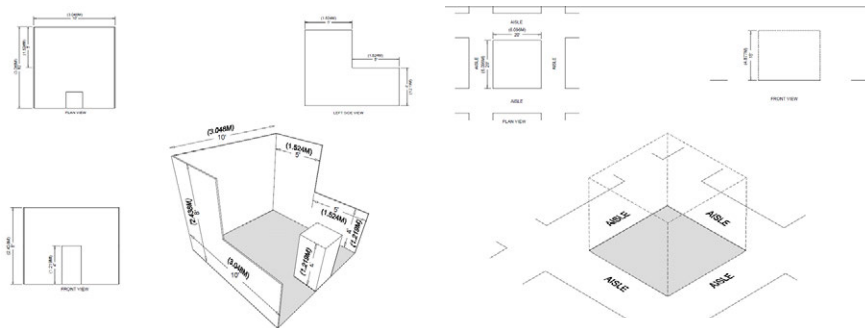


FIG. 2.5 The spatial requirements of exhibitions (IAEE, 2014)

Exhibitions and daily public sports are also usually held in indoor sports arenas, especially for the arenas serving campuses or communities. According to the guidelines of the International Association of Exhibitions and Events (IAEE, 2014), an exhibition requires an area to accommodate a number of standard booths (3m × 3m × 3m) and related aisles (figure 2.5). Daily sports for the public require multiple sports courts simultaneously. A modular layout approach based on the

badminton court is widely used in different countries. The design guide of Sport England (2012) summaries a series of layouts for various sports courts, based on the module of badmintons (figure 2.6).

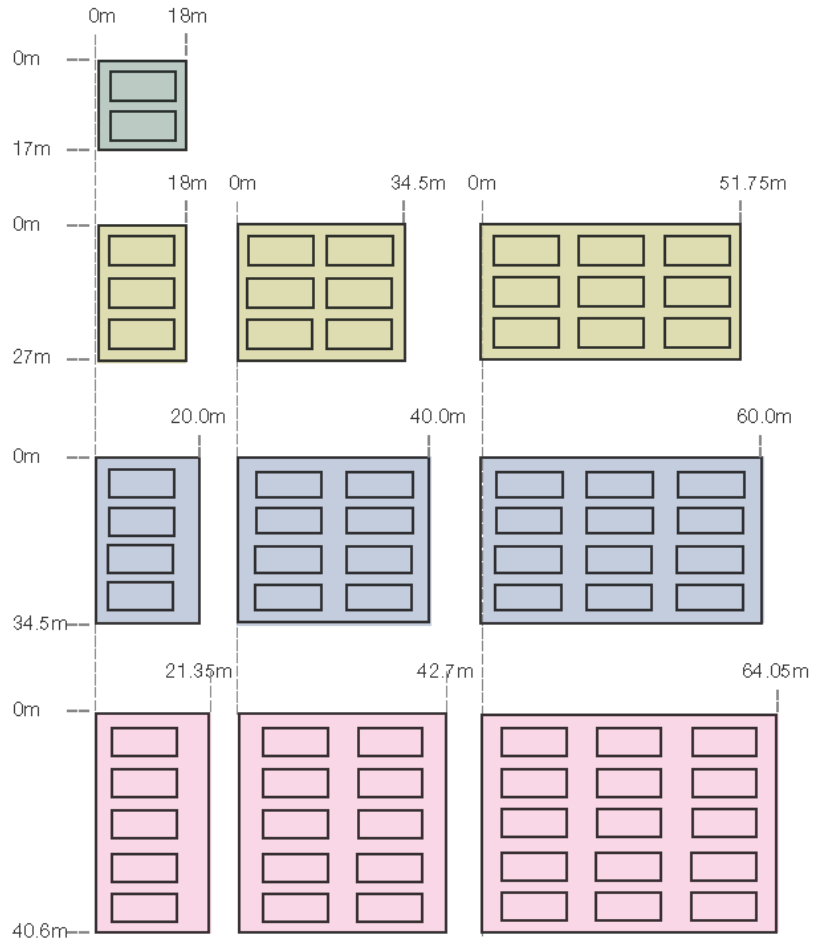


FIG. 2.6 The badminton-court-based modular layout approach for multiple sports courts (Sports England, 2012)

Based on the analyses above, two design parameters related to the pitch can be formulated:

- P_Size: the dimensions of the pitch. The shape of the pitch is usually rectangle, round, or oval. The oval pitch is frequently used for indoor athletics, track cycling, and track speed skating. For other arenas, rectangle pitch is frequently used, since most of the sports competition courts are rectangle. This research also focuses on the rectangle pitch. The dimensions of the pitch (length, width, and height) influence the capacity for various activities. It also influences the seating tiers, since the outline of the pitch is also the inner boundary of the seating tiers.
- Pt_Stage: the position of the stage for stage performances. For stage performances (e.g. concerts, drama), as mentioned, there are three basic types of stage-setting: end-stage, side-stage, and centre-stage. The size of the stage varies in design practice, but to simplify, during conceptual design, a typical stage size can be directly used. The location of the stage impacts the arrangement of the temporary retractable seats in the pitch as well as the views of spectators in fixed seats (details are elaborated in section 2.3.1.2).

2.2.2 Seating tiers (stands) for spectators

A seating tier is a continuous grandstand composed of a series of seating rows, which are set around the pitch in different levels in an arena. The seating tiers can be generated based on two steps and defined by two sets of parameters (figure 2.7). First, based on a defined pitch (figure 2.7, A), a raw seating bowl is generated according to a series of design parameters (figure 2.7, B). Then an outer boundary curve is defined by another set of parameters, and the final seating bowl can be generated by using the boundary curve to cut the raw seating bowl (figure 2.7, C). This method has been proposed and used in practice (Sun et al., 2013; Pan et al., 2019) to generate various types of seating tiers (figure 2.7, D).

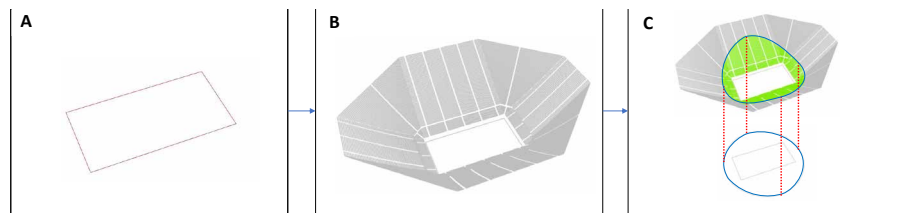
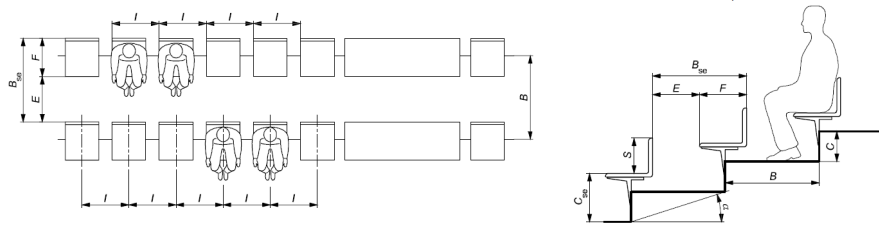


FIG. 2.7 Seating tiers in a typical arena and a two-steps generation process (Pan et al., 2019)

2.2.2.1 Formulation of a raw seating bowl

The seating tiers are regulated by design codes. Taking the Eurocode EN 13200-1:2012 Spectator Facilities (CEN, 2012) as an example, the regulations about seating tiers are related to the accommodation, the passage and evacuation, and the view of spectators. For the accommodation of spectators, the width of a seat and the depth of a seating row are regulated. For the passage and evacuation of spectators, the number of the seats between two aisles, the width of aisles, etc. are regulated (figure 2.8).



- Bse dimension of the tread where there are seating places (seating row depth) (Bse = B), min = 700 mm rec = 800 mm
- C riser between each tread
- E clear width for the row-passage, equals Bse – F, min = 350 mm rec = 400 mm
- F depth of seat, min = 350 mm rec = 400 mm
- Cse difference of level between seat and tread or passage below, max = 450 mm rec = 400 mm
- α angle of inclination of the stand, max 35°
- S the height of seat back, min = 300 mm
- I width of lateral boundaries, min = 450 mm rec = 500 mm

FIG. 2.8 The diagram of the regulations about seating tiers according to EN 13200-1:2012 (CEN, 2012)

For the view of spectators, the quality of sightlines is emphasized. A sightline of a spectator is a line between the spectator's eyes (represented by a point) and a focal point in the pitch. The quality of a sightline refers to the extent of a spectator's view which is not covered by the front spectators. To ensure the quality, a calculation process is widely used to define the riser of each seating row. Taking the Eurocode EN 132001: 2012 (CEN, 2012) as an example, to calculate the riser of a certain seating row, the nearest point on the boundary of the court of a certain sports competition is selected as the focal point (figure 2.9), and the riser can be calculated:

$$C = V + \frac{aB}{D} \quad [2.1]$$

Where C is the riser of a seating row, which varies for each row; V is the vertical distance from the eyes of a spectator to the top of the head or the sightline of the spectator in the next row; a is the difference between the height of the eyes and the height of focal point P (the nearest point of focus along the line of sight); B is the distance from one spectator to the spectator behind; D is the horizontal distance between the spectator's eyes situated and the focal point P .

In practice, the ' V ' value is usually regulated by design codes. Taking the Eurocode EN 132001: 2012 (CEN, 2012) as an example, the acceptable and premium values for ' V ' are 120mm and 150mm respectively. Based on equation 2.1, the risers of all the seating rows can be calculated one by one, according to a defined value of ' V ', then the slope of the seating tiers can be defined. Figure 2.10 illustrates seating tiers with different slopes according to different values of ' V '.

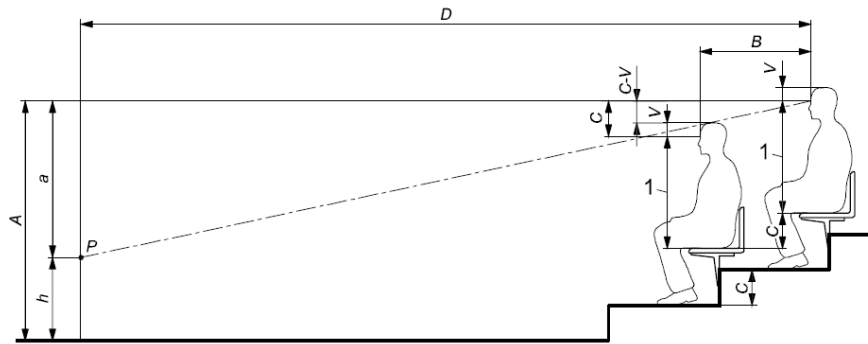


FIG. 2.9 Sightline for a spectator according to EN 13200-1:2012 (CEN, 2012)

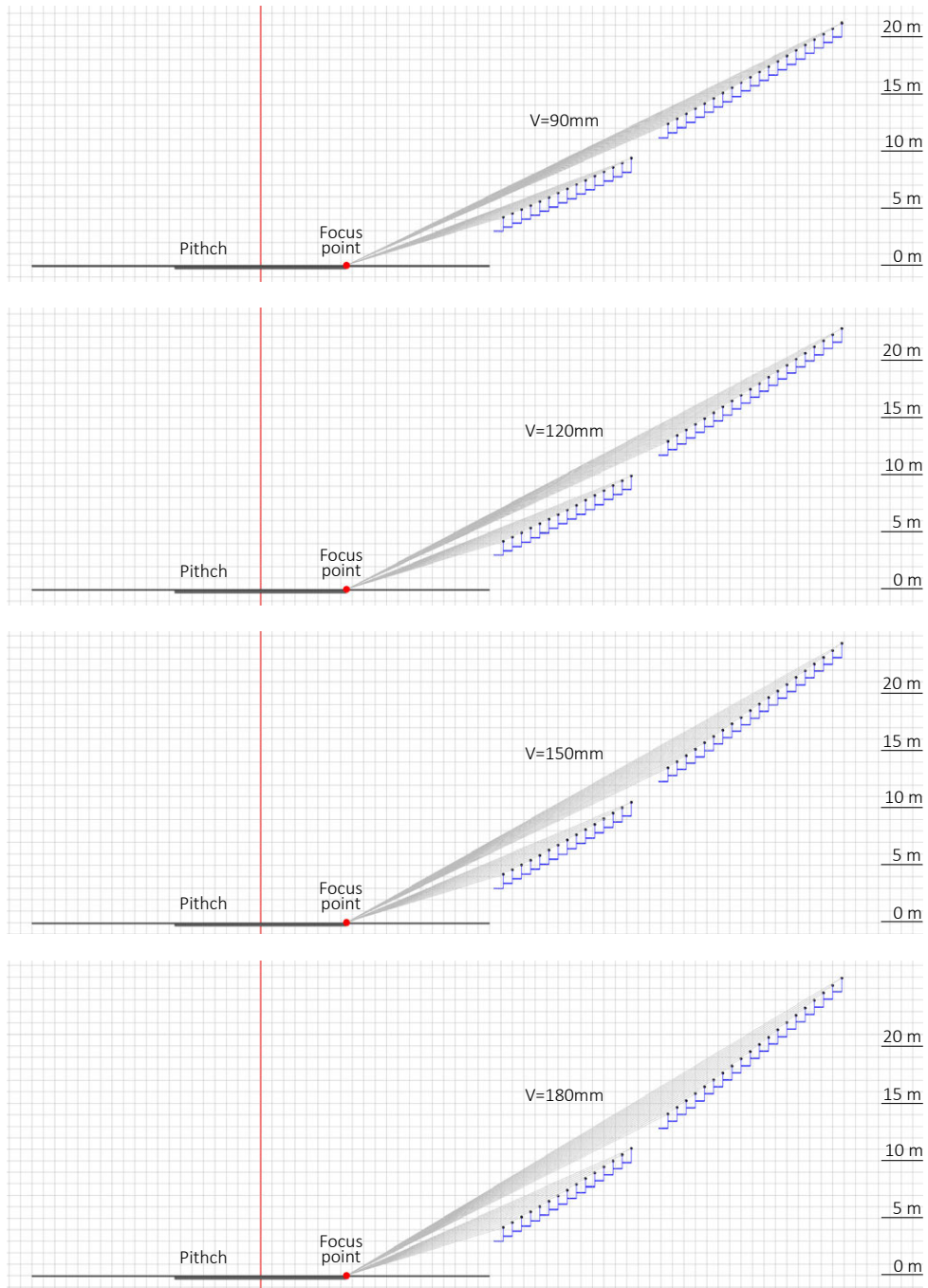


FIG. 2.10 Seating tiers with different slopes caused by different values of 'V'

Based on these regulations, a series of design parameters which are used to generate the raw seating bowl can be formulated:

ST_InBdHeight: the height of the inner boundary of the seating bowl. The first row of the seating tiers is usually higher than the pitch. This parameter is used to define the height from the pitch to the inner boundary of the seating tiers (which is the rim of the floor of the first seating row). The projection of this boundary is usually overlapping the outline of the pitch. Therefore, the size of the pitch (defined by the parameter **P_Size** mentioned above) can impact the slope of the seating tiers (figure 2.11). The parameter here can also impact the slope of the seating tiers (figure 2.12).

ST_Sec: the number of sections of the seating tiers. In a large indoor arena, there can be several parts/sections of seating tiers which are set on different levels. Obviously, the division of the seating tiers, which is defined by this parameter, impacts the overall slope of the seating tiers (figure 2.13).

ST_RowNum: the number of rows for each section of the seating tiers. Based on the division of seating tiers mentioned above, the number of seating rows in each section of seating tiers also impacts the slope (figure 2.14).

ST_OhSb: overhanging or stepping back the upper tiers. For the multi-section seating tiers, the upper tiers can be overhang above the lower tiers (to cover some rows of the lower one) or can be behind the lower tiers and generate an aisle between them. Such different arrangements impact the shape of the seating tiers (figure 2.15).

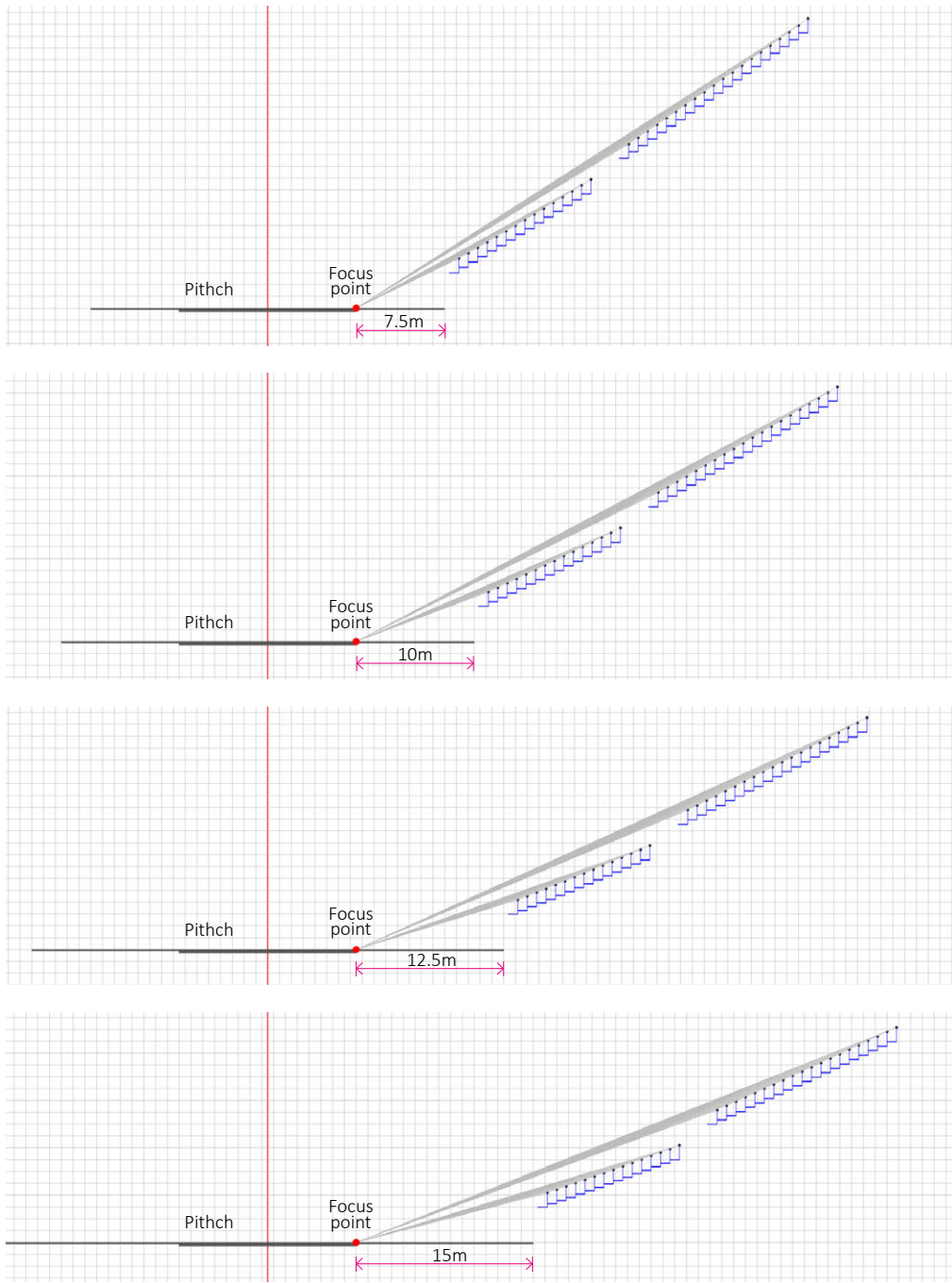


FIG. 2.11 The pitches with different sizes impact the shape of the seating tiers

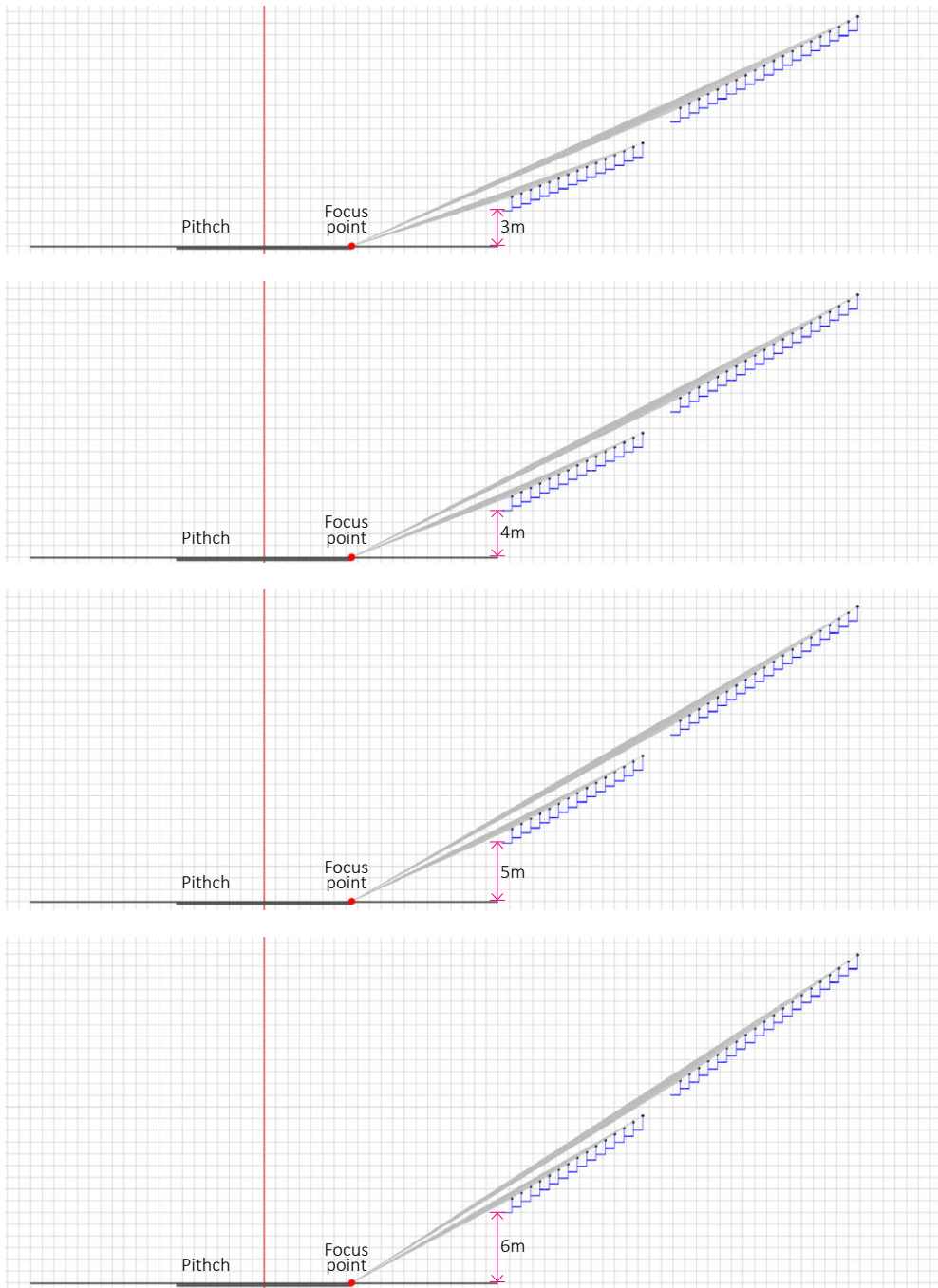


FIG. 2.12 Different heights of the first seating row impact the shape of the seating tiers

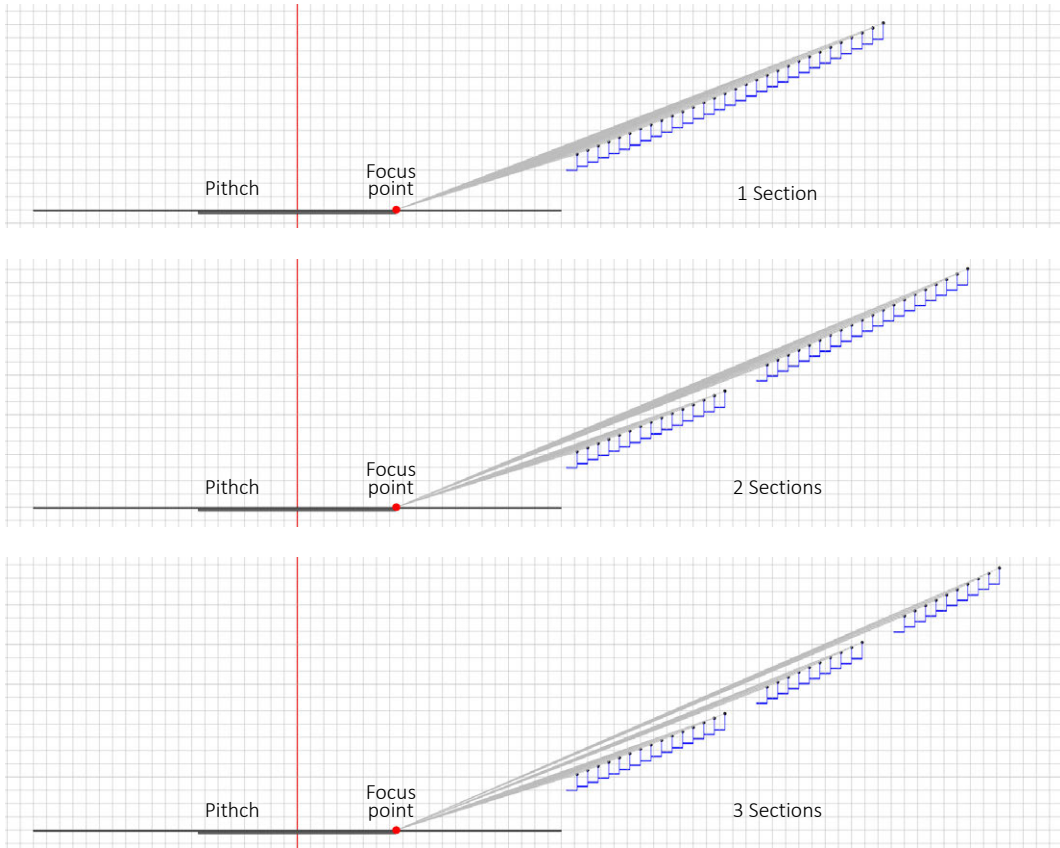


FIG. 2.13 Seating tiers divided into different sections

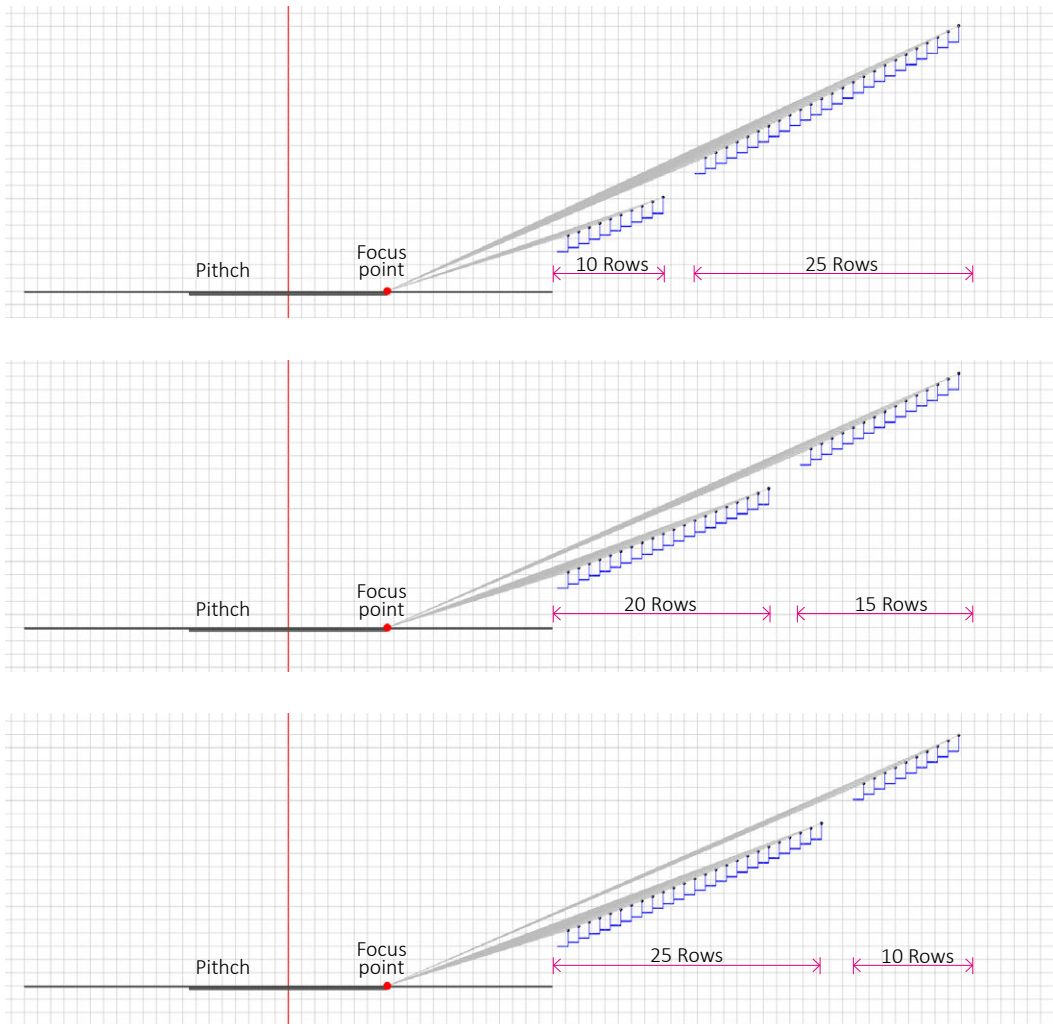


FIG. 2.14 Seating tiers with different number of rows for each section of the tiers

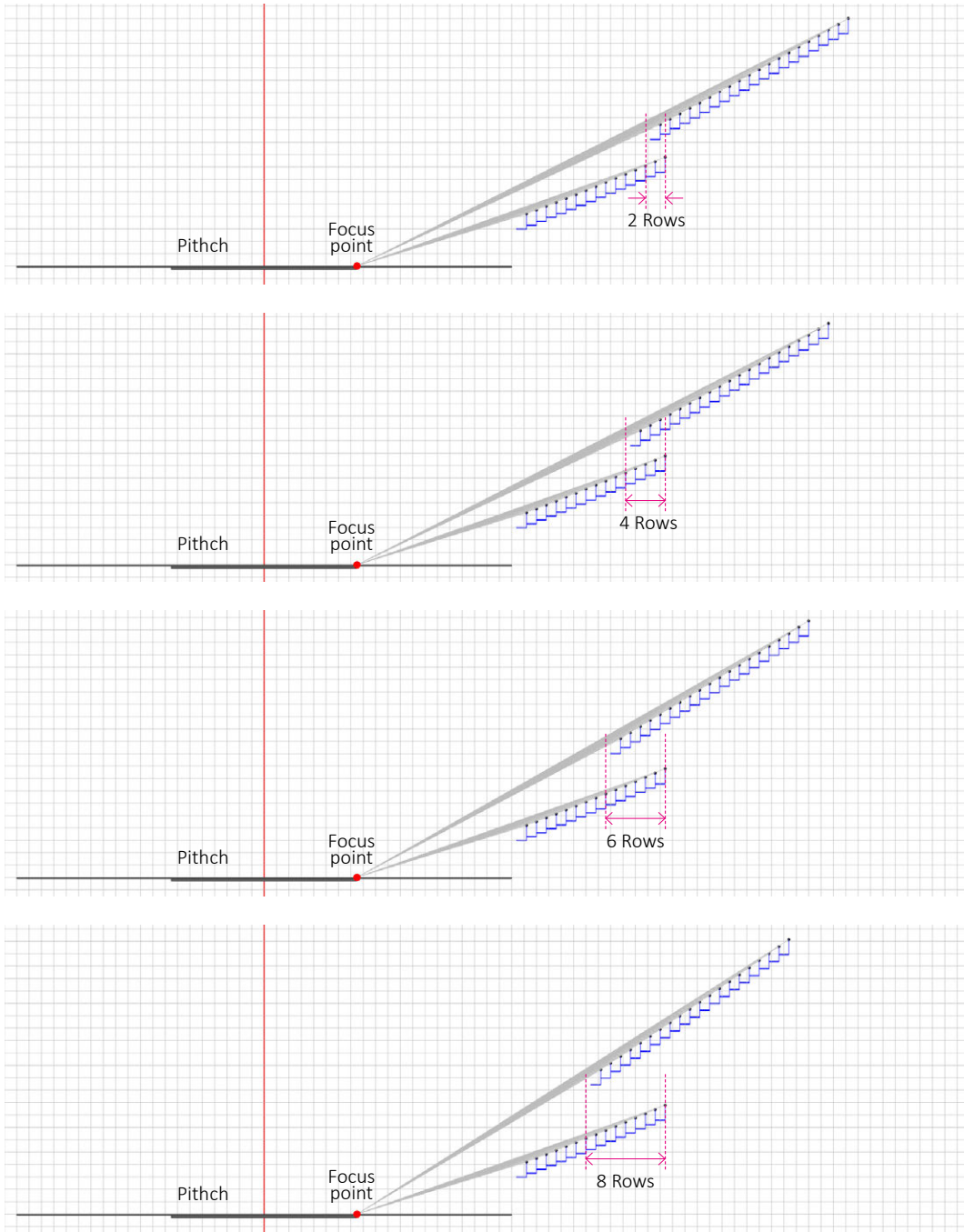


FIG. 2.15 Overhanging or stepping back the upper tiers for two-section seating tiers

2.2.2.2 Formulation of the boundary curve of the seating bowl

The boundary of the seating bowl is an important factor for an indoor arena, since it impacts both the outline of the building and the boundary of the roof structure (which defines the overall span). The projection of the boundary can be defined by control points and the type of the curve (polyline or curve). According to the study on the 129 arenas all over the world (see appendix), several types of polylines/curves are widely used for the boundary, including rectangle, round, oval, hexagon, octagon, and some free form curves based on these basic curves. In this research, the boundary curve is defined by interpolation of eight control points and can be poly line or curve), which can generate all these types of polylines/curve as well as some types of curves which have not been used in the current arenas (figure 2.16).

The boundary curve can be symmetry or asymmetry (along the x-axis or the y-axis) to the pitch. For some indoor arenas which are frequently used for stage-performances (e.g. concerts) and assemblies, the seating bowls are asymmetric to the pitch (e.g. Philippine arena, O2 arena, Ziggo dome, see appendix), to provide more seats in front of the stage. According to the analysis above, a series of parameters are formulated to define the boundary:

ST_LenX / ST_LenY : the length of the seating bowl boundary along the x-axis or y-axis. These parameters defined the length and width of the building and also the positions of four of the eight control points (figure 2.16).

ST_CPi / ST_CPii / ST_CPiii / ST_CPiv: the corner point of the seating bowl boundary in the I, II, III, or IV quadrant. These parameters define the other four control points of the boundary curve, based on the rectangle defined by the previous parameters and the corners of the pitch (figure 2.16)

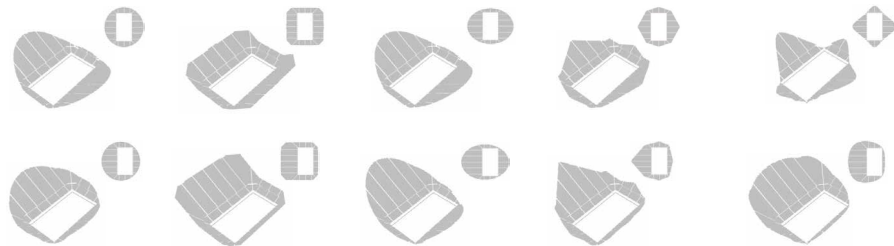


FIG. 2.16 Seating tiers with different outlines

ST_AsyX / ST_AsyY: the asymmetric ratio of the seating bowl boundary along the x-axis or y-axis. These parameters define the asymmetry of the boundary curve based on the pitch. The parameters are ratios. If the seating tiers are symmetric along an axis, then the ratio equals 0. If all the seating tiers are arranging on one side along an axis and there are no any seats on the other side, then the ratio equals 1. Based on these different ratios (between 0 and 1), different shapes for seating tiers can be generated (figure 2.17).

ST_Bdr: the curve degree of the seating bowl boundary. This parameter defines the curve type for the seating bowl boundary. For a polyline, the curve degree equals 1, while for a curve, the degree equals 3.

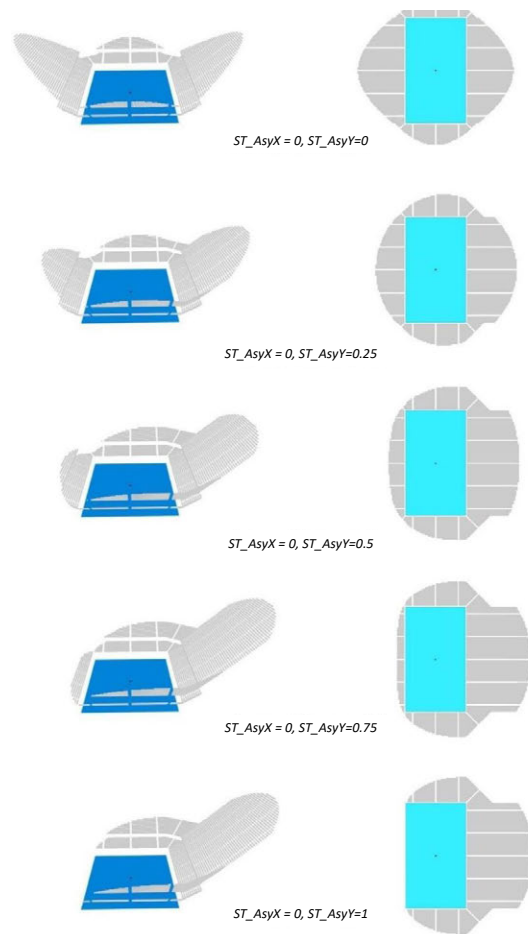


FIG. 2.17 Seating tiers with different asymmetry ratios

2.2.3 Long-span roof and the structure

As mentioned, for an indoor arena, there is a long-span roof to cover the whole multi-functional space (the pitch and seating tiers). The geometry of the roof, which is related to the boundary of the seating tiers, impacts the structural performance, the acoustics of the multi-functional space, and the overall form of the building. In the following sections, the geometries of the long-span roofs of indoor arenas (section 2.2.3.1) and the related long-span structural types are studied (section 2.2.3.2), based on which the design parameters of long-span roof structures of indoor arenas are formulated (section 2.2.3.3).

2.2.3.1 Geometry of the long-span roof

In design practice, the combination of the pitch and the seating tiers is called the 'bowl' (which is defined as the multi-functional space in this thesis), and the roof can be seen as the 'cap' of the 'bowl'. The geometry of the roof is crucial which impacts different aspects of the building. The roof structure and the related ceiling as well as the hanging equipment cannot invade the multi-functional space or obstruct the sightlines of spectators. The roof geometry impacts the structural performance as well as the acoustics of the indoor space. Moreover, the combination of the multi-functional space and long-span roof mainly defines the overall form and the indoor space of the building.

Engle (1997) classified the geometries of long-span roofs into four groups: flat, single-curved surface (zero Gaussian curvature), dome surface (positive Gaussian curvature), saddle surface (negative Gaussian curvature) (table 2.2). These roof geometries can be found in the 129 representative arenas all over the world (Appendix). For the roofs of the 129 arenas, 40 are flat, 38 are single-curved surface (zero Gaussian curvature), 34 are dome surface (positive Gaussian curvature), and 9 are saddle surface (negative Gaussian curvature).

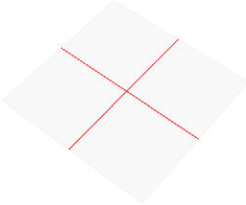
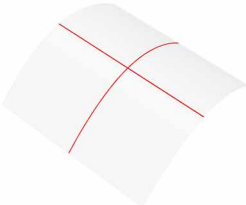
A flat roof can be used for an arena in which the boundary of the seating tiers (the rim of the bowl) is high enough, since it determines whether the flat roof and the hanging equipment invade the overall space (O/A) of the pitch. A flat roof reduces the space volume (comparing with the convex roof), which can potentially improve the performance of acoustics and save energy consumption.

A single curved surface roof can be considered as a barrel vault. It can be generated by sliding a plane curve (section curve) along a straight line (rail curve) which is perpendicular to the plane curve. If the section curve is convex, then it is a convex single curved roof. Such a roof usually increases the floor-to-ceiling height of the pitch, which is suitable for small or medium arenas, but for a large scale arena, it increases additional indoor space.

A Positive Gaussian curvature (PGC) surface can be generated by sliding a convex plane curve (section curve) along another convex plane curve (rail curve). A PGC roof is suitable for some types of structures, but it also increases the indoor volume and the surface area. Besides, a PGC roof can potentially impact the acoustics, since it can converge the reflections of the sound wave and generate a focal point of sound over the pitch. Concave PGC roofs (in which both the section and rail curves are concave) are seldom used for indoor arenas, since it is difficult to drain the rain and snow away from these roofs.

A Negative-Gaussian curvature (NGC) surface can be generated in a similar way of a PGC surface, except that the section curve should be convex when the rail curve is concave or vice versa. The Negative-Gaussian curvature (NGC) surface is also called saddler shape or hyperboloid. In general, this shape can efficiently follow the multi-functional spaces of most of the large arenas. In London Aquatics centre, the saddle shape roofs guide spectators' sightlines to the pools and reduce the volume by decreasing the roof height at the ends. In London Velodrome, the saddle roof is set correspondingly to the saddle shape track and related tiers. Such a roof also helps to control the temperature over the track which should meet the regulations of the competition. Saddle shape roofs may obstruct spectators' sightlines, which happened for the temporary tiers of London Aquatics centre and should be carefully checked during design.

TABLE 2.2 Classification of structural geometry (Engle, 2007)

Geometry	Generation
<p data-bbox="189 213 297 236">Flat/folding</p> 	<p data-bbox="504 248 1053 271">Flat surface is a plane that defined by an enclosed plane boundary.</p> <p data-bbox="504 275 1218 322">Folding surface is composed of flat surfaces which are not in the same plane and share one side with each other.</p>
<p data-bbox="189 481 675 504">Single curved surface (Zero Gaussian curvature surface)</p> 	<p data-bbox="504 516 1203 587">A single curved surface can be generated by "Sliding a horizontal straight line (generatrix / section curve) along a curve (directrix / rail curve) that lies in a plane at right angle to the generatrix. "</p>
<p data-bbox="189 751 636 774">Dome surface (Positive Gaussian curvature surface)</p> 	<p data-bbox="504 786 1218 834">A dome surface can be generated by "Rotating a plane curve of geometric or free form, the generatrix (section curve), around a vertical axis"</p> <p data-bbox="504 837 1160 885">The dome surfaces (sphere surfaces) are special conditions of Positive Gaussian Curvature surface (PGC surface).</p> <p data-bbox="504 889 1218 936">In mathematics, a PGC surface is defined as the product of the maximum and minimum curvature of the surface should large than 0.</p>
<p data-bbox="189 1021 654 1044">Saddle surface (Negative Gaussian curvature surface)</p> 	<p data-bbox="504 1056 1218 1104">A saddle surface can be generated by "sliding a hanging parabola (generatrix / section curve) along upright parabola (directrix / rail curve), or reversely".</p> <p data-bbox="504 1107 1218 1155">The saddle surfaces (Hpseudospherical / hyperbolic surfaces) are special conditions of Negative Gaussian Curvature surface (NGC surface).</p> <p data-bbox="504 1158 1232 1206">In mathematics, an NGC surface is defined as the product of the maximum and minimum curvature of the surface should smaller than 0.</p>

2.2.3.2 Typologies of long-span roof structure

For the large column-free spaces in various large-scale public buildings, long-span structures are necessary to support the large roofs (Majowiecki, 2000). There are various types of structures which organize various structural elements in different ways and have different characteristics in mechanics. Majowiecki (2000) points out that long-span structures are widely used in sports buildings and classified the structures into five groups (table 2.3). Engel (2007) classifies building structures into seven groups, according to how the structure systems redirect/transfer the forces/loads. For each of these groups, the definition, span, characteristics, typical structure types and related examples are elaborated (table 2.4). Dong et al. (2012) proposed a new classification for spatial structures (table 2.5), according to the combinations of five basic structural elements: plate (slab), beam, bar, cable, and membrane, based on which 38 types of structures are included and classified into 17 groups.

TABLE 2.3 Classification of structural types (Majowiecki, 2000)

Group	type
Space structures	Single layer girds Double and multi layers grids Single and double curvature space frames
Cable structures	Cable stayed roofs Suspended roofs Cable trusses Single and multi-layer nets
Membrane structures	Pre-stressed anticlastic membranes Pneumatic membranes
Hybrid structures	Tensegrity systems Beam-cable systems
Convertible roofs	Overlapping sliding system Pivoted system Folding system

TABLE 2.4 Classification of structural types for long-span roofs according to the transfer of loads (Engel, 2007)

Group	Definition	Structure types	Span (m)
Form-active structure	Structure system of flexible, non-rigid matter, in which the redirection of forces is affected through particular from design and characteristic form stabilization. It also includes the rigid matter whose form is correspond to the redirection of forces and the section are subjected only normal stress (no bending or torsion stress).	Cable structure	50-500
		Tent structures	10-80
		Pneumatic structures	10-220
		Funicular Arch structures	8-90
Vector-active structure	Structure systems of solid straight-line elements (bars, rods), in which the redirection of forces is affected through vector partition. The structural elements are subjected to compression or tension	Flat trusses	20-80
		Transmit flat trusses (spatial truss beam or rigid frame)	20-100
		Curved trusses (grid shell)	50-190
		Space trusses (space frame)	25-100
Section-active structure	Structure systems of solid, rigid linear elements, in which the redirection of forces is affected through mobilization of sectional forces. The sections of the elements are subjected to bending stress.	Beam	7-25 (steel) 10-30 (reinforced concrete)
		Rigid frame	15-70 (steel) 4-25 (reinforced concrete)
		Beam grid	12-30 (steel) 8-20 (reinforced concrete)
		Slab	4-15
Surface-active	Structure systems of flexible, or compression-, tension-, shear-resistant surfaces, in which the redirection of forces is affected by surface resistance and particular surface design. The elements are subjected to membrane stresses (the stresses parallel to the surface)	Plate	10-50
		Folded plate	15-150
		Shell	40-150
Hybrid structure	Structural systems in which the redirection of forces is affected through the coaction of two or several mechanisms from different structure group	Superposition systems	-
		Coupling systems	-

TABLE 2.5 Classification of structural type according to the combinations of structural elements (Dong, 2012)

combination of structural elements	Structure types
01. Plate (slab)	Thin shell Folded plane Corrugated arch shell
02. Plate (slab) + Beam	Ribbed shell Ribbed folded plate Double-layer shell
03. Plate (slab) + Cable	Suspended shell
04. Beam	Single-layer lattice shell Open-web space truss Open-web lattice shell Tree-type structure Polyhedron space frame
05. Beam + Plate (slab)	Open-web sandwich plate Composition lattice shell
06. Beam + Bar + Cable	Beam string structure Suspend-dome Cable dome-lattice shell
07. Beam + Bar + Membrane	Tensegrity
08. Bar	Space truss (space frame) Spatial truss Double-layer lattice shell
09. Bar + Beam	Partial double layer lattice shell
10. Bar + Cable	Pre-stressed grid structure Truss string structure Cable-stayed grid structure Pre-stressed segmental structure
11. Bar + Plate (slab) + Beam	Composite space truss
12. Cable	Cable structure Cable nets
13. Cable + Bar	Tensegrity Cable-truss structure Cable truss Cable grids
14. Cable + Bar + Membrane	cable dome
15. Membrane	Air-inflated membrane structure Air-supported membrane structure
16. Membrane + Beam	Membrane structure with rigid supports
17. Membrane + Cable	Membrane structure with flexible supports

A series of materials can be used for long-span structures, including steel, timber, reinforced concrete, cable, membrane, etc. According to the classifications above and the study about the 129 typical arenas (see appendix), steel is widely used in long-span structures (125 in 129), for its high strength, convenient construction, and recycling use. Moreover, different types of steel structures can generate various geometries for long-span roofs, which makes steel structure flexible to adapt to diverse building forms. For steel structures, three types of structures are frequently used for arenas: space frame, truss beam, and single-layer grid shell (112 in 129, see appendix). The reasons may lay on: a) these types are structurally efficient, b) these types of structures can satisfy different design requirements efficiently in practice; c) for these structural types, the characteristics of mechanic are fully comprehended by engineers, and the related design methods as well as construction technologies are mature. This research focuses on these three types of structures (in steel).

A space frame structure can be considered as a latticed slab which can retain bending stress in different directions. In practice, it usually used to cover a wide space. Since its good performance in bending resistance, the space frame is adaptable for various shapes. Nowadays, it is frequently used to achieve various free-form buildings. London aquatic centre (a venue of the 2012 Olympic summer games) is a representative example, in which the space frame supported by three columns (maximum span 100m) generates a complex saddle-shape and variable-depth roof (figure 2.18, left). Another example is the Rio velodrome (venue for the 2016 Olympic summer games), in which the space frame also generates a saddle-shape long-span roof (figure 2.18, right).

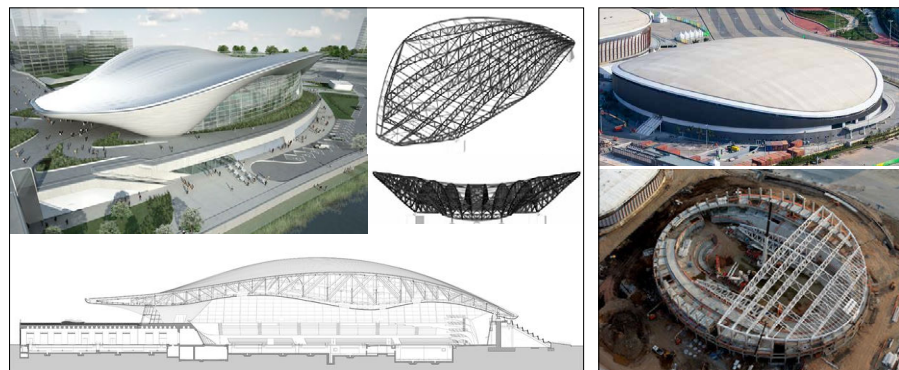


FIG. 2.18 Space frame structures of London aquatic centre (left: Detail, 2012) and Rio velodrome (right: theB1M, 2012 and Wikipedia, 2012)

A truss beam can be considered as a latticed beam and is composed of upper and bottom chords as well as webs. In practice, a series of truss beams are organized in parallel rows and connected by secondary structure bars to generate a spatial structural system. Such a structural system can resist bending moment along the span direction, therefore, it is widely used for the space in which the long axis is much longer than the short axis. In indoor arena design, truss beams are also used to achieve discrete roofs with step-shape (figure 2.19). For these roofs, sky windows for daylight and natural ventilation can be set between the steps. Two typical examples are the gymnasium of China Agricultural University in Beijing, China (a venue of 2008 Olympic summer games, figure 2.19, left) and the aquatics centre of Guangzhou, China (a venue of 2010 Asian games, figure 2.19, right).

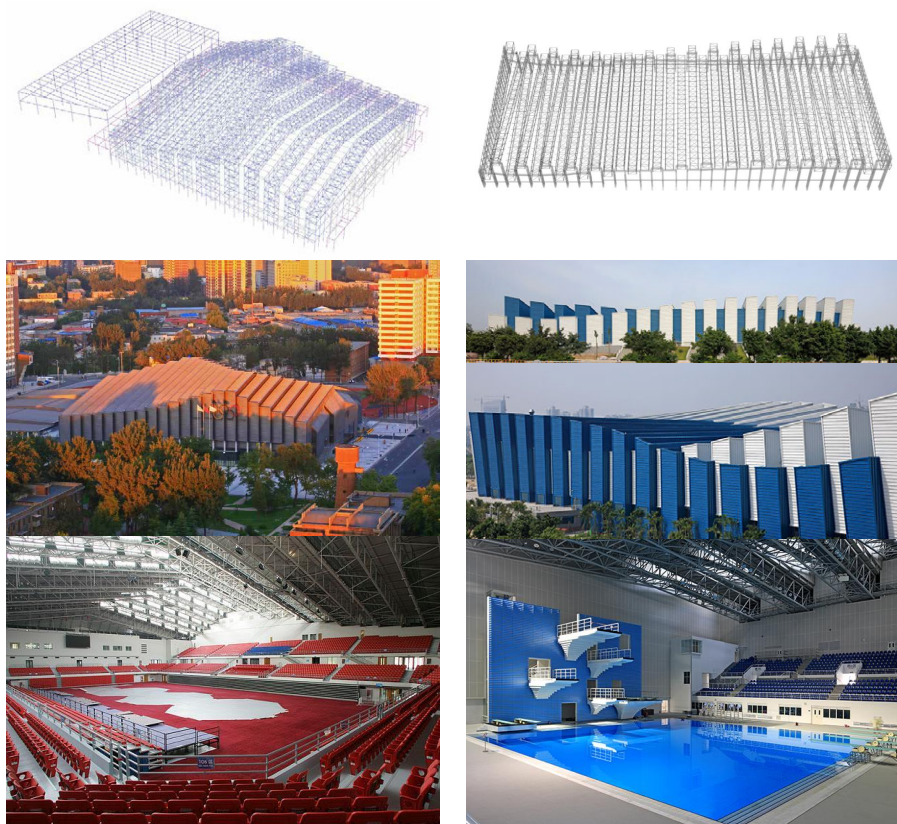


FIG. 2.19 Truss beam structures of the gymnasium of China Agricultural University (left: SCUTAD, 2008a) and the aquatic centre of Guangzhou (right: SCUTAD, 2010)

A grid shell can be considered as a latticed thin shell. Being similar to thin shells, grid shells are form-active structures which are sensitive to shape (the performance is largely impacted by the shape). It is suitable for the arena which needs a dome-shape or convex-shape symbol. Grid shell is also easy to encounter global buckling which should be avoided by special design. Nevertheless, a grid shell is an efficient structure which is usually composed of one-layer bars, so that has less material and less self-weight. A typical example is the Gymnasium of Beijing University of Technology in Beijing, China (a venue of the 2008 Olympic summer games, figure 2.20, left). In this building, to avoid global buckling for the long-span roof structure, a cable network is set under the one-layer grid shell to support it. Another example is Chang'an Sports Arena (Dongguan, China) which applies a dome-shape single-layer grid shell (figure 2.20, left).



FIG. 2.20 Grid shell structures of the Gymnasium of Beijing University of Technology (left: SCUTAD, 2008b) and Chang'an sports arena (right: SCUTAD, 2014)

In practices, for each of the structural type, there are various topologies for the arrangements of the elements/bars, which are also called tessellations. Generally, there are at least three frequently used types of tessellations: radiate, perpendicular crossing, and Voronoi (Engel, 2007). Radiate tessellations are mostly used in round roofs or regular polygons. Crossed tessellations are mostly used for roofs in free forms, rectangles. Voronoi tessellations, which are related to Delaunay triangle, is widely used in recent decades. Beijing aquatic centre (a venue of the 2008 Olympic summer games) is a famous example. Figure 2.21 illustrates the basic tessellation types. The tessellation of right-angle crossing grid is considered in this research, since it is frequently used in various structures.

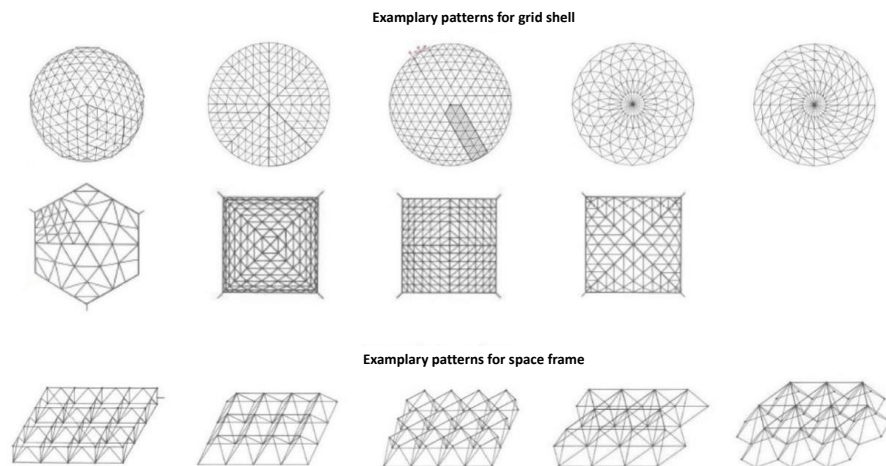


FIG. 2.21 Some basic structural tessellations (Engel, 2007)

2.2.3.3 Design parameters of long-span roof structure

According to the studies on the geometries and structures of long-span roofs, the related design parameters are formulated.

- Str_Bdr-CPi: the height of the i^{th} control point of the structural boundary. The boundary of the long-span roof structure is a curve set above the seating bowl boundary. The projection of the structure boundary overlaps the projection of the seating bowl. The specific shape of the structural boundary is defined by eight control points corresponding to the eight control points of the seating bowl boundary. The parameter 'Str_Bdr-CPi' is used to define the height of the i^{th} control point. The detail about the generation of the structural boundary are elaborated in chapter 4.
- Str_FCHeight: the floor to ceiling height of the roof structure at the central point of the pitch. This parameter defines the height between the floor (the centre point of the pitch) and the roof (the bottom of the structure). The floor to roof height impacts both the geometry of the roof and the shape of the indoor space. It should also ensure the ceiling and the hanging facilities under the roof do not invade into the overall space (O/A) of the pitch and do not obstruct the sightlines of spectators. (figure 2.22).
- Str_DepCen, Str_DepBdr: the structural depth of the roof structure at the central point or on the boundary. The space frame and truss beams considered in this research are composed of two-layer chords. The depth of a structure (the distance between the two-layer chords) can be varied. These two parameters define the depths in the central point of the roof and on the boundary, respectively (figure 2.22).
- Str_RidgeX, Str_RidgeY: the curve degree of the roof ridge along the x-axis or y-axis. Based on the previous parameters, the ridges curves along the x-axis and y-axis of the building (which are the section curve and rail curve mentioned above) can be generated. These parameters define the curve type (polyline or curve) of the ridges (figure 2.22).

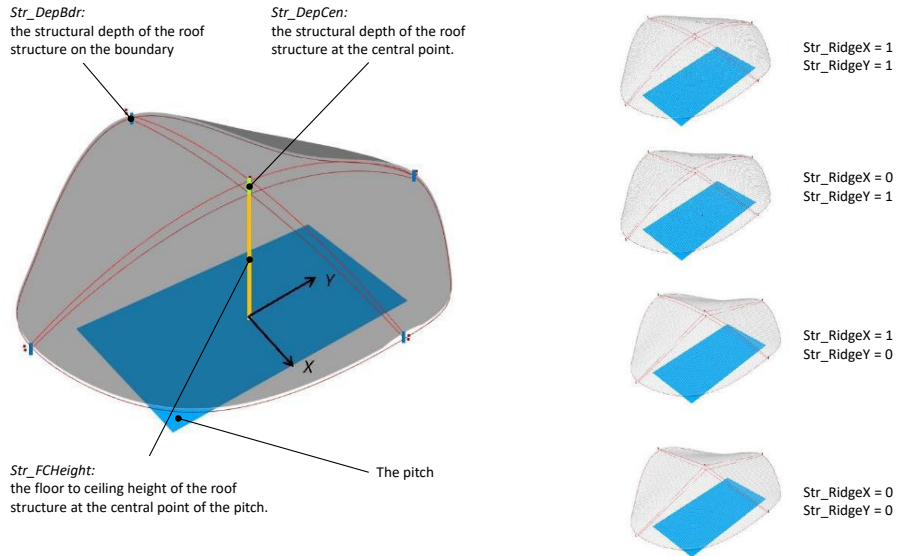


FIG. 2.22 Design parameters of the geometry of long-span roof

- **Str_Type**: the structural types of the long-span roof. This parameter defines a specific structural type (gird shell, or space frame, or truss beam) for a design.
- **Str_Grid**: the grid size of structural tessellation. As mentioned above, the structural tessellation of right-angle crossing grid is considered in this thesis. This parameter defines the size of the grid.
- **Str_Mtr**: structural material. As mentioned above, the structural material of steel is considered in this thesis. According to design codes, there are various types of steel, which are usually labelled according to their yield strength. Take the Eurocode EN 1993-1-1:2005 (CEN, 2005a) as an example, the steel of S275, S355, S420 can be used for long-span roof structures, the numbers are the values of the yield strength in MPa. This parameter defines the specific steel material for a design.
- **Str_CrSec**: structural cross-section. Various cross-sections can be used for the elements in steel structures (e.g. round tube, box, I-shape). This set of parameters define the shape, size, and thickness of the cross-section.

2.2.4 **Interrelationships between the multi-functional space and long-span roof structure**

According to the review and analyses above, in an arena, the configuration of the multi-functional space (pitch and seating tiers) and long-span roof structure are highly interrelated and the combination of them mainly defines the overall form of the building.

The outline of the pitch defines the inner boundary of the seating tiers. The shape of the seating tiers is related to the quality of the sightline which should be defined according to the focal point related to the pitch. The outer boundary or the seating tiers impacts the overall shape of the building and also defines the boundary of the structure. The geometry of the structure is defined based on the parameters related to the pitch and the seating tiers. These interrelationships are crucial for the formulation of an indoor arena.

2.3 **Design requirements and the related assessments of indoor arenas**

A design should satisfy a series of design requirements. During the design process, designs should be assessed to see whether they can satisfy these requirements. As mentioned, these design requirements can be divided into quantitative ones that can be measured and assessed based on numeric data and qualitative ones which are difficult to be assessed based on numeric data and require visual investigation of designers according to their experience and knowledge.

Specifically for the integration of the multi-functionality and long-span roof structure in the conceptual design of indoor arena, the quantitative design requirements are mainly related to the aspects of the multi-functionality and the structure, since these aspects directly related to the basic elements (pitch, seating tiers, and long-span roof) of an indoor arena and should be taken into account during conceptual design. For the qualitative design requirements, to support the related visual investigations, it is crucial to provide the overall forms/geometries of various designs to designers during conceptual design.

In the following sections, for the quantitative design requirements, the aspects related to the multi-functionality of indoor arenas (sec. 2.3.1) and long-span roof structures (sec. 2.3.2) are reviewed and studied, respectively, based on which the quantitative design requirements are concluded (sec. 2.3.3). After that, the qualitative design requirements are reviewed and studied (sec. 2.3.4).

2.3.1 **Design requirements and the related assessments of multi-functionality**

Multi-functionality is still considered as the key driver of the development of sports venues, according to the interview of C. Poterson and G. Sherlock (principals of Populous, a famous design company focusing on sports venues) (Pan Stadia & Arena Management, 2014). Poterson thought multi-functional venues are those can cater for everything while keeping the quality of fan experience. Such venues can be hubs of their areas which can increase the revenue of the owner and surrounding business. Besides, the multi-functionality of indoor arenas can increase the usage rate of venues, which makes the buildings more sustainable (Pan Stadia & Arena Management, 2014).

To further study the multi-functional indoor arena, a definition of multi-functionality of indoor arenas is formulated according to the discussion above:

The multi-functionality of indoor arenas is the capacity of the venues to satisfy the basic requirements of different activities, including but not limited to sports events, stage-performances and assemblies, exhibitions, and daily sports for the public.

These basic requirements for these activities are related to spatial capacity, game/performance watching (spectator view) and listening (acoustics). For different activities, these requirements and the related assessments can be varied, which need to be analysed specifically. In the following sections, the basic requirements of the different activities (sports event, stage performances and assemblies, exhibition, and daily sports for the public) are studied, to formulate the assessment criteria of the multi-functionality of indoor arenas.

1 Spatial capacity

The professional competitions include but are not limited to the matches of multiple sports (e.g. Olympic games, Asian games, National games), world championships or world cups for single sports (e.g. artistic gymnastics world championships), regional league match for single sports (e.g. NBA, NHL) and sports competitions in other levels.

The most basic requirement is about the spatial capacity of the match and the spectators, which are usually provided by the developers or owners of the arena. Two indicators are used to assess the satisfaction of the requirement.

- SE_TypeSp: the types of sports events accommodated in the arena. The values can be obtained by simply comparing the pitch size and the sizes of different courts (see table 2.1 and figure 2.3)
- SE_NumSpct-x: the number of spectators for a certain sport event 'x' accommodated in the arena. The value can be obtained by simply counting the fixed seats and the retractable seats.

2 Spectator view

For a spectator, the most important experience during a sports event is the game watching. In section 2.2.2, the viewing quality, which refers to the extent of the view of a spectator that is not be obstructed by the spectators in front, is used to calculate the risers of seating rows. Besides, the viewing distance and viewing angle mainly determine the game watching experience (figure 2.23).

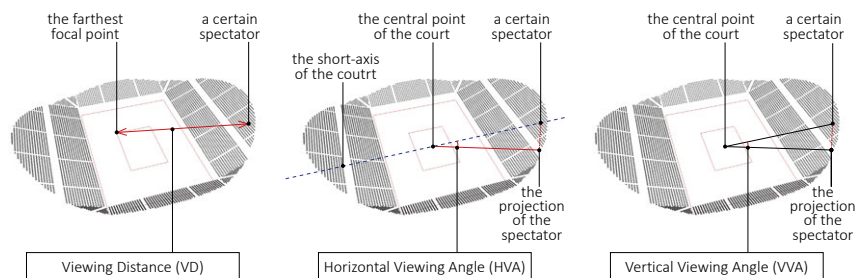


FIG. 2.23 Definitions of viewing distance, horizontal viewing angle, and vertical viewing angle for sports events

For viewing distance, three indicators can be used to assess the game watching experience.

- SE_avrVD-x: the average viewing distance of the seats for a certain sport event 'x'. The value can be obtained by the measurements in the model of the design.
- SE-maxVD-x: the maximum viewing distance of the seats for a certain sport event 'x'. The value can be obtained by the measurements in the model of the design, which should not larger than the maximum viewing distance regulated by design codes. For example, the Eurocode EN 13200-1:2012 (CEN, 2012) regulated the maximum viewing distances for various competitions (table 2.6).
- SE_PctPVD-x: the percentage of the seats with the premium viewing distance for a certain sports event 'x'. This indicator depends on the values of premium viewing distance for a certain sports event 'x'. A seat, whose viewing distance for a certain sport event 'x' is smaller than the premium viewing distance, is considered to be a premium seat for the game watching for this sport event. The premium viewing distance (PVD) for a certain sport event is calculated according to the size of the object to be watched and the visual angle (Stadia, 2010):

$$PVD = \frac{S}{2 \tan v_a} \quad [2.2]$$

where v_a the visual angle and S the size of the object to be watched. According to the theory about human vision, the minimum visual angle v for people to see something clear is about $4'$ (Stadia, 2010), and when the angle v_a equals $16'$ ($16/60$ degree), the view would be ideal. Based on this, the calculation can be simplified as:

$$PVD \approx 107.53S \quad [2.3]$$

Table 2.6 listed the PVDs for different sports calculated according to equation 2.3.

TABLE 2.6 Premium Viewing Distance (PVD) and accepted viewing Distance for different sports

Sports	Size of the object (m)		Viewing distance (m)	
			Premium (PVD) calculated based on equation 2.3 by using visual angle ($\alpha=16^\circ$)	The accepted viewing distance regulated by EN 13200-1:2012 (CEN,2012)
Basketball	ball	0.24	51.57	110
Volleyball	ball	0.21	36.10	110
Boxing	arm	0.40	68.76	110
Trampoline Jumping	arm	0.40	68.76	110
Artistic gymnasium	arm	0.40	68.76	110
Badminton	ball	0.12	20.628	85
Fencing	sword	0.40	68.76	85
Football (five a side)	ball	0.22	37.82	85
Ice sport artistic	arm	0.40	68.76	85
Judo	arm	0.40	68.76	85
Taekwondo	arm	0.40	68.76	85
Wrestling	arm	0.40	68.76	85
Rhythmic gymnastic	arm	0.40	68.76	85
Tennis	ball	0.06	11.1735	85
Handball	ball	0.20	34.38	80
Ice hockey	ball	0.08	13.75	80
Table tennis	ball	0.04	6.88	80

The viewing angle of a spectator, which is related to the position of the seat, is also important for the game-watching experience (Ding and Mei, 2018). The viewing angle can be divided into a horizontal and a vertical angle.

The horizontal viewing angle (HVA) is defined as the angle between the projection of the sightline of a spectator and the middle line of the pitch (figure 2.23). It is used to assess whether a seat is good for watching competitive ball matches (e.g. basketball, volleyball, handball, ice-hockey). For these matches, the seats along the sides of the court are considered to be better than other seats, since the spectators in these seats can clearly see the conversions of attacks and defences in the competitions. For some other ball matches (e.g. badminton, tennis, table tennis), views at the ends are better than those along the side. However, for these competitions (except tennis), the courts are usually laid along the short axis of the rectangle pitch, then the seats along the sides of the pitch are actually at the ends of the courts, which means these seats are still better in watching the matches. Hence, the seats along the side of the pitch are usually preferred by spectators. For the seats along the pitch sides, the ones being closer to the middle line of the pitch are better, since the

spectators on these seats do not need to turn their head a lot to see the furthest end of the pitch. To assess seating tiers based on the horizontal viewing angle, a threshold can be set by designers, and a related indicator can be used.

- SE_PctPHVA-x: the percentage of the seats whose horizontal viewing angles are smaller or equal the premium horizontal viewing angle for a certain sports event 'x' (figure 2.24). The value of this indicator can be obtained based on measurement in the model of the design.

The vertical viewing angle of a seat is defined as the angle between the sightline (the focal point is the central point of the court) and its projection (figure 2.23). A large VVA may lead to distortion of the objects in the view of the spectator and influence the game-watching experience (Ding and Mei, 2018). Hence the maximum vertical viewing angle in a seating bowl should be limited in accepted range (e.g. less than 40 degrees), based on which an indicator can be set.

- SE_maxVVD-x: the maximum vertical viewing angle of seats for a certain sport event 'x' (figure 2.24). The value of this indicator can be obtained based on measurement in the model of the design.

Furthermore, Hudson et al. (2015) proposed the 'A-value' as an indicator to assess spectators' views. The A-value is defined as the area of the pitch that is projected onto the spectator's view-plane. A large A-value for a spectator indicates that when watching the competition, the spectator does not need to swing his/her head frequently, since most part of the pitch can be seen without any adjustment of his/her view. However, in the real world, it is acceptable for spectators to swing their heads slowly to adjust their views. Besides, for most of the spectators, swinging the eyeballs without swinging the heads, can also adjust the view for the competitions with medium courts but fast-moving objects (e.g. tennis, badminton, table tennis). Furthermore, it is obvious that the A-value must be higher for the spectators in upper seating rows (with a larger viewing distance) comparing with those in lower rows (with a smaller viewing distance). The A-value is also higher for the spectators seating at the end of the pitch comparing with those seating along the side of the pitch. However, this is opposite to the aforementioned assessment criteria based on viewing distance and horizontal viewing angle. Hence, because of these contradictions, the A-value is not widely used in practice.

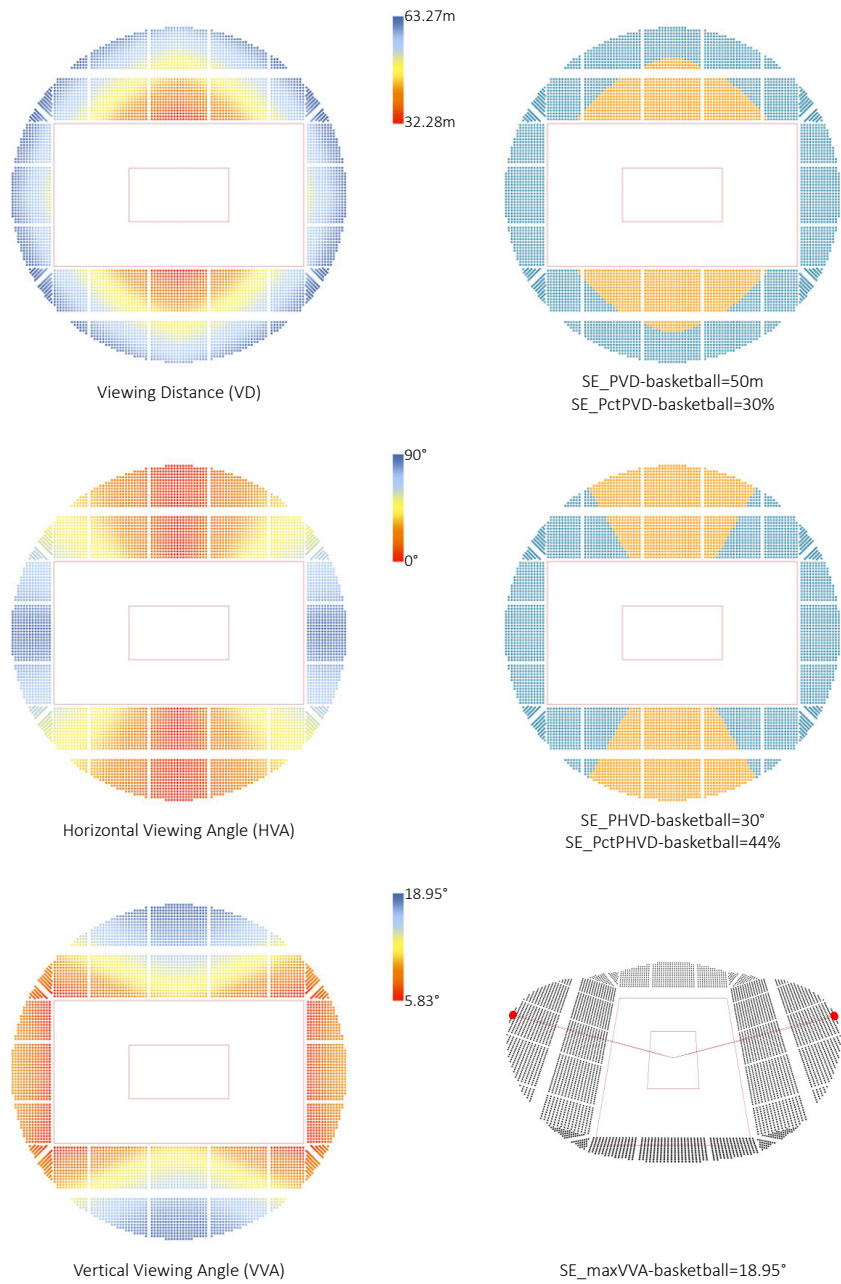


FIG. 2.24 Assessments of seating tiers for basketball according to the indicators related to viewing distance, horizontal viewing angle, and vertical viewing angle

1 Spectator view

Watching experience is also crucial for the spectators of stage-performance and assemblies. Correspondingly, the indicators related to viewing distance, horizontal viewing distance, and vertical viewing distance are also used to assess the spectator view for stage performances. It worth noting that these indicators are related to the size and the position of the stage (side-stage and end-stage). The sizes of the stages can be varied, and designers can define a typical stage for the assessments during conceptual designs.

For stage performance, the seats behind the stage are not available. Hence, the indicator about the percentage of the available seats is necessary for the assessment of the seating bowl.

- SP_{side_PctAS} / SP_{end_PctAS} : the percentage of the available seats for a stage performance with a side- or end-stage. The value can be obtained based on the measurement in the model of the design. Designers should define a reference line based on the front or back edge of the stage, to define the available seats (seats behind the reference line are not available).

For the measurement of the viewing distance for the seating bowl, the focal point can be the central point or the farthest point of the stage (figure 2.25). In this research, the central point is used as the focal point. Based on this focal point, three indicators can be used to evaluate the seating tiers, according to viewing distance.

- SP_{side_avrVD} / SP_{end_avrVD} : the average viewing distance of the available seats for a stage performance with a side- or end-stage. The value can be obtained based on the measurement in the model of the design.
- SP_{side_maxVD} / SP_{end_maxVD} : the maximum viewing distance of the available seats for a stage performance with a side- or end-stage. The value can be obtained based on the measurement in the model of the design.
- SP_{side_PctPVD} / SP_{end_PctPVD} : the percentage of the available seats with the premium viewing distance for a stage performance with a side- or end-stage. The PVD can be calculated based on equation 2.3 (the results are listed in table 2.7). The value can be obtained based on the measurement in the model of the design. An example is illustrated in figure 2.26 and figure 2.27.

The horizontal viewing angle for a stage performance, in this thesis, is defined as the angle between the sightline (a line from the spectator to the middle point of the back edge of the stage) and the axis of the stage (figure 2.25). Obviously, the seats in front of the stage, whose HVAs are close to 0 degrees, are better than other seats. Designers can define a threshold for the angle, called the premium horizontal viewing angle, based on which an indicator can be used to assess the seating bowl.

- SPside_PctPHVA / SPend_PctPHVA: the percentage of available seats whose horizontal viewing angles are smaller or equal to the premium horizontal viewing angle (defined by designers) for a stage performance with a side- or end-stage. The value can be obtained based on the measurement in the model of the design. An example is illustrated in figure 2.26 and figure 2.27.

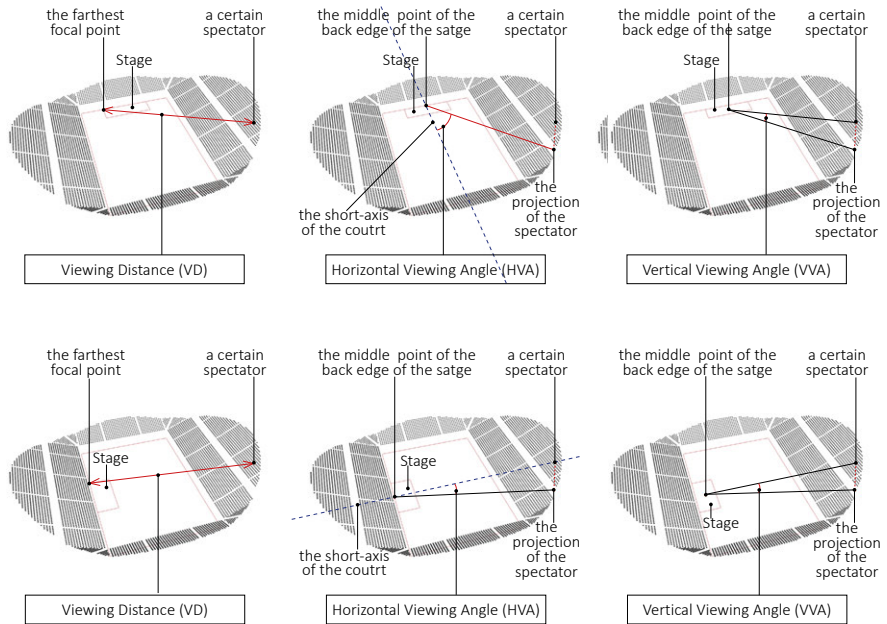


FIG. 2.25 Definitions of viewing distance, horizontal viewing angle, and vertical viewing angle for stage performance

TABLE 2.7 Premium Viewing Distance (PSV) for stage-performances

object	Size of the object S (m)	Premium Viewing Distance (PVD) calculated based on equation 2.3 by using visual angle ($\alpha=16^\circ$)
Human body	1.7	68.76
Head	0.2	36.10
Arm	0.4	51.57

Vertical viewing angle for stage performances is defined as the angle between the sightline (the line between the spectator and the central point of the stage) and its projection (figure 2.25). It should also be limited to avoid large distortion of the objects watched by spectators.

- $SP_{side-maxVVA}$ / $SP_{end-maxVVA}$: the maximum vertical viewing angle of the available seats for a stage performance with a side- or end-stage. The value can be obtained based on the measurement in the model of the design. An example is illustrated in figure 2.26 and figure 2.27.

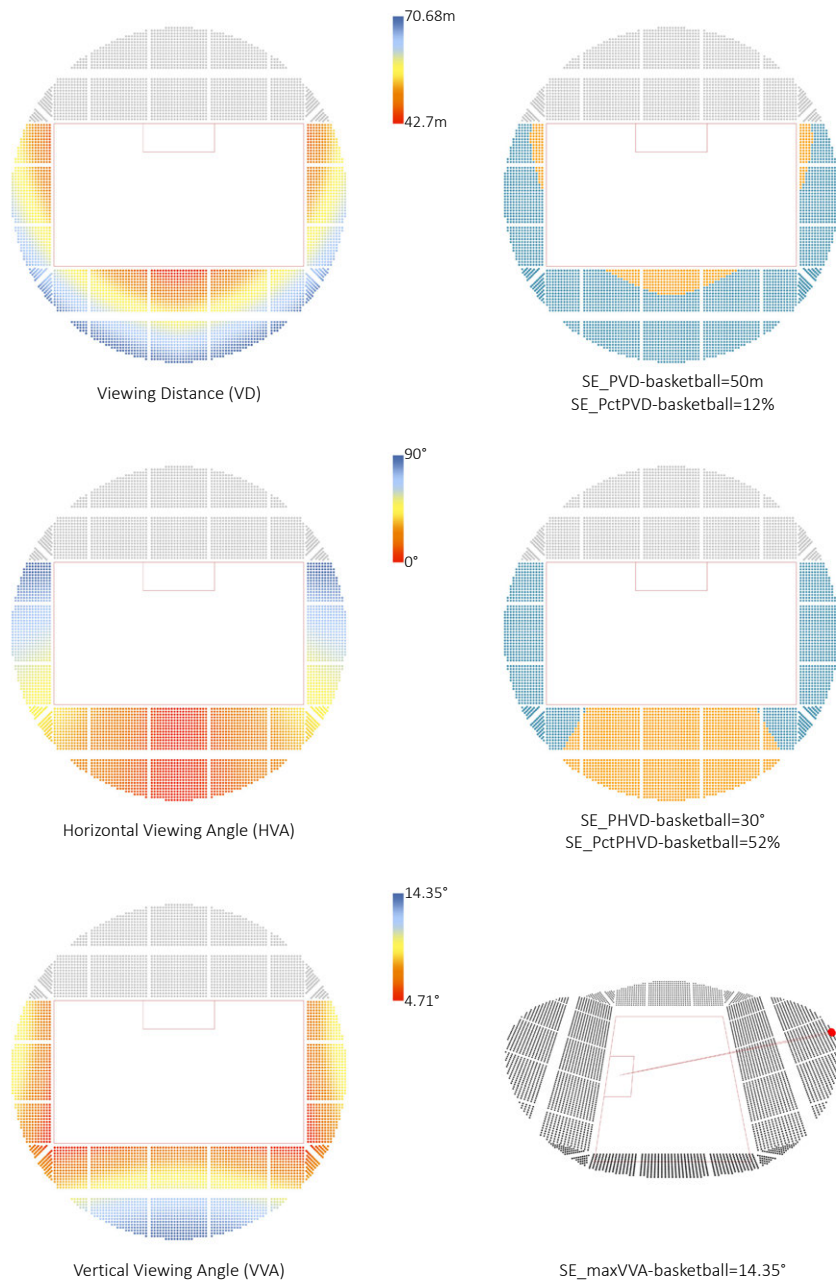


FIG. 2.26 Assessments of seating tiers for stage performance (side-stage) according to the indicators related to viewing distance, horizontal viewing angle, and vertical viewing angle

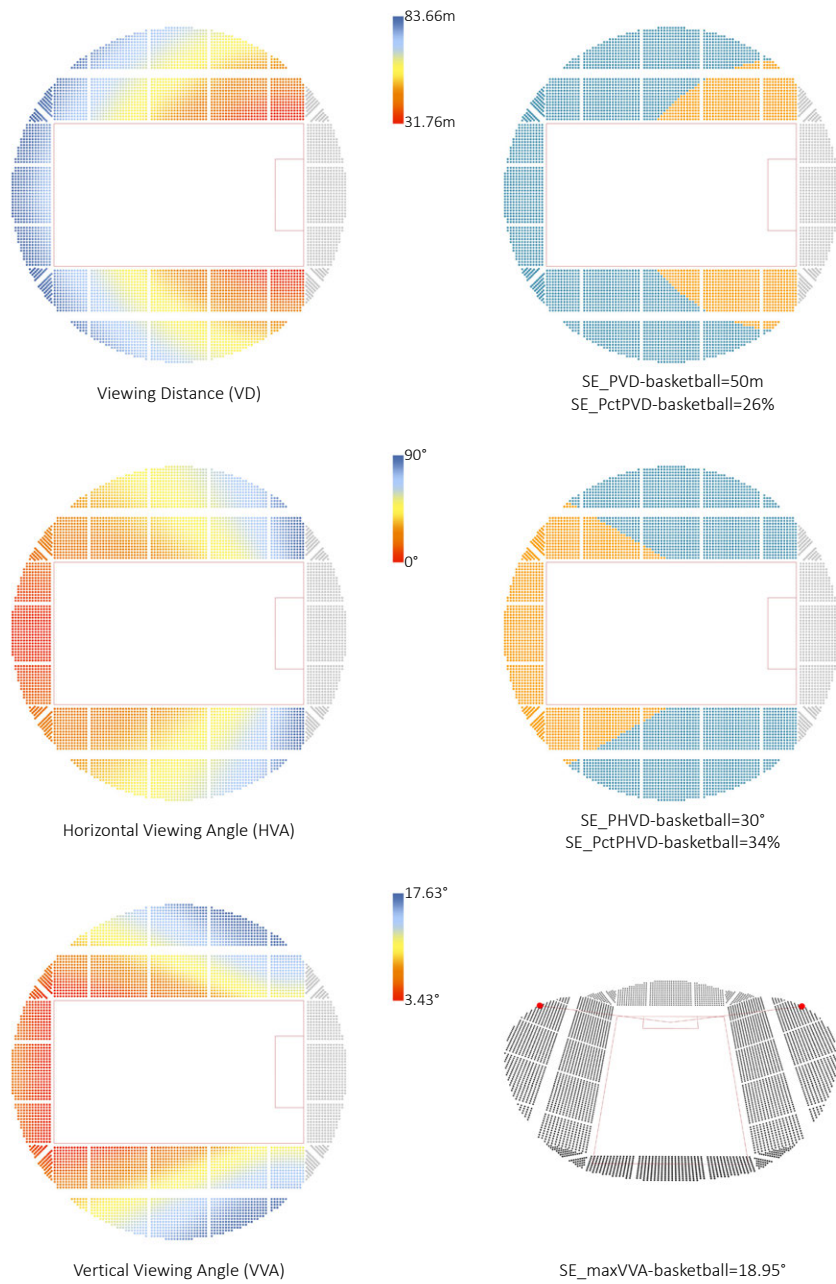


FIG. 2.27 Assessments of seating tiers for stage performance (end-stage) according to the indicators related to viewing distance, horizontal viewing angle, and vertical viewing angle

2 Acoustics

For stage performances, especially for concerts, the hearing experience of the spectators is also crucial and can be more important than the visual experience. The hearing experience is directly related to acoustics. In acoustics, the sound is considered as mechanical waves that are generated by sound sources and propagate in mediums, which can be described by sound pressure level, frequency, and wavelength (Soru, 2014).

The sound pressure level is used to describe the amplitude which can be simply considered as the volume of a sound and is determined by the magnitude of the pressure fluctuation (Salter, 1998), and the unit is decibel (dB). The frequency of a sound is defined as the number of wave cycles in per second, and the unit is Hertz (Hz). Human beings can hear the sounds whose frequencies are between 20 Hz to 20,000 Hz. Room acoustics focuses on the low-frequency sound around 125 Hz to 2000 Hz (Salter, 1998).

Room acoustics is a sub-field of acoustics, which focuses on the propagation of the sounds in closed space (Barron, 2010). Since the boundary of the closed space and the facilities as well as people inside the space, the sound does not only propagate directly but also reflect and scatter. For room acoustics, reverberation time is an important indicator.

In a room, when a sound is generated by a sound source, the sound waves propagate to different directions. Except some waves are received by listeners directly, other waves are reflected by objects (walls, ceiling, facilities, people, etc.). The reflected waves lose some energy since some of them are absorbed by the objects they touched, and the sound pressure levels decrease. Some waves can be reflected many times, and the reflected waves are received by listeners later than the directly received waves. Therefore, there is an interval between the time that sound waves emit from the source and the time that all the waves received by listeners. Specifically, the interval between the time that sound waves emitting from the source to the time that the reflected sound waves received by listeners decrease to 60 dB is defined as the reverberation time (RT60) (Salter, 1998). The reverberation time for the sound with the frequencies of 125 to 2,000 Hz is an important indicator for room acoustics, and different activities require different values of RT60. A long reverberation time leads to echoes which make speech unclear but may be preferred by some types of music. The preferences of different activities on reverberation time are illustrated in figure 2.28.

In this research, reverberation time is directly related to the indoor space defined by the integration of multi-functional space and long-span roof. To measure the RT60 for a defined indoor space, both the empirical methods based on Sabine and Eyring Equations and the acoustic simulation based on software can be used, which are elaborated in chapter 3.

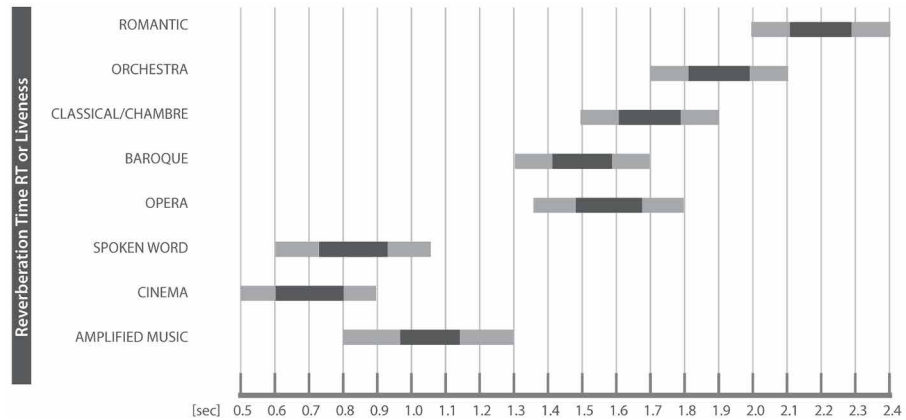


FIG. 2.28 Reverberation time for different activities (Soru, 2014)

For the conceptual design of multi-functional indoor arenas, the task about the acoustic aspect is to provide a proper space without acoustic defects for the following professional acoustic design. Some professional aspects for acoustics (e.g. setting amplifiers, stereo systems, and acoustical materials on the walls and ceilings, which are necessary for the stage-performances and assemblies in indoor arenas) should be designed by professional acoustic designers during the professional design stage. For the conceptual design of indoor arenas in this research, reverberation time is used to evaluate the overall acoustical performance of the indoor space. Besides, the treble ratio and the bass ratio, which are calculated based on reverberation time, are also used as the indicators for acoustic evaluations.

- $RT_{60_{all}}$: the reverberation time for the octave band frequencies of 125 to 2000Hz, which equals the average values of the RT_{60} for the different octave band frequencies.
- TR: the treble ratio indicating whether a sound in a concert hall is bright, clear, and rich in harmonics, which is usually limited between 0.75 and 0.95 and can be calculated based on reverberation times for different octave band frequencies (van Dorp Schuitman, 2010; Soru, 2014):

$$TR = \frac{RT_{60_2000} + RT_{60_4000}}{RT_{60_500} RT_{60_1000}} \quad [2.4]$$

where TR is the treble ration, RT_{60_500} , RT_{60_1000} , RT_{60_2000} , and RT_{60_4000} are the reverberation time in the octave band frequencies of 500Hz, 1000Hz, 2000Hz, and 4000Hz, respectively.

- BR: the bass ratio indicating the liveness or fullness of bass tones, which is usually limited between 0.9 to 1.5 and can be calculated based on reverberation time (Beranek, 1962; Soru, 2014):

$$BR = \frac{RT_{60_125} + RT_{60_250}}{RT_{60_500} RT_{60_1000}} \quad [2.5]$$

where BR is the bass ration, RT_{60_125} , RT_{60_250} , RT_{60_500} , and RT_{60_1000} are the reverberation time in the octave band frequencies of 125Hz, 250Hz, 500Hz, and 1000Hz, respectively.

2.3.1.3 Exhibitions and daily sports for the public

For exhibitions and daily sports, the requirement is to accommodate as many standard exhibition booths or sports courts as possible. The numbers of the booths and sports courts are used as the indicators.

- EX_NumEB: the number of standard booths accommodated in the pitch for an exhibition. The value can be obtained based on the measurement in the model of the design.
- DS_NumSC: the number of courts of a popular sport (defined based on local culture) accommodated in the pitch. The value can be obtained based on the measurement in the model of the design.

2.3.2 **Design requirements and the related assessments of long-span roof structure**

The requirements about structure during conceptual design can be divided into three parts: a) able to carry the expected design loads, b) being safe, and c) being efficient, economical, and sustainable. For each aspect, there are indicators to assess the satisfaction of the requirements.

2.3.2.1 **Load-carrying capacity**

One of the most important goals for structures is to transfer the load to the ground (foundation) (Engle, 2007). Taking the Eurocode EN-1990:2002 (CEN, 2002a) and En-1991-1-1:2002 (CEN, 2002b) as an example, according to real conditions and the regulations of design codes, design loads include permanent loads, live imposed loads, as well as wind and snow loads. The loads related to seism and exploration are usually considered in professional structural design.

1 Permanent loads

Permanent loads include the loads led by the structural self-weight and other permanent components supported by the structure. For a long-span roof structure, permanent loads include the structural self-weight (G1), the weight of cladding and ceiling (G2), and the weight of suspended facilities (G3). The structural self-weight can be simply calculated according to the geometry, section, and material of the structure. The cladding and ceiling weight can be considered as linear even loads along with the upper and bottom elements of the grid structure. Suspending facilities are usually hanged on some nodes of a grid structure, and the related load can be directly added on these nodes in the loading model.

2 Variable loads (imposed loads, wind loads, and snow loads)

Imposed loads include the loads led by the weights of people and movable facilities. For most of the indoor arenas, the fixed roofs are not designed to support people (except for maintenance) or movable facilities. Hence, imposed loads are not considered in this research.

Wind loads (Q_1) can be considered as a pressure (passive or negative) on the roof, which is related to the shape, size, location, and the dynamic properties of the structure, according to Eurocode 'EN-1991-1-4: 2005' (CEN, 2005a). To obtain the wind load, the basic velocity pressure is firstly calculated, based on which the wind load can be calculated according to the shape and dimensions of the roof (CEN, 2005a). To obtain the wind load, both the calculations based on the equations in design codes and performance simulation based on computer software can be used, which are elaborated in chapter 3.

Snow loads can be considered as temporary even loads on the roof. The distribution of the load is related to the roof geometry, and the value of the load is related to the climates. According to the Eurocode EN 1991-1-3:2003 (CEN, 2003), the snow loads should be calculated based on the roof shape, climate, thermal properties of the roof, etc. First, the snow load on the ground is calculated according to the zone (location) and altitude, based on which, the snow load on the roof can be calculated according to the dimensions of the roof. To obtain the snow load, both the calculations based on the equations in design codes and performance simulation based on computer software can be used, which are elaborated in chapter 3.

3 Load combinations (actions)

In the real world, a structure will encounter different situations in which the structure should bear different combinations of loads. Such a loads combination is composed of simultaneously acting individual loads, as introduced above. During the design process, the strength of the structure is evaluated under the actions of all the load combinations regulated by design codes.

According to Eurocode En-1991-1-1:2002 (CEN, 2002b), for a roof structure, the imposed loads, snow load, and wind load should not be applied simultaneously. As mentioned, the roofs of arenas are usually not accessible roofs (i.e. not for the general public, only for maintenance), so the imposed loads are not considered. According to the regulations of A1.3 and A1.4 in En-1991-1-4:2005, this research considers three load combinations for ultimate limit states (ULS) and serviceability limit states (SLS). In these combinations, each load should multiply with a factor regulated by design codes (table 2.8).

Combination/Action 1: Permanent loads (self-weight G_1 + cladding and ceiling G_2 + hung facilities G_3)

$$E_{d1} = \gamma_G (G_1 + G_2 + G_3) \quad [2.6]$$

Combination/Action 2: Permanent loads (self-weight G_1 + cladding and ceiling G_2 + hung facilities G_3) + wind load Q_1

$$E_{d2} = \gamma_G (G_1 + G_2 + G_3) + \gamma_Q Q_1 \quad [2.7]$$

Combination/Action 3: Permanent loads (self-weight G_1 + cladding and ceiling G_2 + hung facilities G_3) + snow load Q_2

$$E_{d3} = \gamma_G (G_1 + G_2 + G_3) + \gamma_Q Q_2 \quad [2.8]$$

TABLE 2.8 Factors of different loads for different states according to En-1990:2002 (CEN,2002a)

Limit state		Permanent loads	Variables loads
Ultimate limit state (ULS)	Unfavourable	$\gamma_G = 1.35$	$\gamma_Q = 1.50$
	favourable	$\gamma_G = 1$	$\gamma_Q = 0$

2.3.2.2 Safety

1 Deflection of the whole structure

The deflection of a structure (labelled as 'dlf' in this thesis) or a structural element is the deformation which is perpendicular to a reference axis or a reference plan. There are vertical deflection and horizontal deflection. For a long span roof, the vertical deflection in the mid-span is a key indicator to evaluate the overall structural deformation, which should be limited in a range to ensure the safety of the structure.

According to Eurocode EN-1990:2002 (CEN, 2002a) and EN-1993-1-1:2005 (CEN, 2005b), under the unfavourable condition of serviceability limit state (SLS), the deflection should be less than a certain value related to the main span, which is specifically regulated by the national annex of different countries. For the Netherlands, the value is 1/250 of the main span.

2 Stress in element

The loads acting on a structure are transformed into internal forces resisted by elements. For each element, the cross-sections resist and transfer the internal forces. For a specific cross-section, it resists normal force (tension or compression) which is perpendicular to the section, shear force, which is parallel with the section, bending moment which is in plane that is perpendicular to the section, and torsion moment which is parallel to the section.

Stress is the force that acts on a unit area. All the forces and moments mentioned above can be represented by a series of stresses. The normal force and bending moment can be represented by normal stresses, and the shear force, and torsion moment can also be represented by shear stresses. The stresses usually distribute unevenly on the cross-section. The maximum stresses (labelled as ‘ σ_{max} ’ for the normal stress and ‘ τ_{max} ’ for shear stress in this thesis) should be smaller than an acceptable value related to the material. Takes the Eurocode EN-1990:2002 (CEN, 2002a) and EN-1993-1-1:2005 (CEN, 2005b) as an example, the design strength for normal and shear stresses can be calculated by:

$$\sigma_{x,Ed} = \frac{f_y}{\gamma_M} \quad [2.9]$$

$$\tau_{x,Ed} = \frac{f_v}{\gamma_M} \quad [2.10]$$

Where $\sigma_{x,Ed}$ is the design strength of normal stress; $\tau_{x,Ed}$ is the design strength of shear stress; f_y and f_v are the yield strengths of the material for normal and shear stress, respectively; γ_M is the partial factors (material factor) regulated by design codes.

1 Self-weight

Structural Self-Weight (labelled as 'SW' in this thesis) is an important indicator of structure. For most of the building structures, the self-weight is the main load, and reducing the self-weight means reducing the load for the structure. Moreover, for a building, using less structural material means the structure is more efficient and more economical. Specifically, for a long-span roof, the self-weight per unit area is used as an indicator to assess the structural performance (von Buelow et al. 2016, Cui et al., 2014, Mueller and Ochsendorf, 2015, Yang et al. 2018, Pan et al. 2019, Pan et al. 2020).

2 Embodied energy

The sustainability of buildings is emphasized by both designers and researchers. For long-spans structures, reducing embodied energy is one of the main approaches to achieve sustainability. The Embodied Energy (labelled as 'EE' in this thesis) of a structure here refers to the energy consumed during the processes of producing, transportation, and construction of the structure, which is directly related to the mass and material of the structure. Hammond and Jones (2008) proposed a series of material-related coefficients for the calculations of embodied energy, based on which the embodied energy of a structure can be obtained by multiplying the structural mass by the related coefficient. Brown et al. (2015) applied this method to calculate the embodied energy, therefore to assess long-span structures.

3 Strain energy

Strain Energy (labelled as 'SE' in this thesis) is potential energy caused by the deformation led by loads, which equals the product of the loads and displacements. Strain energy indicates the overall stiffness of a structure under given loads. Less strain energy indicates the structure is more rigid. Cui et al. (2014) and Pan et al. (2019, 2020) used strain energy to assess long-span structures.

2.3.3 Qualitative design requirements and the related assessments

Qualitative design requirements in this paper are related to humanity and social science, which are difficult to be assessed based on numeric data, and still need to be assessed based on visual investigations of human designers according to their experience and knowledge. The qualitative design requirements are related to various aspects (including aesthetics, psychological feeling related to architectural space, cultural and historical attribute, the relationships with the urban context, etc.) which are crucial for architecture. Cenek (2013) argued that sustainability architecture focusing on ecological and economic aspects of buildings is emphasized by both researchers and designers, but, as a holistic approach, it should also include social and cultural aspects, and most importantly, it should fulfil the aesthetic expectations of the society.

2.3.3.1 Qualitative design requirements and the overall form/geometry of buildings

In general, the qualitative aspects are related to various elements of a building (e.g. the overall form/geometry, material, pattern or tessellation of envelope, tectonic). Among these elements, the overall form/geometry of a building, which is one of the main focuses during conceptual design, usually impacts the qualitative aspects a lot. In architectural theory, the form is usually related to specific meaning, content, or is interpreted as a symbol and social significance (Erzen, 2015). Heys (1984) emphasized that architecture is essentially related to socioeconomic, political, and technological processes. He considered architecture as an instrument of culture, for which architectural form and culture should correspond to each other, the form should efficiently represent the values of the culture.

Specifically, for an indoor arena or a semi-outdoor stadium, which is a large-scale public building and usually serves as landmarks for cities, the qualitative aspects are more crucial. It is important for designers to define the overall form/geometry satisfying the requirements related to these aspects, during conceptual design. Several typical examples can be found in the designs of various real arenas all over the world. Philippine arena, designed by Populous (a world-famous British design company focusing on sports buildings), is the largest indoor arena in the world (figure 2.29, left). The overall form of the arena is inspired by a Narra tree (red sandalwood) which is the mother tree of Philippine and the root of a banyan tree (Haeahn Architecture, 2013), while the roof is designed like a Nipa nut (Arcangel, 2014). All the trees and nuts are related to the local culture. The aquatic

centre of Guangzhou in China (designed by Atelier Sun of the Architectural Design and Research Institute of South China University of Technology) is the swimming and diving venue of the 2010 Asian games (figure 2.29, middle). The overall form of the arena is designed like a double helix structure of DNA, which provides a metaphor that lives come from the water (Sun et al. 2010). The new national stadium designed by Kengo Kuma (a world-famous Japanese architect) is the main stadium of the 2020 Tokyo Olympic summer games (figure 2.29, right). The overall form is composed of several horizontal elements, which mimics a famous traditional Japanese building, the Gojunoto pagoda at Horyuji Temple (Bickersteth, 2020).

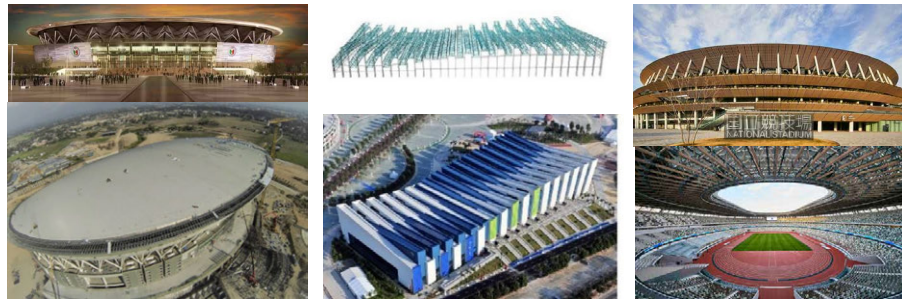


FIG. 2.29 Examples of sports buildings for which the overall form satisfying the requirements related to qualitative aspects (left: Philippine arena, picture sources: Populous, 2011; middle: Guangzhou aquatic centre, pictures sources: SCUTAD, 2010; right: Tokyo national stadium, picture sources: Tokyo 2020, 2019)

2.3.3.2 Assessments of qualitative aspects based on visual investigations in interactive designs

To assess designs about the satisfactions of the qualitative design requirements, various methods have been proposed based on mathematical analyses of building geometry or space. However, in general, these methods are not efficient, since the relationships between the qualitative aspects and building geometry are quite complex and implicit. Moreover, different designers can have different judgments about the qualitative aspects of buildings, which cannot be effectively indicated according to some basic rules or criteria. In other words, so far, there are no clear numeric criteria which can efficiently assess the qualitative aspects of designs.

Hence, during the conceptual design in practice, it is necessary for designers to visually investigate various design alternatives with diverse forms, according to their own knowledge and experience, to assess the satisfaction of the qualitative design requirements. A representative example can be found in the observation of Harding (2014) about the conceptual design phase of the Escher Tower project by Bjarke Ingels Group (BIG, a world-famous architectural design company in Denmark), in which architects worked out and visually studied various physical models of different design concepts until they defined a concept for the following design process.

With the development of computational design, computers aided design (CAD) is frequently applied in design processes. Some of these CAD processes are automatic, and to some extent, tend to delegate human designers' work. However, as mentioned above, for the qualitative design requirements of architecture, the experience of human designers (including physical, sensual, cognitive, emotional, cultural background, etc.) is still indispensable (Fallman, 2008). Specific for sports buildings (including stadia and indoor arenas), the integration and honest expression of their architecture and engineering are at a uniquely high level. Moreover, since the venues are usually the icons to inspire people and attract investment and are also the social catalyst which connects to the urban context, the designs of the roof structures for the venues are more challenging (Leach et al., 2019).

To combine these factors with the algorithm, interactive design methods are proposed (Alben 1996, Fallman, 2003 & 2008, Mueller et al. 2015, von Buelow et al. 2016, Harding et al. 2018). In an interactive design, the factors of human designers are used as inputs for the computational design process, and human designers are allowed to control and intervene the process. Therefore, the experience of designers can be used to generate and assess design alternatives with emphasized on qualitative aspects. To achieve an efficient interactive design, which deals with the qualitative aspects of buildings (e.g. aesthetics), a holistic exploration of numerous design alternatives is crucial (Fallman, 2008), especially for the aforementioned challenging designs of sports venues.

2.4 Basic demands of the conceptual design of indoor arenas

In the previous sections of this chapter, the composition and the related design parameters of indoor arenas are studied, based on which the integration of the multi-functional space and long-span roof structure are analysed, and the diversity of the overall form is studied. Moreover, both the quantitative and qualitative design requirements and the related assessments of indoor arenas are reviewed and studied. These studies formulate the foundation of the conceptual design of indoor arenas.

Conceptual design, as mentioned, is the early stage of the whole design process, which aims to generate promising concepts which satisfy a series of design requirements and can be developed in the following design processes (Turrin, 2014). Such a process is composed of a divergent step in which concepts are generated and a convergent step in which concepts are assessed and selected (Okudan and Tauhid, 2008).

During conceptual design, both the divergent and convergent steps are dynamic and complex. The generated design concepts need to be modified iteratively, according to the assessments, and the criteria of the assessments can be varied as designers gradually understand the design problem (Wortmann et al., 2015). In this light, the process of conceptual design can be seen as a kind of exploration. Design exploration is generally a process that studies different design alternatives according to given assessment criteria, in order to find ideal solutions. It is continuously solving 'what if' problem (Schon, 1992) by exploring possible solutions outside the current paradigms which can be related to technology, economics, function, and style (Ehn, 1988). In this light, three basic demands of the conceptual design of indoor arenas can be formulated.

2.4.1 Generating numerous and diverse design alternatives for conceptual design exploration

The conceptual design exploration first needs a large number of solutions/design-alternatives, which is the divergent step defined by Okudan and Tauhid (2008). Moreover, for these design alternatives, the diversity is important (Wang, 2002; Liu et al., 2003; Okudan and Tauhid, 2008; Chong, et al., 2009; Turrin, 2014).

The reason is obvious, similar solutions are usually similar in the satisfaction of the requirements of various aspects, therefore, in order to search for promising solutions, a large range of different design alternatives is necessary. It also corresponds to the aforementioned observation of Harding (2014) in which designers proposed a number of diverse geometries at the early stage of the conceptual design of a high-rise building. A similar observation can also be found in practice.

However, in the traditional design process of architecture, since the limitations of time and technologies, designers have to focus on a small number of design alternatives which narrows the searching range and limited the emergence of promising solutions (Josephson et al., 1998; Liu et al., 2003; Turrin, 2014). These limitations can be overcome by using a parametric model (the details are elaborated in chapter 3). Nevertheless, the diversity of design alternatives, which is crucial for design exploration, does not get enough emphasis in both research and practice. The details of this problem are discussed in chapter 3.

Based on the studies about the composition and the related design parameters of indoor arenas (with emphasis on the integration of multi-functional space and long-span structure), by using a parametric model, it is possible to generate numerous and diverse design alternatives of indoor arenas.

2.4.2 **Obtaining adequate information of design alternatives for the assessments of various design requirements**

To define promising design(s) in the convergent step, the numerous generated design alternatives need to be assessed according to various design requirements, including quantitative and qualitative ones which are mentioned above. To support the assessments, it is necessary to obtain the information of the generated designs.

The quantitative design requirements and the related assessments in this thesis are related to multi-functionality and structural performance of indoor arenas, which have been studied in section 2.3.1 and section 2.3.2. To assess a design's satisfaction of these requirements, the values of a series of related indicators are necessary. The qualitative design requirements should be assessed by visual investigations of designers (according to the analysis in section 2.3.3), which requires the information about the overall geometries of the designs.

Moreover, since the large amount of the generated design alternatives, it is impractical for designers to explore all the alternatives one by one. Therefore, it is necessary to strategically explore specific designs rather than all of them or to organize all the designs with the related information in an efficient way.

2.4.3 **Adapting to different scenarios laying different emphases on quantitative and qualitative design requirements**

Although the satisfaction of both the quantitative and qualitative design requirements are indispensable for a design, in practice, it is possible for designers to lay different emphases or priorities on these two aspects. Hence, there can be three basic scenarios: 1) Emphasizing the quantitative design requirements and prioritizing the numeric assessments over the visual investigations during the exploration of design alternatives. 2) Emphasizing the qualitative design requirements and prioritizing the visual investigations over the numeric assessments during the exploration of design alternatives. 3) Laying the same emphases on both the quantitative and qualitative design requirements and focusing on both numeric assessments and visual investigations during the exploration of design alternatives. During conceptual design, all these scenarios should be taken into account, to aid designers to explore various design alternatives and to define promising design(s), according to their preferences.

2.5 **Summary**

In this chapter, several aspects of indoor arenas are reviewed and studied. First, in section 2.2, the basic function and composition of indoor arenas are studied. Specifically, the attributes, design parameters, generations, and the interrelationships of pitch, seating tiers, and long-span roof structure are reviewed and studied. Special emphasis is placed on the integration of the multi-functional space (pitch and seating tiers) and long-span roof structure. Based on these studies, a generation process of the indoor arena based on the integration of multi-functional space and long-span roof structure is formulated, and the related design parameters are also defined.

Moreover, in section 2.3, various design requirements related to indoor arenas are reviewed and studied. The design requirements are divided into quantitative ones and qualitative ones. The quantitative design requirements are related to multi-functionality and structural performance. Specifically, the multi-functionality refers to the spatial capacities, view of spectators, and acoustics for multiple activities. The design requirements, assessments, and related indicators of all these aspects are reviewed and studied. For the qualitative design requirements, according to the review of literature, the assessments during conceptual design should be based on the visual investigations about the overall geometries of designs by human designers according to their knowledge and experience.

In section 2.4, based on the reviews and studies above and according to the aim and the divergent-convergent process of conceptual design, three basic demands of the conceptual design of indoor arena (with emphasis on the integration of multi-functional space and long-span roof structure) are formulated.

- 1 Generating numerous and diverse design alternatives of indoor arena based on the integration of multi-functionality and long-span roof structure. The studies in section 2.2 provide a basic generation process and related design parameters.
- 2 Obtaining adequate information of design alternatives for the assessments of various design requirements. The information includes the values of indicators related to the numeric assessments of qualitative design requirements (about multi-functionality and structural performance) and the overall geometries for visual investigations of designers to assess the qualitative design requirements. The studies in section 2.3 provide the foundation of both the numeric assessments and visual investigations.
- 3 Adapting to different scenarios laying different emphases on quantitative and qualitative design requirements. Three scenarios, in which designers can lay different emphases on the quantitative and qualitative design requirements, are taken into account, therefore, to allow designers to define promising design(s) according to their preferences.

In the next chapter, several computational design methods are reviewed to investigate their potentials and limitations in satisfying these basic demands of conceptual designs.

References

- Alben, L. (1996) Quality of experience: defining the criteria for effective interaction design, *Interactions* 3(3) pp.11-15. DOI: 10.1145/235008.235010
- Arcangel, X (2014). "INC's Philippine Arena a 'challenge' for firm behind London's O2". GMA News. Retrieved July 23, 2014. <https://www.gmanetwork.com/news/money/companies/371285/inc-s-philippine-arena-a-challenge-for-firm-behind-london-s-o2/story/>
- Atelier Sun (2006a): the pictures are from the proposal document provided by Atelier Sun of the Architectural Design and Research Institute of South China University of Technology.
- Atelier Sun (2006b): the pictures are from the proposal document provided by Atelier Sun of the Architectural Design and Research Institute of South China University of Technology.
- Atelier Sun (2008): the pictures are from the proposal document provided by Atelier Sun of the Architectural Design and Research Institute of South China University of Technology.
- Atelier Sun (2009): the pictures are from the proposal document provided by Atelier Sun of the Architectural Design and Research Institute of South China University of Technology.
- Barron, M. (2010). *Auditorium Acoustics and Architectural Design*, 2nd ed., Spon Press, London and New York.
- Bickersteth, R., (2020) Tokyo 2020 Olympics venues: the retrofit games. *Architects' Journal*. <https://www.architectsjournal.co.uk/news/culture/tokyo-2020-olympics-venues-the-retrofit-games/10044238.article>
- Brown, N.C., Mueller, C.T. (2016). Design for structural and energy performance of long span buildings using geometric multi-objective optimization, *Energy and Building*, 127, pp. 748–761, DOI: 10.1016/j.enbuild.2016.05.090.
- CEN (2015a). EN-1993-1-1:2005. Design of steel structures - Part 1-1: General rules and rules for buildings.
- CEN, (1995) En-1991-2-4:1995. Actions on structures - Part 1-4: General actions -Wind actions
- CEN, (2002) EN-1990:2002. Basis of structural design. F
- CEN, (2003) EN 1991-1-3:2003. Actions on structures - Part 1-3: General actions -Snow Loads.
- CEN, (2005b) EN-1991-1-4:2005. Actions on structures - Part 1-1: General actions – Densities, self-weight, imposed loads for buildings.
- CEN, (2012). EN 13200: Spectator Facilities-Part 1: General characteristics for spectator viewing area.
- Cenek, M., (2013) ARCHITECTURE: CONCEPT, FORM AND AESTHETICS FROM THE PERSPECTIVE OF SUSTAINABILITY, In: *Proceeding of Central Europe towards Sustainable Building 2013 (CESB 2013)*. Prague http://www.cesb.cz/cesb13/proceedings/4_design/CESB13_1390.pdf
- Chong, Y.T., Chen, C.H., Leong, K.F., (2009) A heuristic-based approach to conceptual design. In: *Research in Engineering Design*, 20(2), pp.97-116.
- Cui, C.Y., Jiang, B.S.(2014). A morphogenesis method for shape optimization of framed structures subject to spatial constraints, *Engineering Structure*. 77, pp. 109–118, DOI: 10.1016/j.engstruct.2014.07.032.
- Culley, P., Pascoe, J. (2009) *Sports Facilities and Technologies*. Routledge, Abingdon, Oxon. ISBN 978-0-415-45868-9
- Detail (2012). London 2012 – Aquatics Centre. <http://www.detail-online.com/article/london-2012-aquatics-centre-16400>. [Accessed: 1-June-2020].
- Ding, J., Mei, H. (eds) (2017) *Manual of Architectural design (book six)*, China Architectural and Building Press, Beijing, China. ISBN 978-7-112-20944-6
- Dong, S., Zhao, Y., Xing, D. (2012). Application and development of modern long-span space structures in China, *Frontier Structure and Civil Engineering*. 6, pp.224–239, DOI: 10.1007/s11709-012-0166-6.
- Ehn, P.(1988) *Work-oriented Design of Computer Artifacts*. Arbetslivscentrum, Stockholm. ISBN: 91-86158-45-7
- Engel, H. (2007). *Structure systems.pdf*, Hatje Cantz Verlag, Berlin.
- Erzen, J.N. (2015) From and meaning in architectural theory. İzmir University original scientific article. <https://www.scribd.com/document/379079071/SAJ-2015-01-J-Erzen>. [Accessed: 14-March-2020]
- Fallman, D. (2003) Design-oriented human-computer interaction. In: *Proceedings of the SIGCHI conference on Human factors in computing systems (CHI '03)*, Association for Computing Machinery, New York, NY, USA. 5(1), pp.225-232. DOI: 10.1145/642611.642652

- Fallman, D. (2008) The interaction design research triangle of design practice, design studies, and design exploration, *Design Issues*, 24(3), pp. 4-18. <https://www.mitpressjournals.org/doi/pdf/10.1162/desi.2008.24.3.4>
- Haeahn Architecture (2013) "Philippine Arena" Archived from the original on August 19, 2013. Retrieved August 19, 2013. https://archive.is/20130819071954/http://haeahn.com/front/project/04_byyear_01.htm?index=251&idx_num=286
- Hammond, G.P., Jones, C.I. (2008). Embodied energy and carbon in construction materials, in: *Proc. Inst. Civ. Eng. - Energy*, 2008, pp. 87-98. DOI:10.1680/ener.2008.161.2.87
- Harding, J. (2014) Meta-parametric design: Developing a computational approach for early stage collaborative practice. EngD. University of Bath.
- Harding, J., Brandt-Olsen, C. (2018). Biomorpher: Interactive evolution for parametric design. *International Journal of Architectural Computing*, 16, pp. 144-163. DOI: 10.1177/1478077118778579.
- Hays, K.M. (1984) *Critical Architecture: Between culture and form*, *Perspecta*, 21, pp. 14-29 doi:10.2307/1567078
- Hudson, R., Westlake, M. (2015). Simulating human visual experience in stadiums, in: *Proceeding of the Symposium on Simulation for Architecture and Urban Design*, pp. 164-171. <http://dl.acm.org/citation.cfm?id=2873021.2873044>. [Accessed: 7-April-2019]
- IAEE (2014) Guidelines for Display Rules and Regulations. www.mromarketing.aviationweek.com/downloads/mro2017/ERC_Documents/Documents/17_Am_IAEEguidelines.pdf. [Accessed: 7-April-2019]
- John, G., Sheard, R., Vickery, B. (2013) *Stadia: the Populous Design and Development Guide* (fifth edition), Routledge, London. ISBN: 978-0-415-52271-7
- Josephson, J.R., Chandrasekaran, B., Carroll, M., Iyer, N., Wasacz, B., Rizzoni, G., Li, Q., Erb, D.A. (1998) An Architecture for Exploring Large Design Spaces, In: *Proceedings of the 15th National Conference on Artificial Intelligence, AAAI'98*, Madison, Wisconsin, USA (1998).
- Liu, Y.C., Blight, T., Chakrabarti A., (2003) Towards an 'ideal' approach for concept generation. In: *Design Studies*, Vol. 24(4), pp.341-355.
- Majowiecki, M. (2000). Concept and Reliability of Widespan Structure. *Wide span roof structure*, Barnes, M., Dickson, M. (eds) London, UK: Thomas Telford. 2000, pp. 50-61
- Mueller, C., Ochsendorf, J. (2015). Combining structural performance and designer preferences in evolutionary design space exploration, *Automation in Construction*, 52, pp. 70-82. DOI: 10.1016/j.autcon.2015.02.011.
- Okudan, Gul E., Tauhid, S., (2008). Concept selection methods - a literature review from 1980 to 2008, *International Journal of Design Engineering* 1 (3), pp. 243-277. DOI: 10.1504/IJDE.2008.023764.
- Pan Stadia & Arena Management, (2014) <http://populous.com/venuesofthefuture/>
- Leach, J., Fowler, M. (2019) Flexible Design, Pan Stadia & Arena Management, 2nd Quarter 2019, pp.42-43.
- Pan, W., Turrin, M., Louter, C., Sariyildiz, S., Sun, Y. (2019). Integrating multi-functional space and long-span structure in the early design stage of indoor sports arenas by using parametric modelling and multi-objective optimization. *Journal of Building Engineering*, 22, pp. 464-485. DOI: 10.1016/j.jobe.2019.01.006.
- Pan, W., Sun, Y., Turrin, M., Louter, C., Sariyildiz, S. (2020), Design exploration of quantitative performance and geometry typology for indoor arena based on self-organizing map and multi-layered perceptron neural network. *Automation in Construction*, 114, pp. DOI: 10.1016/j.autcon.2020.103163
- Pollstarpro.com (2016). 2016 Mid-Year Worldwide Ticket Sales Top200 Arena Venues. <https://www.pollstarpro.com/files/Charts2016/2016MidYearWorldwideTicketSalesTop200ArenaVenues.pdf> [Accessed: 7-April-2019]
- Salter C. (1998). *Acoustics: Architecture, Engineering, the Environment*. 1st edition. Richmond, CA, USA: William Stout Publishers.
- Schon, D.A. (1992) Designing as reflective conversation with the materials of a design situation, *Research in Engineering Design*, 3, pp. 131-147. DOI:10.1007/BF01580516
- Sciencephoto.com (2021). Colosseum in Rome. <http://www.sciencephoto.com/media/540800/view/colosseum-in-rome-artwork>. [Accessed: 1-June-2020].
- Soru, M. (2014). *A Spatial Kinetic Structure Applied to an Active Acoustic Ceiling for A Multipurpose Theatre*, Delft University of Technology, 2014.
- SportsEngland (2015). Comparative Size of Sports Pitch and Courts (INDOOR) [online]. Available at: <https://www.sportengland.org/media/4381/comparative-sizes-indoor.pdf>

- SportsEngland (2012) Sports Halls Design and Layouts (Updated and Combined Guidance), <https://www.sportengland.org/media/4330/sports-hallsdesign-and-layouts-2012.pdf> [Accessed: 7- April-2019]
- Sun, Y., Leng, T., Shen, Y., Tao, L., (2010) Meditative Mind among Clouds and Waters: Design for the Aoti Aquatic Centre, *Architectural Journal*, 2010(10), pp.54-59. DOI: 10.3969/j.issn.0529-1399.2010.10.012
- Sun, Y., Xiong, L., Su, P. (2010). Grandstand Grammar and its Computer Implementation, in: *ECAADe 31*, 2013: pp. 645-654.
- The B1M (2016). The Building of Rio 2016. <http://www.theb1m.com/video/the-buildings-of-rio-2016>. [Accessed: 1-June-2020].
- Turrin, M. (2014), Performance Assessment Strategy: a computational framework for conceptual design of large roofs. PhD. Delft University of Technology.
- von Buelow, P. (2016). Genetically enhanced parametric design in the exploration of architectural solutions, In: Cruz, P.J.S. (Ed) *Structures and Architecture beyond their limits: proceedings of the third International Conference on Structures and Architecture (ICSA2016)*, London, UK: Boca Raton. pp. 675-683, DOI: 10.1201/b20891-93.
- van Dorp Schuitman, J. (2010) Auditory modelling for assessing room acoustics. PhD thesis at Delft University of Technology.
- Wang, J., (2002), Improved engineering design concept selection using fuzzy sets. In: *International Journal of Computer Integrated Manufacturing*, Vol 15 (1), pp.18-27.
- Wekipeida (2021). Rio Olympic Velodrome. http://en.wikipedia.org/wiki/Rio_Olympic_Velodrome. [Accessed: 1-June-2020].
- Wortmann, T., Costa, A., Nannicini, G., Schroepfer, T. (2015). Advantages of surrogate models for architectural design optimization. *Analysis and Intelligence for Engineering Design*, 29 (4), pp.471-481. DOI: 10.1017/S0890060415000451.
- Yang, D., Ren, S., Turrin, M., Sariyildiz, S., Sun, Y. (2018). Multi-disciplinary and multi-objective optimization problem re-formulation in computational design exploration: a case of conceptual sports building design, *Automation in Construction*, 92, pp.242-269. DOI 10.1016/j.autcon.2018.03.023.
- SCUTAD (2008a). The Wrestling Arena of 2008 Beijing Olympic Summer Games (The gymnasium of China University of Agriculture). <http://www.scutad.com.cn/index.php?a=show&m=Product&id=148>. [Accessed: 1-June-2020].
- SCUTAD (2008b). The Badminton Arena of 2008 Beijing Olympic Summer Games (The Gymnasium of Beijing University of Technology). <http://www.scutad.com.cn/index.php?a=show&m=Product&id=149>. [Accessed: 1-June-2020].
- SCUTAD (2010). The Aquatics Centre of 2010 Guangzhou Asian Games. <http://www.scutad.com.cn/index.php?a=show&m=Product&id=92>. [Accessed: 1-June-2020].
- SCUTAD (2014). Dongguan Chang'an Arena. <http://www.scutad.com.cn/index.php?a=show&m=Product&id=102>. [Accessed: 1-June-2020].
- Populous (2011). Populous Designs Worlds Largest Arena in Manila in the Philippines. <https://populous.com/populous-designs-worlds-largest-arena-in-manila-in-the-philippines>. [Accessed: 1-June-2020].
- Tokyo 2020 (2019). Olympic Stadium Officially Opened. <https://tokyo2020.org/en/news/olympic-stadium-officially-opened>. [Accessed: 1-June-2020].

3 Literature review: Computational design methods for architectural conceptual design

According to the aforementioned basic demands of the conceptual design of indoor arenas (with an emphasis on the integration of multi-functional space and long-span roof structure), this chapter aims at clarifying the potential and limitations of several computational design methods in supporting the conceptual design exploration of indoor arenas. These methods are frequently used in architectural conceptual designs, including parametric modelling, building performance simulations, multi-objective optimization, surrogate model based on supervised learning, clustering based on self-organizing map. Based on the studies on the potential and limitations, a hypothesis of the proposed method is formulated to support the conceptual design of indoor arenas.

3.1 Introduction

With the rapid developments of computer science and technology, various computer-based tools and technologies are applied in architectural designs to support designers to fulfil various design tasks. Against this background, computational design, which focuses on using computational tools and methods to improve design processes, emerged in recent decades. Sariyildiz (2012) defined computational

design as: a design approach which uses computational tools, methods, and techniques to facilitate designers to formulate the design need, requirements, and rules, and translate them into algorithms that generate designs. Harding (2014) considered computational design as the study of how programmable computers can be integrated into the design process (in which the process itself is emphasised ahead of the final results) by developing computer algorithms.

Within the field of computational design, Performative Computational Design (PCD) has been widely used in architectural conceptual design to support design explorations of design alternatives according to numeric assessments related to multiple quantitative design requirements (Shea et al., 2005; Holzer et al., 2007; Sariyildiz, 2012; Gerber, 2012; Lin et al., 2013; Turrin et al., 2011; Turrin et al., 2012; von Buelow, 2012; Mueller, 2015; Yang et al., 2018; Pan et al., 2019a). In general, this process consists of form generation based on parametric modelling, performance evaluation based on numeric assessments and Building Performance Simulations (BPSs), and 'well-performing' design search based on Multi-Objective Optimization (MOO). Specifically, the parametric modelling generates parametric design alternatives based on the association of elements of the building and predefined geometric relations. BPSs can obtain the numeric data of different quantitative aspects (e.g. functionality, structure, HVAC, energy, acoustics, daylighting) and support the related numeric assessments. By using MOO, the 'well-performing' ones can be found among numerous design alternatives according to specific assessment criteria related to quantitative design requirements. These three components are iterated in order to generate and assess a large number of design alternatives, based on which, the PCD shows remarkable potential to support the conceptual design of indoor arenas (Yang et al., 2015, Turrin et al., 2016, Yang et al., 2018).

However, the workflow of the PCD should be customized based on the specificity of indoor arenas. In fact, though various aspects have been combined into architectural conceptual designs based on PCD, little attention has been paid to the integration of the multi-functional space and long-span structure of indoor arenas. Moreover, for the PCD itself, there are also limitations in supporting conceptual designs. In practice, the parametric model in PCD is usually not flexible enough so that the geometries of the relative parametric design alternatives are usually fixed in several types, which narrows the range for design exploration and excludes diverse design alternatives. Furthermore, optimizations only focus on the 'well-performing' designs selected according to numeric assessment criteria related to quantitative design requirements, but for architectural designs, qualitative design requirements are of equal importance.

Besides the process of PCD, machine learning methods are also applied to support architectural conceptual design in recent years. Surrogate model based on supervised learning can rapidly predict the numeric data related to multiple quantitative design requirements of numerous design alternatives, based on parametric modelling and building performance simulations. It allows designers to investigate various design alternatives according to both numeric data (related to quantitative design requirements) and visual investigations (related to qualitative design requirements). However, the problem is that it is difficult for designers to investigate mass information of numerous designs.

Unsupervised clustering, which is a subset of machine learning, can be used to group numerous designs into different clusters according to their geometry features. It allows designers to have an overview of different types of designs, which is crucial for the visual investigations of various design alternatives. However, this process is not related to the numeric data of quantitative design requirements.

In section 3.2 to 3.6, the backgrounds, applications in architectural designs, as well as the potential and limitations (in supporting the conceptual design of indoor areas) of parametric modelling, Building Performance Simulations (BPSs), Multi-Objective Optimization (MOO), surrogate model based on supervised learning, and unsupervised clustering are reviewed and studied, respectively. Based on these studies and according to the basic demands of the conceptual design of indoor arenas, a hypothesis of the proposed method is formulated in section 3.7. Based on the hypothesis, a formal method is proposed and elaborated in chapter 4.

3.2 Parametric modelling: a process to associate elements and generate design alternatives

3.2.1 Background

In general, parametric design is considered as a design process by using parametric modelling (Barrios, 2005; Hudson, 2010; Turrin, 2014). In parametric modelling, a model is formulated based on parameters, which can extend the intellectual range of design dynamically (Woodbury, 2010; Emami, 2019). Barrios (2005) defined parametric modelling as a process of formulating a geometrical representation of a design with parametrized components and attributes. Within this definition, parametrization is considered as a process to define which components of the model can be varied and how the variation occurs. Hudson (2010) defined parametric modelling as a process of developing a computer model which is based on relationships between objects controlled by parameters. By changing the values of the parameters, the model can be changed, and a range of alternatives can be generated. Similarly, Harding (2014) defined parametric modelling as a generation of geometry based on input parameters and by defining relationships between functions which manipulate the parameters.

According to these definitions, it can be found that parametric modelling process is composed of two aspects: defining objects and their interrelationships and defining parameters to formulate these relationships. Harding (2014) used a simple example to illustrate this process (figure 3.1, a). Such an example can also be achieved by other definitions of parameters and relationships (figure 3.1, b). These two parametric definitions can generate different sets of alternatives, since the definitions based on different problem descriptions. Hudson (2010) stated that to understand the design problem and describe it in parameters is the beginning of parametric modelling.

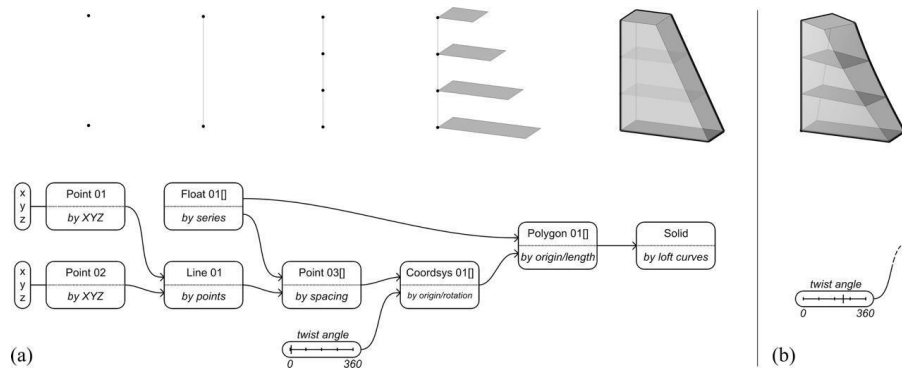


FIG. 3.1 Two different parametric definitions (a) and (b) for a similar design concept (Harding, 2014)

Based on these analyses, in this research, parametric modelling is defined as a process of defining a changeable geometry model based on parameters, according to the interrelationships among objects (elements of the building). The formulation of such interrelationships is based on the understanding of design problems.

The interrelationships among objects (elements of the building) are usually organized by a hierarchy structure. Within this structure, the input data go through different components and are processed, then finally become geometries (in usual). Hence, the parameters and the related hierarchy structure should be defined at the beginning, so that the constraints and the freedoms of the parametric model can be determined (Kilian, 2006). In most of the parametric design tools, this hierarchy structure is illustrated by a directed acyclic graph (DAG) (Christofides, 1975). A specific design alternative is generated by computing the DAG according to the values of the parameters (Cormen et al. 2001). In this light, parametric modelling can also be considered as a process of formulating an algorithm in visual form as DAG (Dino, 2012). Such algorithm represents the interrelationships between objects (e.g. parts or components of the building).

By computing the DAG with different sets of parameter values, various design alternatives can be generated. Each design alternative, which is called as an instance of the parametric model, represents a unique set of transformations based on the values assigned to the parameters (Barrios, 2005). All the instances (design alternatives) of the parametric model constitute a design space of the model, and the amount of the instances can be dozens or billions, which depends on the setting of the parameters. Generally speaking, once the definition of the parametric model (the hierarchy DAG) is fixed, the solution space is also fixed (Dino, 2012).

3.2.2 Applications of parametric modelling

Comparing to engineering and industrial designs in which parametric design has been widely used and well established for decades (Myung and Han, 2001), the parametric architectural design started late. However, with the rapid development of computer-aid architectural design (CAAD) and based on a series of parametric design computer programs, the application of parametric architectural design in practice increased rapidly in the last decade (Barrios, 2005; Hudson, 2010; Gane and Haymaker 2010). So far, parametric design is well established in the computational design community (Harding, 2014).

Several tools can be used to perform parametric architectural designs, including Dynamo in Revit (Autodesk), 3D Max (Autodesk), Maya (Autodesk), Dynamo (Autodesk), Catia (Dassault Systemes), Solidworks (Dassault Systemes), Generative Components (GC, Microstation), Grasshopper (GH, McNeel & Associates), etc. Among these computer applications, Grasshopper, a plugin of Rhinoceros 3D (a NURBS-based modelling software developed by McNeel & Associates) is widely used in architectural design and related research.

Parametric designs can be applied in different design tasks during the whole architectural design process. Hudson (2010) systematically formulated five parametric strategies for architectural designs, based on various case studies. The strategies are: knowledge development strategy (kDev), knowledge capture strategy (kCap), model construction strategy (mCon), design investigation strategy (dInv), and construction documents strategy (cDoc). The workflows based on these strategies are illustrated in figure 3.2 and elaborated in the following paragraph, according to Hudson (2010).

At the beginning of design, when the design problem is unclear, the knowledge development strategy (kDev) is used to facilitate designers to clarify the problem. Parametric modelling is used to undertake an experimental design exploration. During the exploration, the parametric model is used as a test object to be iteratively defined, invested, and redefined, until the design problem is well-defined. Here, the process of defining the design problem is considered as a knowledge development.

For a defined design problem, the knowledge capture strategy (kCap) can be used to parametrize and refine it. Here, the knowledge means the definition of the design problem or the design intent, and capture means parametrizing it into parametric models. A design exploration is used to test whether the design content is correctly captured.

The model construction strategy (mCon) and the design investing strategy (dInv) are actually embedded in kDev and kCap in terms of design exploration. The mCon aims to externalize the defined design problem or intent. The dInv aims to test whether the design problem is correctly defined (for kDev) or parametrized (for kCap)

The construction document strategy (cDoc) is employed with mCon and dInv, to share information with other stakeholders by considering different design representations in the early design phase.

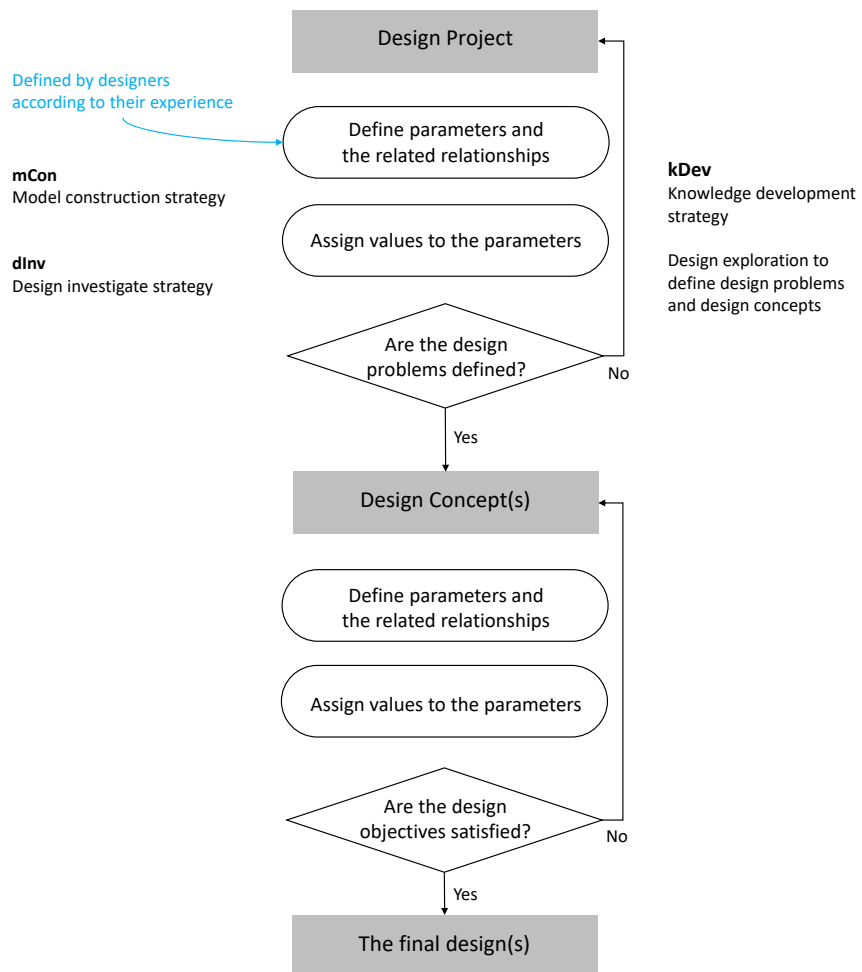


FIG. 3.2 Workflow of an architectural design concluding four parametric design strategies according to Hudson (2010)

The kDev and kCap are related to two steps design phases, respectively. The first step, kDev, can be considered as conceptual design, which defines design concept(s) based on design exploration. The second step, kCap, furtherly refine the design concepts to satisfy design objectives related to various aspects. However, with the increasing emphasis on integrated design, a series of engineering aspects, which are highly related to the overall form of the building, are considered in conceptual design (Turrin, 2014). In this light, the step of kDev and kCap should be achieved in one design process. Specifically, the kDev provides various design alternatives, which correspond to the aforementioned divergent step proposed by (Okudan and Tauhid, 2008), while the kCap assess and refine the alternatives to meet multiple design objectives related to design requirements, which correspond to the convergent step.

3.2.3 Diversity of design alternatives: a further requirement of parametric modelling

According to the discussion in section 2.4 of chapter 2, in the divergent-convergent design process proposed by (Okudan and Tauhid, 2008), within the divergent step, the diversity of design alternatives is crucial. Traditional parametric modelling approaches usually focus on one or several specific types of design alternatives in each design project. As a result, although there can be numerous design alternatives in the design space, they may be similar in geometry. However, in practice, designers usually prefer to study diverse design concepts at the beginning (Harding, 2014) to evaluate the alternatives according to qualitative aspects (as elaborated in chapter 2). An example can be found in the conceptual design phase of the Escher Tower project performed by Bjarke Ingels Group (BIG) (figure 3.3, left), in which the architects worked out various types of designs (Harding, 2014). Moreover, as mentioned above, the satisfactions of some quantitative design requirements are highly related to the overall geometry of the building, and different designs with different types of geometries can perform differently to satisfy these requirements. In this light, to define proper design concepts which satisfy both the quantitative and qualitative design requirements, it is necessary to provide a broader design space containing numerous design alternatives with diverse types of geometries.



FIG. 3.3 Various design concepts proposed by Bjarke Ingels Group architects for Escher Tower project (left) and Various concepts with diverse types of geometries generated by 'Embryo' (right) (Harding, 2014)

However, the flexible parametric models, which can generate diverse design alternatives, are usually difficult to achieve. In the above example of BIG, although the architects worked out various design concepts, it is time-consuming to translate all the concepts into parametric models one by one to make a parametric design exploration (Harding, 2014). To overcome the challenge, a parametric design tool 'embryo' was proposed based on form grammar and genetic programming to generate geometries with diverse topologies (Harding, 2014). By using 'embryo', various designs with diverse types of geometries can be generated by one parametric model (figure 3.3, right).

Specifically, for indoor sports arenas, as elaborated in chapter 2, the spatial topology is fixed (a pitch surrounded by a seating bowl with a roof cap), but the geometry typology can be varied. A seating bowl can be round, rectangle, polygon, oval, or irregular form, and the geometry of a roof can be a surface of plane, zero Gaussian surface (e.g. vault), positive Gaussian surface (e.g. dome), negative Gaussian surface (e.g. saddle) or free form. However, so far, it lacks a flexible parametric model for indoor arenas to generate design alternatives with diverse types of geometries, based on the integration of the multi-functional space and long-span structure.

3.2.4 Parametric design for sports buildings

For the sports building designs, parametric modelling has been applied to generate the pitch and seating bowl. Hudson (2010) formulated a reusable parametric model, Seating Bowl Modeller (SBM), for grandstands of outdoor stadiums. The model is generated by a hierarchical structure, including a basic model and four additional levels (figure 3.4). The basic model generates the basic shape of the seating bowl,

based on which more details are added at each level. Being similar to SBM, another reusable parametric model for seating bowl generation, STaG: stadium generator is proposed by Arup (an international engineering firm) (Arup, 2014; Binkley et al., 2014). However, in these models, the outer boundary of seating tiers is fixed in planner rectangles (figure 3.5), which excludes other shapes of seating bowls.

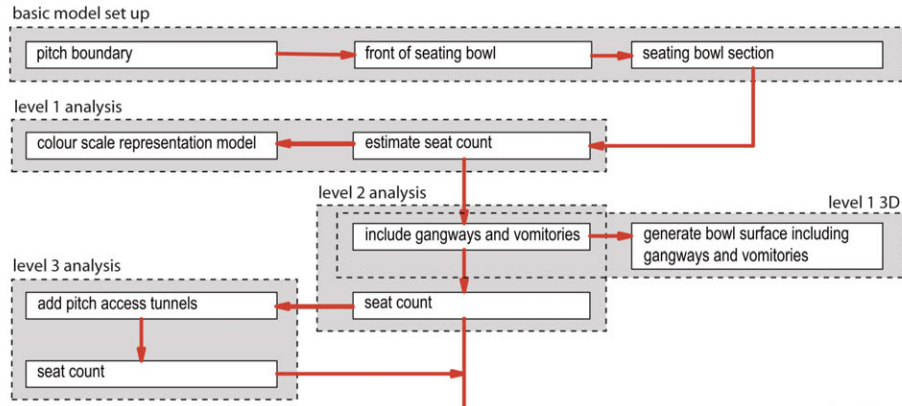


FIG. 3.4 The hierarchical structure of Seating Bowl Modeller (SBM) (Hudson, 2010)



FIG. 3.5 Four typical seating bowls generated by SBM (Hudson, 2010)

To overcome the limitation related to the outer boundary of seating tiers generated by SBM and STaG, Sun et al. (2013) formulated a flexible model for the one-side grandstand of stadiums by using shape grammar in parametric modelling software. This model also generates the seating bowl based on the inner outline and the section, but it also allows designers to define the geometry of the grandstand by an outer outline which can be polyline or a curve (figure 3.6). Therefore, more diverse grandstand can be generated. Nevertheless, it still lacks a reusable and versatile parametric model to integrate the multi-functional space and long-span roof structure and generate design alternatives with diverse geometries based on the integration.

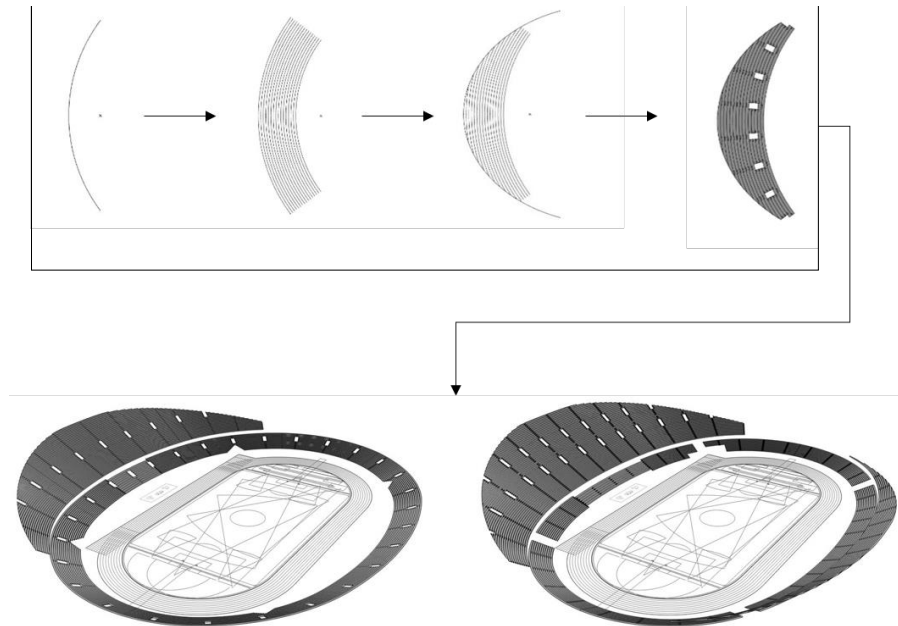


FIG. 3.6 A one-side grandstand generated by a changeable outer outline (Sun et al., 2013)

3.3 Building Performance Simulations (BPSs) for indoor arenas

In performance-based computational design (PCD), the design alternatives, which are generated by the parametric model, should be assessed by numeric indicators related to various quantitative design requirements. It is impossible to do real experiments for the measurements to obtain the values of the indicators, but simulation based on computers can be used to fulfil these measurements.

Turrin (2014) has mentioned the definitions of 'simulation' according to Cambridge English Dictionaries and Collins English Dictionary. According to Cambridge English Dictionaries, a simulation is 'a model of a set of problems or events that can be used to teach someone how to do something, or the process of making such a model'. According to Collins English Dictionary, a simulation is 'a representation of a problem, situation, etc., in mathematical terms, especially using a computer; and specifically referring to mathematics, statistics, and computing, as the construction of a mathematical model for some process, situations, etc., in order to estimate its characteristics or solve problems about it probabilistically in terms of the model'.

Besides, according to Oxford English Dictionary, simulation is 'a situation in which a particular set of conditions is created artificially in order to study or experience something that could exist in reality'. According to Longman English Dictionary, simulation is 'the activity of producing conditions which are similar to real ones, especially in order to test something, or the conditions that are produced'. According to Webster's English Dictionary, simulation is 'the imitative representation of the functioning of one system or process by means of the functioning of another'.

Specifically, in the context of building designs, one of the main tasks for simulation is to represent real conditions for designs to obtain the values of indicators related to specific performance without performing real measurements based on experiments which are usually impractical. For example, to obtain the stress and strain of a specific structural element of a building design under a combination of loads, it is unpractical to build a real structure and apply loads to achieve the measurements. It is also expensive and time-consuming to make a miniature model to achieve the measurements, especially for numerous designs. However, it is feasible to create an artificial condition in computers according to some assumptions and calculations on mechanics (e.g. FEM: finite element method), therefore, to mimic a real condition for the design and obtained the values of the indicators.

In this light, this research defines a Building Performance Simulation (BPS) as a numeric model which imitates a specific real physical system (e.g. gravity, thermal, daylight, airflow, sound wave) to test and measure design objects (including related geometries and materials), therefore, to obtain values of related indicators.

With the rapid developments of computer science and CAAD, a series of tools of Building Performance Simulations (BPSs) have been developed for various engineering aspects, including structure, thermal and energy, daylighting and solar radiance, acoustics, wind and ventilation, etc. These BPS tools are widely used in building design to support integrated designs which aim to combine engineering aspects into architectural conceptual designs (Turrin, 2014). For the architectural aspect, besides the indicators only related to geometry which can be directly measured, there are BPS tools related to space connection, crowd movement and evacuation, etc. Furthermore, some BPS tools can be directly used in parametric modelling applications. Table 3.1 lists some exemplary BPS tools.

TABLE 3.1 Exemplary simulation/analysis tools for different aspects

Aspects	Independent tools	Plug-ins for Rhino grasshopper
Structure	ANSYS DIANA FEA Abaqus SP2000	Karamba Gangroo (for Form-finding) Vault (for form-finding based on Graphic Statics)
Thermal and energy	EnergyPlus ESP-r IDA ICE IES VE TRNSYS	Ladybug honeybee
Daylighting and solar radiance	EnergyPlus IDA ICE	Ladybug Honeybee
Ventilation	Ventseim-3d ADINA-CFD	Honeybee
Acoustics	COMSOL Multiphysics Simulia EASE Odeon	Pachyderm acoustics Acoustic shoot

As mentioned in chapters 1 and 2, this research focuses on the conceptual design of indoor arenas based on the integration of multi-functional space and long-span roof structure. Specifically, for the quantitative design requirements, the emphasis lays on multi-functionality (spatial capacity, view of spectators, and acoustics for multiple activities) and structural performance. BPS tools with the related theories corresponding to these aspects are reviewed and studied in the following sections.

3.3.1 Simulations of spatial capacity and the view of spectators

For the spatial capacity and the view of spectators for multiple activities, the related requirements, indicators and assessment criteria have been reviewed and studied in chapter 2. All the indicators are only related to geometry which can be directly measured in parametric models.

3.3.2 Simulations of acoustics

In the field of room acoustics, several methods are applied to obtain the indicators related to acoustical performance, among which empirical methods, wave-based methods, geometrical acoustics methods are three main methods that are frequently used.

3.3.2.1 Empirical methods

Empirical methods apply equations formulated based on experiments and statistics. Sabine and Eyring formula are two famous methods. The Sabine equation, which is proposed by Wallace Clement Sabine based on the experiments for several rooms in Harvard University, is the first equation to calculate reverberation time (Sabine, 1922):

$$RT_{60} = \frac{0.161V}{\sum \alpha_{s,i} S_i + 4mV} \quad [3.1]$$

Where RT_{60} is the reverberation time, V is the volume of the room in m^3 ; $\alpha_{s,i}$ is the absorption coefficient for the i^{th} surface (see table 3.2), S_i is the area of the i^{th} surface; m is the energy attenuation constant for sound traveling through air in m^{-1} .

Sabine formula is based on the assumption that a sound wave impacts the surface 'one after another' (Cremer and Mueller, 1982; Beranek, 2006) and its energy diffuses equally when it travels through the room. Eyring argued that all the sound wave impacts all the surface at the same time, the impacts can happen many times and each impact is diminished by the average room absorption coefficient (Beranek, 2006). Based on this assumption, Eyring equation is formulated as (Eyring, 1929):

$$RT_{60} = \frac{0.161V}{S_{tot} - 2.30 \log_{10}(1 - \alpha_{ey}) + 4mV} \quad [3.2]$$

$$\alpha_{ey} = \frac{\sum \alpha_{e,i} S_i}{S_{tot}} \quad [3.3]$$

where α_{ey} is the average absorption coefficient for all the surface S_{tot} ; $\alpha_{e,i}$ is the sound absorption coefficient of the i^{th} surface (the coefficients of some typical materials used in arenas are listed in table 3.2), S_i is the area of the i^{th} surface. Although the assumption of Eyring equation is more consistent with the behaviour of sound wave in theory, the reverberation time calculated by Sabine formula is closer to the measured data (Salter, 1998).

TABLE 3.2 Exemplary absorption coefficients for different areas of indoor arenas (Bork, 2005)

Area	Material	Absorption Coefficient Octave band frequency in Hz						
		125	250	500	1k	2k	4k	8k
Pitch floor	Rubber on concrete	0.02	0.03	0.03	0.03	0.03	0.02	-
Seating tier floor	Audience floor, two layers 33mm on sleepers over concrete	0.09	0.06	0.05	0.05	0.05	0.04	-
walls	Fabric-covered panel, 6 pcf rockwool core	0.21	0.66	1.0	1.0	0.97	0.98	0.98
Spectator area	Audience area, 1 person / m ²	0.16	0.29	0.55	0.80	0.92	0.90	-
Ceiling	Metal panel ceiling, backed by 20mm Sillan acoustic tiles, panel width 85 mm, panel spacing 15 mm, cavity 35 cm.	0.59	0.80	0.82	0.65	0.27	0.23	-

3.3.2.2 Geometrical acoustic methods

In the assumption of geometrical acoustic methods, sound waves, which propagate in straight lines, emit to all directions from sound sources with energy, and then travel through the air and are reflected by objects (Elorza, 2005). During their travels and reflections, the energy reduces. Based on the decayed energy and the sound waves received by the receiver, a series of indicators of the sound waves can be calculated (Voländer, 2013). Since the assumption is based on energy, the geometrical acoustics methods are also called energy-based methods. The accuracy of the results is acceptable if the relevant dimensions of the room are larger than the wavelengths (Voländer, 2013).

Based on the assumption, several acoustical simulation tools are developed to simulate sound waves in architectural design, among which Pachyderm Acoustics (van der Harten, 2015) and Acoustic Shoot (Meunier, 2012) can be used in grasshopper. These two tools are based on the ray-tracing model which is one of the two main models for geometrical acoustics. Another main model is the image sources model (Voländer, 2013). The ray-tracing model considers sound waves as a number of rays that carry energy and emit from the sound sources in all directions. When the sound waves go through the air and are reflected by objects, the energy decreases since the absorptions of the air and the objects. Finally, some rays attain the defined receivers, and the energy decays during this process can be obtained. Thus a series of indicators related to the sound waves can be obtained. To use the simulation tools based on the ray-tracing model, users should define the positions of sound sources and receivers, the number of the rays emitted from each sound source, and the geometry and materials of the objects which reflect and absorb sound.

3.3.2.3 Wave-based methods

Wave-based methods intend to use numerical way to approximate the wave equations. In these methods, the room space is divided into elements whose sizes are much smaller than the wavelength. These elements interact with each other according to the characteristics of wave movement. Wave-based methods are suitable for the acoustics of small and medium sized rooms in which the geometrical acoustic methods are usually fail (Volander, 2013). These methods include FEM (finite element method), BEM (boundary element method), FDTD (finite-difference time domain method) (Elorza, 2005).

3.3.2.4 Simulation of acoustics for architectural conceptual design of indoor arenas

For room acoustics, in which the room dimensions are larger than the sound wavelengths, both empirical methods and geometrical acoustic methods can be applied. For empirical methods, the related factors are the volume of the room and the areas of different absorption surfaces, which can be directly measured in the three-dimensional model. Moreover, the calculation is simple and fast. For the methods based on the ray-tracing model, the computation time is usually long for one design. Moreover, the definitions of the sound sources and the number of rays in the digital ray-tracing model require professional knowledge of acoustics, which may need the consultants of acoustics. In general, the accuracy of geometric acoustic methods is higher, but considering the level of architectural conceptual design which aims at providing good geometries for other engineering aspects, the accuracy for empirical methods is also acceptable (Ding et al., 2018).

3.3.3 Structural analysis tools

The simulations of structures are based on the calculations and analyses of mechanics. In mechanics analysis, there are five important factors: structural geometry, structural topology, structural cross-section, structural material, and loads (Li et al., 2016). The first four factors are discussed in chapter 2 as the design parameters for the long-span roof of indoor arenas. The factor of loads is applied during the mechanics analysis to assess a structure. In the following sections, four main mechanic analysis methods and loading models are reviewed and discussed, respectively (section 3.3.3.1 and section 3.3.3.2), based on which the structural simulation for the architectural conceptual design of indoor arenas are reviewed and studied (section 3.3.3.3).

1 Static equilibrium of determinate structure

For a statically determinate structure, the reaction forces and internal forces can be calculated by using the equations of static equilibrium. However, for statically indeterminate structure, there are redundant restraints, and the number of the reactions of all the restraints is larger than the number of the equations based on static equilibrium. Hence, it is impossible to calculate the reaction forces based on these equations. Most of the real structures are indeterminate, since indeterminate structures are usually more stable, with fewer deflections, and have redundancies in carrying loads. To analyse indeterminate structures, force method and displacement method are used (Leet et al., 2002).

2 Force method of statically indeterminate structures

The force method (or the flexibility method or the method of consistent deformation) can be used to calculate the reaction forces and internal forces of a statically indeterminate structure. In this method, an indeterminate structure is transformed into a determinate one (called the released structure or the basic determinate structure), by replacing redundant restraints with related reaction forces or moments (Leet et al., 2002). For the replaced redundant restraints, the related displacements should equal zero, which can be expressed by equations (called compatibility equations). The number of the compatibility equations equals the number of redundant restraints. Therefore, by combining the compatibility equations with the statics equilibrium equations, there are sufficient equations to calculate all the reactions of the restraints.

The force method is straightforward and easy-understood and is efficient in the calculation of simple indeterminate structures. However, for a complex structure with numerous restraints, the number of equations will be too large to be efficiently calculated.

3 Displacement method of statically indeterminate structures

The displacement method (or the stiffness method) is another method to analyse statically indeterminate structures. Nowadays, most of the analyses for real complex structures and most of the computer programs for mechanic analysis are based on this method.

In this method, for each node of a structure, the resultant force should equal zero (Leet et al., 2002). According to this, a set of basic equations can be formulated, and the number of the equations equals the number of nodes multiple three (for a two-dimensional problem) or six (for a three-dimensional problem). Some strategies can be used to reduce the number of the equations, since some of them are not independent, but when using computer software, all the equations are calculated (Leet et al., 2002).

For a certain node of a structure, the force on this node is the sum of the forces led by the displacements of all the nodes of the structure and the forces led by loads, which should equal zero. The force in a certain node (i.e. the i^{th} node) led by loads can be labelled as F_i and can be calculated based on the load constant related to the type of the load. The load constant can be calculated based on the slope-displacement method.

The force in a certain node led by the displacements of all the nodes of the structure can be calculated based on the stiffness of this node and the displacements of all the nodes of the structure. The stiffness of the i^{th} node (written as k_{ij}) refers to the force in the i^{th} node led by a unit displacement in the j^{th} node. For the i^{th} node of a structure with n nodes, the stiffness is a vector. For all the nodes of the whole structure, the stiffness is a matrix (the element stiffness matrix). Each item in the vector or matrix can also be calculated by the slope-displacement method.

$$K = \begin{bmatrix} k_{11} & k_{12} & \dots & k_{1j} & \dots & k_{1n} \\ k_{21} & k_{22} & \dots & k_{2j} & \dots & k_{2n} \\ \vdots & \vdots & & \vdots & & \vdots \\ k_{i1} & k_{i2} & \dots & k_{ij} & \dots & k_{in} \\ \vdots & \vdots & & \vdots & & \vdots \\ k_{n1} & k_{n2} & \dots & k_{nj} & \dots & k_{nn} \end{bmatrix} \quad [3.4]$$

Since stiffness is related to the force led by a unit displacement, and the force led by a displacement can be simply calculated by multiplying stiffness k_{ij} with the related displacement u_j (the displacement in the j^{th} node). The displacement of all the n nodes in the structure is a vector.

$$\{u\} = [u_1 \quad u_2 \quad \dots \quad u_j \quad \dots \quad u_n] \quad [3.5]$$

Hence, the resultant force in a certain node, which equals zero, can be written as:

$$R_i = \sum_{j=0}^n k_{ij} u_j + F_i = 0 \quad [3.6]$$

Then, for the whole structure, the equations can be written as:

$$\left\{ \begin{array}{l} R_1 = \sum_{j=0}^n k_{1j} u_j + F_1 = 0 \\ R_2 = \sum_{j=0}^n k_{2j} u_j + F_2 = 0 \\ \vdots \\ R_i = \sum_{j=0}^n k_{ij} u_j + F_i = 0 \\ \vdots \\ R_n = \sum_{j=0}^n k_{nj} u_j + F_n = 0 \end{array} \right. \quad [3.7]$$

or written as matrix:

$$F = K[u] = \begin{bmatrix} k_{11} & k_{12} & \dots & k_{1j} & \dots & k_{1n} \\ k_{21} & k_{22} & \dots & k_{2j} & \dots & k_{2n} \\ \vdots & \vdots & & \vdots & & \vdots \\ k_{i1} & k_{i2} & \dots & k_{ij} & \dots & k_{in} \\ \vdots & \vdots & & \vdots & & \vdots \\ k_{n1} & k_{n2} & \dots & k_{nj} & \dots & k_{nn} \end{bmatrix} \begin{bmatrix} u_1 \\ u_2 \\ \vdots \\ u_i \\ \vdots \\ u_n \end{bmatrix} \quad [3.8]$$

Since k_{ij} and F_i can be respectively calculated by the slope-displacement method, the u_j can be calculated by the set of equations. Based on the displacements of each node, the moment and normal force for the element between the nodes can be calculated.

It should be noticed that all the mechanic analysis methods are based on some assumptions of material mechanics, which may be invalid if the whole structure is too much simplified. Besides, for the calculation itself, when using the displacement method to calculate the displacements, a group of partial differential equations (PDE) should be calculated, which is impossible for a complex structure (e.g. a grid shell with 4,000 bars for an arena-roof).

4 Finite Element Method (FEM) of indeterminate structures

To overcome the aforementioned problem, the Finite Element Method (FEM) was proposed by Hrennikoff (1941) and Richard Courant (1942). FEM approximately translates the PDE group (of the displacement method) into ordinary differential equations (ODE) by dividing the domain into segments called elements. The number of the elements is large but finite, and the more elements the domain is divided into, the more accurate the results would be.

Correspondingly, in the mechanic analysis, FEM divides a complex structure into numerous simple elements. For example, a 4,000-bar grid shell as the roof structure of an arena can be divided into 4,000 elements, and each bar is an element.

The basic steps for FEM can be formulated into:

- Discrete the structure into elements which are connected to each other by nodes and identify each element and node;
- Calculate the local stiffness matrix of each element;
- Assemble the elements into an intact structure by combining the stiffness of each element into a global stiffness matrix
- Introduce boundary conditions which can be defined as fixing the movements or rotations in some directions of some nodes.
- Formulate the global equilibrium equations in the form of equation 3.8, based on the global stiffness matrix and given loads; and calculate the displacement vector.
- Calculate the normal force, bending moment, stress, and strain of each element based on the nodal displacements.

3.3.3.2 Loading model

The combination of loads according to design codes (e.g. Eurocode) is reviewed in chapter 2. As mentioned in chapter 2, in this research, the combination of loads is composed of permanent load (structural self-weight and the weights of cladding, ceiling, and hanging facilities under the roof), wind load, and snow load. The structural self-weight, as mentioned in chapter 2, can be directly obtained based on the volume and the material of the structure. The weights of cladding, ceiling, and hanging facilities hanging under the roof are set as evenly distributed loads on structural bars or concentrated loads on some nodes. However, the definitions of wind and snow loads are complex. There are at least three methods to define wind and snow loads for a structure during conceptual design: calculation based on design codes, simplified method, and simulation based on computational fluid dynamics (CFD).

1 Calculation based on design code

Wind load can be considered as a pressure (positive or negative) on the roof, which is related to the shape, size, and the dynamic properties of the structure. A series of equations are used to calculate the wind load. Taking Eurocode EN 1991-1-4:2005 (CEN, 2005) as an example, the wind force for the along-wind direction of a structure is calculated by:

$$F_w = C_s C_d C_f q_p(z_e) A_{ref} \quad [3.9]$$

$$C_s C_d = \frac{1 + 2k_p I_v(z_s) \sqrt{B^2 + R^2}}{1 + 7I_v(z_s)} \quad [3.10]$$

$$I_v(z_s) = \frac{k_1}{c_0(z) \ln \frac{z}{z_0}} \quad [3.11]$$

$$q_p(z) = \frac{[1 + 7 \ln(z)] \rho v_m(z)^2}{2} \quad [3.12]$$

$$v_m(z) = C_r(z)C_0(z)v_b \quad [3.13]$$

Where F_w is the wind force, $C_s C_d$ are the structural factors, C_f is the force coefficient related to the geometry of the structure, some examples of simple geometries are demonstrated in EN 1991-1-4:2005 (CEN, 2005); $q_p(z_e)$ is the peak velocity pressure of the wind at the height z_e ; A_{ref} is the reference area of the structure on which the wind is acting; k_p is the peak factor; $I_v(z_s)$ is the turbulence intensity at the height z_s ; B is the background factor; R is the resonant factor; k_t is the turbulence factor equalling one, according to the recommendation EN 1991-1-4:2005 (CEN, 2005); $c_0(z)$ is the orography factor according to EN 1991-1-4:2005- Netherlands annex (CEN, 2005); z_0 is roughness length; ρ is the density of air, which equals 1.225kg/ m³; $v_m(z)$ is the mean wind velocity at the height z ; $c_r(z)$ is the roughness factor; v_b is the basic wind velocity.

The five equations above are the basic equations, in which there are still some unknown indicators which should be calculated by other equations. An intact calculation procedure of the wind force acting on a building from one direction at a specific height z is demonstrated by Estrado (2019), in which the partial wind load is obtained based on the calculations of twenty equations. Therefore, to calculate the wind force for the whole structure, it required a set of complicated calculations. Specifically, for the design of indoor arenas, the geometry of the roof can be complex free form, and it is more difficult to define the force coefficient C_f according to the simple shapes demonstrated in EN 1991-1-4:2005. Besides, the calculations regulated by EN 1991-1-4:2005 are simplified, which makes the results are conservative (Cook, 2007; Estrado, 2019). Hence, the EN 1991-1-4:2005 recommends using wind tunnel and/or numerical models as a supplement to the calculations (CEN, 2005).

Snow loads can be considered as temporary loads related to the roof geometry and the climates. According to Eurocode EN 1991-1-3:2003 (CEN, 2003), snow load should be calculated based on the roof shape, climate, thermal properties of the roof, etc. To calculate snow load, firstly, the snow load on the ground S_k should be defined. The calculation of S_k is varied for different locations (see EN 1991-1-3:2003, Annex 3, table C.1, CEN, 2003). Taking the Netherlands (in the climate region of central west) as an example, the snow load on the ground is:

$$S_k = 0.164Z - 0.082 + \frac{A}{966} \quad [3.14]$$

Where S_k is the characteristic snow load on the ground in the unit of kN/m^2 ; Z is the zone number on the map in Eurocode, and $Z=2$ for most of the land in the Netherlands; A is the altitude of the location (m), $A=0$ for the case of the Netherlands. Being similar to the calculations of wind loads, in the calculation of the snow load, a force shape coefficient related to the roof shape is needed. However, for the design exploration of indoor arenas, there are numerous roofs with free form shapes, and it is difficult to define the force shape coefficient for these shapes according to the simple examples provided by EN 1991-1-3:2003.

2 Simplified method

During the design exploration, numerous design alternatives with diverse geometries are assessed. Moreover, the geometries of the long-span roofs can be complex. Thus, it can be difficult to define the snow and wind loads according to design codes.

Alternatively, considering the level of analysis typically used in architectural conceptual design, the wind and snow loads can be simplified into full and asymmetric vertical loads in a fixed value for the roof research (Brown et al., 2015; Kim et al., 2016; Pan et al., 2019a). Brown et al. (2016) used simplified snow and wind loads in an optimization of three types of long-span roof structures, in which 3.48kN/m^2 is assigned to the wind and snow loads, and both full and asymmetric distributions of the loads are considered. Similarly, Pan et al. (2019a) used a similar simplified load for design optimizations of large roofs of indoor arenas, in which 3kN/m^2 is defined as the fixed value for wind and snow loads. Moreover, several distributions of this vertical load are considered, including the distribution on the whole roof, and the distributions on one-side of the roof (east-, west-, north-, and south-side, respectively).

Although the simplified method can be used for the design exploration during the architectural conceptual design, in the following design processes, it is still necessary to assess the design alternatives selected from the design exploration, according to the wind and snow loads calculated based on design codes, wind tunnel, or numerical model.

3 Computational fluid dynamics (CFD)

Computational fluid dynamics (CFD) is a process to solve a series of governing equations of fluid dynamics by using numerical methods (Mohotti et al., 2014). Based on CFD, the movements of a fluid (can be liquid, gas, and plasma) and its actions on other objects can be simulated. One of the main steps for CFD is meshing

which divides the study range into a series of sub-ranges (meshes). Based on meshing, the governing equations can be solved for each sub-range and then for the whole study range. Finite differential method (FDM), finite volume method (FVM), and finite element method (FEM) can be used to fulfil this step (Estrado, 2019), and FDM is frequently used in CFD software (Anderson, 1995).

CFD has been widely used for the study of wind, and several programs can be used for building designs, e.g. Autodesk Flow Design, ANSYS Fluent, OpenFOAM, Butterfly, GH Wind. Estrado (2019) reviewed and compared these programs and used butterfly and GH wind (which are the plugins for rhino-grasshopper) as the simulation tools of wind environment to optimize the geometry and structure of a high-rise tower building.

3.3.3.3 Structural simulations in architectural conceptual design

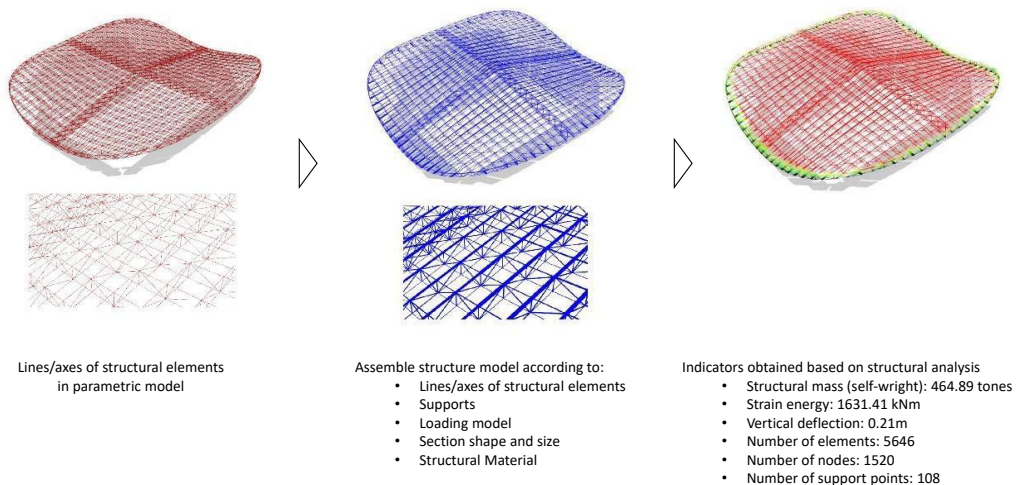


FIG. 3.7 An example about the assembly and analysis of a structure model based on Karamba 3d

Table 3.1 lists a series of structural simulation tools. In this research, Karamba 3d (Preisinger et al., 2013), a plugin of grasshopper for FEM analysis is selected for its capacity in supporting structural conceptual designs.

The process of Karamba 3d can be divided into two steps: assembly and analysis (figure 3.7). In the assembly step, geometric elements in grasshopper are transferred into structural elements. Two components support these processes: line-to-beam, mesh-to-shell. Besides, a series of parameters including nodal constraints, support points, sectional shape and size, material, loads also need to be defined.

Based on the assembled structure model, a series of calculations based on FEM are fulfilled by karamba 3d automatically, and various indicators can be obtained as outputs. The frequently used calculations (called algorithms in Karamba) are first order analysis, second order analysis, deformation analysis, buckling analysis, etc. The indicators (the outputs of the calculations) including mass (weight), strain energy, normal force in each element, nodal and elemental displacements, shear stress, bending moment, etc. Details about Karamba 3d can be found in the manual (Karamba3D, 2020)

3.4 Optimization based on heuristic algorithm

3.4.1 Background

Generally, optimization is a process to find the optimal ones from a number of objects within a defined range, according to specific criteria. In mathematics, mathematical optimization is a process to minimize or maximize one or several real functions, by systematically selecting the input data (objects) in a defined range (searching space) and satisfying some defined requirements (Nguyen et al., 2014). Such a function is called the fitness function or objective function. The inputs are called variables, and the defined range for each variable is called the domain of definition which is composed of lower boundary and upper boundary. The requirements are called constraints which can be expressed in equalities and inequalities. A typical optimization problem can be expressed as (Amaran et al., 2016):

$$\begin{aligned}
 & \min. f(\mathbf{x}) \\
 \mathbf{x} = & \begin{bmatrix} x_{11} & x_{12} & \cdots & x_{1j} & \cdots & x_{1n} \\ x_{21} & x_{22} & \cdots & x_{2j} & \cdots & x_{2n} \\ \vdots & \vdots & & \vdots & & \vdots \\ x_{i1} & x_{i2} & \cdots & x_{ij} & \cdots & x_{in} \\ \vdots & \vdots & & \vdots & & \vdots \\ x_{m1} & x_{m2} & \cdots & x_{mj} & \cdots & x_{mn} \end{bmatrix}
 \end{aligned} \quad [3.15]$$

subject to:

$$\begin{aligned}
 & l_i \leq x_{ij} \leq u_i \\
 l = & \begin{bmatrix} l_1 \\ l_2 \\ \vdots \\ l_i \\ \vdots \\ l_m \end{bmatrix} \\
 u = & \begin{bmatrix} u_1 \\ u_2 \\ \vdots \\ u_i \\ \vdots \\ u_m \end{bmatrix}
 \end{aligned} \quad [3.16]$$

$$A_{eq} \cdot x - b_{eq} = 0 \quad [3.17]$$

$$A \cdot x - b \leq 0 \quad [3.18]$$

Where $f(\cdot)$ is the fitness or objective function, which is minimized during optimization; \mathbf{x} is the matrix of variables representing the objects in the domain of definition; n is the number of objects, each object is represented by variables and m is the number of the variables of each object; \mathbf{l} and \mathbf{u} are the vectors of the lower and upper boundaries of the variables, respectively; A_{eq} , b_{eq} , A , and b are the coefficients for constraint functions.

If the objective function is linear, then the optimization is called linear programme in mathematics, which can be quickly solved by taking a derivative of the function. If the objective function is nonlinear, then the optimization is called nonlinear optimization which can be solved by calculating the derivative or gradient of the function.

In engineering design, the objects in the defined domain are the design alternatives in the design space generated by the parametric model. The objective function and constraint functions are the design objectives and constraints, respectively, which are related to the numeric indicators of multiple kinds of performance. For most of the complex engineering designs, the relationships between input variables and the outputs of the objective function cannot be directly expressed by numerical equations. In other words, there is a complex system between the input variables and the outputs, which is a black box for the optimizer. It means the approach of taking derivatives or gradients are difficult to solve the optimization problems. To overcome the problem, stochastic optimizations are used (Nguyen et al., 2014). Moreover, in engineering designs, there are usually multiple objectives, then the optimization is a Multi-Objective Optimization (MOO). In integrated designs, if the variables, objectives, constraints, or the relationships among them are related to different disciplinary criteria, then the optimization is a Multi-Disciplinary Optimization (MDO).

3.4.2 Simulation-based stochastic optimization

3.4.2.1 Black-box system

For most complex problems, as mentioned above, it is usually difficult to use algebraic equations to formulate objective functions. In other words, for some problems, the fitness $f(\mathbf{x})$ in equation 3.15 is not a real function but a complex system. The relationships between the values of $f(\mathbf{x})$ and \mathbf{x} cannot be simply expressed in equations. Such a system is a black box for the optimizer.

In engineering design, the system between the inputs (design variables) and outputs (data related to indicators of multiple aspects) are the parametric model and simulations. A complex parametric model can be a black box. For this kind of models, the interrelationships between the inputs (design variables) and outputs (geometries) are not explicit. A simulation tool is also a black box, in which the relationships between the input (data and the geometry generated by parametric model) and the outputs (data related to indicators of multiple aspects) are implicit. The design process, which combines parametric modelling and building performance simulations, is called 'parametric simulation method' (Nguyen et al., 2014), and the optimization of such problems is called simulation-based optimization. Moreover, as mentioned, for these black-box systems, stochastic optimization is used, so that the optimization is simulation-based stochastic optimization. For such optimizations, searching algorithms are used to find 'well-performing' solutions.

3.4.2.2 Algorithms for simulation-based stochastic optimization

Various searching algorithms can be used to support stochastic optimizations. Carson & Maria (1997) classified these algorithms into six types of methods according to their characteristics. Amaran et al. (2016) classified the algorithms into seven types of methods in terms of the problem they solved.

To elaborate each of the algorithms is out of the range of this research. In order to apply simulation-based optimization in architectural design, it is worthy to define the characteristics of the design problems first and then select suitable algorithms. According to Amaran et al. (2016), these problems can be classified as: finding global or local optimal, the variables are continuous or discrete, the design space is finite or infinite/large, and the exploration to different extents, etc.

With respect to architectural conceptual design, as mentioned, it is a black-box problem, which means some of the objectives cannot be represented by numerical formulae, then it is difficult to use gradient-based algorithms which require derivable objective functions. For the design variables in architectural design, some are continuous, and some are discrete. But in real design, especially in conceptual designs, to simplify the problem and to consider the fabrication and construction, designers usually modify the continuous variables into discrete ones. Moreover, since the increasing emphasis on integrated design, more aspects are considered during the conceptual design phase, then the number of variables increases, which enlarges the design space. Therefore, the ranking and selection method, which requires a finite and fixed number of design alternatives, is not suitable for complex design problems.

Another issue should be noticed that algorithms aiming to find the optimal solutions within bounded time can take extensive long computation time for optimization problems in practice (Bianchi et al., 2009). Therefore, metaheuristics, which aim to find as good as possible or 'well-performing' solutions (not necessarily the optimal ones) within a reasonable time, are widely used in practice (Bianchi et al., 2009). In this light, considering the characteristics of architectural design problems, metaheuristics are highlighted in this research.

3.4.2.3 Metaheuristic algorithms

The word heuristics is from Greek, which means 'to find', and heuristics are approximation algorithms to search for good or 'well-performing' solutions (not necessarily the global optimal) in a solution space within an acceptable computational time (Bianchi et al., 2009). Meta is also from Greek, which means 'beyond, in an upper level', and metaheuristics are a framework of heuristic algorithms (Bianchi et al., 2009). Blum and Roli (2003) defined metaheuristics as:

“metaheuristics are high level concepts for exploring search spaces by using different strategies. These strategies should be chosen in such a way that a dynamic balance is given between the exploitation of the accumulated search experience (which is commonly called intensification) and the exploration of the search space (which is commonly called diversification). This balance is necessary on one side to quickly identify regions in the search space with high quality solutions and on the other side not to waste too much time in regions of the search space which are either already explored or don't provide high quality solutions.”

Besides those reviewed by Carson et al. (1997) and Amaran et al. (2005), some other typical metaheuristics algorithms that are frequently used in building design are listed below.

- Brute-force search (exhaustive enumeration)
- Hill-climbing (greedy algorithm)
- Tabu search
- Evolutionary algorithm (EA)
- Genetic algorithm (GA)
- Genetic programming
- Evolution programming
- Evolution strategy
- Simulated annealing (SA)

- Particle swarm optimization (PSO)
- Ant Colony optimization (ACO)

According to the statistic from Evins (2013), half of the reviewed optimizations for building designs used Genetic algorithms. According to the statistic from Nguyen et al. (2014), 40 of the 200 reviewed optimizations for building performance analyses used the Genetic Algorithm (GA). Harding (2014) made a simple test to compare four algorithms: Brute-force search, Hill-climbing, Simulated Annealing, Genetic Algorithm. This test indicated that, to some extent, Simulated Annealing and Genetic Algorithm are more efficient in obtaining the global optimal solution. Considering the frequent application and the efficiency in searching well-performing solutions, this research highlights Genetic Algorithm (GA) (Harding, 2014; Evins, 2013).

1 Genetic algorithm

Genetic Algorithm is a subset of evolutionary algorithms, which mimic the biological evolution based on genetic operations. Genetic algorithm was first proposed by Holland (1962; 1975), then Goldberg and Holland (1998) formulated a formal form of genetic algorithm which are widely used. Genetic algorithm runs iteratively. For each iteration, a population of solutions (called a generation of individuals) are generated. The first population is generated randomly. Based on the fitness (the satisfaction of the objectives) of the previous population, the next population is generated based on a series of operations (figure 3.8):

- Score: all the individuals in the current generation are ranked according to their fitness values.
- Select: a number of individuals with the best fitness values are selected as elites.
- Pass elite: the elites survive in the next population.
- Crossover: a number of individuals are selected as parents, and some elements in their variable vectors are exchanged according to certain criteria to generate crossover children as new individuals for the next generation.
- Mutation: a number of individuals are selected for mutation; some elements of their variable's vectors are changed according to certain criteria.

Generally, based on iterations, the values of the fitness function become smaller (if the objective is minimizing the fitness function). The iteration will stop when one of the terminal conditions is satisfied: the number of iterations reaches the maximum value (defined by the user), the average relative change in the fitness function value is smaller than the function tolerance (defined by the user), which means there is no progress for new iterations.

2 Interactive genetic algorithm

Since the performance data obtained by simulations are related to the quantitative design requirements, simulation-based optimizations can only search 'well-performing' designs based on quantitative design requirements. To combining the assessments of qualitative design requirements into these processes, interactive genetic algorithms are proposed. In these processes, designers are allowed to visually investigate the designs in each generation, and to control or dynamic orient the optimization, according to their design preferences and judgments on the qualitative design requirements.

von Beulow (2016) proposed 'ParaGen', to support multi-objective design optimization by using an interactive genetic algorithm called Non-Destructive Dynamic Population Genetic Algorithm (NDDP GA). In the selection step of a standard genetic algorithm, the old generation of individuals (except the elites) are removed when the new ones are generated. But in the NDDO GA, all the old individuals with their fitness values are stored in a database (SQL), and can be selected as parents to generate new individuals based on the operations of crossover or mutation. Designers are allowed to select the parents based on visual investigations of the designs (individuals) and the related fitness values.

Similarly, Mueller et al. (2015) proposed a genetic algorithm in which the operations of selection, crossover, and mutation can be handled by designers during iterations. The related workflow is illustrated in the right chart in figure 3.8. In the selection step of each generation, instead of a selection function, designers can visually investigate the designs and obtain the related fitness values, and then select the parents and elites. In the crossover step of each generation, designers can dynamically define how many new individuals (designs) are generated based on the crossover of parents. In the mutation step, instead of a fixed rate, designers can define the mutation rate.

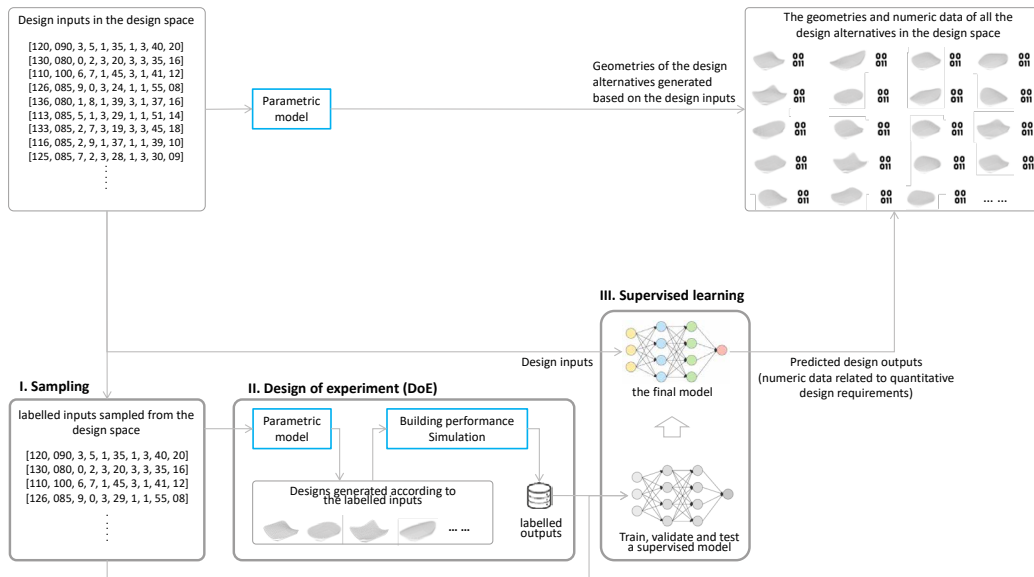


FIG. 3.8 An exemplary workflow of genetic algorithm (left) and interactive genetic algorithm (right) (Mueller et al., 2015)

3.4.3 Multi-Objective Optimization (MOO)

For the simulation-based stochastic optimizations applied for engineering designs, the number of design objectives (fitness functions) is usually more than one. Such optimizations are Multi-Objective Optimizations (MOOs). The fitness/objective function is modified based on equation 3.15:

$$\min. \{f_1(\mathbf{x}), f_2(\mathbf{x}) \cdots f_k(\mathbf{x})\} \quad [3.19]$$

where k is the number of the objectives and $k \geq 1$.

One of the challenges of MOO lays on the conflicts between different objectives. To find a trade-off among the conflicts in MOO, the theory of 'Pareto efficiency/optimality' proposed by Velfredo Pareto is used. In MOO, Pareto optimality is a statement in which the objects are not dominated to each other (Nguyen et al., 2014), and the set of all the non-dominated objects is called Pareto set or Pareto frontier.

Among several algorithms applying to search for Pareto solutions for MOO, NSGA-II (Non-dominated sorting genetic algorithm II) (Deb et al., 2002) is a frequently used genetic algorithm. In NSGA-II, a non-dominated rank is used to solve the assessment problem during iterations. Taking the procedure illustrated in figure 3.9 as an example, according to the ranking regulation of NSGA-II, in a population, if one individual (e.g. S6) is dominated to another individual (e.g. S13) and rank higher, it means S6 is better than S13 in at least one objective (fitness function), and no worse than S₁₃ in all other objectives (fitness functions). If some individuals do not dominate each other, they are a set of un-dominated individuals and will share the same rank. Based on the final rank, the following steps are similar to those of a standard genetic algorithm.

The result of the multi-objective optimization is a set of un-dominated individuals/designs which called Pareto Front. The number of these individuals/designs are predefined by users as a percentage of the population size. With respect to how to select ideal individuals/designs among Pareto solutions, there are several methods elaborated and compared by Ferreira et al. (2007). However, for architectural conceptual design, it is an important task for designers to select promising designs based on visual investigations according to their judgments on qualitative aspects (Brown et al., 2016)

3.4.4 Multi-Disciplinary Optimization (MDO)

As mentioned above, the integrated design of buildings, which considers a building as a complex system involving aspects related to multiple disciplines (of architecture, structure, HVAC, daylighting, energy, etc.), is emphasized during the conceptual design phase. Such a design process involves aspects related to multiple disciplines, and the performance of the multi-disciplinary system is determined by both the performance of each discipline and their interaction (Martins et al., 2010).

For the multi-disciplinary systems, multi-disciplinary optimizations (MDOs) are applied to search for 'well-performing' designs. Schmit (1960) involved other disciplines during structural optimization, which is considered as the first MDO. After that, MDOs were first widely used in aeronautics, especially in aircraft designs which involve the disciplines of structure, controls, aerodynamics, etc. So far, MDOs have been widely applied in various fields. For the applications of MDOs, one of the most important issues is how to organize the disciplinary analysis models (performance simulations) and the optimization tool according to the problem formulation (Martins et al., 2010). Such a combination of organization and problem formulation is called

MDO architecture. Various MDO architectures are elaborated and compared by researchers (Haftka et al. 1992; Cramer et al. 1994; Balling et al. 1996; Kroo, 1997; Martins et al., 2009).

With respect to the integrated design of buildings, Díaz et al. (2017) proposed strategies of MDO applying in the AEC industry, based on literature reviews. The strategies focus on the tool integration for MDO, which includes 1) selecting and determining tools according to the requisites of MDO, 2) testing the tools according to the requirements on component interoperability, automation, and parameterization, and 3) testing the integration of the tools in case studies. Specifically, for sports building designs, Yang et al. (2015; 2018) proposed MDO procedures for the envelope design of indoor sports buildings, which focused on three objectives: satisfying lighting comfort, reducing the energy consumption of artificial lighting by enhancing daylighting use, and reducing the weight of the structure. Turrin et al. (2016) proposed a framework of computational methods for sports building designs, which includes MDO. This research proposed an MDO design process for indoor arenas focusing on searching good solutions in wide design spaces containing diverse design alternatives generated based on the integration of multi-functional space and long-span roof structure (Pan et al., 2019a).

3.4.5 MOO-based conceptual design and its limitations

In building designs, to support integrated design involving multiple disciplines and to search for 'well-performing' designs according to quantitative design requirements, performance-based computational design (PCD), a process combining parametric model, building performance simulations, and multi-objectives optimization, is proposed and widely used (Sariyildiz, 2012; Turrin et al., 2011; Turrin et al., 2012; Gerber et al., 2012; Evins, 2013; Lin et al., 2014; von Buelow, 2012; Mueller et al., 2015; Yang et al. 2018; Pan et al. 2019a).

However, the limitations of MOO-based PCD are also discussed by researchers. First, it usually takes an extremely long time since the time-consuming building performance simulations, which makes it become unpractical (Wortmann et al., 2015; Tseranidis et al., 2016). Within a limited time of real design, the designs provided by MOO-based PCD may not be optimal but just some designs with mediocre or even poor performance (Wortmann et al., 2015).

Second, in practice, a design problem is usually ill-defined at the beginning (since there are no clear criteria for the assessments of some quantitative design

requirements), and the design process is usually non-linear and dynamic in which designers usually evaluate designs alternatives according to changing assessment criteria related to various aspects (Wortmann et al., 2015). However, in an optimization, the criteria should be predefined and unchangeable. Moreover, within the defined criteria, the number of design objectives is limited. When the objectives are more than three, it is difficult to find non-dominated solutions based on existing algorithms (IEEE Computational Intelligence Society, 2018).

Third, an optimization with a heuristic algorithm can find ‘well-performing’ designs with extreme values of design objectives, based on numeric assessments related to quantitative design requirements. However, it is limited in supporting further exploration of the whole design space. Most of the design alternatives in the design space are excluded. Comparing to accepting the ‘well-performing’ designs selected by optimization, a wide exploration is more crucial for architectural conceptual design to study diverse design alternatives (Tseranidis et al., 2016). Although interactive optimization allows designers to explore other designs within various generations during optimization iterations (von Buelow, 2012; Mueller et al., 2015; Harding et al., 2018), the range of the exploration is still limited.

3.5 Surrogate models based on supervised learning

3.5.1 Surrogate models

To overcome the time-consuming problem of simulation-based optimization and to support dynamic and wide design exploration, surrogate model method has been widely used in engineering fields to replace the building performance simulations (Wortmann et al., 2015). Surrogate model can approximate a high-fidelity but time-consuming function in reasonable accuracy by simple and fast computation, based on sampled data obtained by Design of Experiments (DoEs) of the high-fidelity function (Koziel, 2011; Tseranidis et al., 2016). This method has been applied in building designs (Hajela, 1992; Wortmann, 2015; Tseranidis et al., 2016; Yang, 2016; Pan et al., 2020), in which a surrogate model can be considered as a

mapping between design variables (inputs) and performance values (outputs) to replace the combined system of parametric model and BPSs. Surrogate models are usually achieved by regressions which can approximate the relationships between inputs and outputs.

In general, regression can be considered as a process to formulate a new mapping to approximate an unknown mapping according to a number of inputs and their related outputs (Koziel, 2011). The mapping represents the interrelationships between the inputs and outputs. The inputs and outputs are obtained by measurements in Design of Experiments (DoEs). In some cases, the measurements can be time-consuming or expensive, and it is necessary to select a limited number of inputs to perform DoEs and obtain the related outputs. The selection is called sampling.

The number of sampled inputs is related to the specific problem and defined by experience. A large number of sampled inputs need more time for the DoEs to obtain the related outputs, while a small number of them can decrease the accuracy of data approximation (Tseranidis et al., 2016; Koziel et al., 2011). There are many sampling methods, among which random, Monte Carlo, grid, and Latin Hypercube sampling, are frequently used. Based on the sampled inputs and the related outputs, which are called labelled data, a series of supervised learning methods can be used to perform regression and achieve surrogate models.

3.5.2 Supervised learning methods for surrogate models

Supervised or predictive learning is a process that learns a mapping between the inputs and outputs of a system, based on a labelled set of input-output pairs (training set) (Murphy, 2012). Specifically, for building designs, in general, the process can be divided into several steps (figure 3.9):

- 1 sample the input space to obtain a number of labelled inputs;
- 2 obtain the labelled outputs related to the labelled inputs by Design of Experiments (DoEs);
- 3 train, validate, and test the predefined supervised learning model, therefore, to obtain a defined model.

Based on the defined model, the design outputs (the numeric data related to quantitative design requirements) related to all the design inputs in the design space can be predicted. Moreover, based on the parametric model, the related geometries of all the design inputs can also be obtained.

Specifically, for step 3, a general training-validation-test approach can be further divided into:

- A use a part of the labelled set (training set) to train the model and learn the mapping between the inputs and outputs;
- B use another part of the labelled set (validation set) to validate the model;
- C repeat step a and b until the errors of the model for both the training set and validation set are acceptable;
- D use the last part of the labelled set (test set) to test the model.

If the error is still acceptable, then the model is defined. Besides this general training-validation-test approach, there are different approaches for this process (e.g. k-fold cross-validation, resubstitution, hold-out, and random subsampling) ((Murphy, 2012).

Various supervised learning models are used to achieve surrogate model. Some of them have been used in engineering or architectural designs, including Multi-Layer Perceptron Neural Network (MLPNN) (Tseranidis et al., 2016; Bre et al., 2018; Pan et al., 2020), poly-nominal regression and Response Surface Method (RSM) (Yang et al., 2016; Hiyama et al., 2015; Liu et al., 2019; Zhang et al., 2018), Random Forest (RF) (Tseranidis et al., 2016; Wang et al., 2018; Smarra et al., 2018), Radial Basis Function Network (RBFN) (Wortmann et al., 2015; Tseranidis et al., 2016), kriging (Tseranidis et al., 2016; Yi, 2016a; Yi, 2016b). Tseranidis et al. (2016) used and compared these methods to support the surrogate models for a long-span building design focusing on structural self-weight and energy consumption. The results of the case study indicated that the Multi-Layer Perceptron Neural Network (MLPNN) is the best method in the data approximation of structural weight and energy consumption for the example since it has the fastest speed and smallest errors.

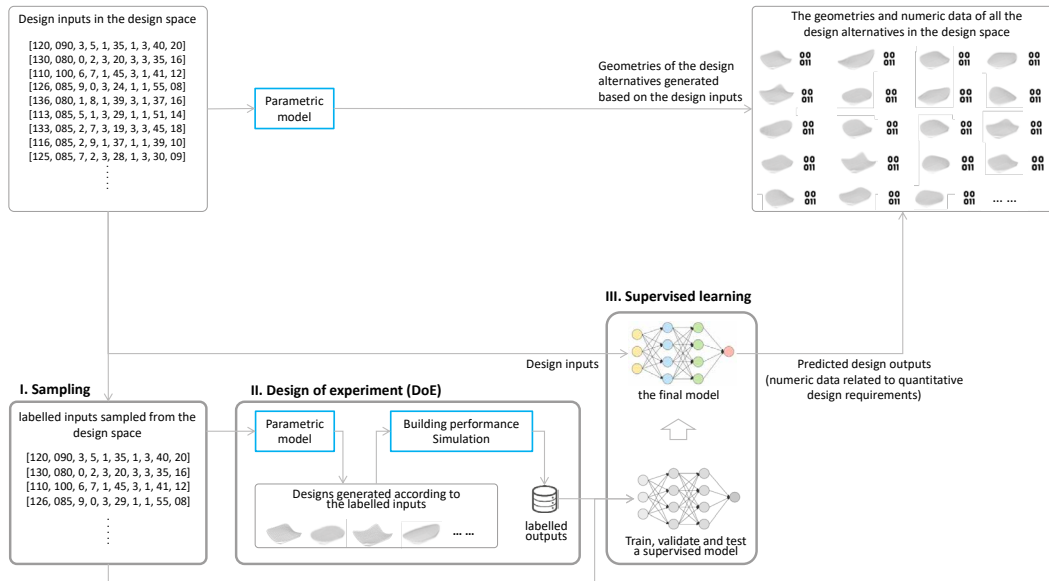


FIG. 3.9 A typical workflow of a surrogate model supported by supervised learning in architectural design

3.5.2.1 Multi-layer perceptron neural network

In general, a Multi-Layer Perceptron Neural Network (MLPNN) is composed of neural networks of an input layer, an output layer, and multiple hidden layers (figure 3.10, a). The input layer is related to the input data, and the number of the neurons on the layer equals the dimensions of the input data, while the output layer is related to the output data. Between them, multiple hidden layers connecting the output and input layers, which are used to learn a mapping between the inputs and outputs according to sampling data (labelled data).

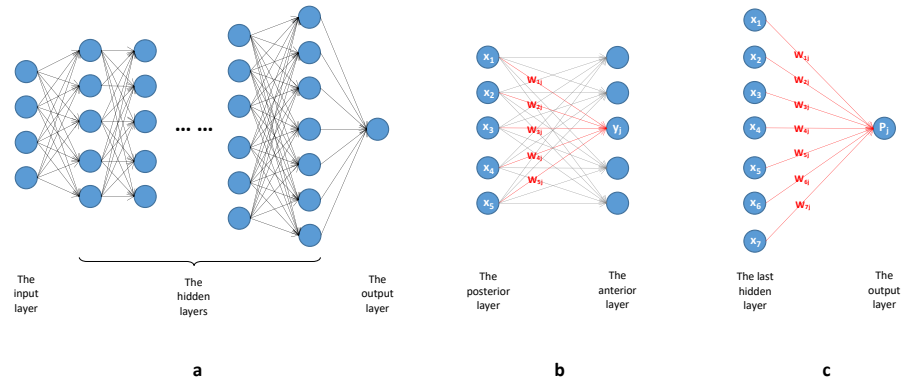


FIG. 3.10 An exemplary scheme of a Multi-Layer Perceptron Neural Network (MLPNN)

The connection between the neurons of two adjacent layers (figure 3.10, b) is based on the calculation related to activation function, bias, and the weighted sum of the values of the anterior neural layer (Murphy, 2012). In this paper, the calculation is expressed by the following equation:

$$y_j = f \left(b_j + \sum_{i=1}^n w_{ij} x_i \right)$$

$$j \in 1, m \quad [3.20]$$

$$j \in \mathfrak{N}$$

Where y_j is the value for the j th neuron in the posterior layer, $f(\cdot)$ is the activation function defined by users (table 3.3 lists some frequently used activation functions), b_j is the bias for this neuron, w_{ij} is the weight of the i th neuron in the anterior layer related to both the i th neuron in the anterior layer and the j th neuron in the posterior layer, x_i is the value of the i th neuron of the anterior layer, n and m is the number of the neurons in the anterior and posterior layers, respectively.

For the output layer (figure 3.10, c), according to (Murphy, 2012), the value of the neuron is calculated by:

$$P_j = \sum_{i=1}^s w_{ij} x_i$$

$$j \in 1, r \quad [3.21]$$

$$j \in \mathfrak{N}$$

Where P_j is the value for the j th neuron in the output layer, s is the number of the neurons on the last hidden layer, r is the number of the neurons in the output layer. For regression problems, r equals one, and for classification problems, r equals the number of the classes.

The neural networks learn the mapping between the inputs and outputs by adjusting the weights and bias for each neuron, until the error function is minimized, which is obviously an optimization process. The error/cost function (table 3.3) can be Mean Squared Error (MSE), Root Mean Squared Error (RMSE), average absolute error, coefficient of domination (R^2), relative average absolute error, etc. (Tseranidis et al., 2016). Backpropagation is used to feed back the error to the neural networks, therefore, can accelerate and improve the optimization process (Rumelhart et al., 1987; Werbos, 1990). The details of MLPNN can be found in (Murphy, 2012; Shanmuganathan, 2016).

For MLPNNs, the capability of universal approximation is verified (Cybenko, 1989), and they are also used as a universal function approximators in recent years (Shanmuganathan, 2016). Specifically, for the building designs, MLPNNs are widely used for the predictions of energy consumptions (Ahmad, et al., 2014; Rubio-bellido, et al., 2017; Amasyali, et al., 2018; Singaravel, et al., 2018; Series, 2019) structural analysis and design (Hajela, et al., 1992; Salehi, et al. 2018; Hashemi, et al., 2019) and integrated design (Tseranidis et al., 2016).

It worth noting that for the applications of MLPNN, the structures of neural networks (the number of the hidden layers, the amount of the neurons on each hidden layer) can be different. In fact, to define a proper network to obtain promising performance of data approximation is one of the main challenges of the applications of MLPNNs. Using growing neural networks as well as pruning techniques are two of the ways to find proper networks for specific problems (Shanmuganathan, 2016). Besides, the uncertainty of MLPNNs in data approximation is another main challenge of the applications of MLPNNs, which includes input uncertainty, parameter uncertainty, and structure uncertainty (Kasiviswanathan et al., 2016). A series of methods are proposed to quantify the uncertainties, therefore, to help users to evaluate the networks (Kasiviswanathan et al., 2016).

TABLE 3.3 Some activation functions and error functions for MLPNN

Activation functions	
Logistic/sigmoid function	$f(x) = \sigma(x) = \frac{1}{1 + e^{-x}}$
Gauss	$f(x) = e^{-x^2}$
TanH	$f(x) = \tanh(x) = \frac{e^x - e^{-x}}{e^x + e^{-x}}$
ElliotSig	$f(x) = \frac{x}{1 + x }$
Inverse square root linear unit (ISRLU)	$f(x) = \frac{x}{\sqrt{1 + \alpha x^2}}$
Piecewise linear unit (PLU)	$f(x) = \max\left(\left(\alpha(x + c) - c, \min(\alpha(x - c) + c, x)\right)\right)$
Rectified linear unit (ReLU)	$f(x) = \begin{cases} 0, & x \leq 0 \\ x, & x > 0 \end{cases}$

>>>

TABLE 3.3 Some activation functions and error functions for MLPNN

Activation functions	
Leaky rectified linear unit (Leaky ReLU)	$f(x) = \begin{cases} 0.01x, & x < 0 \\ x, & x \geq 0 \end{cases}$
Parametric rectified linear unit (PReLU)	$f(x) = \begin{cases} \alpha x, & x < 0 \\ x, & x \geq 0 \end{cases}$
Gaussian Error Linear unit (GELU)	$f(x) = x\mathcal{O}(x) = \frac{x(1 + \operatorname{erf}(\frac{\sqrt{2}}{2}x))}{2}$
SoftPlus	$f(x) = \ln(1 + e^x)$
Bent identity	$f(x) = \frac{\sqrt{x^2 + 1} - 1}{2} + x$

>>>

TABLE 3.3 Some activation functions and error functions for MLPNN

Error/cost functions (Tseranidis et al., 2016)	
Coefficient of domination (R2)	$1 - \frac{\sum_{j=1}^h (y_j - a_j)^2}{\sum_{j=1}^h (y_j - \bar{y})^2}$
Mean squared error (MSE)	$\frac{\sum_{j=1}^h (y_j - a_j)^2}{h}$
Root mean squared error (RMSE)	$\sqrt{\frac{\sum_{j=1}^h (y_j - a_j)^2}{h}}$
Root mean squared normalized error (RMSNE)	$\sqrt{\frac{\sum_{j=1}^h \frac{y_j - a_j}{y_j}}{h}}$
Average absolute error (AAE)	$\frac{\sum_{j=1}^h y_j - a_j }{n}$
Relative average error (RAAE)	$\frac{\sum_{j=1}^h y_j - a_j }{h \cdot STD(y)}$

y_j is the j th predicted output, a_j is the j th labelled output, h is the number of both predicted outputs and labelled outputs, \bar{y} is the average of all the predicted outputs

$$\bar{y} = \frac{\sum_{j=1}^h y_j}{h}$$

3.5.2.2 Poly-nominal regression and response surface method

A poly-nominal regression can approximate a mapping between independent variables (labelled inputs) and dependent variables (outputs) based on a formulated poly-nominal basis function (Murphy, 2012). Linear regression is the foundation of poly-nominal regression:

$$y = \mathbf{w}^T X + \bar{\epsilon} \quad [3.22]$$

In which, y is the labelled output, x is the labelled input, w is the weight of x and also the parameter of the regression model, ϵ is the residual error, n is the amount of the pair of labelled data. The function can be written in matrix notation as:

$$\begin{bmatrix} y_1 \\ y_2 \\ \vdots \\ y_j \\ \vdots \\ y_n \end{bmatrix} = \begin{bmatrix} 1 & x_1 \\ 1 & x_2 \\ \vdots & \vdots \\ 1 & x_j \\ \vdots & \vdots \\ 1 & x_n \end{bmatrix} \begin{bmatrix} w_0 \\ w_1 \end{bmatrix} + \begin{bmatrix} \epsilon_1 \\ \epsilon_2 \\ \vdots \\ \epsilon_j \\ \vdots \\ \epsilon_n \end{bmatrix} \quad [3.23]$$

However, for most of the practical problems, the mappings between the inputs and outputs are non-linear, which cannot be held by linear regression. Poly-nominal can deal with non-linear mapping by introducing complex non-linear function in the model of linear regression:

$$\begin{bmatrix} y_1 \\ y_2 \\ \vdots \\ y_j \\ \vdots \\ y_n \end{bmatrix} = \begin{bmatrix} 1 & x_1 & x_1^2 & \cdots & x_1^i & \cdots & x_1^m \\ 1 & x_2 & x_2^2 & \cdots & x_2^i & \cdots & x_2^m \\ \vdots & \vdots & \vdots & & \vdots & & \vdots \\ 1 & x_j & x_j^2 & \cdots & x_j^i & \cdots & x_j^m \\ \vdots & \vdots & \vdots & & \vdots & & \vdots \\ 1 & x_n & x_n^2 & \cdots & x_n^i & \cdots & x_n^m \end{bmatrix} \begin{bmatrix} w_0 \\ w_1 \\ \vdots \\ w_i \\ \vdots \\ w_m \end{bmatrix} + \begin{bmatrix} \epsilon_1 \\ \epsilon_2 \\ \vdots \\ \epsilon_j \\ \vdots \\ \epsilon_n \end{bmatrix} \quad [3.24]$$

Where m is the order/degree in the poly-nominal for the labelled inputs.

The transformation from equation 3.23 to equation 3.24 is called basis functional expansion, in which the model is still linear for the parameter w , therefore, the poly-nominal regression here is still a linear regression (Murphy, 2012). Furthermore, in the model of poly-nominal regression, multiple inputs can be added, which is multivariant poly-nominal regression. Take a two degree model for a three inputs problem as an example, the model can be written as:

$$\begin{bmatrix} y_1 \\ y_2 \\ \vdots \\ y_j \\ \vdots \\ y_n \end{bmatrix} = \begin{bmatrix} 1 & x_{11} & x_{12} & x_{13} & x_{11}^2 & x_{12}^2 & x_{13}^2 & x_{11}x_{12} & x_{11}x_{13} & x_{12}x_{13} \\ 1 & x_{21} & x_{22} & x_{23} & x_{21}^2 & x_{22}^2 & x_{23}^2 & x_{21}x_{22} & x_{21}x_{23} & x_{22}x_{23} \\ \vdots & \vdots \\ 1 & x_{j1} & x_{j2} & x_{j3} & x_{j1}^2 & x_{j2}^2 & x_{j3}^2 & x_{j1}x_{j2} & x_{j1}x_{j3} & x_{j2}x_{j3} \\ \vdots & \vdots \\ 1 & x_{n1} & x_{n2} & x_{n3} & x_{n1}^2 & x_{n2}^2 & x_{n3}^2 & x_{n1}x_{n2} & x_{n1}x_{n3} & x_{n2}x_{n3} \end{bmatrix} \begin{bmatrix} w_0 \\ w_1 \\ \vdots \\ w_9 \end{bmatrix} + \begin{bmatrix} \varepsilon_1 \\ \varepsilon_2 \\ \vdots \\ \varepsilon_j \\ \vdots \\ \varepsilon_n \end{bmatrix} \quad [3.25]$$

Where the x_{jk} is the k^{th} element of the j^{th} input vector. Obviously, the item of the input matrix increases a lot for multiple inputs problems. The learning process of the poly-nominal regression is to estimate the parameter w , to minimize the error. Least square estimation is frequently used to support the process. In the equation 3.25, if $m > n$, according to ordinary least squares estimation, there is (detail can be found in Murphy, 2012):

$$\hat{w} = (\mathbf{X}^T \mathbf{X})^{-1} \mathbf{X}^T \vec{y} \quad [3.26]$$

$$\sum_{j=1}^n \varepsilon_j^2 = \sum_{j=1}^n (y_j - w_j x_j)^2 \quad [3.27]$$

To learning the mapping between the inputs and outputs, the parameter w is adjusted to minimize the sum of the squared residual errors (equation 3.27). The respond surface method is based on poly-nominal regression, specifically for the cases in which the dimensions of inputs are more than one (multivariant poly-nominal regression). RSM has been used in architectural designs as surrogate

models to accelerate the optimization processes (Yang et al., 2016; Hiyama, et al., 2015; Liu et al., 2019; Zhang et al., 2018).

As mentioned above, the transformation of the model from linear regression (equation 3.23) to poly-nominal regression (equation 3.24) is called basis function expansion. In this expansion, the basis function of linear regression expands to a new one which includes higher degree of inputs and multiple inputs. In general, various machine learning methods are based on different basis functions (Murphy, 2012).

One of the main drawbacks of poly-nominal regression is that the basis function is non-local, which means the fitting of one set of inputs depends on other sets of inputs far away in the input space, which can lead to expensive computation (Magee, 1998). Some methods based on 'local' basis function are proposed, e.g. radial basis function network and local linear mapping based on self-organizing map.

3.5.2.3 Radial Basis Function (RBF) network

A typical radial basis function network (RBFN) is a three-layer neural network (figure 3.11) using RBF function as the activation function for the neurons on the hidden layer (Faris et al., 2017).

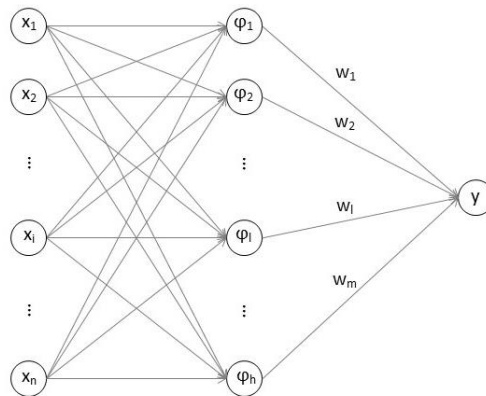


FIG. 3.11 A typical radial basis function network

A radius basis function (RBF) is a function of the norm (usually Euclidean) between the inputs x and the fixed centres c . The function can be Gaussian, multi-quadric, inverse quadratic, inverse multi-quadric, poly-harmonic spline, thin plate spline, etc. A gaussian RBF for a neuron of the hidden layer of an RBFN can be written as (Faris et al., 2017):

$$\varphi_l(x - c_l) = \exp\left(-\frac{\|x - c_l\|^2}{2\sigma^2}\right) = \exp\left(-\frac{\sum_{i=1}^n (x_i - c_{li})^2}{2\sigma^2}\right) \quad [3.28]$$

where $\varphi_l(\cdot)$ is the radius basis function of the l^{th} neuron on the hidden layer, x_i is the i^{th} element of the input vector x , n is the dimension of the input data, c_l is the centre vector of the l^{th} neuron on the hidden layer (which is usually obtained by unsupervised clustering), c_{li} is the i^{th} element of the vector c_l , h is the number of the neurons on the hidden layer (see figure 3.11), σ is the width of the Gaussian distribution.

Based on the activation function of each neuron of the hidden layer, the value of the output can be calculated (Faris, et al. 2017):

$$y(x) = \sum_{l=1}^h w_l \varphi(x - c_l) \quad [3.29]$$

where $y(x)$ is the output based on the input x ; h is the number of the neurons of the hidden layer; w_l is the weight of the l^{th} neuron of the hidden layer (see figure 3.11). To learning the mapping between the inputs and outputs, the parameters of w are adjusted to minimize the error function (MSE).

For Gaussian distribution, there is:

$$\lim_{(x-c_l) \rightarrow \infty} \varphi(\|x - c_l\|) = \lim_{(x-c_l) \rightarrow \infty} \exp\left(-\frac{\|x - c_l\|^2}{2\sigma^2}\right) = 0 \quad [3.30]$$

Hence, for the input x which is far away from the fixed centre c_l in the input space, the value of the activation function is small, and the effect of changing the weight w_l is small. For the input x , which is close to c_l , the value of the RBF is large, and the effect of changing the weight w_l is large. It means the RBF is a 'local' basis function.

The vector of the centre c (for each neuron on the hidden layer) is usually obtained by unsupervised clustering methods (e.g. k-means, self-organizing map) which can cluster input data points into different groups and obtained the vector of the centre for each group. Details of unsupervised clustering are elaborated in section 3.6.

RBFN has been used in building designs to support surrogate models in predicting various kinds of performance data (Ramedani et al., 2014; Assareh et al., 2015; Wortmann et al., 2015; Tseranidis et al., 2016).

3.5.2.4 Local Linear Mapping (LLM) based on Self-Organizing Map (SOM)

Local Linear Mapping (LLM) is another supervised learning method based on local basis functions. Being similar to RBFN, a clustering method is used to find the centres in input space to support the local basis function in LLM. Local Linear Map based on Self-Organizing Map (SOM-LLM) was proposed by Aupetit et al. (2014) based on the original Local Linear Map (LLM) which is formulated by using linear interpolation and additional weights (Moshou et al., 1997):

$$S_i(M) = N_i^{[out]} + A_i^T (M - N_i^{[in]}) \quad [3.31]$$

$$A_i^T = \sum_{j=1}^{n-1} \frac{(N_i^{[out]} - N_j^{[out]})(N_i^{[in]} - N_j^{[in]})}{\sum_{h=1}^p (|N_j^{[in]}[h] - N_i^{[in]}[h]|)^2} \quad [3.32]$$

$$S(M) = \sum_{i=1}^n \omega_i(M) \cdot S_i(M) \quad [3.33]$$

Equation 3.31 demonstrates a linear interpolation method, in which $S_i(M)$ is the output of the interpolated data calculated by the i^{th} reference data point, and M is the input of the interpolated data. [out] and [in] are the output and input of the i^{th} reference data point, respectively, which are known; A_i^T is the slop which can be calculated according to equation 3.32 in which j is the index of all the reference data point without the i^{th} one, n is the number of the reference data point, and p is the dimensions of the all the data which is related to the problem itself. In equation 3.33, each output (calculated by each reference data point according to equation 3.31) is

weighted by (M) (the weight of the i^{th} reference data point for the interpolated point M). (M) is the calculated output of the interpolated data point M. The weight $\omega_i(M)$ is calculated by the distances of between the reference points $N[in]$ and interpolated points M, and the sum of all the weights should equal one (Aupetit et al., 2014; Moshou et al., 1997):

$$d_{\alpha} \left(M, N_i^{[in]} \right) = \sum_{h=1}^p \left(\left| M_{[h]} - N_{i[h]}^{[in]} \right| \right)^{\alpha} \quad [3.34]$$

$$\omega_i (M) = \frac{\prod_{k=1, k \neq i}^n d_{\alpha} \left(M, N_k^{[in]} \right)}{\sum_{j=1}^n \left[\prod_{k=1, k \neq j}^n d_{\alpha} \left(M, N_k^{[in]} \right) \right]} \quad [3.35]$$

$$\sum_{i=1}^n \omega_i (M) = 1 \quad [3.36]$$

Equation 3.34 is a distance function which calculates the distance between the input of the interpolated data point M and the input of the i^{th} reference data point [in]. p is the dimension of the input data, and α is related to the type of distance (e.g. for the square of Euclidean distance $\alpha=2$). Equation 3.35 calculates the weight (M) by a series of distances calculated by equation 3.36.

Since each new interpolated data point is largely impacted by the nearby reference data, it is crucial to find the nearby reference data (from all the data) to calculate the interpolated data. Aupetit et al. (2014) used self-organizing map (SOM), a single-layer competition neural network proposed by Teuvo Kohonen (Kohonen, 1982; 2014), to find the cluster and neighbour clusters of each given interpolated point within a high dimension input data space. The details of SOM are elaborated in section 3.6, in which unsupervised clustering models are reviewed and discussed.

The trained SOM network can capture the whole input data space and preserve the topology of the data distribution, then projects them into an approximately 2D network. On the network, every input data point belongs to a cluster represented by the related neuron. This neuron and its neighbour neurons can be considered as

the nearby reference data points which are used to calculate the output of this input data point. The input vectors of all the neurons are the results of SOM, which means that the reference data are not pre-defined, and their related outputs should be obtained by design experiments or simulations.

Besides, in the SOM-LLM, in order to increase the accuracy, neighbouring influence kernel is proposed to modify the weights (M) (Aupetit et al., 2014). First, to define the influence region for a neuron (reference data point), natural cubic spline function (NCS) is introduced (Aupetit et al., 2014), in which, for any real number a and b, there is:

$$NCS(A, B) = \begin{cases} 0, & (b < 0) \cup ((a > b) \cap (b > 0)) \\ 1 - 3\left(\frac{a}{b}\right)^2 + 2\left(\frac{a}{b}\right)^3, & a \in [0, b] \\ 1, & (a < 0) \cap (b > 0) \end{cases} \quad [3.37]$$

Then a neighbouring influence function is defined (Aupetit et al., 2014):

$$A = \sqrt{d_2(M, N_h^{[in]})} + \sqrt{d_2(M, N_i^{[in]})} - \mu \sqrt{d_2(N_i^{[in]}, N_h^{[in]})} \quad [3.38]$$

$$B = \gamma \sqrt{d_2(N_i^{[in]}, N_h^{[in]})} \quad [3.39]$$

$$\sigma_{i,h}(M) = NCS(A, B) \quad [3.40]$$

$$\varphi_i(M) = 1 - NSC \sum_{h=1}^v (\sigma_{i,h}(M)), 1 \quad [3.41]$$

Where μ is the width of the fully activated region around the neighbouring neurons and γ is the width of the area between 0 and 1 of the neighbouring influence kernel; $N_i^{[in]}$ is the input vector of the i^{th} neuron representing the cluster the current interpolated data M belongs to, which is the result of SOM; $N_h^{[in]}$ is the input vector of the h^{th} neuron (one of the neighbouring neurons of the i^{th} neuron), according to the result of SOM; $\sigma_{i,h}(M)$ is the influence of the i^{th} and h^{th} neurons for the interpolated data point M ; and $\phi_i(M)$ is the total influence of the i^{th} neuron for the interpolated data point M .

Therefore, the $\omega_i(M)$ in equation 3.35 is modified as (Aupetit et al., 2014):

$$\omega_i(M) = \frac{\prod_{k=1, k \neq i}^n \left[1 + \varphi_k(M) \cdot \left(d_2(M, N_k^{[in]}) - 1 \right) \right]}{\sum_{j=1}^n \left[\prod_{k=1, k \neq j}^n \left[1 + \varphi_k(M) \cdot \left(d_2(M, N_k^{[in]}) - 1 \right) \right] \right]} \quad [3.42]$$

Finally, the output of the interpolated data point (M) can be calculated by equation 3.31 and equation 3.33 with the modified weights calculated by equation 3.42.

Comparing with poly-nominal regression, SOM-LLM is computationally cheap and can be used to solve high-dimensional problems. Comparing with Multi-Layer Perceptron Neural Network (MLPNN), a two-dimensional problem had been used to verify the SOM-LLM has equivalent performance in functional approximation (Shepard, 1968). Besides, SOM-LLM is considered to be able to limit the interference and avoid the optimization of a non-convex cost function which can be stuck in local minima but is necessary for MLPNN (Aupetit et al., 2014).

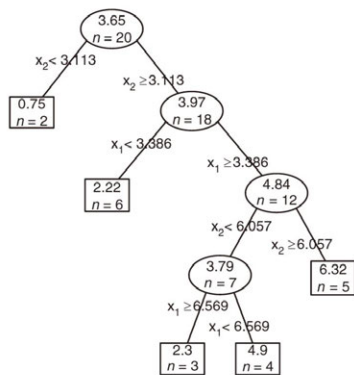
3.5.2.5 Decision/regression tree

Decision tree is an inverse tree-shape model composed of nodes (figure 3.12, left). Each of the nodes split the input data set into groups which have high probabilities related to one output (Olson and Wu, 2017). It can be used for both classification tasks and regression tasks for continuous outputs. Specifically, the decision trees for the numeric predictions in regression tasks are defined as regression trees (Witten and Frank, 2005; Olson and Wu, 2017).

A typical example of regression tree is provided by Torgo (2017) and illustrated in figure 3.12. In the inverse tree-shape (figure 3.12, left), the node in the top consists of all the inputs. The node is divided into two in the sequent level, and correspondingly the input space is also divided into two domains (figure 3.12, right). These two nodes can be further divided into other nodes in different levels of the inverse tree-shape model, until the bottom level. The nodes of the bottom level are called leaves, which correspond to the sub domains in the input space. Each of the sub domains is related to an output. Based on this model, the relationships between the inputs and outputs are formulated.

To learn the relationships, recursive partitioning algorithm is used. In the algorithm, the results of the best logical test about one of the outputs are selected. According to the results, the input space is divided into two parts. The first part includes the inputs which are related to the selected outputs, and the other part includes other inputs. This process repeats to divide the input space into many parts, until the square error is minimized. As a result, a large tree with many leaves is formulated, and then a pruning tree process is used to cut the tree to decrease the leaves, aims at avoiding overfitting. Details of the algorithm and the pruning tree process can be found in (Torgo, 2017)

Example regression tree



Partitioning of the predictors' space

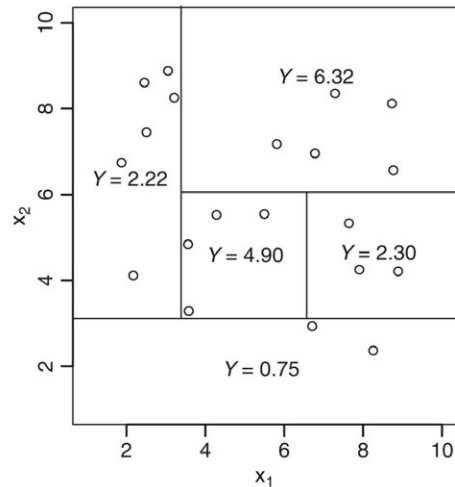


FIG. 3.12 A regression tree (left) and the related predictors' space (right) (Torgo, 2017)

Specifically, for building designs, Yu et al. (2010) use decision a tree for building energy demand modelling. Tseranidis et al. (2016) use regression trees to predict

the structural weight and energy consumption for long-span buildings. Wang et al. (2018) use regression trees to predict hourly building energy.

3.5.3 **Limitations of surrogate models based on supervised learning**

The reviewed and studies above show that various supervised learning methods are proposed and applied to achieve surrogate models in building designs to predict different performance data, which saves much time for the design process and supports dynamic design exploration that designers can arbitrarily investigate any design (in theory). However, there are still limitations.

- 1 It lacks an efficient organization for the numerous designs and the related information (numeric data and geometries). Each design alternative is independent in the design space. Although the related numeric data related to quantitative design requirements and geometry can be easily obtained, it is impractical for designers to deal with a mass of information about the numerous design alternatives during design exploration.
- 2 There are uncertainties in the application of supervised learning methods, including input uncertainty, parameter uncertainty, and structure uncertainty (Kasiviswanathan et al., 2016). The input uncertainty is related to the errors in sampling and DoEs. The parameter uncertainty refers to that it cannot ensure to find a unique set of the best parameters for a specific model. The structure parameters are related to the simplification of the mathematical processes in explaining complex nature phenomena. In this research, since the sampled inputs and the outputs obtained by the parametric model and simulations are considered as trusted data, the input uncertainty is not considered. However, the parameter and structure uncertainty can influence the design exploration. For a supervised learning model, the errors may be acceptable in the training-validation-testing process but may become too large when the model is applied for other data, and designers may perform design exploration based on incorrect data unknowingly. Kasiviswanathan et al. (2016) reviewed some methods to quantify the uncertainties of supervised learning models, but the methods cannot guarantee the elimination of the uncertainties.

3.6 Unsupervised clustering based on Self-Organizing Map (SOM)

3.6.1 Clustering

Unsupervised learning is another subset of machine learning, in which the main task is clustering (Murphy, 2012). Generally, clustering can be considered as a process to arrange objects into various groups (clusters) according to specific features identified by their related data, so that the objects within the same cluster are similar in the features, while the objects in different clusters are different (Jain et al., 1988; Xu et al. 2015). The similarity/dissimilarity for the objects is defined by distances related to the input data (Xu et al. 2015).

Various methods can be used to perform clustering, which can be classified into twelve types (Sexena et al., 2017). These methods are widely used in various fields. Specifically, for building designs (among various applications), K-means clustering is used to cluster design alternatives in each generation of interactive optimizations, according to their geometry features (Harding et al., 2018). Hierarchical clustering to group design alternatives selected by MOO, according to their geometry feature (Pan et al., 2019b). Self-Organizing Maps (SOMs) are used to group design alternatives of the whole design space according to the geometry features (Harding, 2016; Pan et al., 2018; 2019b; 2020). Among these methods, self-organizing map is considered to be suitable to cluster numerous design alternatives and reflect the design space according to geometry typology (Harding, 2016; Harding et al. 2018).

3.6.2 Self-Organizing Map (SOM)

Self-Organizing Map (SOM), an artificial neural network (ANN) model proposed by Teuvo Kohonen (Kohonen, 1982), is considered as a model-based algorithm (Sexena et al., 2017) which uses a predefined model to cluster objects. In SOM, to cluster the objects, the nodes of a predefined artificial neural network move to and capture different objects iteratively, according to specific functions and regulations. The objects captured by the same nodes belong to the same clusters. Such a process is fulfilled based on a series of steps (Kohonen, 2014):

- 1 Before the iteration, a neural network is formulated by users to define the number of neurons and the topology of the network.
- 2 For each iteration, every input data point (object in the input data space) is investigated one by one, to find the nearest neuron on the network, according to a distance function (e.g. Euclidean distance). The nearest neuron, which is called the Best Matching Unit (BMU) for the input data point, then moves to the related data point (object) in a step.
- 3 The neighbour neurons near the BMU, which are defined by a neighbourhood function, also move with it.
- 4 The above two steps repeat for each iteration, and this phase is called 'the ordering phase'. During this phase, the length of the step, with which the BMUs and their neighbour neurons move to the related data points (objects), reduces gradually from a given learning ratio to 0 until the iteration times meets the terminal condition. Such reduction makes the network transforming largely at the beginning of the phase and becoming stable at the end.
- 5 Following the ordering phase is a 'tuning phase'. For each iteration within this phase, step 2 is repeated, but only the BMUs move to the related data points (objects) without taking the neighbours, and the length of the moving step will also gradually reduce from another given learning ratio to 0 until the iteration times meet the terminal condition. Such a phase makes the BMUs getting closer to the related data points, then the network can furtherly capture the input space while keeping the overall topology learnt during the ordering phase.

Comparing to other frequently used clustering algorithms (e.g. k-means, hierarchical clustering), one of the advantages of SOM is that it not only groups similar objects in the same cluster but also gather similar clusters closely and make different clusters being far away on the network (map) (Kohonen, 2014). This characteristic of SOM illustrates the distribution of the objects, based on which designers can have a quick glimpse of the data space and select preferred clusters.

3.6.3 Design exploration of different types of geometries based on SOM

Based on the general process of SOM introduced above, every input data point can be captured by one neuron of a predefined two-dimensional SOM network, and all the data points captured by the same neuron are grouped in the same cluster and are represented by this neuron. On the network, similar neurons are located closely while the different ones are far away, which reflects the intrinsic topology of the input data set (Harding et al., 2016).

In this light, SOM clustering can be used to group design alternatives according to the features related to the input data. One of the applications of SOM clustering in architectural design is to group design alternatives according to their geometry features, and to present the representative design for each group on the network, therefore, to reflect the design space. Based on the information, designers can have an overview of the design space and visually investigate each type of design alternatives, according to their experience and knowledge about qualitative design requirements. Moreover, designers can select several types/clusters of design alternatives to make further exploration based on the visual investigations of the design alternatives in each of the selected type/cluster. This method has been applied in the design explorations of architectural design (Harding, 2016; Harding et al. 2018) (Figure 3.13).

In this method, the design parameters (directly related to building geometry) of each design alternative within design space are used as the inputs to train a predefined two-dimensional SOM-network. Since the design parameters related to geometry are used as the inputs, design alternatives with similar geometries are grouped in the same clusters based on the algorithm of SOM. For each cluster, the vector of the neuron can be obtained during the training process, and the vector is actually the design parameters of the neural/node design (which represents all the designs within this cluster). By using the parametric model, the geometries of the neural/node designs can be generated according to the vectors. All the neural designs representing their own clusters of designs are presented on the trained two-dimensional SOM network, and similar ones are closed while different ones are far away, which can reflect the design space. Therefore, designers can have a quick glimpse of the whole design space and explore all the design alternatives based on geometry typology.

However, this method does not deal with numeric data of design alternatives related to quantitative design requirements, which is a limitation in supporting design exploration.

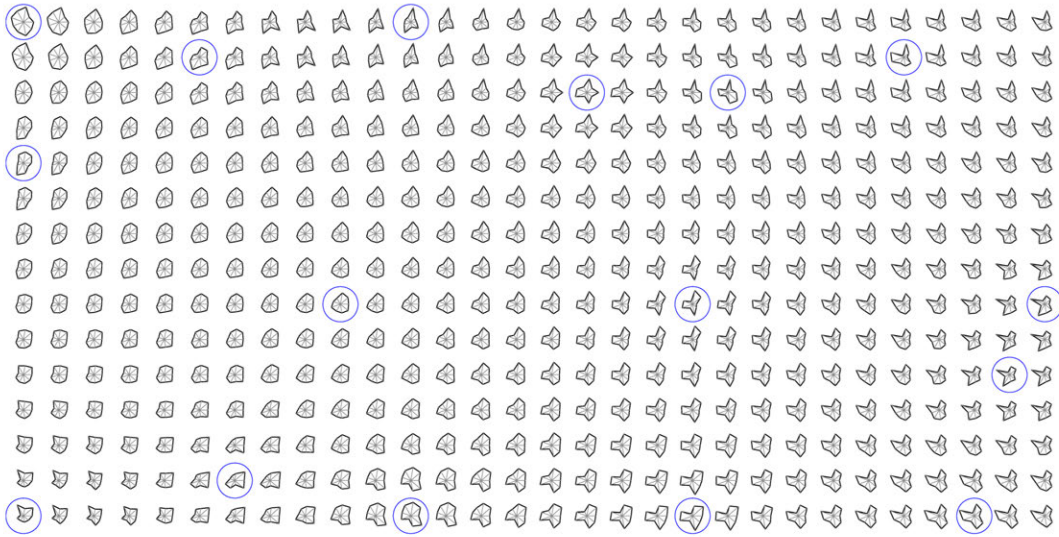


FIG. 3.13 An example of using SOM clustering to group design alternatives to geometry features (Harding, 2016).

3.7 Assumption of a computation method for the conceptual design of indoor arenas

In chapter 2, three basic demands of the conceptual design of indoor arenas with emphasis on the integration of the multi-functional space and long-span roof structure are formulated.

- 1 Integrating the multi-functional space and long-span roof structure and generating numerous and diverse design alternatives.
- 2 Obtaining adequate information to support the exploration of the generated designs based on both numeric data and visual investigations, therefore, to support designers to assess the satisfactions of both quantitative and qualitative design requirements.

- 3 Supporting designers to select promising designs according to the assessments, in which designers' different emphases on quantitative or qualitative design requirements should be taken into account.

Based on the review and studies of computational methods above, a hypothetical method is proposed to satisfy the demands based on different components.

- 1 To satisfy the first demand, parametric modelling is used to integrate the multi-functional space and long-span roof structure and generating numerous and diverse design alternatives. To overcome the limitation related to the lack of diversity of the generated design alternatives in conventional parametric models, a versatile and flexible parametric model specifically for indoor arenas should be proposed, which can generate most of the feasible indoor arena designs based on the integration of multi-functional space and long-span roof structure.
- 2 To satisfy the second demand, the parametric modelling provides the geometries of design alternatives, therefore, to support the visual investigations related to the assessments of the qualitative design requirements. A series of numeric indicators and related Building Performance Simulations (BPSs) corresponding to multi-functionality and structural performance are used to support the designers to assess the satisfactions of quantitative design requirements. However, it is impractical to demonstrate all the information of numerous generated designs. More components are needed to facilitate designers to strategically explore the design space, with consideration of different scenarios in practice.
- 3 To satisfy the third demand, based on the parametric model and BPSs, MOO, surrogate model based on supervised learning, and SOM-clustering are used to facilitate designers to strategically explore the design space in different ways, with consideration of different scenarios in practice. Corresponding to the three scenarios formulated in chapter 2, three different workflows are proposed.
 - A For the scenario in which designers prioritize numeric assessments related to quantitative design requirements, MOO based on the versatile and flexible parametric model for indoor arenas is used to search 'well-performing' designs based on quantitative design requirements. Then, designers can visually investigate these designs according to their experience and knowledge about the qualitative requirements.
 - B For the scenario in which designers prioritize visual investigations related to qualitative design requirements, SOM-clustering is used to reflect the design space according to geometry typology, therefore, to support designers to

visually investigate different types/clusters of designs and select the preferred types. Then, MOO can be used for these types of designs to search for 'well-performing' designs according to numeric assessments related to quantitative design requirements.

- c For the scenario in which designers place the same priority to both numeric assessments related to quantitative design requirements and visual investigations related to qualitative design requirements, both surrogated model and SOM-clustering are used to obtain the information of design alternatives and to organize and demonstrate the information in an efficient way.

3.8 Summary

This chapter reviews and studies several computational design methods which are frequently used for architectural conceptual designs. Based on the review and studies, the capabilities and limitations of these methods in supporting the conceptual design of indoor arenas are clarified, according to the related basic demands formulated in chapter 2. These methods are parametric modelling, Building Performance Simulations (BPSs), Multi-Objective Optimization (MOO), surrogated model based on supervised learning, and unsupervised clustering based on Self-Organizing Map (SOM).

- 1 Parametric modelling can associate various elements of the building into an intact form controlled by parameters, based on which numerous designs can be generated to compose a design space. Conventional parametric models are usually fixed in one or several types of design. It lacks a versatile and flexible parametric model for indoor arenas to integrate the multi-functional space and long-span roof structure and generate diverse types of designs.
- 2 Building Performance Simulations (BPSs) can obtain the numeric data of various indicators related to quantitative design requirements. Nevertheless, it is necessary to formulate specific numeric assessment criteria for indoor arena related to quantitative design requirements about multi-functionality (the spatial capacity, spectator's view, and acoustics) and structure and to specify related BPS tools to the criteria.

- 3 MOO can be used to search for 'well-performing' designs according to numeric criteria related to quantitative design requirements. However, it excludes other designs in the design space. Moreover, the criteria cannot be changed, and the number of design objectives cannot be more than three during MOO, which limits the dynamic exploration of various design objectives. Besides, since the 'well-performing' designs are selected based on numeric assessment, a standard MOO limits the visual investigations of most of the design alternatives in the design space, which are crucial for the assessments of the qualitative design requirements.
- 4 Surrogate model based on supervised learning can predict numeric data of designs related to quantitative design requirements. Therefore, it is possible to obtain the information about the geometry and numeric data of numerous designs, based on the parametric model and the surrogate models. However, it is impractical for designers to investigate mass information which is not organized and demonstrated in an efficient way.
- 5 SOM-clustering can support designers to have an overview of the design space according to the geometry features of the designs and to visually investigate and select designs based on geometry typology, according to their knowledge and experience of qualitative design requirements. However, this process does not deal with numeric assessments related to quantitative design requirements.

Based on the capabilities and limitations of the methods, a hypothetical method is proposed. In the methods, a versatile and flexible parametric model for indoor arenas and a series of numeric indicators with related simulations tools (focusing on multi-functionality and structural performance) are proposed as the foundation. Based on the foundation, MOO, surrogate model based on supervised learning, and SOM-clustering are used to support designers to strategically explore design alternatives in the design space in three different ways, to support the three scenarios (in which designers place different emphasis on numeric assessments related to quantitative design requirements and visual investigations related to qualitative design requirements).

Reference

- 3ds Max (Autodesk), <https://www.autodesk.co.uk/products/3ds-max/overview>
- Ahmad, A.S., Hassan, M.Y., Abdullah, M.P., Rahman, H.A., Hussin, F., Abdullah, H., Saidur, R. (2014) A review on applications of ANN and SVM for building electrical energy consumption forecasting, *Renewable and Sustainable Energy Reviews*, 33, pp.102–109. DOI: 10.1016/j.rser.2014.01.069.
- Amaran, S., Sahinidis, N.V., Sharda, B., Bury, S.J. (2016) Simulation optimization: a review of algorithms and applications, *Annals of Operation Research*, 240, pp.351–380. DOI: 10.1007/s10479-015-2019-x.
- Amasyali, K., El-gohary, N.M. (2018) A review of data-driven building energy consumption prediction studies, *Renewable and Sustainable Energy Reviews*, 81, pp.1192–1205. DOI: 10.1016/j.rser.2017.04.095.
- ANDERSON, J. D. (1995). *Computational fluid dynamics : the basic with applications*, New York, McGraw-Hill.
- ARUP (2014) STAG:Stadium Generator ,2014. <https://www.arup.com/expertise/services/buildings/architecture>. [Accessed: 7-April-2019]
- Assareh, E., Biglari, M. (2015) A novel approach to capture the maximum power from variable speed wind turbines using PI controller, RBF neural network and GSA evolutionary algorithm, *Renewable and Sustainable Energy Reviews*, 51, pp. 1023-1037. DOI: 10.1016/j.rser.2015.07.034
- Aupetit, M., Couturier, P., Massotte, P. (2014) Function Approximation with Continuous Self-Organizing Maps using Neighboring Influence Interpolation, in: Bothe, H., Rojas, R., Fyfe, C. (Eds.), *Proceedings of Neural Computing.*, International Computer Science Conventions, Berlin, 2014.
- Balling, R. J., Sobieszczanski-Sobieski, J. (1996). Optimization of Coupled Systems: A Critical Overview of Approaches. *AIAA Journal*, 34(1), pp. 6–17. DOI: 10.2514/3.13015.
- Barrios, C. (2005), *Transformations on Parametric Design Models*. In: *Computer Aided Architectural Design Futures*, Springer, Netherlands, pp. 393-400.
- Beranek L. L., Analysis of Sabine and Eyring equations and their application to concert hall audience and chair absorption. *Journal of the Acoustical Society of Americas*, 120(3), pp.1399-1410. DOI: 10.1121/1.2221392
- Bianchi, L., Dorigo, M., Maria, Gambardella, L. M., Gutjahr, W. J. (2009) A survey on metaheuristics for stochastic combinatorial optimization. *Natural Computing*, 8, pp. 239-287. DOI: 10.1007/s1147-008-9098-4.
- Binkley, C., Jeffries, P., Vola, M. (2014) Design computation at Arup, in: Spiegelhalter, T., Andia, A. (Eds.), *Post-Parametric Automation in Design and Construction*, Artech House Publishers, London, 2014, pp. 112–120. ISBN-10: 1608076938
- Blum, C., Roli, A. (2001) Metaheuristics in Combinatorial Optimization: Overview and Conceptual Comparison, *ACM Computing Surveys* 35, pp.268-308. DOI: 10.1145/937503.937505.
- Bork, I. (2005). Report on the 3rd round robin on room acoustical computer simulation -Part II: calculations, *Acta Acustica united with Acustica*. 91 (4) 753–763.
- Bre, F., Gimenez, J.M., Fachinotti, V.D. (2018) Prediction of wind pressure coefficients on building surfaces using artificial neural networks, *Energy and Buildings* 158, pp. 1429–1441. doi:10.1016/j.enbuild.2017.11.045.
- Brown, N.C., Mueller, C.T. (2016). Design for structural and energy performance of long
- Carson, Y., Maria, A. (1997). *Simulation Optimization: Methods and Applications*. In: 1997 winter Simulation Conference. Atlanta, Georgia, USA: IEEE, pp. 118-126.
- Catia (Dassault Systems), https://www.3ds.com/products-services/catia/?wockw=card_content_cta_1_url%3A%22https%3A%2F%2Fblogs.3ds.com%2Fcatia%2F%22
- CEN (1995) En-1991-2-4:1995. Actions on structures - Part 1-4: General actions -Wind actions
- CEN (2003) EN 1991-1-3:2003. Actions on structures - Part 1-3: General actions -Snow Loads.
- Christofides, N. (1975) *Graph theory: An algorithmic approach*. Academic press, New York.
- Cook, N. (2007). *Designers' Guide to EN 1991-1-4 Eurocode 1 - Actions on Structures, General Actions, Part 1-4: Wind Actions*, ICE Publishing.
- Cormen, T.H., Leiserson, C.E., Rivest, R.L., Stein, C. (2001) *Introduction to algorithms*. MIT press.
- Courant, R. (1943). Variational methods for the solution of problems of equilibrium and vibrations. *Bulletin of the American Mathematical Society*. 49(1), pp.1-23. DOI:10.1090/s0002-9904-1943-07818-4.
- Cramer, E. J., Dennis Jr., J. E., Frank, P. D., Lewis, R. M., and Shubin, G. R., (1994) Problem Formulation for Multidisciplinary Optimization, *SIAM Journal on Optimization*, 4(4) pp. 754–776. DOI:10.1137/0804044.

- Cremer, L., Mueller, H. (1982). Principles and Applications of Room Acoustics, Vol. 1, English translation with additions by T. J. Schultz (Applied Science Publishers, Essex, England) and in USA and Canada (Elsevier, New York). Originally published in German (1978) by Hirzel, Stuttgart. [Referred to throughout his article as C&M.]
- Cybenko, G. (1989) Approximation by Superpositions of a Sigmoidal Function, *Mathematics of Control, Signals and Systems*, 2, pp.303–314. <https://link.springer.com/article/10.1007/BF02551274> [Accessed: 7-April-2019]
- Deb, K., Pratap, A., Agarwal, S., Meyarivan, T. (2002) A fast and elitist multiobjective genetic algorithm: NSGA-II, *IEEE Transactions on Evolutionary Computing* 6 (2), pp. 182–197, DOI: 10.1109/4235.996017.
- Díaz, H., Alarcón, L. F., Mourgues, C., García, S. (2017) Multidisciplinary Design Optimization through process integration in the AEC industry: Strategies and challenges. *Automation in Construction*, 73, pp. 102–119. DOI: 10.1016/j.autcon.2016.09.007
- Ding, J., Mei, H. (eds) (2017) *Manual of Architectural design* (book six), China Architectural and Building Press, Beijing, China. ISBN 978-7-112-20944-6.
- Dino, I.G. (2012). Creative Design Exploration by Parametric Generative Systems in Architecture. *METU Journal of Faculty of Architecture*, 29(1), pp. 207–224. DOI:10.4305/metu.jfa.2012.1.12.
- Dynamo Revit (Autodesk), <https://dynamobim.org/>.
- Elorza, D. (2005) Room Acoustics Modelling using the Ray-tracing Method: Implementation and evaluation. M.Sci, Universtiy of Turku.
- Emami, N. (2019) Untangling parameters: A formalized framework for identifying overlapping design parameters between two disciplines for creating an interdisciplinary parametric model. *Advanced engineering informatics*, 42, pp.1–13. DOI: 10.1016/j.aei.2019.100943.
- Estrado E. (2019) Optimisation of complex geometry buildings based on wind load analysis. Delft University of Technology. <http://resolver.tudelft.nl/uuid:bea970ba-da91-40e5-b31d-53cf0cb15ec3>
- Evins, R. (2013) A review of computational optimisation methods applied to sustainable building design, *Renewable and Sustainable Energy Review*, 22, pp.230–245. DOI: 10.1016/j.rser.2013.02.004.
- Eyring, C. F. (1929) Reverberation Time in Dead Rooms. *The Journal of the Acoustical Society of America*, 1(2A), pp. 217–241. DOI: 10.1121/1.1901884
- Faris H., Aljarah, I., Mirjalili, S. (2017) Evolving radial basis function network using moth-flame optimization. In: *Handbook of Neural Computation*, Academic press, pp. 537–550. DOI.10.1016/B978-0-12-811318-9.00028-4
- Ferreira, J. Fonseca, C., Gaspar-Cunha, A. (2007). Methodology to select solutions from the pareto-optimal set: a comparative study. In: the 9th annual conference on Genetic and evolutionary computation. New York, New York, USA: ACM, pp.789–796
- Gane, V., Haymaker, J., (2010). Design Scenarios: Enabling Requirements-Driven Parametric Design Spaces. In: Stanford Center for Integrated Facility Engineering Technical Report # 194. https://stacks.stanford.edu/file/druid:pk865yz9898/TR194_0.pdf
- Generative Components (Bentley Systems), https://communities.bentley.com/products/products_generativecomponents/w/generative_components_community_wiki
- Gerber, D., Lin, S., Pan, B., Solmaz, A. (2012). Design Optioneering: Multidisciplinary Design Optimization through Parameterization, Domain Integration and Automation of a Genetic Algorithm, in: *Symp. Simul. Archit. Urban Des.*, 2012: pp. 23–30.
- Goldberg, D.E., Holland, J.H. (1988). Genetic algorithms and machine learning. *Machine learning*, 3 (2), pp. 95–99. DOI: 10.1023/A:1022602019183
- Grasshopper (GH, McNeel & Associates) Robert McNeel & Associates, grasshopper, (n.d.). <http://www.grasshopper3d.com>
- Haftka, R. T., Sobieszczanski-Sobieski, J., and Padula, S. L., (1992) On Options for Interdisciplinary Analysis and Design Optimization, *Structure Optimization*, 4, pp. 65–74
- Hajela, H., Berke, L. (1992). Neural networks in structur analysis and design: an overview, *Computing Systems in Engineering*, 3 (1–4), pp. 535–538. DOI:10.1016/0956-0521(92)90138-9
- Harding, J. (2014) Meta-parametric design: Developing a computational approach for early stage collaborative practice . EngD. University of Bath.

- Harding, J. (2016). Dimensionality reduction for parametric design exploration. In: Adriaenssens, S., Gramazio, F., Kohler, M., Menges, A., Pauly, M. (Eds.) *Advances in Architectural Geometry AAG 2016*. Zürich, Switzerland: vdf Hochschulverlag AG an der ETH Zürich, pp. 274–287. doi:10.3218/3778-4.
- Harding, J., Brandt-Olsen, C. (2018). Biomorpher: Interactive evolution for parametric design. *International Journal of Architectural Computing*, 16, pp. 144–163. doi:10.1177/1478077118778579.
- Hashemi, S., Sadeghi, K., Fazeli, A., Zarei, M. (2019) Predicting the Weight of the Steel Moment-Resisting Frame Structure, *International Journal of Steel Structures*, 12, pp.168–180. DOI: 10.1007/s13296-018-0105-z.
- Hiyama, K., Wen, L. (2015) Rapid response surface creation method to optimize window geometry using dynamic daylighting simulation and energy simulation, *Energy and Buildings* 107, pp. 417–423. DOI:10.1016/j.enbuild.2015.08.035.
- Holland, J. H. (1962). Outline for a logical theory of adaptive systems. *Journal of the Association for Computing Machinery*, 3, pp. 297–314.
- Holland, J. H. (1975). *Adaptation in natural and artificial systems*. Ann Arbor, MI: University of Michigan Press.
- Holzer, D., Tengono, Y., Downing S.(2007) Developing a framework for linking design intelligence from multiple professions in the aec industry. In: *Proceedings of the 12th International CAAD Conference*, Springer Netherlands, 2007, pp. 303–316. DOI: 10.1007/978-1-4020-6528-6
- Hrennikoff, A. (1941). Solution of Problems of Elasticity by the Frame-Work Method. *ASME J. Appl. Mech*, 8, A619–A715. <https://www.ingentaconnect.com/content/iass/piass/2015/00002015/00000020/art00015>
- Hudson, 2010; Hudson, R. (2010). Strategies for parametric design in architecture: an application of practice led research. PhD. University of Baths.
- IEEE Computational Intelligence Society (2018) IEEE CIS Task Force on Many-Objective Optimisation, IEEE Computational Intelligence Society. <https://www.cs.bham.ac.uk/~limx/MaOP.html>
- Jain, A., Dubes, R. C. (1988) *Algorithm for clustering data*. Englewood Cliffs, New Jersey, USA: Prentice Hall. ISBN 0-13-022278-x
- Karamba3D (2020) <https://manual.karamba3d.com/2-getting-started/2-getting-started-1>
- Kasiviswanathan, K.S., Sudheer, K.P., He, J. (2016) Quantification of Prediction Uncertainty in Artificial Neural Network Models, In: Shanmuganathan, S., Samarasinghe, S. (Eds.), *Artificial Neural Network Modelling*, Vol. 628. Berlin, Germany: Springer. pp. 145–159. DOI:10.1007/978-3-319-28495-8.
- Kilian, A. (2006) *Design Exploration through Bidirectional Modeling of Constraints*, Massachusetts Institute of Technology (MIT)
- Kim, J., Ryu, H., Cho, D., Song, K. (2016) Structural design of Philippine Arena. *Journal of Civil Engineering and Architecture*, 10, pp. 405–416. doi.org/10.17265/1934-7359/2016.04.002.
- Kohonen, T. (1982) Self-Organized Formation of Topologically Correct Feature Maps, *Biological Cybernetics*, 43(1), pp.59–69.
- Kohonen, T. (2014) *MATLAB Implementations and applications of the Self-organizing map*. Helsinki, Finland: Unigrafia. ISBN: 978-952-60-3678-6
- Koziel, S., Ciaurri, D.E., Leifsson, L. (2011). Surrogate-based methods, in: Koziel, S., Yang, X.S. (Eds.), *Computational Optimization, Methods and Algorithms*. Studies in Computational Intelligence, Vol. 356. Berlin, Germany: Springer. pp. 33–59. DOI 10.1007/978-3-642-20859-1_3.
- Kroo, I. M. (1997). MDO for Large-Scale Design. In: Alexandrov, N., Hussaini, M. Y., (Eds.) *Multidisciplinary Design Optimization: State-of-the-Art*, Philadelphia, PA, USA: SIAM. pp. 22–44.
- Leet, M. K., Uang C., Gilbert, A. M. (2002) *Fundamentals of structural analysis*, McGraw-Hill, Boston, MA
- Li, Q., Borgart, A., Wu, Y. (2016) How to Understand 'Structural Morphology'?, *Journal of the International Association of Shell and Spatial Structure* 57(2), pp.148-158. DOI: 10.20898/j.iass.2016.188.765.
- Lin, S., Gerber, D. (2014). Designing-in performance: A framework for evolutionary energy performance feedback in early stage design, *Automation in Construction*, 38, pp.59–73. doi:10.1016/j.autcon.2013.10.007
- Liu, T., Lee, W. L. (2019) Using response surface regression method to evaluate the influence of window types on ventilation performance of Hong Kong residential buildings. *Building and Environment*, 154, pp. 167–181. DOI: 10.1016/j.buildenv.2019.02.043
- Magee, L. (1998) Nonlocal Behavior in Polynomial Regressions, *the American statistician*, 52(1), pp. 20-22

- Martins, J. Lambe, A. (2010) Multidisciplinary Design Optimization: A Survey of Architectures. *AIAA journal*, 2013; 51 (9), pp. 2049–2075. DOI: 10.2514/1.J051895
- Martins, J. R. R. A., Marriage, C., Tedford, N. (2009) pyMDO: An Object-Oriented Framework for Multidisciplinary Design Optimization, *ACM Transactions on Mathematical Software*, 36(4), pp. 20:1–25. doi:10.1145/1555386.1555389.
- Maya (Autodesk), <https://www.autodesk.com/products/maya/overview>
- Meunier, G. (2012) Acoustic Shoot, <https://www.grasshopper3d.com/group/acoustic-shoot>
- Mohotti, D., Mendis, P., NGO, T. (2014). Application of Computational Fluid Dynamics (CFD) in Predicting the Wind Loads on Tall Buildings: A Case Study. In: 23rd Australasian conference on the mechanics of structures and materials (ACMSM23), Southern Cross University (SCU), Australia. <https://epubs.scu.edu.au/acmsm23/169/>
- Moshou, D., Ramon, H. (1997) Extended Self-Organizing Maps with Local Linear Mappings for Function Approximation and System Identification, In: *Work. Self-Organizing Map WSOM'97*, Helsinki University of Technology, Helsinki, Finland, 1997.
- Mueller, C., Ochsendorf, J. (2015). Combining structural performance and designer preferences in evolutionary design space exploration, *Automation in Construction*, 52, pp. 70–82. doi:10.1016/j.autcon.2015.02.011.
- Murphy, K. P. (2012) *Machine Learning: A Probabilistic Perspective*. The MIT press, Cambridge, Massachusetts, 2012. <https://mitpress.mit.edu/books/machine-learning-1> [Accessed: 7-April-2019]
- Myung, S., Han, S. (2001) Knowledge-based Parametric Design of Mechanical Products based on Configuration Design Method. *Expert Systems with Application*, 21(2), pp. 99–107. DOI: 10.1016/S0957-4174(01)00030-6
- Nguyen, S.T., Reiter, S., Rigo, P. (2014) A review on simulation-based optimization methods applied to building performance analysis, *Applied Energy*, 113, pp. 1043–1058. DOI: 10.1016/j.apenergy.2013.08.061.
- Okudan, Gul E., Tauhid, S., (2008). Concept selection methods - a literature review from 1980 to 2008, *International Journal of Design Engineering* 1 (3), pp. 243–277. doi:10.1504/IJDE.2008.023764.
- Olson, D. L., Wu, D. (2017) *Predictive Data Mining Models*. Singapore: Springer Nature. p. 45 DOI: 10.1007/978-981-10-2543-3
- Pan, W., Sun, Y., Turrin, M., Louter, C., Sariyildiz, S. (2019b). Design exploration of architectural geometries and structural performance for sports arenas based on SOM-clustering and structural performance simulation. In: Cruz, P., ed. *Structure and architecture: Bridging the gap and crossing borders*. London, UK: Taylor & Francis. pp. 342–349. ISBN 978-1-138-03599-7
- Pan, W., Sun, Y., Turrin, M., Louter, C., Sariyildiz, S. (2020), Design exploration of quantitative performance and geometry typology for indoor arena based on self-organizing map and multi-layered perceptron neural network. *Automation in Construction*, 114, pp. DOI: 10.1016/j.autcon.2020.103163
- Pan, W., Turrin, M., Louter, C., Sariyildiz, S., Sun, Y. (2018). Integrating the Multi-Functional Space and Long-Span Structure for Sports Arena Design : A design exploration process based on design optimization and self-organizing map, in: Mueller, C., Adriaenssens, S. (Eds.), *Proceeding of the IASS Symposium 2018: Creativity in Structural Design, Vol 2018*, International Association for Shell and Spatial (IASS), Boston, pp.1-8. <https://www.ingentaconnect.com/content/iass/piass/2018/00002018/00000004/art00015#>
- Pan, W., Turrin, M., Louter, C., Sariyildiz, S., Sun, Y. (2019a). Integrating multi-functional space and long-span structure in the early design stage of indoor sports arenas by using parametric modelling and multi-objective optimization. *Journal of Building Engineering*, 22, pp. 464–485. doi:10.1016/j.jobe.2019.01.006.
- Preisinger, C. (2013), Linking Structure and Parametric Geometry. *Architectural Design*, 83, pp. 110–113. DOI: 10.1002/ad.1564.
- Ramedani, Z., Omid, M., Keyhani, A. Shamshirband, S., Khoshnevisan, B. (2014) Potential of radial basis function based support vector regression for global solar radiation prediction, *Renewable and Sustainable Energy Reviews*, 39, pp.1005–1011. DOI: 10.1016/j.rser.2014.07.108
- Rhinoceros 3D McNeel & Associates) Robert McNeel & Associates, Rhinoceros, (n.d.). www.rhino3d.com
- Rubio-bellido, C., Pino-mejías, R., Alexis, P., Pulido-arcas, J.A. (2017) Comparison of linear regression and artificial neural networks models to predict heating and cooling energy demand, energy consumption and CO₂ emissions, *Energy*, 118, pp.24–36. DOI: 10.1016/j.energy.2016.12.022.

- Rumelhart, D.E., Hinton, G.E., Williams, R.J. (1987) Learning internal representations by error propagation, in: Rumelhart, D.E., McClelland, J.L. (Eds.) *Parallel Distributed Processing: Explorations in the Microstructure of Cognition: Foundations*. Cambridge, MA, USA: MIT Press. pp. 318–362. <https://ieeexplore.ieee.org/document/6302929> [Accessed: 7-April-2019]
- Sabine W. C. (1922) *Collected Papers on Acoustics*. Cambridge, MA: Harvard University Press
- Salehi, H., Burgueño, R. (2018) Emerging artificial intelligence methods in structural engineering, *Engineering Structures*, 171, pp.170–189. DOI: 10.1016/j.engstruct.2018.05.084.
- Salter, C. (1998). *Acoustics: Architecture, Engineering, the Environment*. 1st edition. Richmond, CA, USA: William Stout Publishers.
- Sariyildiz, S. (2012). Performative Computational Design. In: *International Congress of Architecture 2012*. Konya Turkey: Selcuk University, pp. 313–344.
- Saxena, A., Prasad, M., Gupta, A., Bharill, N., Prakash, O. (2017) A review of clustering techniques and developments, *Neurocomputing*, 267, pp.664–681, DOI: 10.1016/j.neucom.2017.06.053.
- Schmit, L., (1960). *Structural Design by Systematic Synthesis*. In: 2nd conference on Electronic Computation, ASCE: New York, pp. 105-132.
- Series, C. (2019) A Methodology for daylight optimisation of high-rise buildings in the dense urban district using overhang length and glazing type variables with surrogate modelling, *Journal of Physics: Conference Series*, 1343, pp doi:10.1088/1742-6596/1343/1/012133.
- Shanmuganathan, S. (2016) Artificial Neural Network Modelling: An Introduction, In: Shanmuganathan, S., Samarasinghe, S. (Eds.), *Artificial Neural Network Modelling*, Vol. 628. Berlin, Germany: Springer. pp. 1-14. DOI: 10.1007/978-3-319-28495-8_1
- Shea, K., Aish, R. and Gourtovaia, M. (2005). Towards Integrated Performance-driven Generative Design Tools. *Automation in Construction*, 14(2), pp. 253-264.
- Shepard, D. (1968) A two-dimensional interpolation for irregularly-spaced data function, In: Blue, R., Rosenberg, A.(Eds.), *Proceeding of the 1968 23rd ACM National Conference*, New York, NY, USA: ACM. pp. 517–523. ISBN: 978-1-4503-7486-6
- Singaravel, S., Suykens, J., Geyer, P. (2018) Deep-learning neural-network architectures and methods : Using component- based models in building-design energy prediction, *Advanced Engineering Informatics*, 38, pp.81–90. DOI:10.1016/j.aei.2018.06.004.
- Smarra, F., Jain, A., De Rubeis, T., Ambrosini, D., Innocenzo, A.D., Mangharam, R. (2018) Data-driven model predictive control using random forests for building energy optimization and climate control, *Applied Energy* 226, pp.1252–1272. DOI: 10.1016/j.apenergy.2018.02.126.
- Solidworks (Dassault Systems), <https://www.3ds.com/products-services/solidworks/?wockw=Solidworks>
- span buildings using geometric multi-objective optimization, *Energy and Building*, 127, pp. 748–761. DOI: 10.1016/j.enbuild.2016.05.090.
- Sun, Y., Xiong, L., Su, P. (2013) Grandstand Grammar and its Computer Implementation, In: Stouffs, R., Sariyildiz, S., (Eds.) *Computation & Performance: Proceedings of the 31st International Conference on Education and Research in Computer Aided Architectural Design in Europe (eCAADe31)*. Delft, NL: eCAADe (Education and research in Computer Aided Architectural Design in Europe) and Faculty of Architecture, Delft University of Technology, pp. 645-654. ISBN: 978-94-91207-04-4 (eCAADe)
- Torgo L. (2017) Regression Trees. In: Sammut, C., Webb, G.I. (Eds) *Encyclopedia of Machine Learning and Data Mining*. Boston, MA , USA: Springer. DOI: 10.1007/978-1-4899-7687-1
- Tseranidis, S., Brown, N.C., Mueller, C.T. (2016). Data-driven approximation algorithms for rapid performance evaluation and optimization of civil structures, *Automation in Construction*, 72, pp. 279–293. DOI: 10.1016/j.autcon.2016.02.002.
- Turrin, 2014 Turrin, M. (2014), *Performance Assessment Strategy: a computational framework for conceptual design of large roofs*. PhD. Delft University of Technology.
- Turrin, M., von Buelow, P., Kilian, A., Stouffs, R. (2012). Performative skins for passive climatic comfort: A parametric design process, *Automation in Construction*, 22, pp. 36–50. doi:10.1016/j.autcon.2011.08.001.
- Turrin, M., von Buelow, P., Stouffs, R. (2011). Design explorations of performance driven geometry in architectural design using parametric modeling and genetic algorithms, *Advanced Engineering Informatics*, 25, pp. 656–675. doi:10.1016/j.aei.2011.07.009.
- Turrin, M., Yang, D., D'Aquilio, A., Šileryte, R., Sun, Y. (2016) Computational Design for Sport Buildings. *Procedia Engineering*, 147, pp. 878-883. DOI: 10.1016/j.proeng.2016.06.285

- van der Harten, A. (2015) Pachyderm Acoustic, <https://www.grasshopper3d.com/group/pachyderm>
- von Buelow, P. (2008) Using evolutionary computation to explore geometry and topology without ground structure. In: Proceeding of the 6th International Conference on Computation of Shell and Spatial Structures (IASS-IACM 2008), Cornell University, Ithaca, NY, USA: IASS. pp. 1-5.
- von Buelow, P. (2009) Parametric exploration of discrete structures using evolutionary computation, In: Proceeding of the International Association for Shell and Spatial Structure (IASS) Symposium 2009, Valencia, Spain: IASS. pp. 577-587.
- von Buelow, P. (2012). Paragen-Performative Exploration of Genetive Systems, Journal of IASS, 53, pp. 271–284.
- von Buelow, P. (2016). Genetically enhanced parametric design in the exploration of architectural solutions, In: Cruz, P.J.S. (Ed) Structures and Architecture beyond their limits: proceedings of the third International Conference on Structures and Architecture (ICSA2016), London, UK: Boca Raton. pp. 675–683, DOI: 10.1201/b20891-93.
- Vorländer, M. (2013). Computer simulations in room acoustics: Concepts and uncertainties. The Journal of the Acoustical Society of America 133, pp. 1203-1213; <https://doi.org/10.1121/1.4788978>
- Wang, Z., Wang, Y., Zeng, R., Srinivasan, R.S., Ahrentzen, S. (2018) Random Forest based hourly building energy prediction, Energy and Buildings 171, pp.11–25. DOI: 10.1016/j.enbuild.2018.04.008.
- Werbos, P. (1990) Backpropagation Through Time : What It Does and How to Do It, In: Proc. IEEE '90, Vol. 78, IEEE, 1990, pp. 1550–1560. DOI:10.1109/5.58337.
- Witten, I. H., Frank, E. (2005) Data mining: practical machine learning tools and techniques, 2nd edn. Amsterdam, NL: Elsevier, ISBN: 0-12-088407-0
- Woodbury, R. (2010) Elements of Parametric Design (1st ed.) Routledge, New York
- Wortmann, T., Costa, A., Nannicini, G., Schroepfer, T. (2015). Advantages of surrogate models for architectural design optimization. Analysis and Intelligence for Engineering Design, 29 (4), pp.471-481. DOI 10.1017/S0890060415000451.
- Xu, D., Tian, Y. (2015) A comprehensive survey of clustering algorithm. Annals of Data Science, 2(2), pp. 165-193. DOI: 10.1007/s40745-015-0040-1
- Yang, D., Ren, S., Turrin, M., Sariyildiz, S., Sun, Y. (2018). Multi-disciplinary and multi-objective optimization problem re-formulation in computational design exploration: A case of conceptual sports building design, Automation in Construction, 92, pp. 242–269. doi:10.1016/j.autcon.2018.03.023.
- Yang, D., Sun, Y., di Stefano, D., Turrin, M., Sariyildiz, S. (2016). Impacts of problem scale and sampling strategy on surrogate model accuracy. In: IEEE Congress on Evolutionary Computing. Vancouver, BC, Canada: IEEE. pp. 4199–4207. DOI: 10.1109/CEC.2016.7744323.
- Yang, D., Sun, Y., Turrin, M., von Buelow, P., Paul, J.C. (2015) Multi-objective and multidisciplinary design optimization of large sports building envelopes : a case study. In: Proceeding of the 2015 Symposium of International Association of Shell and Spatial Structure (IASS 2015), Amsterdam, NL: IASS. pp. 1-14
- Yi, Y.K. (2016a) Adaptation of Kriging in daylight modeling for energy simulation, Energy and Buildings 111, pp.479–496. DOI:10.1016/j.enbuild.2015.11.036.
- Yi, Y.K. (2016b) Dynamic coupling between a Kriging-based daylight model and building energy model, Energy and Buildings 128, pp.798–808. DOI: 10.1016/j.enbuild.2016.05.081.
- Yu, Z., Haghghat, F., Fung, B. C. M., Yoshino, H. (2010) A decision tree method for building energy demand modeling. Energy and Buildings, 42, pp. 1637-1646. DOI: 10.1016/j.enbuild.2010.04.006
- Zhang, S., Sun, Y., Cheng, Y., Huang, P., Olaide, M., Lin, Z. (2018) Response-surface-model-based system sizing for Nearly / Net zero energy buildings under uncertainty, Applied Energy 228, pp.1020–1031. DOI: 10.1016/j.apenergy.2018.06.156.

4 Method development: CDIA – Computational Design of Indoor Arenas

4.1 Introduction

Based on the hypothetical method formulated in chapter 3, this chapter proposes the formal method: Computationally Integrated Design of Indoor Arenas (CDIA), to satisfy the basic demands about the conceptual design of indoor arenas formulated in chapter 2. Figure 4.1 illustrates the scheme of CDIA. Five components are involved in CDIA (the blue boxes in figure 4.1): Indoor Arena Generator (IAG), Framework for numeric assessment of indoor arena (Framework-NAIA), Multi-Objective Optimization (MOO), unsupervised clustering based on Self-Organizing Map (SOM clustering), and Multi-Layer Perceptron Neural Network based on self-organizing map (SOM-MLPNN). In CDIA, IAG and Framework-NAIA are the two components of pre-processing in which the design space is defined based on IAG and the numeric assessment criteria related to quantitative design requirements are formulated based on the Framework-NAIA. Based on the two pre-processing components, MOO, SOM-clustering, and SOM-MLPNN are used in three different workflows corresponding to the three design scenarios discussed in chapter 3.

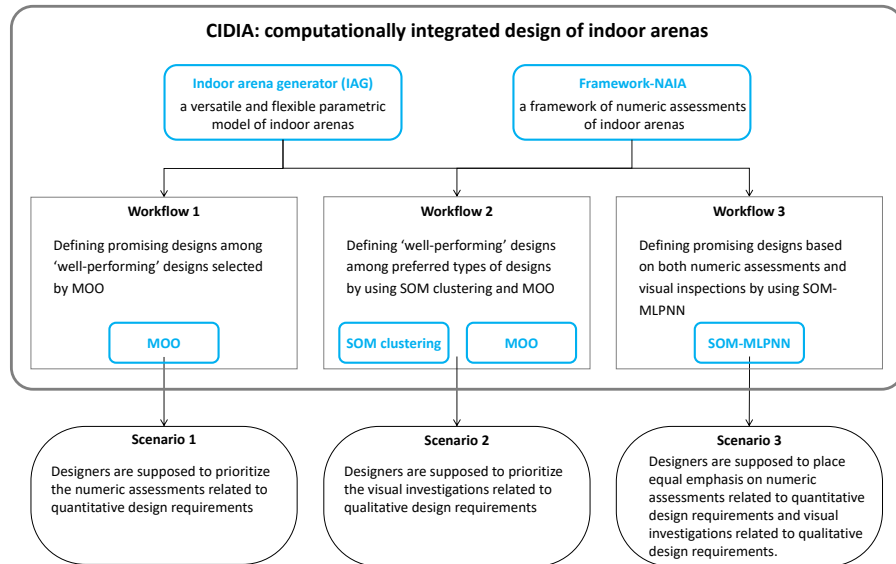


FIG. 4.1 The scheme of CDIA

In section 4.2.1 and section 4.2.2, the two pre-processing components of CDIA, IAG and Framework-NAIA are proposed and elaborated. IAG is a flexible and versatile parametric model for indoor arenas, which is formulated based on the composition and design parameters of indoor arenas reviewed and concluded in chapter 2. It is used to generate various types of building forms with three different structural types based on the integration of the multi-functional space (pitch and seating bowls) and long-span roof structure, which satisfy the first basic demand of the conceptual design of indoor arenas concluded in chapter 2.

Framework-NAIA is proposed based on the studies about the quantitative design requirements of indoor arenas in chapter 2 and the reviews about the related numeric indicators and simulations in chapter 3. It consists of the numeric indicators and related Building Performance Simulation (BPS) tools about the multi-functionality (spatial capacity, view of spectators, acoustics for various activities) and structural performance. Moreover, the framework also provides possible assessment criteria, based on which the indicators can be used as design objectives or constraints to assess a design. Therefore, designers can rapidly customize specific criteria and combine the BPS tools with IAG to assess design alternatives.

Based on the two basic components, IAG and Framework-NAIA, in section 4.3.1 to section 4.3.3, three workflows are formulated based on the components of MOO, SOM clustering, and SOM-MLPNN. The three workflows are applied for the three scenarios in which designers intend to place different emphases on numeric assessment relate to quantitative design requirements and visual investigations related to qualitative design requirements.

The first workflow is proposed for the design scenario in which designers intend to prioritize the numeric assessment related to quantitative design requirements for design alternatives. Multi-Objective Optimization (MOO) is used in this workflow to search for 'well-performing' designs in a wide design space containing diverse design alternatives, according to customized numeric assessment criteria related to quantitative design requirements. Among the 'well-performing' designs selected by MOO, designers can further select promising designs based on visual investigations related to qualitative design requirements.

The second workflow is proposed for the design scenario in which designers intend to prioritize the visual investigations related to qualitative design requirements for design alternatives. In this workflow, unsupervised clustering based on Self-Organizing Map (SOM clustering) is used to cluster all the design alternatives into groups according to geometry features and to reflect the design space based on a two-dimensional SOM network which organizes various typical designs. Based on SOM clustering, designers can explore various types of designs and select promising types based on visual investigations related to qualitative design requirements. All the designs within these types are selected out, among which MOO is used to search for 'well-performing' designs based on numeric assessment related to quantitative design requirements.

The third workflow is proposed for the design scenario in which designers intend to place equal emphases on numeric assessments related to quantitative design requirements and visual investigations related to qualitative design requirements. This workflow is based on SOM-MLPNN. The SOM clustering, being similar to that in the second workflow, is used to cluster designs into groups according to geometry features and generate a typical design for each cluster. Therefore, designers can visually investigate various types of designs. Moreover, the inputs of the typical designs generated by SOM clustering are used as the sampled/labelled inputs for the Design of Experiments (DoEs) and MLPNN to predict the values of the numeric indicators related to quantitative design requirements for all the design alternatives in the design space. Based on data visualization, designers can explore designs and select promising ones, according to both numeric assessments and visual investigations.

The workflows are applied to two examples in the case studies in chapter 5, in which the related effects as well as the potential advantages and limitations are demonstrated and verified.

4.2 Pre-processing components of CDIA: IAG and Framework-NAIA

4.2.1 Indoor Arena Generator (IAG): a versatile and flexible parametric model of indoor sports arenas

Based on the interrelationships of the building elements and the related design parameters formulated in chapter 2, Indoor Arena Generator (IAG) is proposed, which has been published in a journal paper (Pan et al., 2019). In IAG, the multi-functional space (pitch and seating bowl) is integrated with the long-span roof structure, which defines the overall form/geometry of the building. Diverse geometries can be generated based on this integration, and three frequently-used structural types: single-layer grid-shell, double-layer spatial frame, and spatial truss beams are applied.

In IAG, an indoor arena is defined in four steps related to the pitch, seating tiers, roof geometry, and structure. Table 4.1 illustrates the process and lists the related parameters. The four steps of the formulation of IAG are based on the literature review and analyses about the composition of indoor arenas in section 2.2. In this composition, a pitch is in the centre of the building, and seating tiers are set around the pitch. A roof is set to cover the bowl configuration (pitch and seating tiers), and there is a structure system support the roof.

It is worth noting that even though this model includes most formal types of indoor arenas, some special types (e.g. the arena with a discrete roof which is composed of several surfaces) are not yet included. For the long-span structure, this model only focuses on three frequently-used types of lattice steel structures (grid-shell, space-frame, and truss-beam) with quadrilateral topological patterns/tessellations.

Step 1 deals with the pitch and the prototype of the seating bowl (Table 4.1, step 1). The dimension of the pitch, as mentioned in chapter 2, can be determined according to the activities which are planned to be held in the arena. In this step, designers should select a principal activity to define the focal point for spectators' sightlines to generate the seating tiers. The sections of the tiers and the rows for each section should also be defined. In this research, as mentioned in chapter 2, a method which uses one or several specific 'values of V' to calculate the riser of each row, is used to generate the foundation of the seating bowl (see equation 2.1 and figure 2.9 in chapter 2).

In step 2, a variable boundary curve of the seating tiers is formulated to trim the prototype of the seating bowl and define the final bowl (Table 4.1, step 2). For the boundary curve, the formulations process is proposed in section 2.2.2.2. The formulation is based on eight control points and the curve type (polyline or curve). The control points are defined by the lengths along the x- and y-axes of the building, the asymmetric ratios along x- and y-axis, and the corner positions. Thus, based on the formulation process proposed in section 2.2, diverse multi-functional spaces can be generated (see figure 2.16 in chapter 2). The number of the fixed seats for the seating bowl should be examined in this step, according to the number defined before the design process. The height of the last row of the seating bowl should be constrained according to design requirements in practice. In fact, the height can be varied in a large range for different buildings. For the Philippine Arena (50,000 fixed seats), which is the largest indoor arena in the world, the height for the last row is around 60m (Kim et al., 2016)

Based on the pitch and seating tiers, step 3 formulates the roof by using quadrilateral grids (Table 4.1, step 3). First, the structural boundary is generated by eight control points corresponding to the eight control points of the seating bowl boundary in step 2. The initial positions of the control points are on the seating bowl boundary (the blue dash curve in the first chart of step 3 in Table 4.1), then each of the control points (except the highest ones) are allowed to vertically move to a certain position between the original position and its highest position (with the same height as the highest control point). It allows the structural boundary to vary between the seating bowl outline (the blue dash curve in the first chart of step 3 of Table 4.1) and the flat structural boundary (the orange dash curves in the first chart of step3 of Table 4.1). Based on a defined structural boundary, the ridges of the roof along the x- and y-axis of the building are generated based on a design parameter defining the headroom height of the pitch centre and another parameter defining the curve type of the ridge (polyline or curve). Furthermore, the quadrilateral grid can be achieved based on a grid size defined by a parameter.

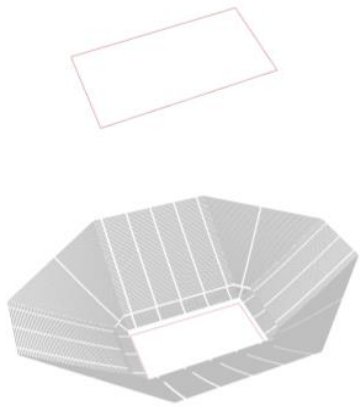
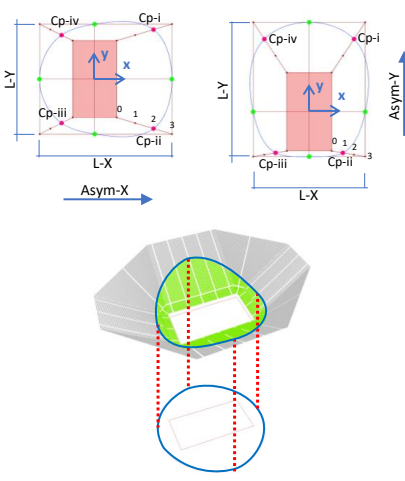
Sequentially, in step 4, based on the quadrilateral grid, three different types of structures can be generated. For a one-layer grid-shell (GS) structure, a quadrilateral pattern is used, and the defined quadrilateral grid (figure 4.2, A) can be directly used as the axes of the structural elements (bars). For a two-layered space frame (SF) structure and a truss beam (TB) structure, a two-layered grid is necessary. Based on the defined quadrilateral grid (the red one in figure 4.2, A and B), an upper grid (the blue one in figure 4.2, B) is generated according to two parameters, *SturDpth-ctr* (the structural depth at the central point of the roof) and *StruDpth-bdr* (the structural depth on the boundary of the roof). For a space frame structure, the upper and bottom grids are directly used as the axes of the upper and bottom chords, and additional vertical as well as diagonal webs are added between them (figure 4.2, C). For a truss-beam (TB) structure, both the x- and y-axis can be the span direction of the beams, which are considered as two subtypes for TB. The cross-section of each truss beam is an inverted triangle (figure 4.2, D), which is composed of two upper chords (generated by offsetting the upper grid lines) and one bottom chord (directly generated based on the bottom grid lines). Additional webs are set between the chords. For all the structural types, steel (S235, S275, or S355) is used as the material, and circle tubes are defined as the cross-sectional shape for the elements. Designers should assign the ranges for the parameters of the diameter and thickness of the tubes.

By using the IAG, a wide design space containing numerous design alternatives with diverse geometries for indoor arenas can be generated, which include not only some conventional geometries (some examples are proposed in figure 4.3, A) but also some special ones (some examples are proposed in figure 4.3, B). It can also be used to mimic the geometries of some real arenas (some examples are proposed in figure 4.2, C). The feasibility of the geometries can be guaranteed by setting the ranges of variables (e.g. the size of the building, the height of the roof) and the constraints of some numeric indicators (e.g. the number of fixed seats, the maximum viewing distance of spectators, the maximum deflection viewing angle of spectators).

To use IAG to define a design space, some parameters in table 4.1 should be selected as design variables which can be changed to generate various design alternatives, while other parameters are fixed. The fixed design parameters are usually defined before design exploration. For example, the parameter of the dimension of the pitch (*P_size*), which is related to activities which are planned to be held in the building, is usually defined during the planning process, therefore, the related parameters can be fixed during conceptual design.

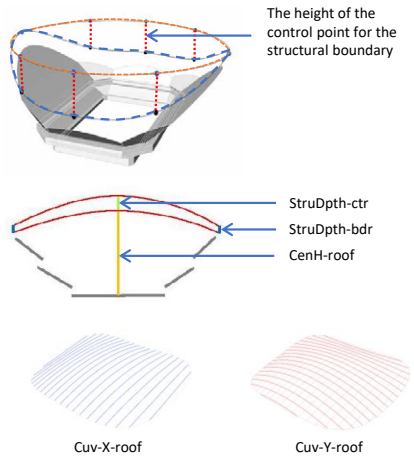
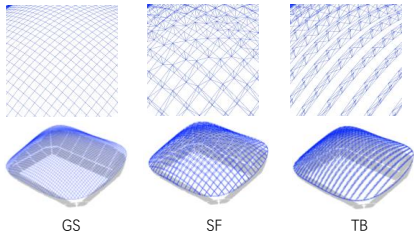
For each of the parameters which are selected as design variables, the related range and interval should be defined. The selections and definitions of the design variables determine the amount and the diversity of the design alternatives within the design space.

TABLE 4.1 Process and parameters of the proposed parametric model (Pan et al. 2019)

Step	Parameter	Description
Step 1		
	P-size	the dimensions of the pitch, decided by designers according to the requirements
	SE-NumSpct-x	the number of spectators for a certain sport event 'x' accommodated in the arena
	SE_Prin	Principal sports event accommodated in the pitch defined by the designers
	V	the vertical distance from eyes of a spectator to the top of the head or the sightline of the spectator in the next row: 120mm
	ST_DepthSR	the depth of a seating-row: $\geq 0.8\text{m}$
	ST_WidthS	the width of a seat: $\geq 0.5\text{m}$
	ST_NumSR	the number of the seats between radical or parallel passageway: ≤ 28
	ST_WidthPW	the width of a passageway: $\geq 1.2\text{m}$
	ST_Sec	the number of the sections of the seating tiers
	ST_RowNum	the number of rows for each section of the seating tiers
Step 2		
	ST_LenX	the length of the x-axis of the seating bowl boundary
	ST_AsyX	the asymmetric ratio of the boundary of the seating bowl along the x-axis (for the performance of side-stage) 0: symmetric in X-axis; 10: totally asymmetric in X-axis
	ST_LenY	the length of the y-axis of the seating bowl boundary
	ST_AsyY	the asymmetric ratio of the boundary of the seating bowl along the x-axis (for the performance of side-stage) 0: symmetric in Y-axis; 10: totally asymmetric in Y-axis
	ST_CPi	the corner point of the seating bowl boundary in the first or second or third or fourth quadrant:
	ST_CPii	0: overlap with the corner of the pitch; 3: overlap with the corner of the outer rectangle.
	ST_CPiii	
ST_CPiv		
ST_Bdr	the curve degree of the seating bowl boundary 1: polyline; 3: curve.	

>>>

TABLE 4.1 Process and parameters of the proposed parametric model (Pan et al. 2019)

Step	Parameter	Description
Step 3		
 <p>The height of the control point for the structural boundary</p> <p>StruDpth-ctr StruDpth-bdr CenH-roof</p> <p>Cuv-X-roof Cuv-Y-roof</p>	Str_BdrCPI	the height of the i^{th} control point of the structural boundary: 0 to 10 when the variable equals to 0, the control point is on the original boundary parallel to the seating bowl outline (the blue one; when it equals to 10, the control point is as high as the highest control point and is on the orange curve.
	Str_FCHeight	the floor to ceiling height of the roof structure at the central point of the pitch: $\geq 18\text{m}$
	Str_Grid	the grid size of structural tessellation for the long-span roof
	Str_RidgeX	the curve degree of the ridge along the x-axis or y-axis: 1: polyline; 3: curve.
	Str_RidgeY	
	Str_DepCen	structural depth of the roof structure at the central point (for space frame and truss beam)
	Str_DepBdr	structural depth of the roof structure on the boundary (for space frame and truss beam)
Step 4		
 <p>GS SF TB</p>	Str_Type	the structural type of the long-span roof: 0: GS (Grid Shell); 1: SF (space frame); 2: TB in X (truss-beam along x-axis); 3: TB in Y (truss-beam along y-axis).
	Str_CrSec	the structural cross-section (shape, size, thickness)
	Str_Mtr	Structural material: Steel (S235, S275, S355)

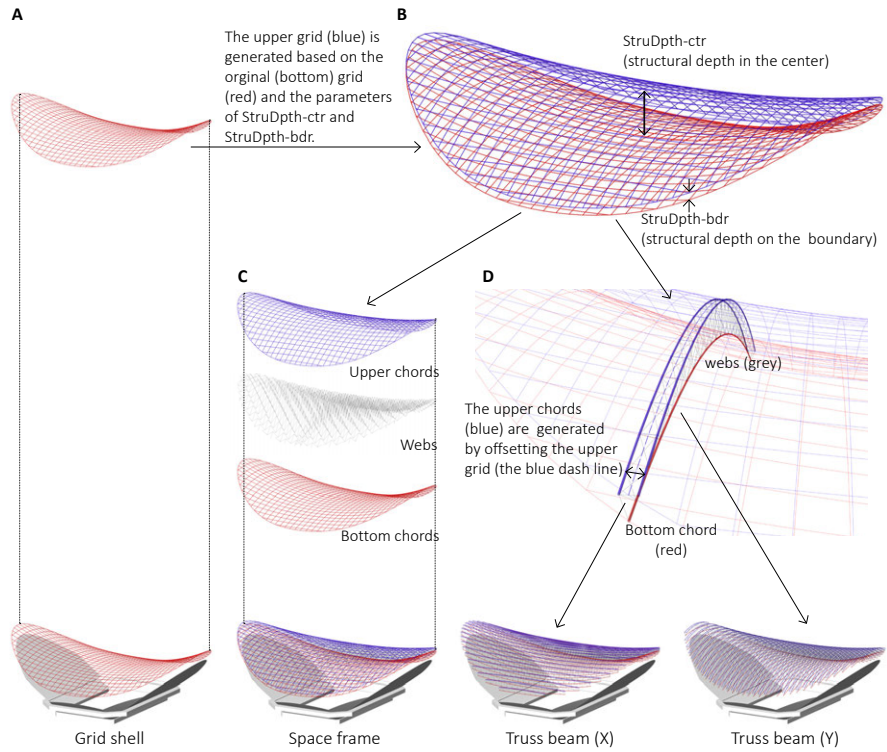
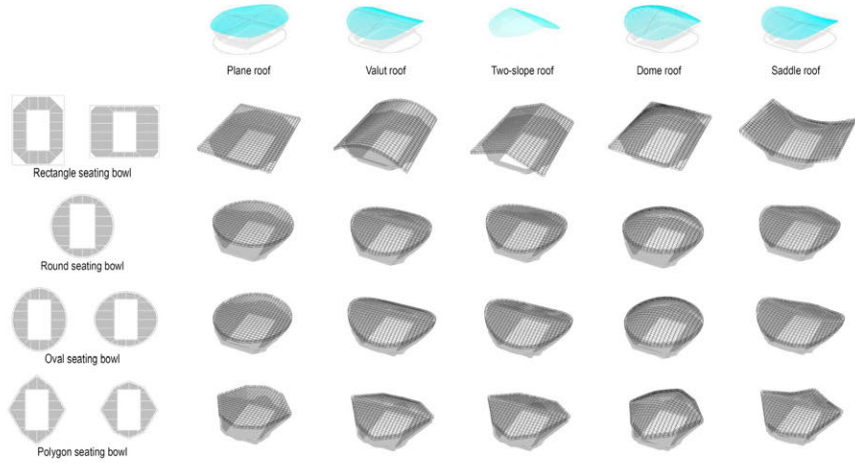
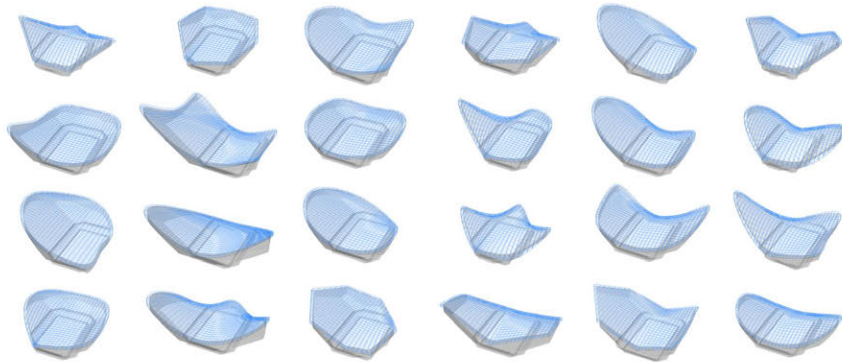


FIG. 4.2 The generation of the roof structure (Pan et al. 2019)

A. Some conventional design alternatives of indoor arenas generated based on IAG



B. Some unconventional design alternatives of indoor arenas generated based on IAG



C. Some design alternatives of real indoor arenas generated based on IAG

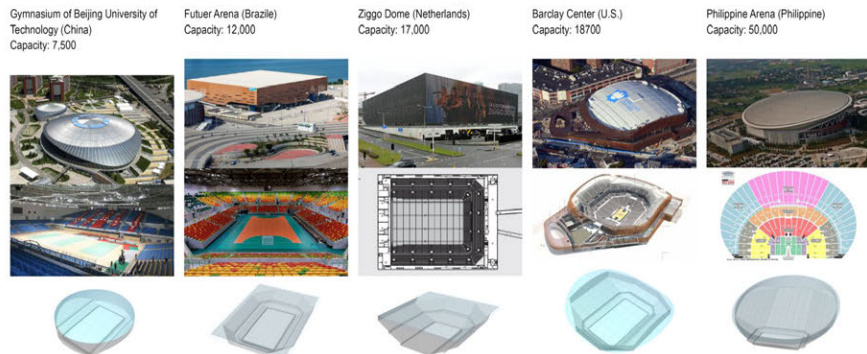


FIG. 4.3 Some design alternatives of indoor arenas generated by IAG (Pan et al. 2019)

4.2.2 **Framework for Numeric Assessments of Indoor Arenas (Framework-NAIA)**

The generated design alternatives should be evaluated based on a series of criteria related to quantitative and qualitative design requirements. For the quantitative design requirements, the satisfaction can be assessed based on numeric data related to a series of indicators. As mentioned in chapter 1 and chapter 2, for the quantitative design requirements of indoor arenas, this research focuses on the multi-functionality (the spatial capacity, views of spectators, and acoustics for multiple activities) and structural performance. The related indicators and Building Performance Simulation (BPS) methods and tools are reviewed and studied in chapter 2 and chapter 3, respectively. By collecting these indicators and the related BPS tools, a Framework for Numeric Assessment of Indoor Arenas (Framework-NAIA) is formulated to support the numeric evaluations of the design alternatives according to quantitative design requirements. Moreover, the Framework provides criteria for each indicator, based on the reviews and studies of related work and design codes in chapter 2, to show how to use an indicator as a design objective or constraint to evaluate a design. Table 4.2 demonstrated the Framework.

TABLE 4.2 Framework for Numeric Assessment of Indoor Arenas (Framework-NAIA)

Aspect	Indicator	BPS tools	Possible criteria (applying the indicator as design objective or design constraints)
Spatial capacity	SE_TypeSpt: the types of sports events accommodated in the arena	Measure in the 3d model	- objective: max. SE_TypeSpt (usually, the types are predefined by designers)
	SE_NumSpct-x: the number of spectators for a certain sports event 'x' accommodated in the arena	Measure in the 3d model	- objective: max. SE_NumSpct-x (usually, the number is predefined by designers)
	DS_NumC: the number of the courts of a popular sport in the pitch for daily sports.	Measure in the 3d model	- objective: max. DS_NumC
	EX_NumEB: the number of standard booths accommodated in the pitch for exhibition	Measure in the 3d model	- objective: max. EX_NumEB
View of Spectator	SE_avrVD-x: the average viewing distance of the seats for a certain sports event 'x'	Measure in the 3d model	- objective: min. SE_avrVD-x:
	SE_VDmax-x: the maximum viewing distance of the seats for a certain sports event 'x'	Measure in the 3d model	- objective: min. SE_VDmax-x - constraint: $SE_VDmax_x \leq$ acceptable value of design codes
	SE_PctPVD-x: the percentage of the seats with the premium viewing distance for a certain sports event 'x'	Measure in the 3d model	- objective: max. SE_Pct_PVDx - constraint: $SE_PctPVD_x \geq$ acceptable value defined by designers
	SE_PctPHVA-x: the percentage of the seats whose horizontal viewing angles are smaller or equal the premium horizontal viewing angle (PHVA) for a certain sports event 'x'	Measure in the 3d model	- objective: max. SE_PctPHVA-x - constraint: $SE_PctPHVA_x \geq$ acceptable value defined by designers.
	SE_maxVVA-x: the maximum vertical viewing angle of seats for a certain sport event 'x'	Measure in the 3d model	- objective: min. SE_maxVVA-x - constraint: $SE_maxVVA_x \leq$ acceptable value of design codes.
	SPside_PctAS: the percentage of the available seats for a stage performance with a side-stage	Measure in the 3d model	- objective: max. SPside_PctAS - constraint: $SPside_PctAS \geq$ acceptable value of defined by designers
	SPend_PctAS: the percentage of the available seats for a stage performance with an end-stage	Measure in the 3d model	- objective: max. SPend_PctAS - constraint: $SPend_PctAS \geq$ acceptable value of defined by designers

>>>

TABLE 4.2 Framework for Numeric Assessment of Indoor Arenas (Framework-NAIA)

Aspect	Indicator	BPS tools	Possible criteria (applying the indicator as design objective or design constraints)
	S _{PSide_avrVD} : the average viewing distance of the available seats for a stage performance with a side-stage.	Measure in the 3d model	- objective: min. S _{PSide_avrVD}
	S _{Pend_avrVD} : the average viewing distance of the available seats for a stage performance with an end-stage.	Measure in the 3d model	- objective: min. S _{Pend_avrVD}
	S _{PSide_maxVD} : the maximum viewing distance of the available seats for a stage performance with a side-stage.	Measure in the 3d model	- objective: min. S _{PSide_maxVD} - constraint: S _{PSide_maxVD} ≤ acceptable value defined by designers
	S _{Pend_maxVD} : the maximum viewing distance of the available seats for a stage performance with an end-stage.	Measure in the 3d model	- objective: min. S _{Pend_maxVD} - constraint: S _{Pend_maxVD} ≤ acceptable value defined by designers
	S _{PSide_PctPVD} : the percentage of seats with premium viewing distance for the stage performances with a side-stage.	Measure in the 3d model	- objective: max. S _{PSide_PctPVD} - constraint: S _{PSide_PctPVD} ≥ acceptable value defined by designers
	S _{Pend_PctPVD} : the percentage of seats with premium viewing distance for the stage performances with an end-stage.	Measure in the 3d model	- objective: max. S _{Pend_PctPVD} - constraint: S _{Pend_PctPVD} ≥ acceptable value defined by designers
	S _{PSide_PctPHVA} : the percentage of seats whose horizontal viewing angles are smaller or equal the premium horizontal viewing angle for a stage performance with a side-stage.	Measure in the 3d model	- objective: max. S _{PSide_PctPHVA-x} - constraint: S _{PSide_PctPHVA-x} ≥ acceptable value defined by designers
	S _{Pend_PctPHVA} : the percentage of seats whose horizontal viewing angles are smaller or equal the premium horizontal viewing angle for a stage performance with a side-stage.	Measure in the 3d model	- objective: max. S _{Pend_PctPHVA-x} - constraint: S _{Pend_PctPHVA-x} ≥ acceptable value defined by designers

>>>

TABLE 4.2 Framework for Numeric Assessment of Indoor Arenas (Framework-NAIA)

Aspect	Indicator	BPS tools	Possible criteria (applying the indicator as design objective or design constraints)
Acoustics	RT _{60-all} : the average value of the reverberation times for the octave band frequencies from 125 to 8000Hz	- Sabine equation, - Eyring equation, - Raytracing based on Pachyderm in grasshopper	- objective: RT _{60-all} get close to the ideal value for a specific stage performance - constraint: to limit the RT _{60-all} within an acceptable range defined by designers
	TR: the treble Ratio indicating whether a sound is bright, clear, and rich in harmonics.		- constraint: 0.75 ≤ TR ≤ 0.95
	BR: the bass ratio indicating the liveness or fullness of bass tones.		- constraint: 0.9 ≤ BR ≤ 1.5
Structure	SW: the structural self-weight of the roof for per square meter of the multi-functional space in the arena	FEM based on Karamba 3D	- objective: min. SW - constraints: SW ≤ accepted value defined by designers
	SE: Strain energy of the roof		- objective: min. SE
	EE: the embodied energy of the roof structure		- objective: min. EE - constraints: EE ≤ accepted value defined by designers
	NumN: Number of the nodes in the roof structure		- objective: min. NumN - constraints: NumN ≤ accepted value defined by designers
	σ_{max} : the maximum normal stress of the structural elements		- objective: min. σ_{max} - constraints: $\sigma_{x,Ed} \leq \frac{f_y}{\gamma_M}$
	τ_{max} : the maximum shear stress of the structural elements		- objective: min. τ_{max} - constraints: $\tau_{x,Ed} \leq \frac{f_x}{\gamma_M}$
	dfI: the vertical deflection of the whole structure		- objective: min. dfI - constraints: $dfI \leq \frac{span}{250}$

Based on the Framework, by selecting indicators and the related BPS tools, designers can quickly customize criteria to assess design alternatives based on quantitative design requirements. The selected BPS tools are then connected to the parametric model (IAG) to obtain the numeric data of the related indicators for the generated design alternatives. It is worth noting that the framework is developable, and more indicators for these aspects and for other aspects (climate and energy, HVAC, daylighting, etc.) can be added.

4.3 **CDIA: a flexible method including three workflows**

Based on the IAG and Framework-NAIA, three workflows of CDIA are proposed based on the components of Multi-Objective Optimization (MOO), unsupervised clustering based on Self-Organizing Map (SOM clustering), and Multi-Layered Perceptron Neural Network. Each of the workflows is proposed for one of the three scenarios in which designers intend to place different emphases on numeric assessments related to quantitative design requirements and visual investigations related to qualitative design requirements.

4.3.1 **Defining promising designs among ‘well-performing’ designs by using MOO**

The first workflow is proposed for the design scenario in which designers intend to prioritize the numeric assessments related to quantitative design requirements. Specifically, designers intend to investigate design alternatives in a wide design space and select ‘well-performing’ ones according to customized numeric assessment criteria related to quantitative design requirements, and then to further visually select the promising ones among the ‘well-performing’ design alternatives according to qualitative design requirements. This workflow has been published in a journal paper (Pan et al., 2019).

In this workflow (figure 4.4), MOO is used to search for 'well-performing' designs according to numeric assessment criteria formulated based on Framework-NAIA, within a wide design space containing diverse design alternatives generated by IAG. To use MOO, the related parameters should be defined, including population size, iteration times, mutation rate, etc. The MOOs in this research are performed based on MATLAB (2020). Moreover, the result data of MOO should be processed and visualized, based on which designers can investigate the 'well-performing' designs and select promising ones based on visual investigations according to their knowledge and experience about qualitative design requirements. The related case studies are performed in section 5.4.1 of chapter 5, which demonstrate the workflow and verify the effects.

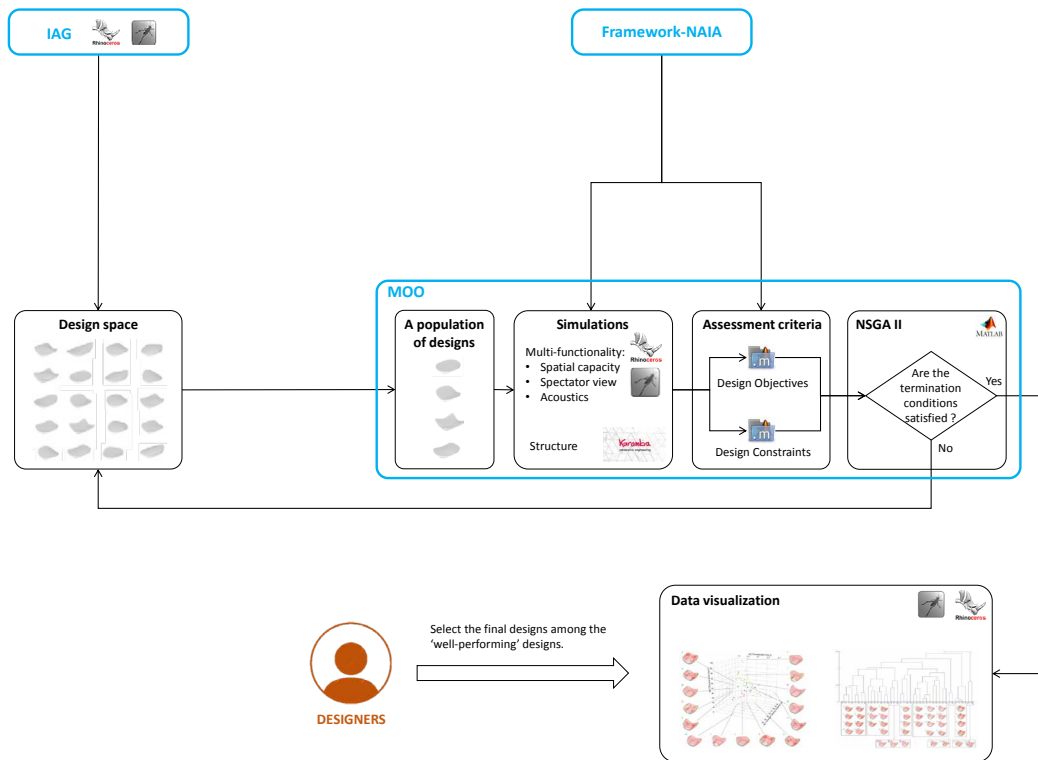


FIG. 4.4 The process of the first workflow by using MOO

4.3.1.1 Search for ‘well-performing’ designs based on heuristic algorithm

Within the defined design space and according to the formulated assessment criteria related quantitative design requirements, Multi-Objective Optimization (MOO) is used to search for ‘well-performing’ designs. NSGA II, which is introduced in section 3.4.3 of chapter 3, is selected as the searching algorithm for MOO in this research. To use NSGA II, a series of parameters should be defined, including population size, iteration times, mutation rate, and parameters related to ranking, selection, and crossover function, etc. The NSGA II based MOO is achieved by the ‘gamultiobj’ function in the optimization toolbox of MATLAB (Mathworks, 2020) in this research. In the ‘gamultiobj’ function, designers can directly use the default or customized values for the parameters. Specifically, to guarantee the diversity of the design alternatives selected by MOO, an adaptive mutation function ‘mutationadaptfeasible’ (Mathworks, 2020) is used to dynamically define the mutation rate during MOO. By using this function, solutions obtaining high scores of fitness functions are given lower mutation rates while the solutions with lower scores are given higher mutation rates (Mathworks, 2020).

4.3.1.2 Result data process and visualization

The result data provided by MATLAB are a series of vectors. Each vector represents one of the designs on the Pareto Frontier and the related values of design objectives and constraints. Based on these vectors, the geometries of the selected ‘well-performing’ designs can be generated and visualized for designers, based on IAG. Moreover, based on the values of the design objectives of these design alternatives, a 3D scatter chart can be used to illustrate the Pareto frontier.

Besides, to support designers to visually investigate these design alternatives according to geometry typologies, hierarchical clustering (introduced in chapter 3) is used. The ‘clusterdata’ function of the statistics and machine learning toolbox in MATLAB (Mathworks, 2020) is used to achieve the hierarchical clustering and formulate the dendrogram. The input parameters for the distance calculation in hierarchical clustering are the design variables directly related to the overall form of these ‘well-performing’ designs. A ‘zero-one’ feature scaling is used to pre-process the input data for the clustering, to guarantee the accuracy. Based on the geometries, scatter chart, and the dendrogram of the ‘well-performing’ design alternatives, designers can further investigate the designs based on visual investigations according to their experience and knowledge about qualitative design requirements and select promising ones.

4.3.1.3 Limitations

MOO is frequently used in building designs to support designers to find 'well-performing' solutions according to quantitative design requirements. In this research, as discussed above, MOO is used with IAG, therefore it can search for 'well-performing' designs in a wide range. However, the process of MOO can be time-consuming, especially for a large design space, since the time-consuming BPSs. Besides, as mentioned in section 3.4.5 of chapter 3, MOO can only efficiently deal with three design objectives, which limits dynamic design exploration focusing on changeable design objectives and constraints.

4.3.2 Defining 'well-performing' designs among preferred types of designs by using SOM clustering and MOO

The second workflow is proposed for the design scenario in which designers intend to prioritize the visual investigations related to qualitative design requirements. Specifically, designers intend to investigate design alternatives and select some of them by visual investigations, according to qualitative design requirements, and then further select the promising ones among the selected designs by numeric assessments, according to quantitative design requirements. This workflow has been published in a conference paper (Pan et al. 2018).

In this workflow (figure 4.5), SOM clustering is used to group design alternatives into different clusters according to geometry features, based on which designers can visually investigate the typical design of each cluster, therefore to select preferred types of designs according to designers' experience and knowledge of qualitative design requirements. Among these selected types of design alternatives, MOO is used to search for 'well-performing' ones based on numeric assessments criteria related to quantitative design requirements. Since the selected types of design alternatives are far less than all the design alternatives within the design space, the computation time of the related MOO can be reduced. The related case studies are performed in section 5.4.2 of chapter 5, which demonstrate the workflow and verifies the effects.

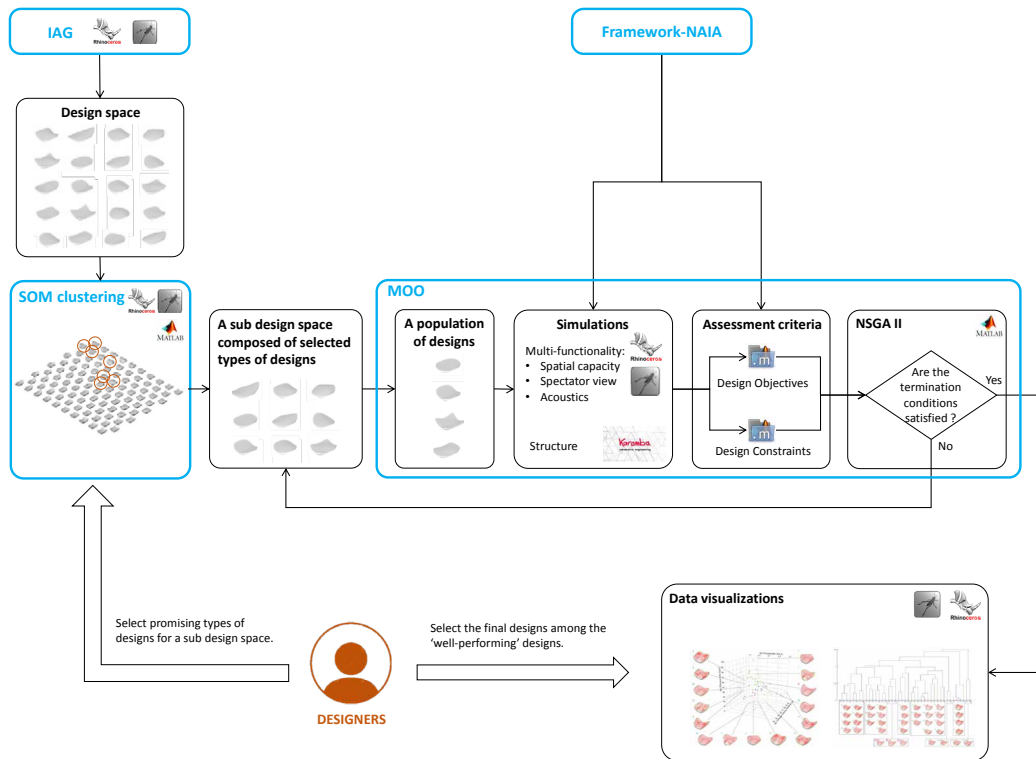


FIG. 4.5 The workflow defining 'well-performing' designs among preferred types of designs by using SOM clustering and MOO

4.3.2.1 Visual investigations of different types of design alternatives by using SOM clustering

As discussed in chapter 1 and chapter 2, the qualitative design requirements of architecture (e.g. aesthetics, sociality, culture, psychology) are difficult to be measured and assessed by numeric data, and so far, designers still intend to assess them based on visual investigations based on their knowledge and experience. It is also one of the most important characters of architectural design. However, it is impossible for designers to visually investigate every design alternative within the design space. One of the feasible ways is to present a small number of representative designs.

As introduced in section 3.6 of chapter 3, SOM clustering can group all the design alternatives within the design space into a number of clusters and generate a representative design for each of the clusters, according to geometry features. Moreover, the representative designs (the node designs) are organized by a two-dimensional SOM network, on which similar designs are close while different ones are far away, to reflect the design space. Based on the representative node designs on the SOM network, designers can have an overview of the design space based on geometry typology, and visually investigate diverse types of designs to select promising types according to their experience and knowledge about qualitative design requirements.

To use SOM clustering to group design alternatives according to geometry features, the inputs for SOM clustering should be the design variables of the design alternatives directly related to the overall geometries. It worth noting that if a large number of variables are used as the inputs of SOM, the SOM clustering can be failed to reflect the design space, since the curse of dimensionality. It is difficult to define a proper number of variables to achieve an efficient SOM clustering. Nevertheless, in a case study performed by Harding (2016), nine variables are used for SOM, in which the SOM clustering can efficiently reflect the design space. Since the variables have different ranges, which can influence the results of SOM clustering, a feature scaling is necessary to make the variables having the same range. In this research, a zero-one scaling is used, which makes all the variables distributed between zero to one.

Besides the variables, a series of parameters of SOM clustering should be defined, including the size of the network, the topology of the network, iteration times, learning rates, and neighborhood function for the ordering phase and the tuning phase (details about these parameters are elaborated in section 3.6.2 of chapter 3).

Specifically, the size of the SOM-network defines how many nodes can be used to capture the object in the input space (the design alternatives in the design space). It equals or is less than the number of the clusters (since some of the nodes may capture no objects/design alternatives). A large size network can group designs into a higher number of smaller clusters. However, too many clusters with too many representative design alternatives (the node designs) can make designers difficult to efficiently investigate these alternatives. Nevertheless, a small size SOM network cannot fully reflect the diversity of the designs in the design space. Hence, there is a trade-off in the definition of the size of the SOM network.

Moreover, the topology of the network is also important. For a two-dimensional SOM network, rectangle and triangle are two of the main topologies, and the triangle one is considered to be more efficient (Lämsiluoto, 2014; Harding, 2016).

4.3.2.2 Search for ‘well-performing’ designs among preferred types of designs according to quantitative requirements by using MOO

Among the selected types of designs, MOO is applied to search for ‘well-performing’ designs according to quantitative assessment criteria. This step is similar to the previous workflow. Since the selected design alternatives are less than all the design alternatives in the design space, the generation size and iteration times for NSGA-II can be reduced, which can save the computational time. Finally, designers should select promising designs among the ‘well-performing’ ones again based on visual investigations according to their knowledge and experience about qualitative design requirements.

4.3.2.3 Limitations

In general, the workflow based on SOM and MOO can support the design scenarios in which designers prioritize visual investigations related to qualitative design requirements. However, the selection of the promising types of designs narrows the searching range for MOO to find the ‘well-performing’ design alternatives. Therefore, the ‘well-performing’ design alternatives here can be ‘worse’ comparing to those directly selected from the design space (like those in the first workflow), according to the same assessment criteria.

4.3.3 **Defining promising designs based on both numeric assessments and visual investigations by using SOM-MLPNN**

The third workflow is proposed for the design scenario in which designers intend to place equal emphases on numeric assessments related to quantitative design requirements and visual investigations related to qualitative design requirements. To achieve the workflow, multi-layered perceptron neural network based on self-organizing map (SOM-MLPNN) is proposed. Figure 4.6 illustrates the workflow. This workflow has been published in a journal paper (Pan et al., 2020).

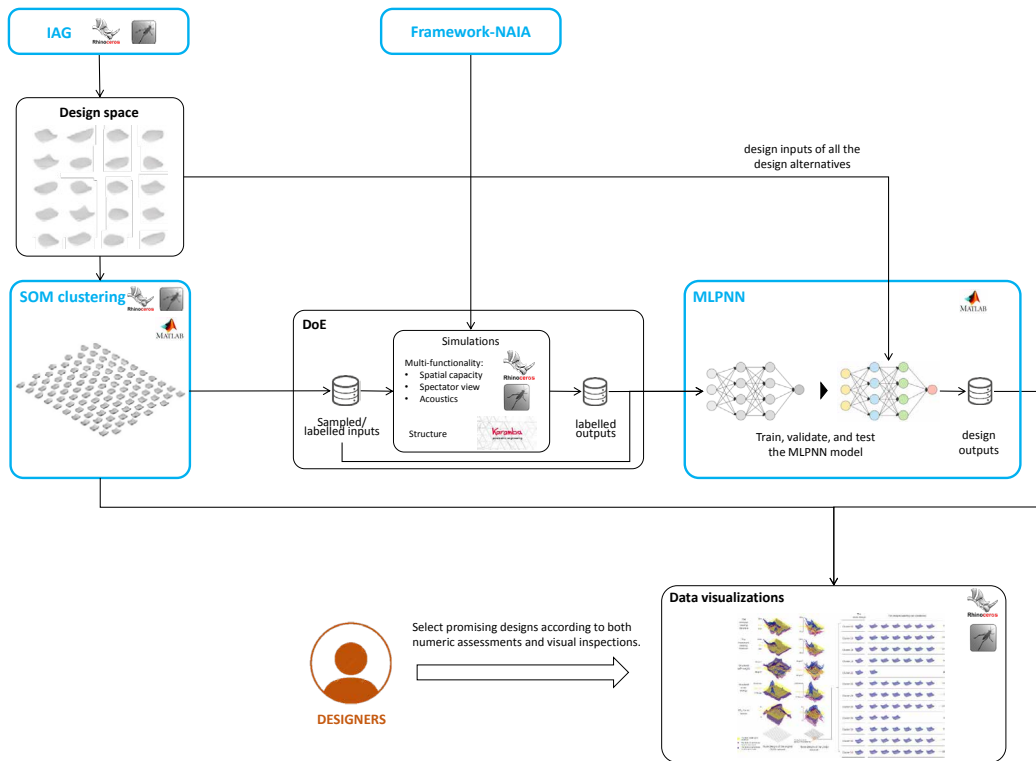


FIG. 4.6 The workflow of SOM-MLPNN to support the design exploration according to both quantitative and qualitative design requirements

In SOM-MLPNN, being similar to that in the second workflow, SOM clustering is used to group design alternatives into clusters according to geometry features and generate related representative node designs which are organized on a two-dimensional SOM network. Thus, the SOM network can be considered as an index system which organizes all the design alternatives according to geometry typology. Besides, the vectors of the nodes on the SOM network (which are also the design variables of the node designs) are used as the sampled inputs for the surrogated model based on MLPNN to predict the numeric data of the indicators (related to quantitative design requirements) for all the design alternatives. According to these predicted numeric data, the information about both geometries and numeric data of all the design alternatives can be demonstrated based on the SOM network (which organizes all the design alternatives according to geometry typology). Thus, designers can explore various design alternatives and select promising ones based on both visual investigations and numeric assessments. The related case studies are

performed in section 5.4.3 of chapter 5, which demonstrate the workflow and verify the effects.

4.3.3.1 Clustering and sampling the design alternatives by using SOM

SOM clustering here is used for two tasks. First, being similar to that in the second workflow, SOM is used to cluster the design alternatives according to geometry features, the results of which are directly used for data visualization (figure 4.6). The design variables which are directly related to the overall geometries of the design alternatives are used as the inputs of SOM clustering. A series of parameters of SOM should be defined, which are elaborated in the second workflow.

Besides, since the SOM network captures the design inputs in the input space by the nodes/neurons, the nodes actually distribute evenly among the design inputs. Thus, the process of SOM clustering can also be considered as a sampling process, in which the vectors of all the nodes on the trained SOM network can be considered as the sampled inputs. These sampled inputs are then used in DoE (figure 4.6).

Comparing to other sampling methods, SOM clustering can 1) adapt to un-uniform distribution of data within design space (which frequently exist in practice since some unfeasible designs are usually eliminated); 2) adapt to high dimensional data and avoid the 'curse of dimensionality'; 3) can preserve the topology of the original data. It is worth noting that SOM clustering is a learning process based on iterations, therefore, the computation time may be longer than those of other sampling methods. Nevertheless, SOM clustering is dispensable to the exploration of diverse types of design alternatives based on visual investigations and to the efficient organization of all the design alternatives.

4.3.3.2 Design of Experiments (DoEs)

The design of experiments (DoEs) aims at generating the labelled outputs for the node designs based on their design inputs (the labelled inputs), by using simulation tools (figure 4.6). First, the geometries of the node designs provided by SOM clustering are sent to DoEs. In DoEs, for each of the node designs, the geometry is generated based on IAG and the numeric data of various kinds of indicators related to the quantitative design requirements can be obtained by specific BPS tools, which

are the labelled outputs. Thus, the labelled inputs (the design inputs of the node designs) and the related outputs compose the pairs of labelled data.

4.3.3.3 Obtain multiple indicators related to quantitative requirements for each design alternatives in the design space

Based on the labelled data obtained in DoEs, a defined MLPNN model is trained, validated and tested to predict the numeric data of the indicators (related to quantitative design requirements) for all the design alternatives in the design space (figure 4.6). For MLPNN, the composition of the networks and the activation function applied for each neuron are usually defined by users/designers empirically, as mentioned in chapter 3, which can influence the approximation results a lot.

To overcome the problems of overfitting in generalization, a validation process is used. The labelled data are divided into three sets: training set, validation set, and test set. Within an iteration of training, the training set is used to train the MLPNN model and the validation set is used to validate the trained model by measuring the difference of the two errors obtained by these two data sets. The iterations will stop until both the errors of the trained model and the difference between the two errors are smaller than an acceptable value defined by the users. After iterations, the final trained model is selected as the best model which will be tested by the test set. If the error is also acceptable, then the model will be used for data approximation. It is worth noting that one MLPNN model can only be trained for predicting the outputs of one indicator for a number of designs. For the predictions of the numeric data related to a number of different indicators, the same number of independent MLPNNs models should be trained, respectively.

4.3.3.4 Data visualization to support the explorations of design alternatives according to both numeric data and visual investigations

Based on the SOM network, and the numeric data predicted by MLPNNs, designers can investigate various design alternatives in different types/clusters according to both numeric data and visual investigations. Moreover, designers can also study the interrelationships between the performance data (related to the quantitative design requirements) and the overall forms/geometries of the designs. A data visualization approach is proposed to support the explorations. The approach simultaneously

presents the input space represented by the node designs for the clusters and the corresponding output spaces demonstrated the values of the indicators for all the design alternatives in each cluster. The details are illustrated in the case studies in chapter 5.

4.3.3.5 Limitations

In general, the workflow of SOM-MLPNN can support the scenarios in which designers place equal emphases on both numeric assessments and visual investigations. However, considering the uncertainties of the surrogate model based on MLPNN, it is difficult to ensure the accuracy of the predicted performance values is acceptable in all cases. Moreover, the definition of an MLPNN model can impact the approximation results. An MLPNN model may be suitable for one case and has acceptable accuracy in data approximation in this case, but it may fail in other cases. However, defining a suitable MLPNN model for a specific case requires professional knowledge and experience, which can be difficult for most designers in practice.

4.4 Summary

This chapter proposes the method of computation-based integrated design of indoor arenas (CDIA), which is the core of the research, to satisfy the three basic demands of the conceptual design of indoor arenas formulated in chapter 2:

- 1 Generating numerous and diverse design alternatives of indoor arena based on the integration of multi-functionality and long-span roof structure.
- 2 Obtaining adequate information of design alternatives for the assessments of various design requirements. The information includes the values of indicators related to the numeric assessments of qualitative design requirements (about multi-functionality and structural performance) and the overall geometries for visual investigations of designers to assess the qualitative design requirements.
- 3 Adapting to different scenarios laying different emphases on quantitative and qualitative design requirements. Three scenarios, in which designers can lay different

emphases on the quantitative and qualitative design requirements, are taken into account, therefore, to allow designers to define promising design(s) according to their preferences.

CDIA is composed of three workflows based on five components (IAG, Framework-NAIA, MOO, SOM clustering, and SOM-MLPNN). The IAG and Framework-NAIA are the two basic components of the pre-process shared by the three workflows. IAG (Indoor Arena Generator) is a flexible and versatile parametric model for indoor arenas, which integrates the multi-functional space and long-span roof structure of indoor arena and can generate diverse designs including most of the possible types of arenas with three frequently used structure (grid shell, space frame, and truss beam).

Framework-NAIA (Framework for Numeric Assessments of Indoor Arenas) collects various indicators as well as the related simulations and assessment criteria of the multi-functionality (the spatial capacity, spectator view, and acoustics of multiple activities) and structural performance of indoor arenas. Such a framework aids designers to rapidly customize criteria to assess designs, according to quantitative design requirements.

By using IAG and Framework-NAIA (containing the BPS tools), numerous design alternatives with diverse geometries can be generated, and the information of geometry and numeric performance data about the alternatives are possible to be obtained, which satisfies the first two basic demands of the conceptual design of indoor arenas. Based on these two components, three workflows of CDIA are formulated by using the techniques of Multi-Objective Optimization (MOO), unsupervised clustering based on self-organizing map (SOM clustering) and multi-layered perceptron neural network based on self-organizing map (SOM-MLPNN). The three workflows are independent and used for the different scenarios in practice, which satisfy the third basic demands of the conceptual design of indoor arenas.

- 1 In the first design scenario, designers intend to prioritize numeric assessments relate to quantitative design requirements. Correspondingly, the workflow uses MOO to search for 'well-performing' designs in a wide design space (generated based on IAG), according to the assessment criteria related to quantitative design requirements (formulated by designers based on Framework-NAIA). Among the 'well-performing' designs, designers can further select promising ones based on visual investigations according to their knowledge and experience about qualitative design requirements. However, since it is based on BPSs, the computation time can be long. Moreover, as mentioned in section 3.4.5 of chapter 3, a standard MOO

can only efficiently deal with no more than three design objectives, which limits the dynamic design explorations.

- 2 In the second design scenario, designers intend to prioritize visual investigations related to qualitative design requirements. Correspondingly, the workflow firstly uses SOM clustering to group numerous designs in a wide design space (generated based on IAG) according to the geometry features, based on which designers can select promising types/groups of design alternatives by visually investing according to their knowledge and experience about qualitative design requirements. Then, MOO is used to search for 'well-performing' ones among the selected types of design alternatives, according to the assessment criteria related to quantitative design requirements (formulated by designers based on Framework-NAIA). Comparing to the computation time of the MOO in the first workflow, the time can be shorter in the second workflow, since fewer iterations and population are set for the smaller searching space. However, the 'well-performing' design alternatives can be 'worse' than the counterpart in the first workflow, since some 'better performing' ones may be excluded from the selected types and cannot be selected by the MOO.
- 3 In the third design scenario, designers intend to place equal emphases on numeric assessments related to quantitative design requirements and visual investigations related to qualitative design requirements. Correspondingly, being similar to that in the second workflow, this workflow uses SOM clustering to group design alternatives according to geometry features and to generate node designs representing different groups/clusters of designs. Moreover, SOM is also used as the sampling tool for the surrogate models based on MLPNN which are used to predict the numeric indicators of all the design alternatives. Based on the SOM network which presents the geometries of various types of designs and the predicted numeric indicators, designers can explore the design alternatives and directly select the promising ones based on both numeric assessment and visual investigations. However, there are uncertainties in the data approximations based on MLPNN, which can lead to large errors and are difficult to identify during generalization.

The three workflows are applied in the case studies of chapter 5, in which their effects and limitations in supporting the design explorations are verified.

References

- 'gamultiobj' [online] <https://www.mathworks.com/help/gads/gamultiobj.html> (19 April, 2020)
- 'mutationadaptfeasible' [online] <https://www.mathworks.com/help/gads/genetic-algorithm-options.html> (19 April, 2020)
- clusterdata' hirachical [online] <https://www.mathworks.com/help/stats/clusterdata.html>(19 April, 2020)
- Harding, J. (2016) Dimensionality reduction for parametric design exploration. In: Adriaenssens, S., Gramazio, F., Kohler, M., Menges, A. and Pauly, M., eds. (2016) *Advances in Architectural Geometry 2016*. Zurich, Switzerland: vdf Hochschulverlag AG an der ETH Zurich, pp. 274-287. ISBN 9783728137777 Available from: <http://eprints.uwe.ac.uk/30096>
- Kim, J., Ryu, H., Cho, D., Song, K. (2016) Structural design of Philippine Arena. *Journal of Civil Engineering and Architecture* 10, pp. 405-416. DOI 10.17265/1934-7389/2016.04.002
- Lämsiluoto, A. (2004) *Economic and Competitive Environment Analysis in the Formulation of Strategy: A Decision-Oriented Study Utilizing Self-Organizing Maps*. Turun Kauppakoekoulun Julkaisuja: Publications of the Turku School of Economics and Business Administration. ISBN: 951-564-230-2 (PDF) 951-564-229-9 (nid.)
- Mathworks. (2020). *Global Optimization Toolbox: User's Guide (R2020b)*. Retrieved 20 April, 2020 from www.mathworks.com/help/pdf_doc/gads/gads_tb.pdf
- Mathworks. (2020). *MATLAB(R2020b)*. Natick, Massachusetts: The MathWorks Inc.
- Matlab [online] https://www.mathworks.com/?s_tid=gn_logo (19 April, 2020)
- Pan, W., Sun, Y., Turrin, M., Louter, C., Sariyildiz, S., (2020) Design exploration of quantitative performance and geometry typology for indoor arena based on self-organizing map and multi-layered perceptron neural network. *Automation in Construction*. 114, pp. 464-485. DOI10.1016/j.autcon.2020.103163
- Pan, W., Turrin, M., Louter, C., Sariyildiz, S., Sun, Y. (2018). Integrating the Multi-Functional Space and Long-Span Structure for Sports Arena Design : A design exploration process based on design optimization and self-organizing map, in: Mueller, C., Adriaenssens, S. (Eds.), *Proceeding of the IASS Symposium 2018: Creativity in Structural Design, Vol 2018*, International Association for Shell and Spatial (IASS), Boston, pp.1-8. <https://www.ingentaconnect.com/content/iass/piass/2018/00002018/00000004/art00015#>
- Pan, W., Turrin, M., Louter, C., Sariyildiz, S., Sun, Y. (2019) Integrating multi-functional space and long-span structure in the early design stage of indoor sports arenas by using parametric modelling and multi-objective optimization. *Journal of Building Engineering*. 22, pp. 464-485. DOI10.1016/j.job.2019.01.006

5 Case studies: applying CDIA in the designs of two typical arenas

5.1 Introduction

In this chapter, CDIA is used in the design examples of two typical indoor arenas (Barclay Centre in New York and O2 Arena in London), aiming to demonstrate the method of CDIA and to verify its effects and limitations in supporting the conceptual design of indoor arenas.

As discussed in section 2.2.2.2 in chapter 2, according to the layout of the seating tiers, all indoor arenas can be divided into three types:

- 1 the seating tiers are symmetric to the pitch,
- 2 the seating tiers are asymmetric along the long-axis of the pitch,
- 3 the seating tiers are asymmetric along the short-axis of the pitch.

Most of the indoor arenas belong to the first and second types, according to the investigation of the 129 representative indoor arenas all over the world (Appendix). The third type of arenas are seldomly used, therefore, it is not considered in these case studies. The first type of indoor arenas mainly serve for sports events and sometimes also serve for stage performances (concerts), and Barclay Centre in New York is a typical one of this type. The second type of indoor arenas serve for both stage performances (with an end-stage) and sports events, and O2 Arena in London

is a typical one of this type. These two typical arenas are selected as the examples for case studies. The backgrounds of these two examples and the details of the related hypothetical designs are introduced in section 5.2.

To apply CDIA to the designs of the two arenas, the pre-process components, IAG and Framework-NAIA, are firstly used to define the design spaces and formulate the quantitative assessment criteria (figure 5.1), which are elaborated in section 5.3. Based on the pre-process, the three design scenarios, in which designers intend to place different emphases on numeric assessments and visual investigations, are considered for the hypothetical designs of the two arenas. The three proposed workflows of CDIA based on MOO, SOM clustering and MOO, as well as SOM-MLPNN are used to support the designs of the three scenarios, respectively (figure 5.1). The related details and results are elaborated in section 5.4. The effects and limitations are verified in the case studies and are discussed in section 5.5.

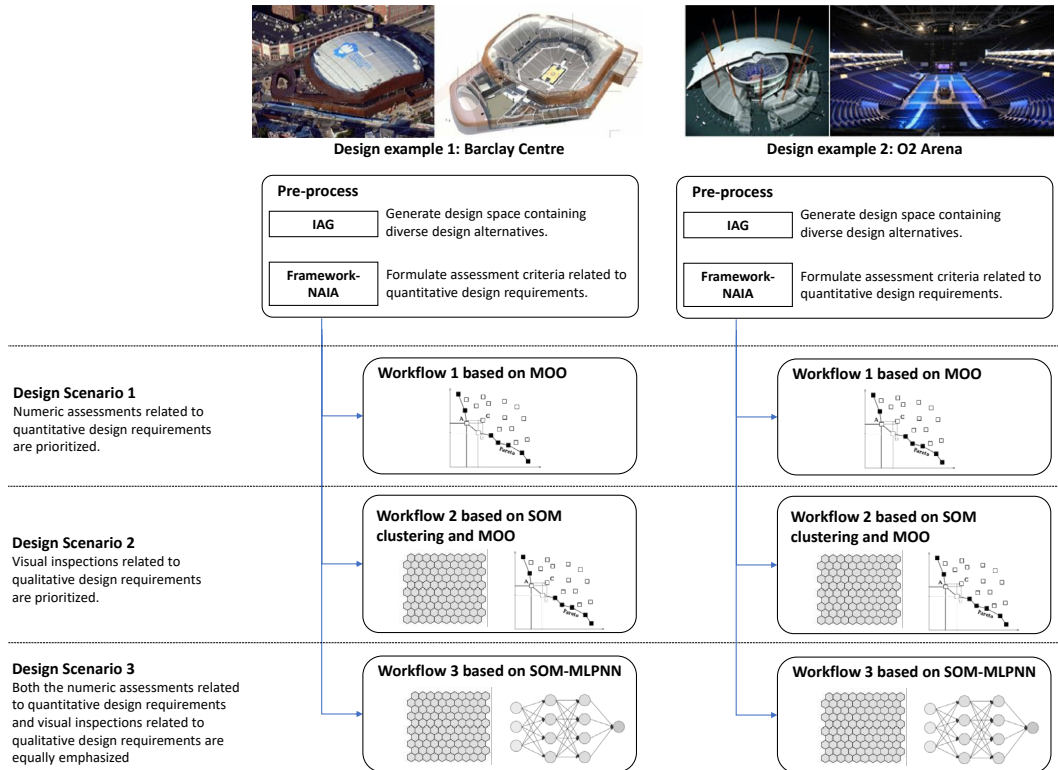


FIG. 5.1 The scheme of the cases studies (the picture sources of Barclay Arena: info-stade, 2013 and Advance Graphics, 2015; the picture sources of O2 Arena: Trip2london, 2014 and Wikipedia, 2016)

5.2 Two typical examples: Barclay Centre and O2 Arena

5.2.1 Barclay Centre: an arena mainly for sports events and sometimes for pop-music concerts

Barclay Centre (figure 5.2, left and middle) is a typical arena which is mainly used for games of basketball (NBA) and ice-hockey (NHL) and is also sometimes used for pop-music concerts. The seating bowl, which contains 18,700 fixed seats, is an approximate octagon being symmetric along both the long (y-) and short (x-) axes of the rectangle pitch. The long-span roof is a shallow dome with a space-frame structure. A similar configuration with a space-frame structure can be generated by using IAG (figure 5.2, right)

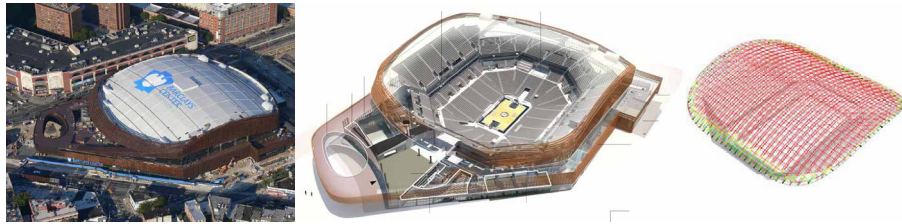


FIG. 5.2 Barclay Centre (left (left: Info-stade, 2013, and middle: Advance Graphics, 2015) and a similar configuration (right) generated by IAG

According to these attributes, a hypothetical design of Barclay Centre in this research is formulated. In this design, the multi-functional space should accommodate the courts of basketball and ice-hockey and about 18,700 fixed seats. The seating bowl should be symmetric along the long (y-) and short (x-) axes, which is suitable for this type of arenas. Besides space frame structure which is used for the long-span roof in the original design, grid shell and truss beam structures are also considered. Based on these general requirements about the configuration, the overall form of the building should be allowed to change in a large extent to generate diverse design alternatives. For the quantitative design requirements, the aspects of spectator view for both the basketball and ice-hockey games, acoustics for pop concerts,

and structural performance are highlighted. For qualitative design requirements, designers are allowed to evaluate design alternatives according to their knowledge and experience. According to these general requirements, a design space and specific quantitative assessment criteria can be formulated in the pre-processing step based on IAG and framework-NAIA, respectively (details are elaborated in section 5.3).

5.2.2 O2 Arena: an arena for both pop-music concerts and sports events

O2 Arena (figure 5.3, left and middle) is used for both pop-music concerts (with an end-stage) and sports events. According to the statistics of 'Pollstar' (a trade industry journal), O2 Arena was the busiest venue for concerts all over the world in 2016 (Pollstarpro.com, 2016). Meanwhile, the O2 Arena is also used for various high-level sports events, including some oversea games of NBA (basketball) and NHL (ice-hockey), tennis matches of ATP, and some matches of the 2012 summer Olympic games (basketball, artistic gymnastics, trampoline). The arena has a rectangle pitch which can accommodate gymnastics match. Around the pitch, the rectangle seating bowl of O2 Arena is asymmetric along the long (y-) axis of the pitch, therefore most of the fixed seats are available for the performances with an end-stage. Although the venue is covered by the famous Millennium Dome (figure 5.3, left), it has an independent roof with a space-frame structure (composed of two main trusses and many small trusses) (NSC2-SSDA, 2008). Therefore, in this research, it is considered as an independent venue without the membrane dome. A similar configuration can be generated by using IAG (figure 5.3, right).



FIG. 5.3 O2 Arena (left: Trip2london, 2014, and middle: Wikipedia, 2016) and a similar configuration (right) generated by IAG

According to the background, the hypothetical design of O2 Arena in this research is formulated. In this design, the multi-functional space should accommodate the courts of basketball, ice-hockey as well as gymnastics and around 20,000 fixed seats. The seating bowl is asymmetric along the long (y-) axes of the pitch, in which the ratio of the asymmetry is allowed to vary to generate different design alternatives. Besides space frame structure which is used for the long-span roof in the original design, grid shell and truss beam structures are also considered. Based on these general requirements about the configuration, the overall form of the building should be allowed to change in a large extent to generate diverse design alternatives. For the quantitative design requirements, the aspects of spectator view for the performances with an end-stage as well as the basketball and ice-hockey games, acoustics for pop concerts, and structural performance are highlighted. For qualitative design requirements, designers are allowed to evaluate design alternatives according to their knowledge and experience. According to these general requirements, a design space and specific quantitative assessment criteria can be formulated in pre-processing step based on IAG and framework-NAIA, respectively (details are elaborated in section 5.3).

5.3 Pre-processing of CDIA based on IAG and Framework-NAIA

In the pre-processing step of CDIA, for a design task, a series of design parameters of IAG (see table 4.1) should be defined to formulate a design space, and a set of numeric assessment criteria related to quantitative design requirements should be also defined based on framework-NAIA.

5.3.1 Defining design space based on IAG

As discussed in section 4.2, to define a design space containing numerous and diverse design alternatives of indoor arenas, the design parameters of IAG should be defined. Some parameters are fixed in certain values, while others can be changed in defined ranges. According to the hypothetical design tasks of Barclay Centre and O2 Arena, the design parameters are defined and listed in tables 5.1 and 5.2, respectively.

For Barclay Centre, since it is mainly used for basketball and ice-hockey games, the parameters of pitch size are defined as rectangle in $65\text{m} \times 36\text{m} \times 18\text{m}$. A series of parameters related to seating tiers are defined according to Eurocode EN 13200-1:2012 (CEN, 2012). Since the seating bowl is symmetric along both the long (y-) and short (x-) axes of the pitch, the related parameters are fixed in 0. The number of the fixed seats is limited between 18,000 to 19,000. The structural steel S275 is selected as the material for the long-span roof structure. Other parameters are selected as design variables (labelled in '*' in table 5.1), and the related ranges and intervals are defined. It is worth noting that, as mentioned in section 4.2.1 of chapter 4, the IAG can automatically eliminate the design alternatives which have too many or too few fixed seats according to the parameters of fixed seat number. Based on the definition, 1,177,200 design alternatives can be generated by IAG to compose the design space.

For O2 Centre, since it is mainly used for both pop-music concerts (with an end-stage) and sports events (gymnastics, ice-hockey, basketball, tennis, etc.), the parameters of pitch size are defined as a rectangle in $40\text{m} \times 70\text{m} \times 18\text{m}$. A series of parameters related to seating tiers are defined according to Eurocode EN 13200-1:2012 (CEN, 2012). Since the seating bowl is symmetric along the short (x-) axes of the pitch, the related parameters are fixed in 0. The number of the fixed seats are limited between 19,000 to 21,000. The structural steel S275 is selected as the material for the long-span roof structure. Other parameters are selected as design variables (labelled in '*' in table 5.2), and the related ranges and intervals are defined. Based on the definition, 1,653,850 design alternatives can be generated by IAG to compose the design space.

TABLE 5.1 The design parameters of the design example of Barclay Centre

1	P-size	the dimensions of the pitch (ice-hockey): 65m × 36m × 18m
2	Seat-Num	the number of the fixed seats: 18, 000 to 19,000
3	SE_Prin	the principal sports event defined by designers: basketball and ice-hockey
4	V	the vertical distance from eyes of a spectator to the top of the head or the sightline of the spectator in the front row: 120mm.
5	ST_DpthSR	the depth of a seating-row: 0.8m
6	ST_WidthS	the width of a seat: 0.5m
7	ST_NumSR	the number of the seats between radical or parallel passageways: ≤ 28
8	ST_WdthPW	the width of a passageway: 1.2m
9	ST_Sec	the number of the sections of the seating tiers: two sections
10	ST_RowNum	the number of rows for each section of the seating tiers: – lower tiers (without retractable seats): 12 rows – Higher tiers: depends on the boundary
11	ST_LenX *	the length of the x-axis of the seating bowl boundary: 100m – 160m
12	ST_AsyX	the asymmetric ratio of the seating bowl boundary along the x-axis: 0
13	ST_LenY *	the length of the y-axis seating bowl boundary: 90m –120m
14	ST_AsyY	the asymmetric ratio of the seating bowl boundary along the y-axis: 0
15	ST_CPi *, ST_CPii *, ST_CPiii *, ST_CPiv*	the corner points of the seating bowl boundary in the 1 st , 2 nd , 3 rd , and 4 th quadrant: 0, 1, 2, 3, 4, 5, 6, 7
16	ST_Bdr*	the curve degree of the seating bowl boundary: 1 (polyline) and 3 (curve)
17	Str_BdrCPi	the height of the ith control point of the structural boundary: 0
18	Str_FCHeight*	the floor to ceiling height of the roof structure at the central point of the pitch: 20m – 45 m
19	Str_RidgeX* Str_RidgeY*	the curve degree of the ridges along the x-axis and y-axis: 1 (polyline) and 3 (curve)
20	Str_DepCen*	the structural depth of the roof structure at the central point (for space frame and truss beam): 2m – 6m
21	Str_DepBdr*	the structural depth of the roof structure on the boundary (for space frame and truss beam): 0.8–3m
22	Str_Type*	the structural types of the long-span roof: 0: GS (Grid Shell); 1: SF (space frame); 2: TBX (truss beam)
23	Str_Grid	the grid size of structural tessellation for the long-span roof: 1.8–2.2 m for Grid-shell; 4–5m for space-frame and truss beam
24	Str_CrSec*	the structural cross-section: Circle hollow, diameter: 0.3 - 0.6m, thickness: 20 – 70 mm.
25	Str_Mtr	the structural material: S275

TABLE 5.2 Design parameters of the example of O2 arena

1	P-size	the dimensions of the pitch (ice-hockey): 70m × 40m × 18m
2	Seat-Num	the number of the fixed seats: 19, 000 to 21,000
3	SE_Prin	the principal sports event defined by designers: basketball and ice-hockey gymnastics
4	V	the vertical distance from eyes of a spectator to the top of the head or the sightline of the spectator in the front row: 120mm
5	ST_DpthSR	the depth of a seating-row: 0.8m
6	ST_WidthS	the width of a seat: 0.5m
7	ST_NumSR	the number of the seats between radical or parallel passageways: ≤ 28
8	ST_WdthPW	the width of a passageway: 1.2m
9	ST_Sec	the number of the sections of the seating tiers: two sections
10	ST_RowNum	the number of rows for each section of the seating tiers: – lower tiers (without retractable seats): 12 rows – Higher tiers: depends on the boundary
11	ST_LenX *	the length of x-axis of the seating bowl boundary: 100m – 160m
12	ST_AsyX	the asymmetric ratio of the seating bowl boundary along the x-axis: 0
13	ST_LenY *	the length of the y-axis of the seating bowl boundary: 90m -120m
14	ST_AsyY	the asymmetric ratio of the seating bowl boundary along the y-axis: 6, 8, 10
15	ST_CPi*, ST_CPiv*	the corner points of the seating bowl boundary in the 1 st and 4 th quadrant: 0, 1, 2, 3
16	ST_CPii*, ST_CPiii*	the corner points of the seating bowl boundary in the 2 nd and 3 rd quadrant: 0, 1, 2, 3
17	ST_Bdr*	the curve degree of the seating bowl boundary: 1 (polyline) and 3 (curve)
18	Str_BdrCPi	the height of the i th control point of the structural boundary: 0
19	Str_FCHeight*	the floor to ceiling height of the roof structure at the central point of the pitch: 20m - 45 m
20	Str_RidgeX* Str_RidgeY*	the curve degree of the ridges along the x-axis and y-axis: 1 (polyline) and 3 (curve)
21	Str_DepCen*	the structural depth of the roof structure at the central point (for space frame and truss beam): 2m – 6m
22	Str_DepBdr*	the structural depth of the roof structure on the boundary (for space frame and truss beam): 0.8-3m
23	Str_Type*	the structural types of the long-span roof: 0: GS (Grid Shell); 1: SF (space frame); 2: TBX (truss beam)
24	Str_Grid	the grid size of structural tessellation for the long-span roof: 1.8-2.2 m for Grid-shell; 4-5m for space-frame and truss beam
25	Str_CrSec*	the structural cross-section: Circle hollow, diameter: 0.3 - 0.6m, thickness: 20 – 70 mm.
26	Str_Mtr	the structural material: S275

5.3.2 Formulate numeric assessment criteria related to quantitative design requirements based on Framework-NAIA

According to the quantitative design requirements about the design tasks, the related numeric assessment criteria can be formulated by selecting indicators and the related BPS tools in framework-NAIA. For Barclay Centre, as mentioned in section 5.2.1, spectator view for basketball and ice-hockey, acoustics for pop-music concerts, and structural performance is emphasised. Therefore, the average viewing distances of basketball and ice-hockey are required to be minimized, the reverberation time of all the octave band frequency is required to get close to 1.3s (which is preferred by pop music, see figure 2.28 in chapter 2), the structure mass is required to be minimized. Besides, to satisfy the regulations of design codes, there are a series of constraints. The maximum viewing distances of basketball and ice-hockey cannot be larger than the acceptable values in Eurocode EN 13200-1:2012 (CEN, 2012). The vertical deflection of the overall structure and the maximum normal stress in elements cannot be larger than the value regulated by Eurocode EN-1990: 2002 (CEN, 2002) and EN-1993-1-1:2005 (CEN, 2005). The assessment criteria for the hypothetical design of Barclay Arena are listed in table 5.3.

TABLE 5.3 Input data of the optimization for the Barclay Centre (OPT-BC).

objectives	1	Minimizing the maximum value of the average viewing distances of both basketball and ice-hockey: min. (max[SE_avrVD-basketball, SE_avrVD-icehockey])
	2	Minimizing the difference between the reverberation time and the value of 1.3s: min. (RT _{60-all} - 1.3s)
	3	Minimizing the structural mass of the roof: min. SW
constraints	1	The maximum viewing distance for ice-hockey SE_maxVD-icehockey ≤ 110m
	2	The maximum viewing distance for basketball SE_maxVD-icehockey ≤ 130m
	4	The normal stress of structural elemental cross section: $\sigma_{x,Ed} \leq \frac{f_y}{\gamma_M}$
	5	Structural vertical deflection: $dfl \leq \frac{span}{250}$

For O2 Arena, as mentioned in section 5.2.2, spectator view for performances (with an end-stage), basketball, ice-hockey, and gymnastics, acoustics for pop-music concerts, and structural performance is emphasized. Therefore, the ratio of seats with premium viewing distance for end-stage is required to be maximized, the average viewing distances of basketball and ice-hockey are required to be minimized, the reverberation time of all the octave band frequency is required to get close to 1.3s, the structure mass and strained energy are required to be minimized. Besides, to guarantee enough available fixed seats for the performance with an end-stage and to satisfy the regulations of design codes, there are a series of constraints. The ratio of multi-functional seats (for both performances and sports events) should not be less than 85%. The maximum viewing distances of basketball and ice-hockey cannot be larger than the acceptable values in Eurocode EN 13200-1:2012 (CEN, 2012). The deflection of the overall structure and the maximum normal stress in elements cannot be larger than the value regulated by Eurocode EN-1990:2002 (CEN, 2002) and EN-1993-1-1:2002 (CEN, 2005). The assessment criteria for the hypothetical design of Barclay Arena are listed in table 5.4. To deal with more design objectives, two MOOs are formulated based on two sets of design objectives, for both the first and second workflows.

TABLE 5.4 Input data of the optimizations for the O2 Arena (OPT-O2).

The first MOO of the design of O2 arena	objectives	1	Minimizing the maximum value of the average viewing distances of both basketball (SE_avrVD-basketabl) and ice-hockey (SE_avrVD-icehockey): min. (max[SE_avrVD-basketball, SE_avrVD-icehockey])	
		2	Minimizing the difference between the reverberation time (RT ₆₀) and the value of 1.3s: min. (RT _{60,all} - 1.3s)	
		3	Minimizing the structural mass (SM) of the roof: min. SW	
	constraints	1	The percentage of the seats available for the stage performances with an end stage should larger than 85% (HVA=90 degrees, end stage size: 25m×10m, the reference points are the back corners of the stage): SPend_PctAS ≥ 85%	
		2	The maximum viewing distance for ice-hockey SE_maxVD-icehockey ≤ 110m	
		3	The maximum viewing distance for basketball SE_maxVD-icehockey ≤ 130m	
		4	The normal stress of structural elemental cross section: $\sigma_{x,Ed} \leq \frac{f_y}{\gamma_M}$	
		5	Structural vertical deflection: $dfl \leq \frac{span}{250}$	
	The second MOO of the design of O2 arena	objectives	1	Maximizing the percentage of the seats whose horizontal viewing angle are not larger than the premium horizontal viewing angle (20 degree) for a stage performance with an end-stage: max. SPend_PctPHVA
			2	Minimizing the difference between the reverberation time and the value of 1.3s: min. (RT _{60,all} - 1.3s)
3			Minimizing the structural strain energy: min. SE	
constraints		1	The percentage of the seats available for the stage performances with an end stage should larger than 85% (HVA=90 degrees, end stage size: 25m×10m, the reference points are the back corners of the stage) SPend_PctAS ≥ 85%	
		2	The maximum viewing distance for ice-hockey SE_maxVD-icehockey ≤ 110m	
		3	The maximum viewing distance for basketball SE_maxVD-icehockey ≤ 130m	
		4	The normal stress of structural elemental cross section: $\sigma_{x,Ed} \leq \frac{f_y}{\gamma_M}$	
		5	Structural vertical deflection: $dfl \leq \frac{span}{250}$	

Specifically, to perform structural simulation, a loading model should be formulated for the structure. According to the discussion in section 3.3.2.2 in chapter 3, three loading combinations are set for the long-span roof structure, which are listing in table 5.5.

TABLE 5.5 Loading combinations for the long-span roof structure

Loading actions	$E_{d1} = \gamma_G (G_1 + G_2 + G_3)$			
	$E_{d2} = \gamma_G (G_1 + G_2 + G_3) + \gamma_Q Q_1$			
	$E_{d3} = \gamma_G (G_1 + G_2 + G_3) + \gamma_Q Q_2$			
Permanent loads	Structural self-weight G1 calculated based on the configuration generated by IAG	Variable loads	Wind load	Q1 = 1.8 kN/m ²
	Ceiling and cladding G2= 2 kN/m ²		Snow load	Q2= 2 kN/m ²
	Hanging facilities G3= 1.5 kN/m ²			
factors	$\gamma_G = 1.35$ (the partial factors of the permanent loads for the ultimate limit state recommended by Eurocode En-1990:2002 (CEN, 2002)) $\gamma_Q = 1.50$ (the partial factors of the variable loads for the ultimate limit state recommended by Eurocode En-1990:2002 (CEN, 2002))			

5.4 Applying CDIA to support conceptual designs in different scenarios

Based on the design space containing numerous design alternatives and the numeric assessment criteria related to quantitative design requirements, the three workflows of CDIA are applied to the design tasks, to support the conceptual designs of the three different scenarios in which designers intend to place different emphases on numeric assessments related to quantitative design requirements and visual investigations related to qualitative design requirements.

5.4.1 Using MOO to support the design exploration emphasizing numeric assessments

By using MOOs, this workflow provides ‘well-performing’ designs according to customized numeric assessment criteria related to quantitative design requirements. Therefore, designers can select promising designs among them, according to their knowledge and experience about qualitative design requirements. It is worth noting that, as discussed in section 3.4.5 chapter 3, a standard MOO can only efficiently deal with design objectives no more than three. For the design example of Barclay Centre, one MOO is used for the set of assessment criteria listed in table 5.4. For the design example of O2 Arena, two MOOs are used for the two sets of assessment criteria listed in table 5.5, respectively, to study how the different assessment criteria influence the ‘well-performing’ design alternatives.

The related parameters for the MOOs are set in table 5.6. Considering the amounts of design alternatives in the two formulated design spaces (1,177,200 for Barclay Centre and 1,653,850 for O2 Arena), the population size is set in 150, and the iteration times are 100, therefore, at most 16,500 design alternatives (double size of population for the first iteration) are investigated during the iterations (some design alternatives can be selected into the populations for several times). ‘mutationadaptfeasible’ function, as mentioned in section 4.3.1.1 of chapter 4 are used to achieve changeable mutation rate during the iterations.

TABLE 5.6 Parameters of the optimizations of the designs of Barclay Centre and O2 Arena

Population size	150 (300 for the initial iteration)
Iterations	100
Searching algorithm	NSGA II
Mutation rate	Using dynamic mutation rate based on ‘mutationadaptfeasible’ function
Selection function	Binary tournament
Pareto ratio	52 %

The application of MOOs for the designs of Barclay Centre and O2 Arena has been studied in a previous paper of the author (Pan et al., 2019). Here, the results are reused to demonstrate and verify the effects and limitations of the workflow. By using the data visualization proposed in the section 4.3.1.2 in chapter 4, the results are demonstrated and the observations are listed in section 5.4.1.1 and section 5.4.1.2.

5.4.1.1 Using MOO for the hypothetical design of Barclay Centre

The results of the MOO for the design example of Barclay Centre is illustrated in figure 5.4. In part A of figure 5.4, the coordinate chart illustrates the values of the three design objectives for the Pareto solutions (the ‘well-performing’ designs alternatives). The solutions are represented by the solid dots, and the hollow circles are the projections of the dots on the three planes of the coordinate system. Different colours of the dots and of the labels for the design alternatives indicate different structural types: green for grid-shell, blue for space-frame, and red for truss-beam. Some selected key ‘well-performing’ design alternatives on the Pareto frontiers of obj.1 vs. obj.3, obj.2 vs. obj.3, and obj.1 vs. obj.2, respectively, are illustrated around the coordinate chart, which presents how the geometry and structural type vary as the change of performance values. Based on these key designs, the relationships between performance values and geometries with different types of structures can be further study to obtain some knowledge.

There are some observations according to the results.

- The Pareto solutions (the ‘well-performing’ design alternatives) are diverse in geometry and in structural types, according to the manual classification of the Pareto solutions illustrated in the part C of figure 5.4. Moreover, some of the Pareto solutions are similar to some real arenas (figure 5.2), which is unpredictable at the beginning of the design. The reason can be attributed to the diversity of the design alternatives generated based on IAG.
- For the Pareto solutions, the geometries and structural types change as the change of the values of the design objectives, according to the key Pareto solutions illustrated around the coordinate charts in part A of figure 5.4. The Pareto solutions perform better than the original design illustrated in Part A of figure 5.4, according to the values of design objectives. It means that to satisfy the different design objectives, different geometries and structural types are necessary.
- There are also design alternatives with other types of geometries in the design space, which are quite different from the Pareto solutions. Some of these design alternatives are randomly selected in the design space and illustrated in part B of figure 5.4. It indicates that there can be more diverse design alternatives in the design space, which are not available to designers by using this workflow.

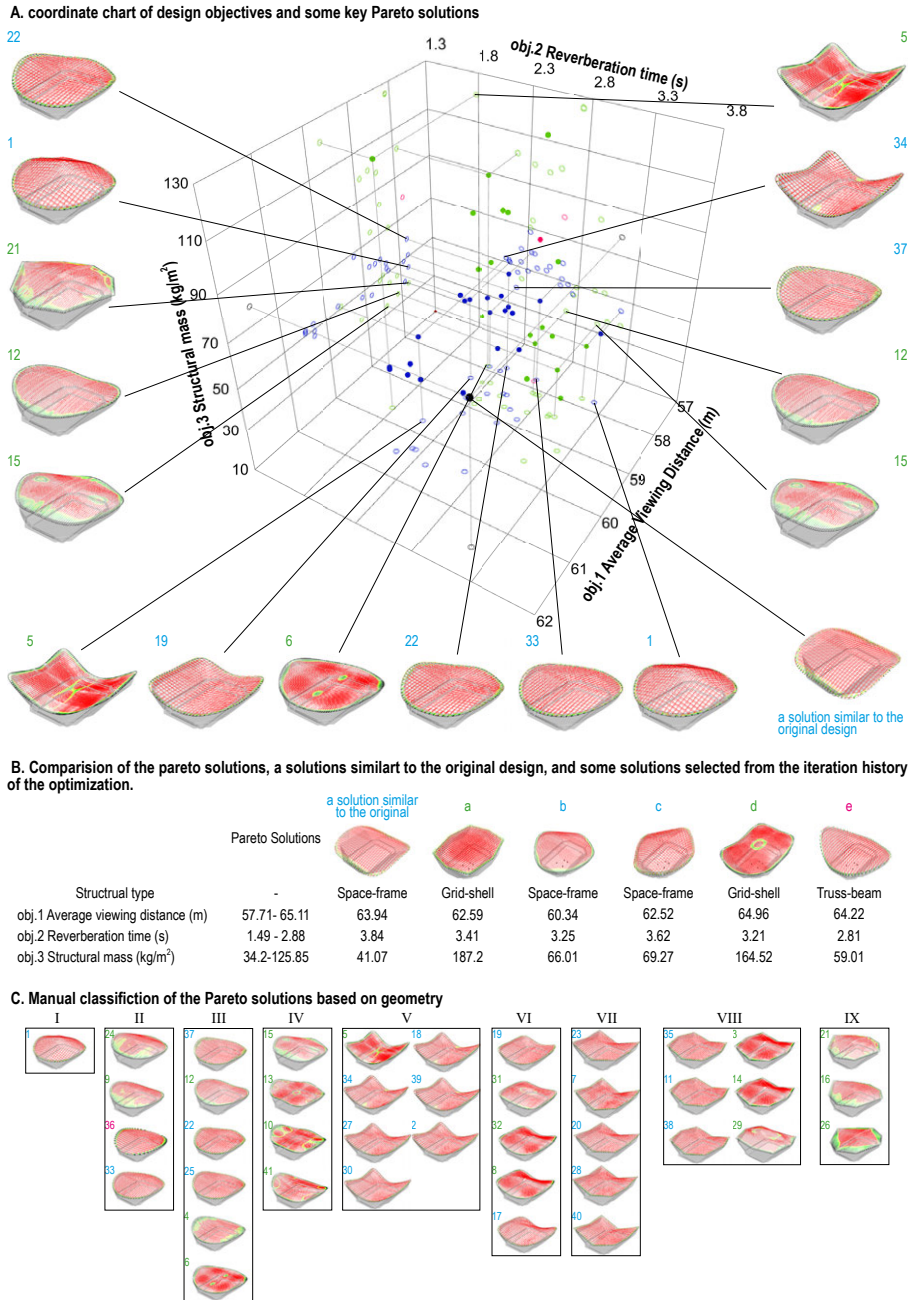


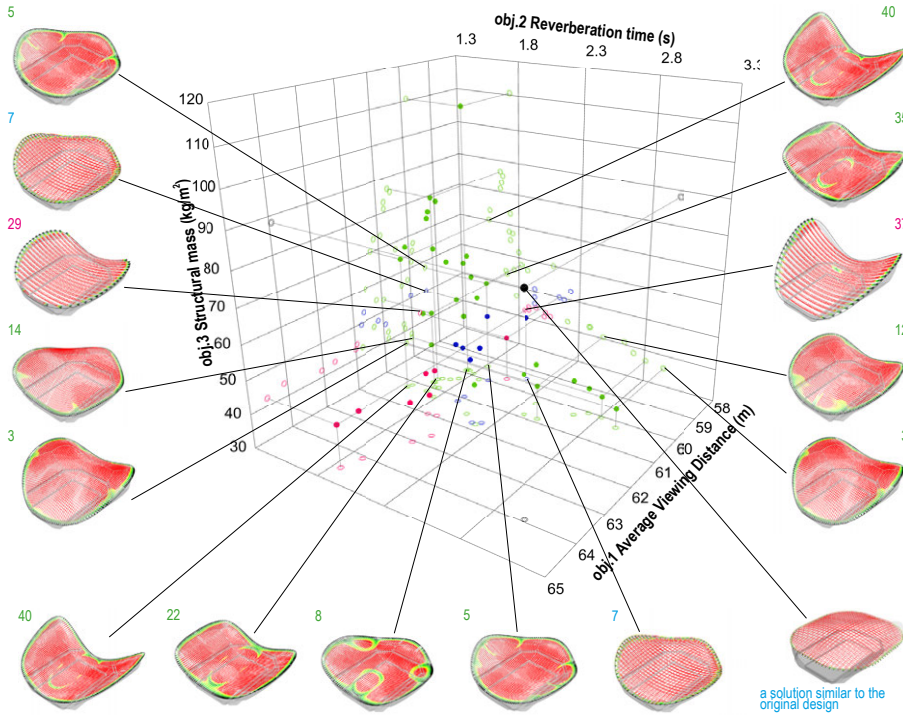
FIG. 5.4 The results of MOO for the design of Barclay Centre

5.4.1.2 Using MOO for the hypothetical design of O2 Arena

As mentioned above, two MOOs with different sets of design objectives are applied for the design of O2 Arena. The results are illustrated in figure 5.5 and figure 5.6, respectively.

The observations in the MOO results for the design of Barclay Centre (section 5.4.1.1) are also obtained in the results of these two MOOs, according to figure 5.5 and figure 5.6. Specifically, in part C of figure 5.5, three Pareto solutions are similar to London Aquatic Centre designed by Zaha Hadid, while in the part C of figure 5.6, two Pareto solutions are similar to Barcelona Arena designed by HOK. Besides, the Pareto solutions of these two MOOs are quite different from those in the MOOs for Barclay Centre (figure 5.4), since the design spaces of the two design tasks and the design objectives of the MOOs are different. Moreover, even for these two MOOs for the design example of O2 arena, which apply the same design space generated by IAG, the Pareto solutions are quite different, since the design objectives are different. This observation further indicates that different design tasks need different design spaces generated based on different formulations of design variables, which can be satisfied by using IAG for its flexibility in providing different design spaces. Furthermore, even for the same design task, different sets of design objectives can select different design alternatives, therefore, it requires a wide design space containing diverse alternatives, which can also be satisfied by using IAG.

A. coordinate chart of design objectives and some key Pareto solutions



B. Comparison of the pareto solutions, a solutions similar to the original design, and some solutions selected from the iteration history of the optimization.

	a solution similar to the original design	a	b	c	d	
Pareto Solutions						
Structural type	-	Space-frame	Space-frame	Truss-beam	Grid-shell	Space-frame
obj.1 Viewing distance (m)	59.44 - 64.55	63.94	65.25	64.42	66.91	61.72
obj.2 Reverberation time (s)	1.55 - 2.94	2.98	2.91	3.09	3.14	3.3
obj.3 Structural Mass (kg/m³)	35.85 - 110.58	88.23	84.92	144.64	213.52	97.24

C. Manual classification of the Pareto solutions based on geometry

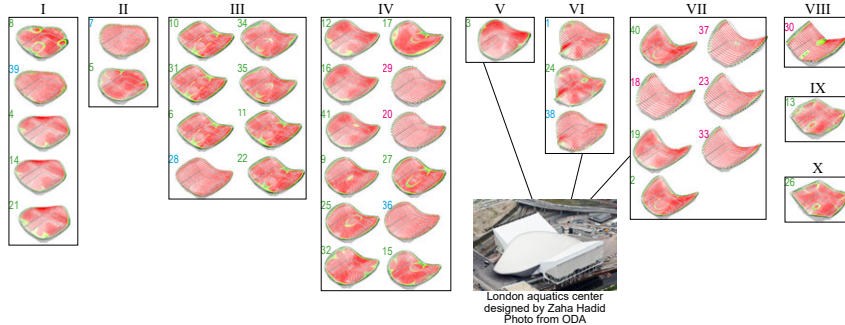
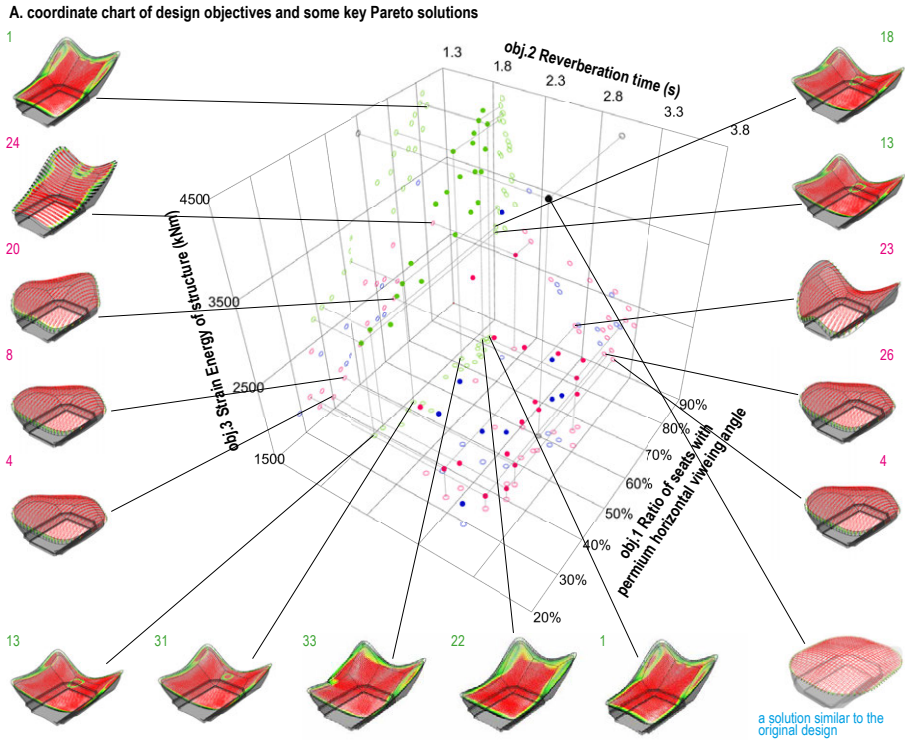


FIG. 5.5 The results of the first MOO for the design of O2 Arena (the Picture source of the London Aquatics Centre: World Para Swimming, 2011)



B. Comparison of the pareto solutions, a solutions similar to the original design, and some solutions selected from the iteration history of the optimization.

	a solution similar to the original design	a	b	c	d	
Pareto Solutions						
Structural type	-	Space-frame	Truss-beam	Space-frame	Grid-shell	Space-frame
obj.1 Ratio of premium seats	22.3 - 67.5%	35.9%	54.9%	38%	52%	28.9%
obj.2 Reverberation time (s)	1.82-3.28	2.98	3.17	3.33	3.11	3.19
obj.3 Strain Energy (kNm)	1659-4358	4322	6073	2132	4149	5242

C. Manual classification of the Pareto solutions based on geometry

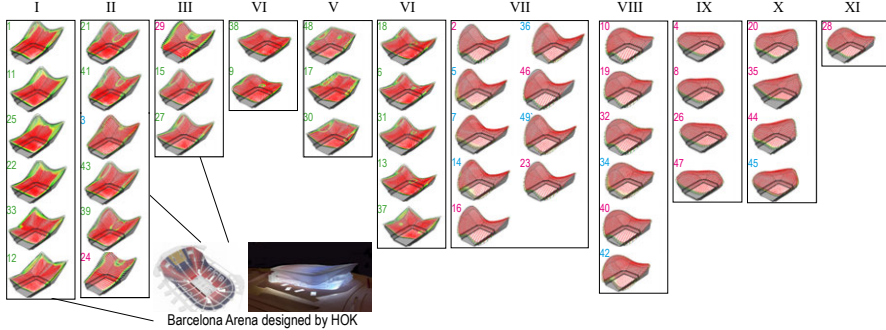


FIG. 5.6 The results of the second MOO for the design of O2 Arena (the picture sources of Barcelona Arena: Architects+Artisans, 2017 and Amalgam, 2016)

5.4.2 Using SOM clustering and MOO to support the design exploration emphasizing visual investigations

As discussed in section 4.3.2 of chapter 4, by using SOM clustering and MOO, the second workflow of CDIA is used for the design scenario in which designers prioritize visual investigations of design alternatives according to their knowledge and experience about qualitative design requirements. By using SOM clustering, it allows designers to have an overview of the design space (generated based on IAG) according to geometry typologies and to select promising types of designs based on visual investigations. Subsequently, a MOO is used to search for 'well-performing' design alternatives among the selected types according to customized numeric assessment criteria (formulated based on framework-NAIA) related to quantitative design requirements (Pan et al., 2018).

In this workflow, first, the design variables defined in pre-processing step (see tables 5.1 and table 5.2) should be further processed and used as the inputs for the SOM clustering. The design variables which are directly related to the overall forms of the buildings are selected out. Among these variables, some implicit ones are modified. For example, the variables of 'Str_FCHeight' and 'Str_DepCen' in tables 5.1 and table 5.2 are implicit and do not directly indicate the overall form, but their sum can directly indicate the height of the central point of the roof. Another example is related to the variable of 'ST_AsyY' in table 5.2, which defines the asymmetric ratio of the outline of the seating bowl implicitly. An approach to make it explicit is to transform it and the variable of 'ST_LenY' (which define the length of the building along the Y-axis, see table 5.2) into two new variables ('ST_LenY1' and 'ST_LenY2') which respectively define the lengths between the middle point of the pitch and the two points of the intersections of the Y-axis and the boundary outline of the seating bowl. These transformations can be automatically processed in IAG (see table 5.7). After the transformations, all the variables are feature scaled (zero-one scaling is used in this research) to eliminate the influences led by the different ranges of the variables.

Besides, the parameters of SOM clustering should be defined (see table 5.7). For both the two design examples, a 10x10 network with triangle topology is used, which can cluster the design alternatives into 100 (or slightly less than 100) groups. All the design alternatives in the design space are used to train the SOM network. In practice, according to the amount of all the design alternatives in the design space and the size of the network, designers can also use a small amount of design alternatives (obtained by sampling the design space) for the SOM clustering to save computation time. For the MOOs, the assessment criteria and the parameters are similar to those in the first workflow (see table 5.3, 5.4, 5.5, and 5.6). The iteration

times of the MOOs here are 40, which are less than the 100 for the MOOs in the first workflow, since the selected types of design alternatives are usually much less than all the design alternatives in the design space and it does not need so many iterations. For the hypothetical designs of both the two examples, the results of the SOM clustering and the MOOs are presented and discussed in section 5.4.2.1 and section 5.4.2.2, respectively.

TABLE 5.7 Inputs and parameters of SOM clustering

Inputs of the SOM clustering for the design examples of Barclay Centre (left) and O2 arena (right)			
Var.1: ST_LenX	ST_LenX \in [100, 160]	Var.1: ST_LenX	ST_LenX \in [92, 120]
Var.2: ST_LenY	ST_LenY \in [90, 150]	Var.2: ST_LenY1	ST_LenY1 \in [49.8, 83]
		Var.3: ST_LenY2	ST_LenY2 \in [37, 46.2]
Var.3: ST_Cpi, ST_Cpii, ST_CPiii, ST_CPiv	ST_Cpi = ST_Cpii = ST_Cpiii = ST_CPiv \in {0, 1, 2, 3}	Var.4: ST_Cpi, ST_CPiv	ST_Cpi = ST_CPiv \in {0, 1, 2, 3}
		Var.5: ST_Cpii, ST_Cpiii,	ST_Cpii = ST_Cpiii \in {0, 1, 2, 3}
Var.4: ST_bdr	ST_bdr \in {1,3}	Var.6: Cuv-BO	ST_bdr \in {1,3}
Var.5: Str_Height	Str_Height = (Str_FCHeight + Str_DepCen) \in [44, 48]	Var.7: Str_Height	Str_Height = (Str_FCHeight + Str_DepCen) \in [44, 48]
Var.6: Str_RidgeX Str_RidgeY	Str_RidgeX = Str_RidgeY \in {1,3}	Var.8: Str_RidgeX Str_RidgeY	Str_RidgeX = Str_RidgeY \in {1,3}
Parameters of SOM clustering			
SOM network	10x10, triangle	Ordering phase	1,000
Distance function	Euclidean distance	Ordering phase	1,000
Initial neighbourhood	3		

5.4.2.1 SOM clustering supporting the visual investigations and selections of design alternatives according to qualitative design requirements

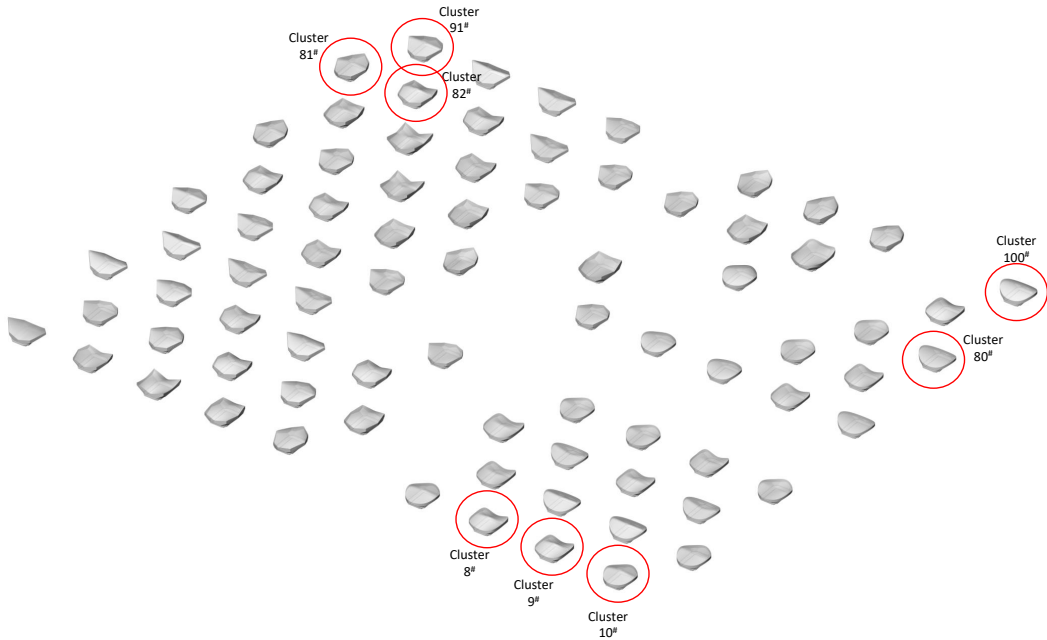
Figure 5.7 and figure 5.8 illustrate the results of the SOM clustering for the design examples of Barclay Centre and of O2 Arena, respectively. The upper charts in figure 5.7 and figure 5.8 illustrate the node designs on the trained SOM network. These node designs represent diverse types of design alternatives in the design space and reflect the intrinsic distributions of the design spaces of the two design examples, respectively. Based on these charts, designers can have overviews of the design spaces according to geometry typology and select promising types of design alternatives based on visual investigations according to their knowledge and experience about qualitative design requirements. In the case studies, designers intend to select several types of design alternatives which are circled in the charts.

The bottom charts in figure 5.7 and figure 5.8 illustrate intrinsic information about the SOM clustering of the two design examples, respectively. The bottom left charts in both the figures indicate the amount of design alternatives captured by the nodes of different clusters. For the results of both the SOMs, there are empty clusters, which indicates that there is no design alternative in somewhere of both the design spaces. The reason can be that some design alternatives in the design spaces are eliminated since the amounts of the fixed seats are out of the ranges defined in table 5.1 and table 5.2, respectively.

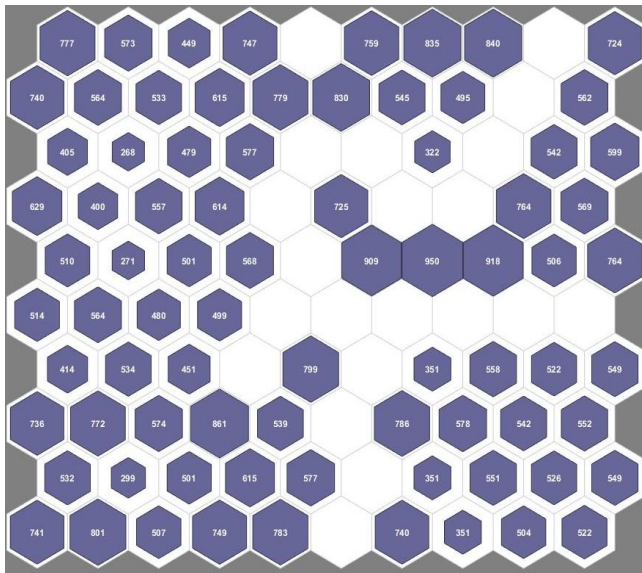
The charts of the 'distances between nodes' in figure 5.7 and figure 5.8, respectively, use colours to indicate the relative distances between the nodes, which can reflect the distribution of the nodes in the design spaces. The darker the colour of the connection between two nodes is, the larger the related distance is.

Each of the smaller charts in the bottom right of figure 5.7 and figure 5.8, respectively, indicates the weights from a certain input of SOM clustering (listed in table 5.7) to the nodes on the SOM network. If the pattern of the weights from two inputs are similar, these two inputs can be considered to be correlative and one of them should be eliminated. According to these charts, there are no correlative inputs.

Node designs on the trained SOM network

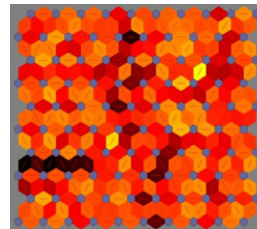


Amount of the design alternatives in each cluster

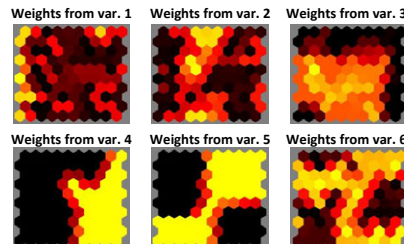


The sizes of the shapes indicate the amounts of the design alternatives in the related clusters. The empty units indicate there is no any design alternatives in the clusters.

Distance between nodes



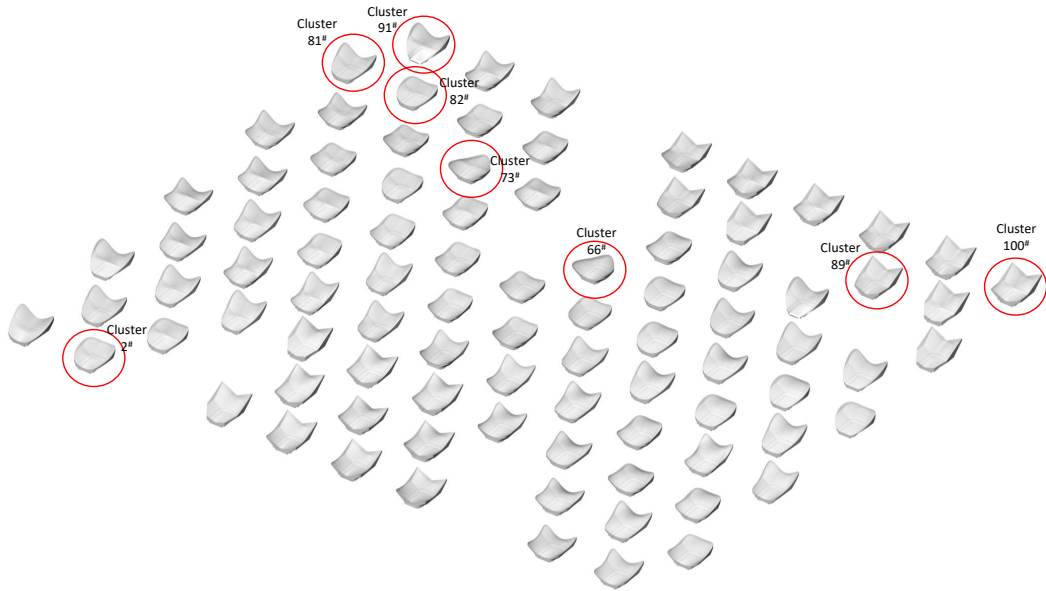
The colour between two nodes indicates the distance between them. The darker the colour is, the longer the distance is.



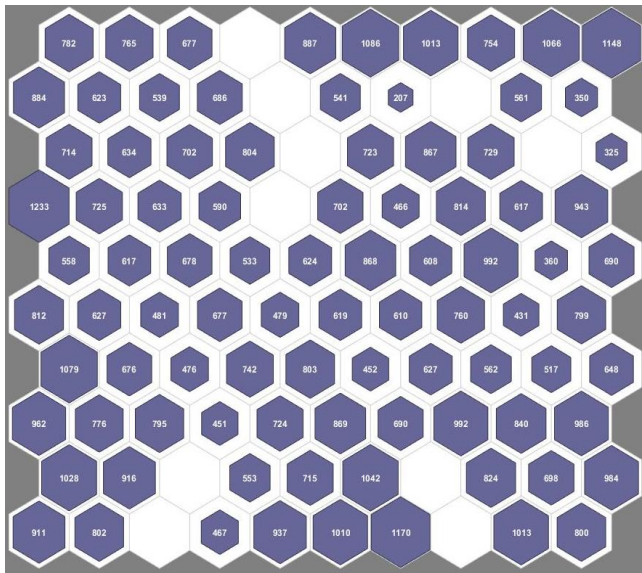
For the weights from the i^{th} variable to the nodes, the most negative connections are shown in black, zero connections in red, and the strongest positive connections in yellow.

FIG. 5.7 The trained SOM network of the design space for the design example of Barclay Centre

Node designs on the trained SOM network

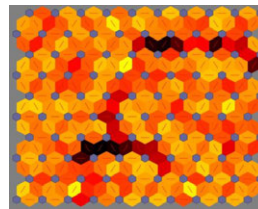


Amount of the design alternatives in each cluster

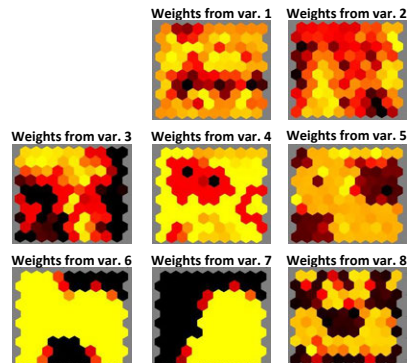


The sizes of the shapes indicate the amounts of the design alternatives in the related clusters. The empty units indicate there is no any design alternatives in the clusters.

Distance between nodes



The colour between two nodes indicates the distance between them. The darker the colour is, the longer the distance is.



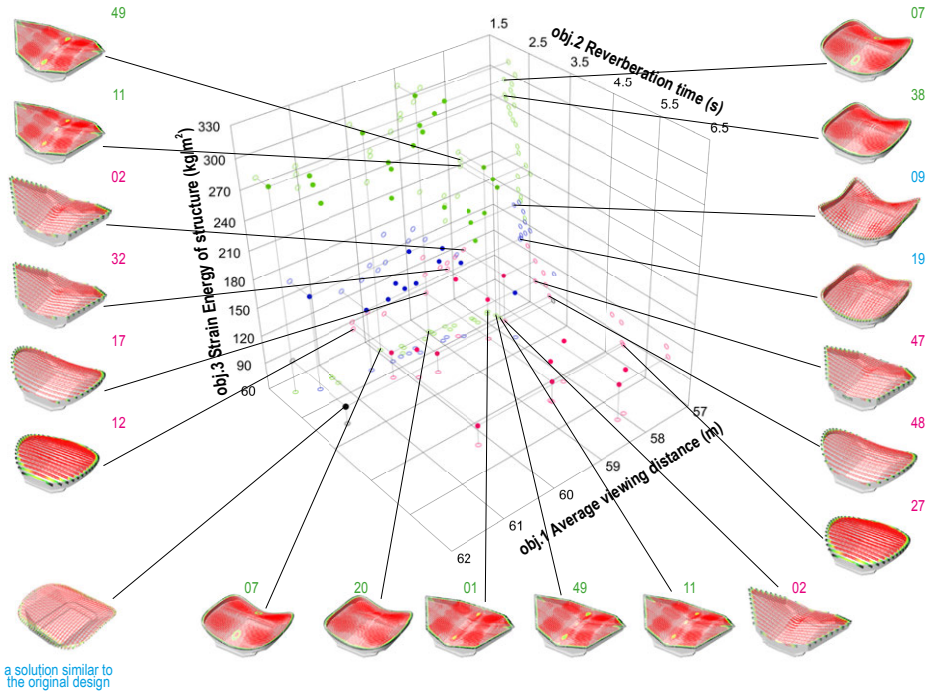
For the weights from the i^{th} variable to the nodes, the most negative connections are shown in black, zero connections in red, and the strongest positive connections in yellow.

FIG. 5.8 The trained SOM network of the design space for the design example of O2 Arena

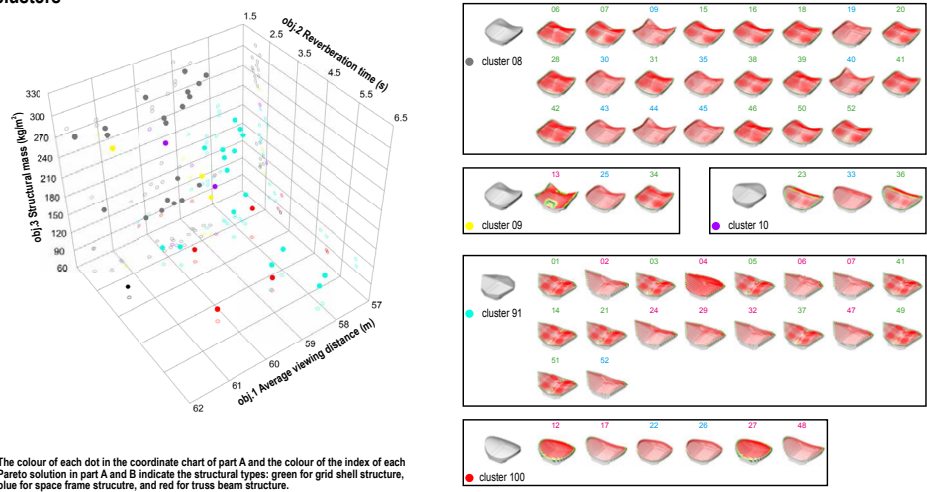
5.4.2.2 Using MOOs to search for ‘well performing’ designs among selected types

Among the types of design alternatives selected based on the trained SOM networks by designers (see the upper charts in figure 5.7 and figure 5.8), MOOs are used to search for ‘well-performing’ design alternatives, according to the numeric assessment criteria formulated in the pre-process step (see table 5.3 and table 5.4). It is worth noting that only a part of design variables are used as the inputs for SOM clustering. Therefore, for each of the selected design alternatives, three more design variables (‘StrDpth-cen’, ‘StrDpth-bou’, and ‘Strtype’) are necessary to be considered. According to the design variables listed in table 5.1 and table 5.2, there are 25 combinations of these variables for each of the selected design alternatives. Therefore, for the design example of Barclay Centre, 119,552 design alternatives are selected out from 1,177,200 ones in the original design space. For the design example of O2 Arena, 155,100 design alternatives are selected out from 1,653,850 ones in the original design space. Since the searching spaces are much smaller than the original design space, the iteration times of MOOs in the second workflow are decreased to 40, which saves computation time. The other parameters of MOOs are similar to those in the first workflow listed in table 5.6. The results of the MOOs for the design examples of Barclay Centre and O2 Arena are illustrated in figure 5.9, figure 5.10, and figure 5.11.

A. the coordinate chart about design objectives of the Pareto solutions



B. the coordinate chart about the design objectives of the Pareto solutions belonging to different selected clusters

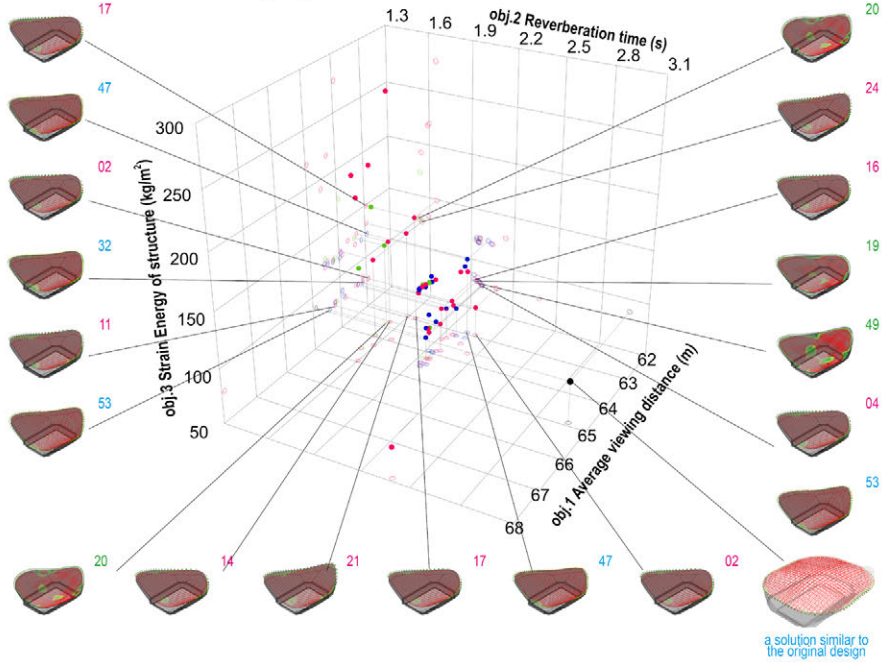


The colour of each dot in the coordinate chart of part A and the colour of the index of each Pareto solution in part A and B indicate the structural types: green for grid shell structure, blue for space frame structure, and red for truss beam structure.

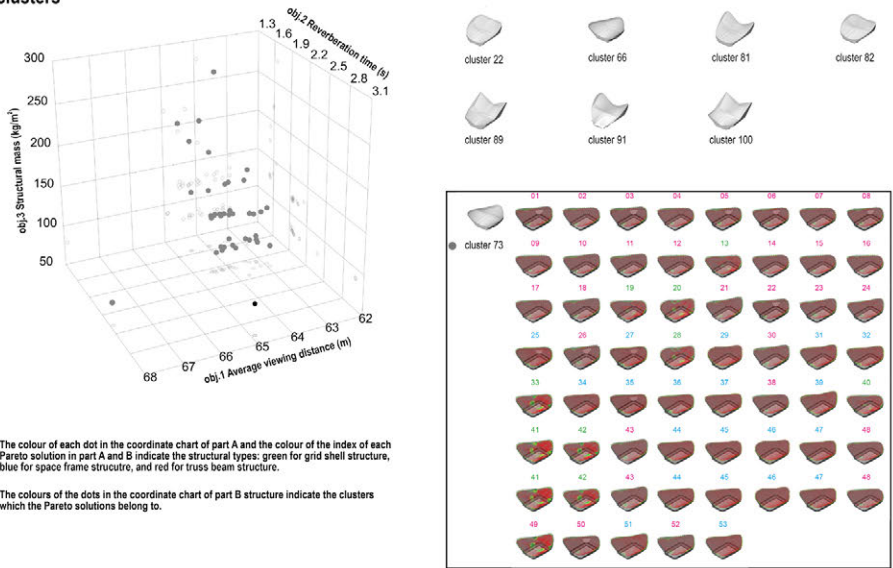
The colours of the dots in the coordinate chart of part B structure indicate the clusters which the Pareto solutions belong to.

FIG. 5.9 The results of the MOO for the selected design alternatives in the design example of Barclay Centre

A. the coordinate chart about design objectives of the Pareto solutions



B. the coordinate chart about the design objectives of the Pareto solutions belonging to different selected clusters

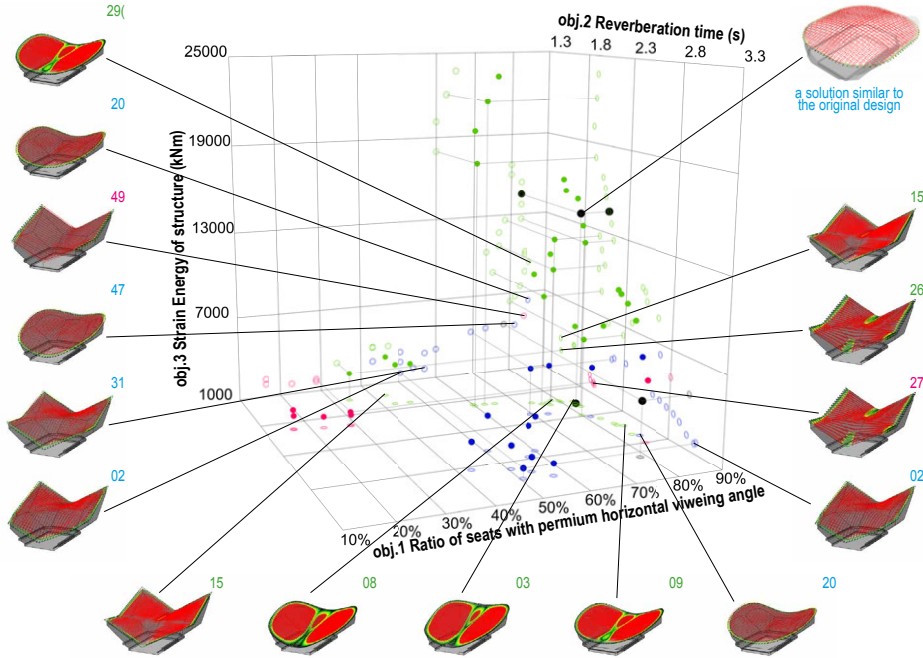


The colour of each dot in the coordinate chart of part A and the colour of the index of each Pareto solution in part A and B indicate the structural types: green for grid shell structure, blue for space frame structure, and red for truss beam structure.

The colours of the dots in the coordinate chart of part B structure indicate the clusters which the Pareto solutions belong to.

FIG. 5.10 The results of the first MOO for the selected design alternatives in the design example of O2 Arena

A. the coordinate chart about design objectives of the Pareto solutions



B. the coordinate chart about the design objectives of the Pareto solutions belonging to different selected clusters

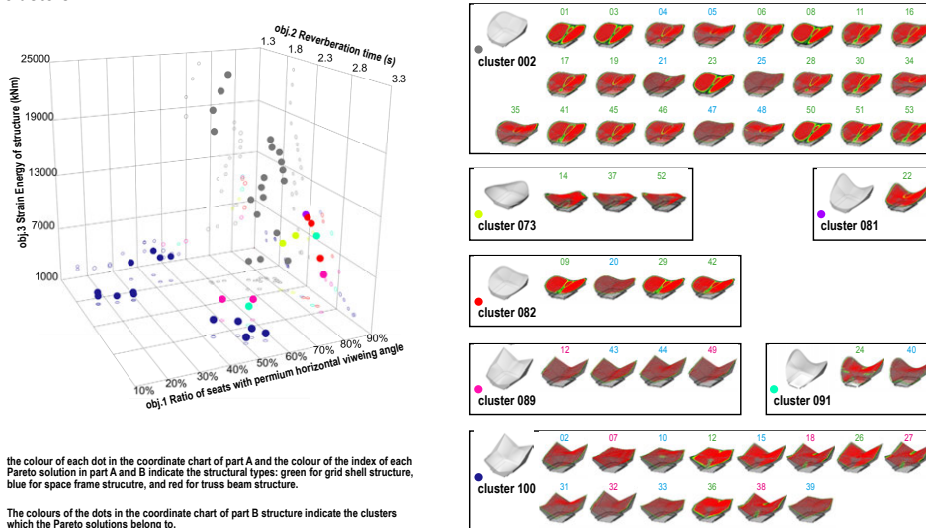


FIG. 5.11 The results of the second MOO for the selected design alternatives in the design example of O2 Arena

According to the results illustrated in figure 5.9, figure 5.10, and figure 5.11, there are a series of observations. The geometry types of the Pareto solutions ('well-performing' designs) searched by the MOOs are included in the types selected from the corresponding SOM networks (figure 5.7 and figure 5.8). It indicates that the goal of the workflow is achieved, which guarantees the geometries of the Pareto solutions are those preferred by designers (the ones selected by designers according to designers' knowledge and experience about qualitative design requirements).

The objectives values of the Pareto solutions ('well-performing' design alternatives) related to quantitative design requirements are worse than the counterparts of the MOOs in the first workflow, according to the criteria listed in table 5.3 and table 5.4. This phenomenon is discussed in section 4.3.2.3 of chapter 4, based on the reason that the selected design alternatives are far less than the design alternatives in the original design space (which is used by the MOOs in the first workflow), which potentially excludes some 'better performing' ones.

The diversity of the Pareto solutions in these MOOs decreases, comparing to the counterparts in the first workflow. Nevertheless, the geometries and the structural types of the solutions also change as the change of the values for the design objectives, which is also observed in the MOO results of the first workflow.

The bottom charts of figure 5.9, figure 5.10, and figure 5.11 illustrate the clusters which the Pareto solutions belong to. For the MOO of the design example of Barclay Centre, eight clusters of design alternatives (cluster 08, 09, 10, 80, 81, 82, 91, and 100, see the upper charts in figure 5.7) are selected for the MOO, but all the Pareto solutions just belongs to five of them (cluster 08, 09, 10, 91, and 100, see figure 5.9). For the design example of O2 Arena, eight clusters of design alternatives (cluster 02, 66, 73, 81, 82, 89, 91, and 100, see the upper chart in figure 5.8) are selected for the two MOOs, but for the first MOO, all the Pareto solutions are belongs to one of the selected cluster (cluster 73, see figure 5.10), for the second MOO, all the Pareto solutions belong to seven of the selected clusters (cluster 2, 73, 81, 82, 89, 91, and 100, see figure 5.11). It indicates that the satisfactory of different design objectives require design alternatives with different types of geometries.

5.4.3 Using SOM-MLPNN to support the design exploration equally emphasizing numeric assessments and visual investigations

The third workflow aims to support design exploration with equal emphases on numeric assessment criteria related to quantitative design requirements and visual investigations related to qualitative design requirements. SOM-MLPNN (multi-layer perceptron neural network based on self-organizing map) is proposed (Pan et al. 2020) to achieve the workflow, which is elaborated in section 4.3.3 of chapter 4.

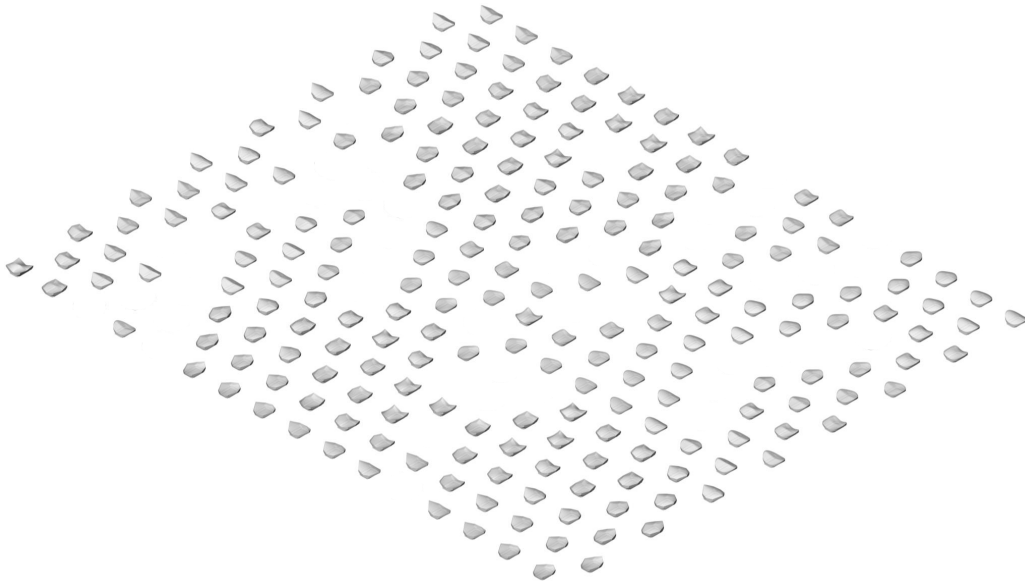
5.4.3.1 SOM clustering, sampling, and Design of Experiments (DoEs)

According to the elaboration in section 4.3.3 of chapter 4 and the demonstration in figure 4.6, SOM clustering is first used to group design alternatives according to geometry features, which is similar to that in the second workflow. It allows designers to visually investigate various types of designs and select clusters of design alternatives.

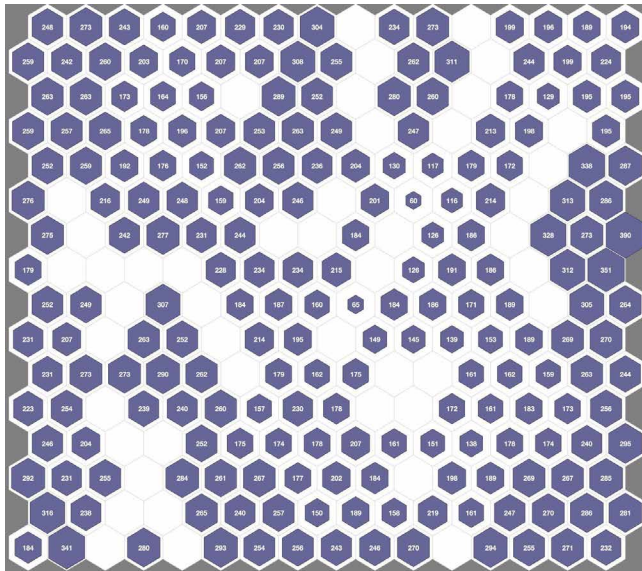
Besides, the node designs on the trained network are used as the sampled designs for the design of experiment (DoE) to obtain the related values of indicators related to quantitative design performance. The design variables of the sampled designs (labelled inputs) and the related to indicator values (labelled outputs) compose of the labelled data to train, validate, and test the predefined MLPNN model.

Considering the proper amount of the node designs (based on which designers can visually investigate diverse types of designs) and the number of labelled data sets for DoE, a 16x16 network is used for SOM clustering. Based on the network, a number (no more than 256) of node designs can be generated, which are not too many for designers to visually investigate diverse types of designs. The SOM clustering results are illustrated in figure 5.12 and figure 5.13.

Node designs on the trained SOM network

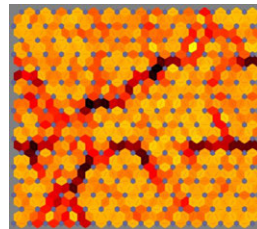


Amount of the design alternatives in each cluster



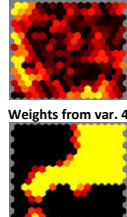
The sizes of the shapes indicate the amounts of the design alternatives in the related clusters. The empty units indicate there is no any design alternatives in the clusters.

Distance between nodes

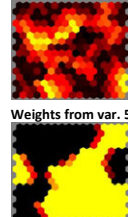


The colour between two nodes indicates the distance between them. The darker the colour is, the longer the distance is.

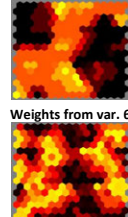
Weights from var. 1



Weights from var. 2



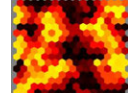
Weights from var. 3



Weights from var. 4



Weights from var. 5

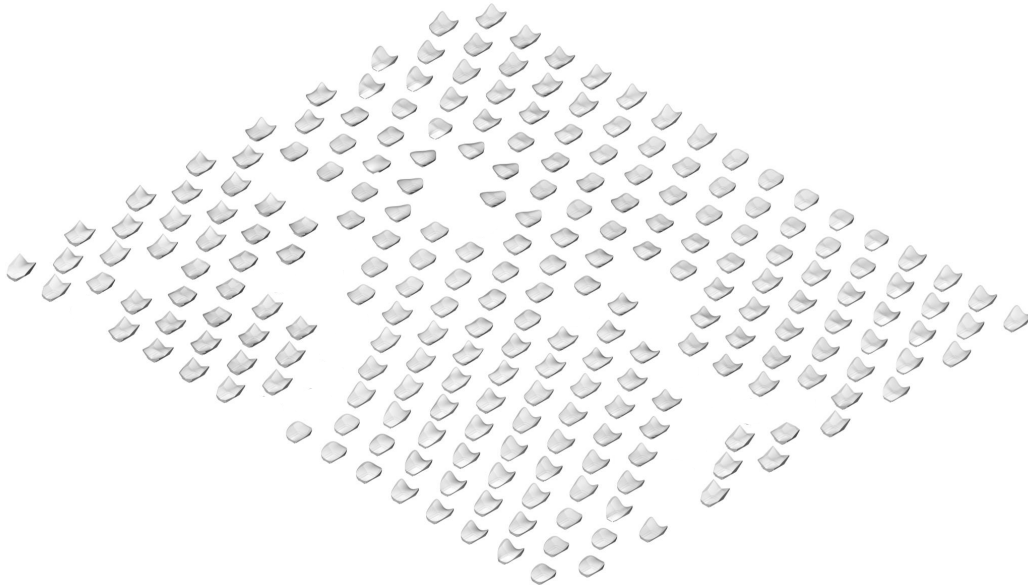


Weights from var. 6

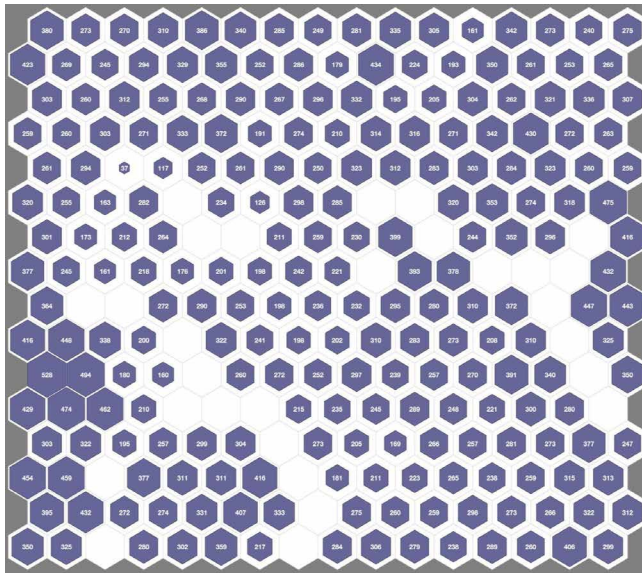
For the weights from the i^{th} variable to the nodes, the most negative connections are shown in black, zero connections in red, and the strongest positive connections in yellow.

FIG. 5.12 The results of SOM clustering in the SOM-MLPNN for the design example of Barclay Centre

Node designs on the trained SOM network

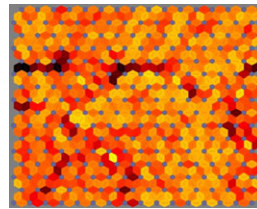


Amount of the design alternatives in each cluster



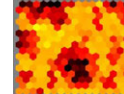
The sizes of the shapes indicate the amounts of the design alternatives in the related clusters. The empty units indicate there is no any design alternatives in the clusters.

Distance between nodes



The colour between two nodes indicates the distance between them. The darker the colour is, the longer the distance is.

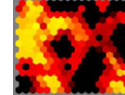
Weights from var. 1



Weights from var. 2



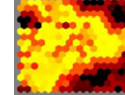
Weights from var. 3



Weights from var. 4



Weights from var. 5



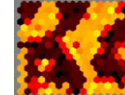
Weights from var. 6



Weights from var. 7



Weights from var. 8



For the weights from the i^{th} variable to the nodes, the most negative connections are shown in black, zero connections in red, and the strongest positive connections in yellow.

FIG. 5.13 The results of SOM clustering in the SOM-MLPNN for the design example of O2 Arena

Moreover, all the 256 node designs can be used for the DoEs. The clusters of some node designs may be empty, since the node on the SOM network do not capture any objects in the input space. Nevertheless, these node designs can also be used for the DoEs. It worth noting that in SOM clustering, only a part of the design variables (directly related to the overall geometry) are used as the inputs, but in DoEs all the design variables should be used as the labelled inputs. Hence, by considering the design variables which are excluded in SOM clustering ('StruType', 'struDpth-ctr' and 'StruDpth-bdr'), based on each node design, 25 design alternatives can be generated. Therefore, 6,400 design alternatives can be used for the DoEs, and their design variables are used as the labelled inputs. By using IAG and the related BPS tools, the corresponding labelled outputs can be obtained.

5.4.3.2 Training, validations, and tests of MLPNN models

The labelled data obtained by the DoEs are used to train, validate and test the predefined multi-layered perceptron neural network (MLPNN) models. For each of the numeric indicators related to quantitative design requirements, an independent MLPNN model is trained to learn the mapping between the labelled inputs (design variables) and the labelled outputs (the value of the indicators). A neural network with 6-6-10 hidden layers is first used to approximate the data, and more hidden layers or neurons on each layer can be added if the results are not acceptable. A backpropagation function 'Leverberg Marquardt' is used as the training algorithm. The parameters of the MLPNN model and training process are listed in table 5.8.

Figure 5.14 and figure 5.16 illustrate the training, validation, and test process of the MLPNN models to approximate the spectator view and acoustic indicators for the two design examples. For the approximations of the structural indicators, the relationships between the inputs and the outputs are different for different structural types, therefore, independent MLPNN models are trained to approximate the structural indicators for each type of structures. The related training, validation, and test process of these MLPNN models for the two design examples are illustrated in figure 5.15 and figure 5.17, respectively.

TABLE 5.8 The parameters of the MLPNN models and the training process

Platform	MATLAB
Neural network (the hidden layers)	6-6-10 (for the approximation of the spectator view and acoustics indicators of the design examples of Barclay Centre and O2 Arena) 6-6-6-10-10 (for the approximation of the structural self-weight and strain energy of grid shell structure in the design examples of Barclay Centre and O2 Arena) 6-6-10-10 (for the approximation of the deflection of grid shell structure in the design examples of Barclay Centre and O2 Arena) 6-6-10-10 (for the approximation of the structural self-weight, strain energy, and deflection of space frame and truss beam structures in the design examples of Barclay Centre and O2 Arena)
Activation function	Sigmoid
Cost function	Mean squared errors (MSE)
Training algorithm	Leverberg Marquardt
Amount of labelled data pairs	6,400
Ratio of training, validation and testing sets	70% for training, 15% for validation, and 15% for test

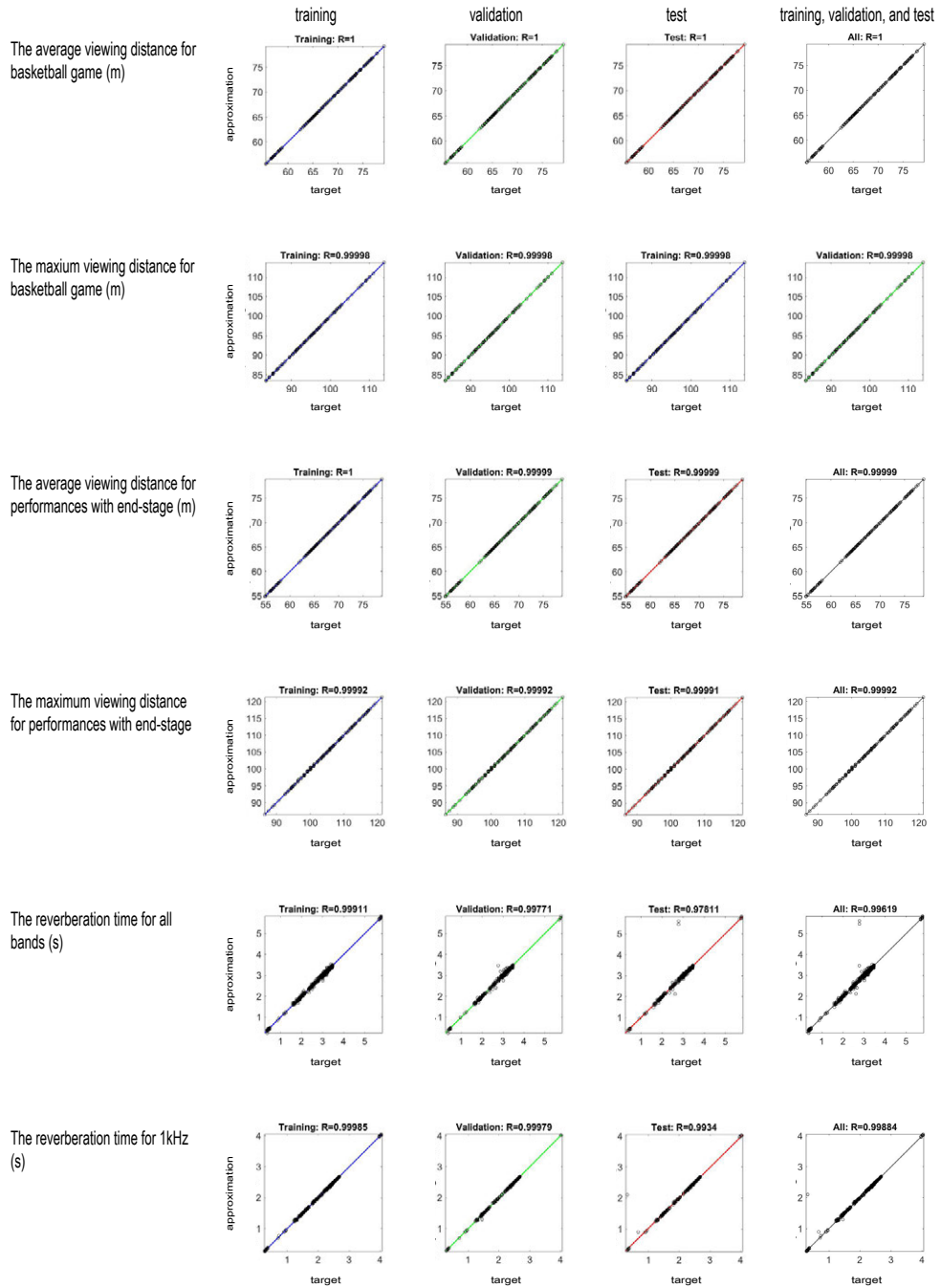


FIG. 5.14 The training, validations, and tests data of the MLPNN models to approximate the indicators of spectator view and acoustics for the design example of Barclay Centre

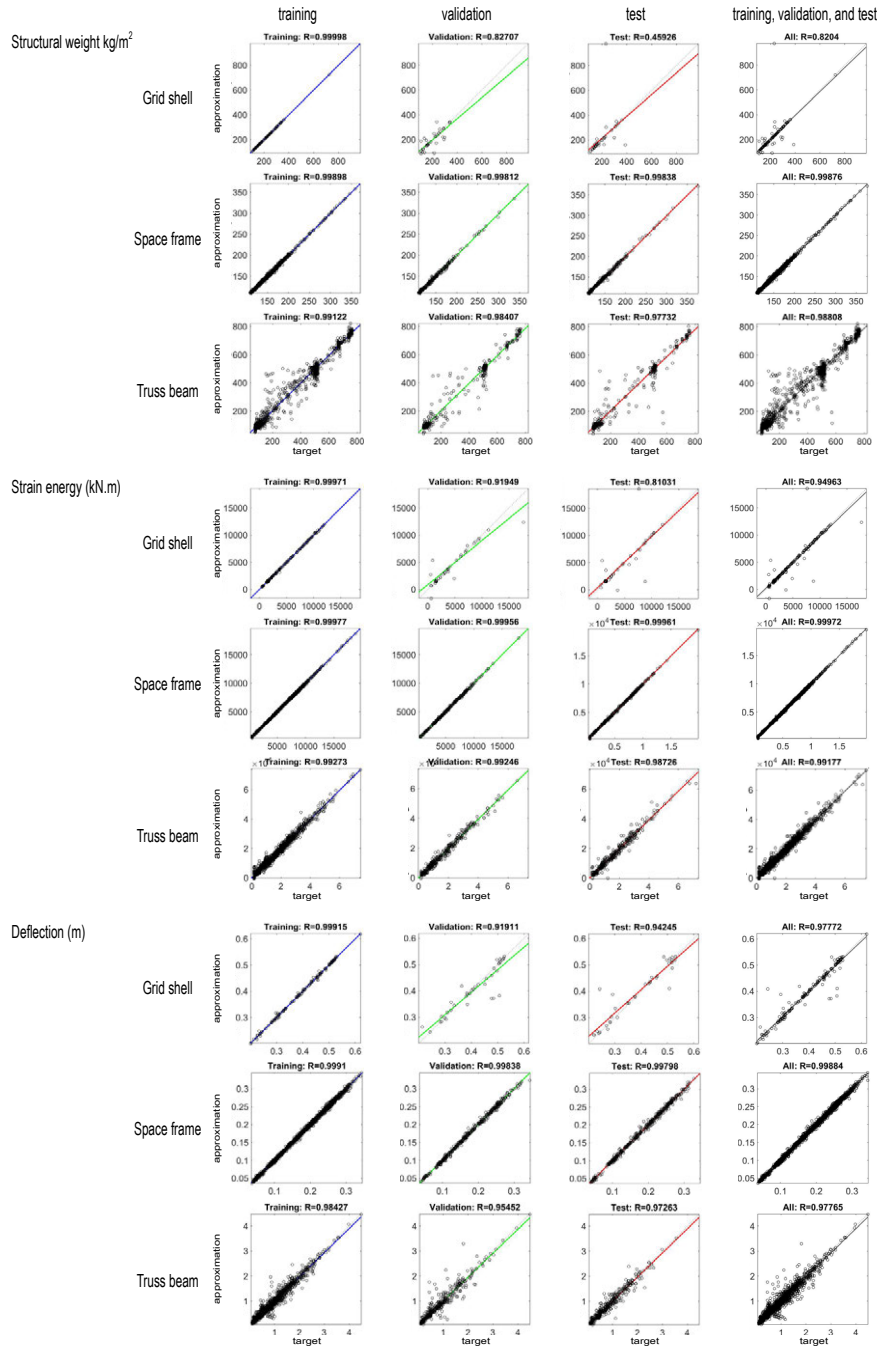


FIG. 5.15 The training, validations, and tests data of the MLPNN models to approximate structural indicators for the design example of Barclay Centre

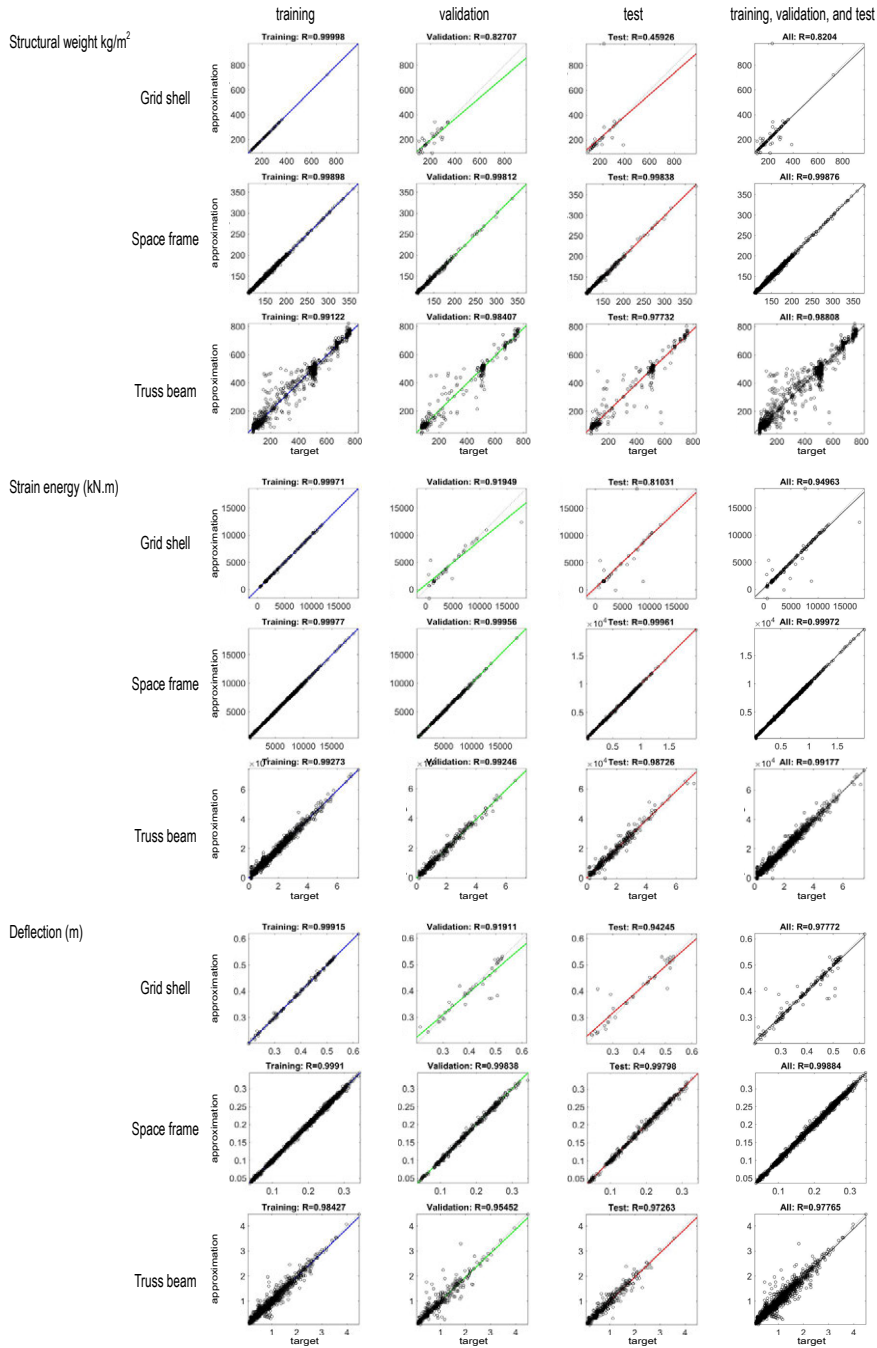


FIG. 5.16 The training, validations, and tests data of the MLPNN models to approximate the indicators of spectator view and acoustics for the design example of O2 Arena

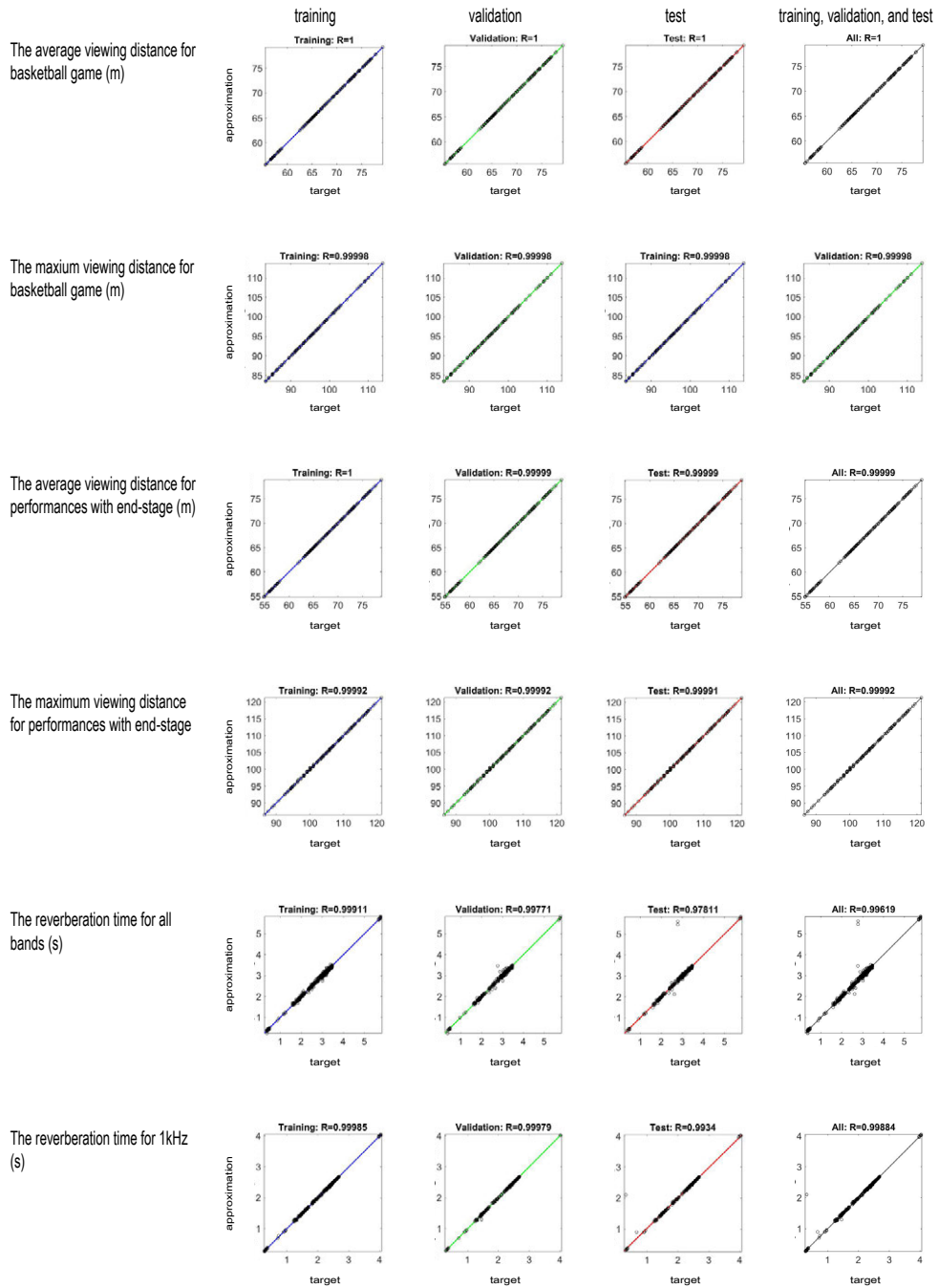


FIG. 5.17 The training, validations, and tests data of the MLPNN models to approximate structural indicators for the design example of O2 Arena

According to the results presented in figure 5.14 and figure 5.16, it is obvious that the approximations of the indicators of spectator view and acoustics are ideal, since all the data points in the charts lay or concentrate along the diagonals. The reason can be that for these indicators, the relationships between the inputs (design variables) and outputs (indicator values) are not complex.

By contrast, the approximations of the structural indicators for both the design examples of Barclay Centre and O2 Arena are more complex (see figure 5.15 and figure 5.17). To improve the approximations, more hidden layers and more neurons on the layers are added for the MLPNN models (see table 5.8). The reason can be that the relationships between the inputs (design variables) and outputs (structural indicator values) are more complex, since the structural simulation is highly non-linear, comparing to the simulations of spectator view and acoustics. Specifically, the approximations of the structural indicators related to the design example of O2 Arena are more complex (figure 5.17) than those of the Barclay Centre (figure 5.15). The reason can be the asymmetric seating bowl which makes the relationships between the geometry (defined by the design variables) and structural indicators more complex.

Besides, these complex approximations can be also caused by the uncertainty of the training model. A series of methods can be used to quantify the uncertainty (Kasisviswanathan, et al., 2016) and using deeper MLPNN or using cross-validation to fully exploit the labelled data can be possible ways to improve the performance. Nevertheless, in general, the approximations of all the indicators for both the design examples are acceptable, since the errors of most of the data points are less than 10%. It worth noting that, in the training, validation, and test process, only a small number of design alternatives are used, and it is impossible for designers to evaluate the performance of the trained MLPNN models in predicting the indicators of other design alternatives. It is still a problem in the application of MLPNNs.

5.4.3.3 Design explorations based on data visualizations

To support designers in exploring design alternatives simultaneously based on both numeric assessments related to quantitative design requirements and visual investigations related to qualitative design requirements, a data visualization is proposed based on the data approximated by the trained MLPNN models. This visualization is introduced in section 4.3.3.4 in chapter 4, which presents the indicator values (related to quantitative design requirements) for various types of design alternatives reflected by the SOM network (based on which designers visually investigate design alternatives according to qualitative design requirements). Figure 5.18 and figure 5.19 illustrate this data visualization for the design examples of Barclay Centre and O2 Arena, respectively.

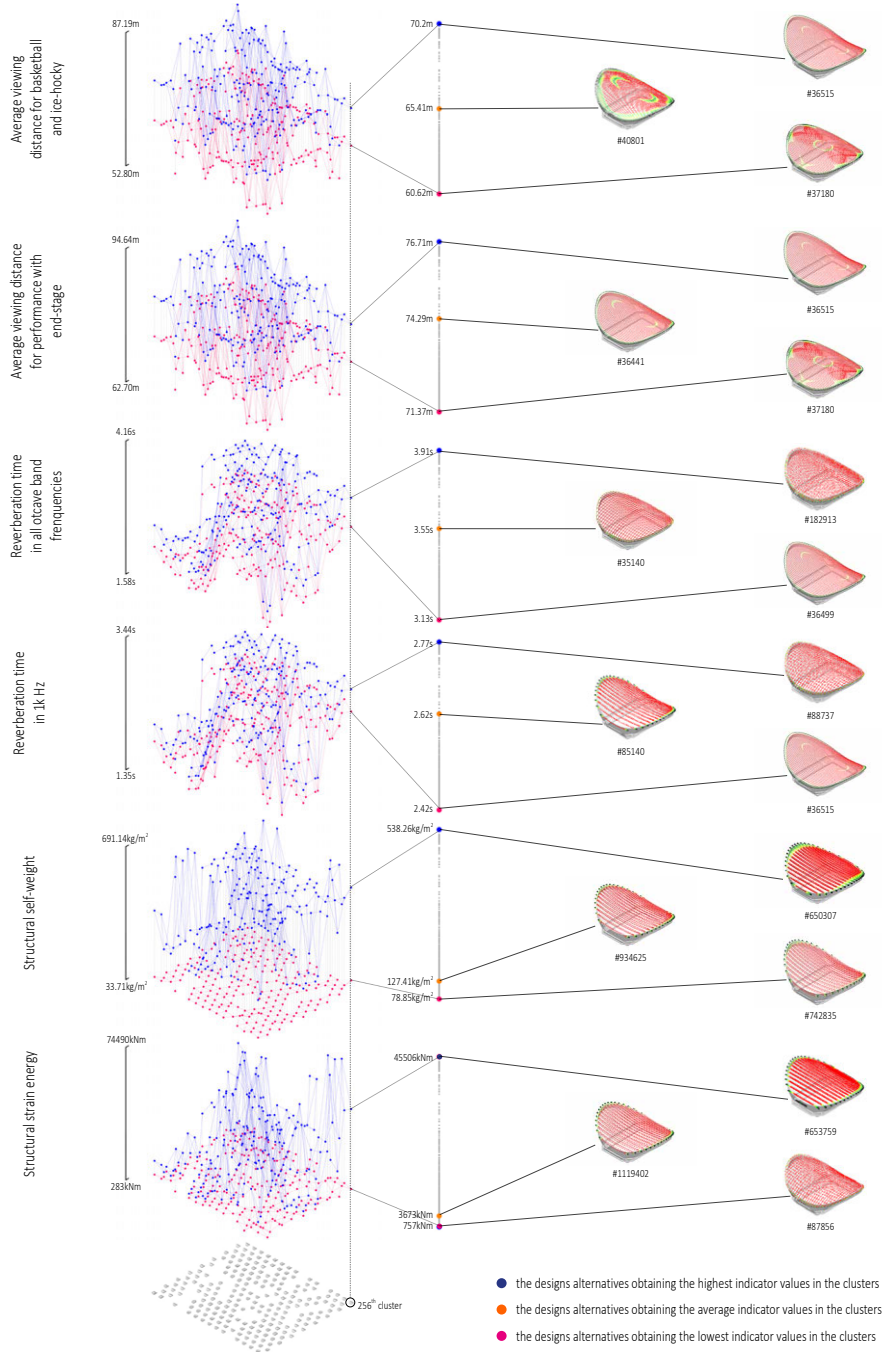


FIG. 5.18 Exploring the output spaces related to various quantitative indicators according to the design alternatives with different geometry types (design example of Barclay Centre)

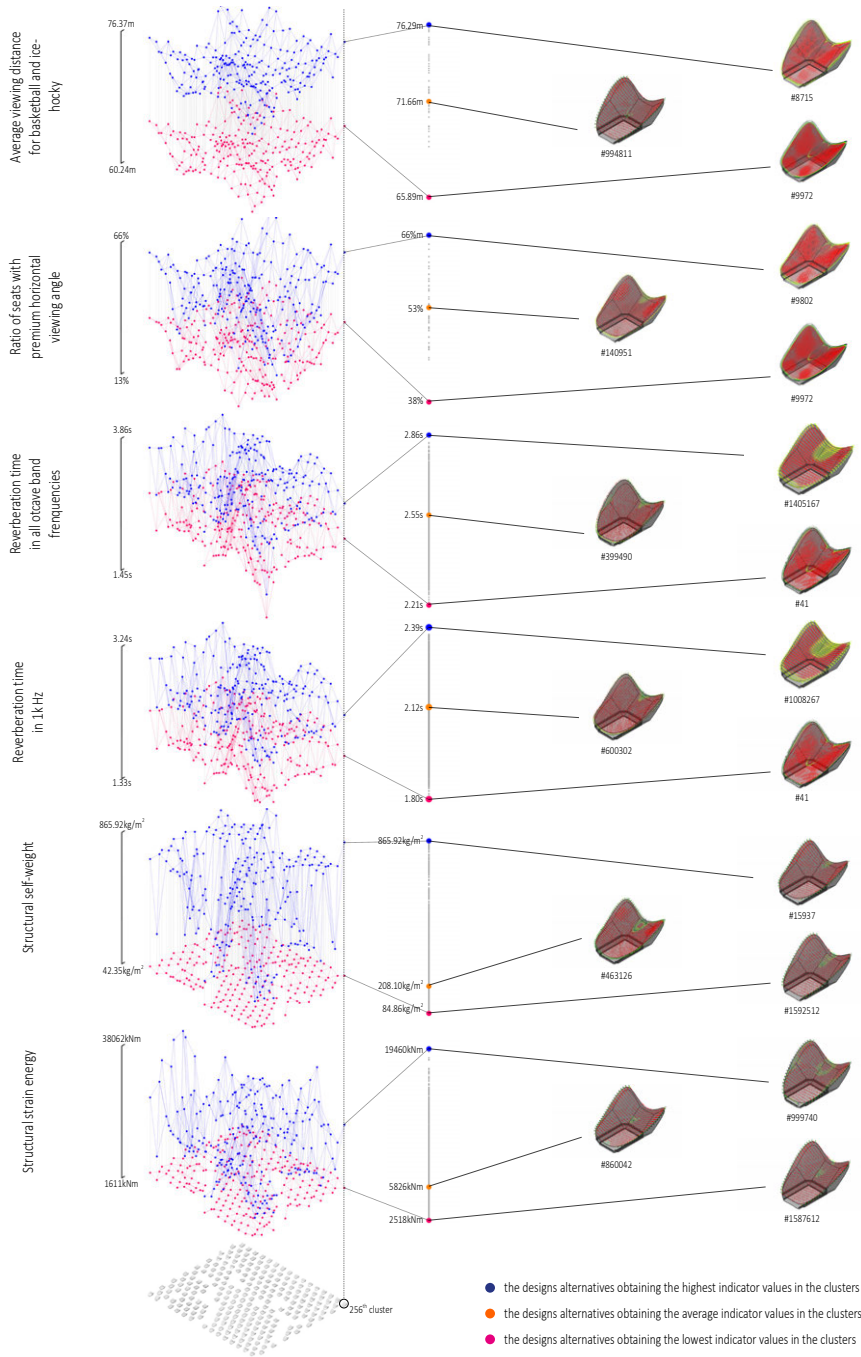


FIG. 5.19 Exploring the output spaces related to various quantitative indicators according to the design alternatives with different geometry types (design example of O2 Arena)

In figure 5.18 and figure 5.19, the SOM networks in the bottom (which are the same with those in figure 5.12 and figure 5.13, respectively) contain node designs representing various types of design alternatives, based on which designers can explore design alternatives based on visual investigations. This kind of exploration is similar to those in the second workflow. Moreover, above the SOM networks, corresponding to each of the node designs, a series of dots (are set for each indicator). To illustrate the details, the dots corresponding to the cluster 256 in both the two design examples are taken as an example (see the charts in the middle columns in figure 5.18 and figure 5.19). The altitudes of all the dots indicate the values of the indicators, according to the vertical scale axis on the left. The blue and red dots respectively represent the design alternatives obtaining the highest and the lowest values of the related indicators within the cluster. Between the blue and red dots, a series of grey dots represent other design alternatives in this cluster, among which the ones obtaining the average values are highlighted in orange. The geometries of the highlighted design alternatives are presented on the right. The geometries of the other design alternatives (corresponding to the grey dots) can also be presented based on IAG. For other clusters, designers can also investigate any design alternatives in this way, based on both numeric assessments according to the indicator values and visual investigations of the geometries of both the node designs and the specific design alternatives.

Besides, for each indicator, two meshes are generated based on the blue dots and red dots, respectively, which represents the upper and lower boundaries of the indicator values. Between the meshes are the output spaces corresponding to the input space below reflected by the node designs organized by the SOM network. The fluctuation of each of the meshes reflects how the value of the related indicator changes among the clusters of design alternatives. It can be used to study the relationships between the numeric indicators and the geometries of various types of design alternatives.

5.5 Discussions and summary

In this chapter, the method of CDIA is demonstrated and verified in the case studies of two design examples. First, the parametrization processes of indoor arena designs for the two typical examples by using IAG are demonstrated (table 5.1 and table 5.2). Based on IAG, numerous and diverse design alternatives are generated (including the ones similar to the original design), which provides a wide design space for design exploration. The framework-NAIA contains multiple numeric assessment indicators and criteria related to quantitative design requirements, based on which nine and ten indicators are selected to formulate two sets of assessment criteria for the two design examples, respectively. The criteria are used in the three workflows to aid designers to evaluate design alternatives.

For the three workflows of CDIA, the results of the case studies verify the effects for the three design scenarios. The first workflow uses MOO, based on IAG and framework-NAIA, to search for well-performing design alternatives in a wide design space according to selected assessment criteria related to quantitative design requirements. The results (figure 5.4, figure 5.5, and figure 5.6) present the 'well-performing' design alternatives on the Pareto fronts about different quantitative design objectives, and designers can study the design alternatives with diverse geometric types and further select the final design(s) based on visual investigations according to their knowledge and experience about qualitative design requirements.

The second workflow uses SOM clustering before MOO, based on IAG, to group all the design alternatives into different clusters according to their geometry features, based on which designers can visually investigate and select design alternatives according to their knowledge and experience about qualitative design requirements. According to the results of the SOM clustering presented in figure 5.7 and figure 5.8, the numerous design alternatives with diverse types of geometries generated by IAG for the two design examples are respectively grouped into 79 and 90 clusters and represented by the node designs organized on the two SOM networks. Based on the clustering results, eight clusters for each of the design examples are supposed to be selected by the designers. The related design alternatives compose of selected design spaces for the two design examples, based on which MOOs are used to search for 'well-performing' design alternatives. According to the results presented in figure 5.9, figure 5.10, and figure 5.11, each of the 'well-performing' design alternatives is similar to one of the node designs selected by the designers. However, the Pareto design alternatives in the MOOs of the second workflow do not perform as well as the counterparts in the first workflow, according to the values related to

the design objectives. The reason, as discussed in section 4.3.2.3 of chapter 4 and section 5.4.2.2, is that the ‘well-performing’ design alternatives in the whole design space can be excluded during the selection of the clusters. Comparing to the results of the first and second workflows, it is obvious that some ‘well-performing’ design alternatives in the first workflow belong to the clusters which are excluded in the second workflow (see figure 5.4 and figure 5.9 for the design example of Barclay Centre and figure 5.5, figure 5.6, figure 5.10 and figure 5.11 for the design example of O2 Arena).

The third workflow uses SOM-MLPNN, based on IAG and framework-NAIA, to group all the design alternatives into clusters according to geometry features (like that in the second workflow) and meanwhile provide the numeric indicator values for all the design alternatives based on the data approximation of MLPNN models. By using this workflow, designers can obtain the information related to geometries and quantitative indicators of various design alternatives, simultaneously. Figures 5.18 and figure 5.19 presents the information provided by the workflows of SOM-MLPNN for the two design examples. Therefore, it is possible to study any design alternatives based on both numeric assessments related to quantitative design requirements and visual investigations related to qualitative design requirements.

According to the results of the case studies and the discussion above, in general, the CDIA method satisfies the three basic demands of the conceptual design of indoor arenas emphasizing the integration of the multi-functional space and long-span roof structure (formulated in chapter 2). Moreover, its three workflows satisfy the demands of the three design scenarios. It is obvious that, among the three workflows, the third workflow based on SOM-MLPNN can provide more information of geometries and quantitative indicators about the design alternative, which can also satisfy the demands of the first and second design scenarios. However, since it uses the data approximations based on MLPNN, in which there are uncertainties and the real errors for generalizations are unknown in practice, the predicted values for the quantitative indicators may be quite different from the real values obtained by simulations. This is the risk in using the surrogate models based on supervised learning. For the first and second workflow, although there are limitations in supporting design explorations, the quantitative indicators are reliable, since they are directly obtained by simulations. Moreover, these workflows satisfy the demands of their own design scenarios, as the discussions above. Hence, the three workflows have their advantages and limitations, and designers can select them according to the design scenarios and their limitations as well as effects.

References

- Advance Graphics (2015). Barclay Center Collage – Planaxon. <https://stblaney.wordpress.com/2015/01/15/barclay-center-collage/>. [Accessed: 3-November-2018].
- Amalgam (2016). Barcelona Sports Arena. <https://www.amalgam-models.co.uk/portfolio-item/dynamic-lighting-on-hok-barcelona-model/>. [Accessed: 3-November-2018].
- Architects+Artisans (2017). Barcelona's New Arena by HOK. <https://architectsandartisans.com/barcelonas-new-arena-by-hok/>. [Accessed: 3-November-2018].
- CEN (2002) EN-1990:2002. Eurocode - Basis of structural design.
- CEN (2005) EN-1991-1-1:2005. Eurocode 3: Design of steel structure – Part 1-1: General rules and rules for buildings.
- Info-stade(2013). Brooklyn Barclay Center. <http://www.info-stades.fr/stade/418/new-york-brooklyn-barclays-center/>. [Accessed: 3-November-2018].
- Kasiviswanathan,K.S., Sudheer, K.P., He, J. (2016). Quantification of prediction uncertainty in artificial neural network models, in: Shanmuganathan, S., Samarasinghe, S. (Eds.), Artificial Neural Network Modelling, 628 Springer, Berlin, 2016, pp. 145–159, <https://doi.org/10.1007/978-3-319-28495-8>.
- NSC2-SSDA (2008). The O2 Arena. <http://www.newsteelconstruction.com/wp/ssda-2008-the-o2-arena-north-greenwich/>. [Accessed: 3-November-2018].
- Pan, W., Turrin, M., Louter, C., Sariyildiz, S., Sun, Y. (2019). Integrating multi-functional space and long-span structure in the early design stage of indoor sports arenas by using parametric modelling and multi-objective optimization. *Journal of Building Engineering*, 22, pp. 464–485. DOI:10.1016/j.jobe.2019.01.006.
- Pan, W., Turrin, M., Louter, C., Sariyildiz, S., Sun, Y. (2018). Integrating the Multi-Functional Space and Long-Span Structure for Sports Arena Design : A design exploration process based on design optimization and self-organizing map, in: Mueller, C., Adriaenssens, S. (Eds.), *Proceeding of the IASS Symposium 2018: Creativity in Structural Design, Vol 2018*, International Association for Shell and Spatial (IASS), Boston, pp.1-8. <https://www.ingentaconnect.com/content/iass/piass/2018/00002018/00000004/art00015#>
- Pan, W., Sun, Y., Turrin, M., Louter, C., Sariyildiz, S. (2020), Design exploration of quantitative performance and geometry typology for indoor arena based on self-organizing map and multi-layered perceptron neural network. *Automation in Construction*, 114, pp. DOI: 10.1016/j.autcon.2020.103163
- Pollstarpro.com (2016). 2016 Mid-Year Worldwide Ticket Sales Top200 Arena Venues. <https://www.pollstarpro.com/files/Charts2016/2016MidYearWorldwideTicketSalesTop200ArenaVenues.pdf> [Accessed: 7-April-2019]
- Trips2London (2014) The O2 Arena London. http://www.trips2london.com/the_o2arena_london.html. [Accessed: 3-November-2018].
- Wikipedia (2016). O2 Arena Hosting a Tennis Match. https://en.wikipedia.org/wiki/The_O2_Arena#/media/File:ATP_World_Tour_Final_Tennis_at_The_O2_Arena_London.jpg. [Accessed: 3-November-2018]
- World Para Swimming (2011). London 2012 Aquatics Centre. <https://www.paralympic.org/news/london-2012-aquatics-centre-finished>. [Accessed: 3-November-2018].

6 Discussions, conclusions and recommendations

6.1 Discussions

This section aims at answering the research questions formulated based on the research goals in chapter 1, according to the literature reviews in chapter 2 and chapter 3 and the proposed CDIA method in chapter 4 as well as the related case studies in chapter 5. Therefore, by answering the questions, the research goals can be achieved, and the related contributions of the research can be formulated.

6.1.1 Answers to the research questions

The research question formulated in chapter 1 is:

How can designers be supported to fulfil the conceptual design of indoor arenas?

The questions are divided into four sub-questions:

- How can the method support designers to formulate diverse design alternatives based on the integration of the multi-functional space and long-span roof structure and generate, by using the proposed method?

- How can the method support designers to obtain adequate information of the generated design alternatives, therefore, to fulfil numeric assessments related to quantitative design requirements (about the multi-functionality and the performance of the long-span roof structure) and visual investigations related to qualitative design requirements (about aesthetics, culture, psychology, etc.), based on the proposed method?
- How can the method support designers to lay different emphases or priorities on numeric assessments and visual investigation of the design alternatives, based on the proposed method?
- How can the method support designers to select the final design(s) as the outcome(s) of the conceptual design?

Using IAG to integrate multi-functional space and long-span roof structure and generated diverse design alternatives for indoor arenas

To address the first sub-question, IAG is proposed in section 4.2.1 based on the literature review about the space compositions and design parameters of indoor arenas in section 2.2 of chapter 2 and about the techniques of parametric design in section 3.2 of chapter 3.

As a parametric model, IAG defines and associates the basic elements (including pitch, seating tiers, and roof structure) of indoor arenas based on a series of parameters, according to the basic composition of indoor arenas. Moreover, IAG includes several types of indoor arenas (including multiple types of seating bowls and various types of roof geometries, which are applied in 129 important worldwide indoor arenas listed in annex 1) and three frequently used types of long-span steel structures. Therefore, by integrating various types of the multi-functional space and three types of long-span roof structures with various geometries, IAG can define the overall forms of indoor arenas and generated diverse design alternatives based on different sets of design parameters.

The key design parameters related to the multi-functional space and long-span roof structure as well as their integration are listed in table 4.1 of chapter 4. A simple but meaningful test of IAG in generating diverse design alternatives is performed and presented in figure 4.3, in which various types of geometries of indoor arenas are generated, some of them are similar to real arenas, some have not been proposed in the real world. Moreover, in the case studies in chapter 5, the hypothetical designs of two typical indoor arenas demonstrate how to select design parameters to define the design variables according to practical design requirements in order to generate

a suitable design space for design exploration (section 5.3.1 of chapter 5). The diversities of the design alternatives generated by the IAG are fully illustrated by the result of the SOM clustering (figure 5.7, figure 5.8, figure 5.12, and figure 5.13).

Obtaining various information of design alternatives by using IAG, BPSs, MOOs, MLPNNs, and SOM clustering

To obtain the information about numeric indicators and geometries, parametric model and BPSs can be used. IAG, as the parametric model mentioned above, can generate the geometries of design alternatives which can be visually investigated by designers according to their knowledge and experience about qualitative design requirements. BPSs can be used to obtain various indicator values of design alternatives. However, as the discussion in section 3.7 of chapter 3, it is unpractical to generate the geometries and obtain the indicator values for numerous design alternatives based on parametric models and BPSs, since the extremely long computation time.

To overcome the challenge, MOOs and MLPNNs are used to obtain the numeric indicators for design alternatives based on IAG and BPSs, in different ways. MOOs can search for 'well-performing' design alternatives within the design space, according to specific numeric assessment criteria provided by designers, while MLPNNs can predict the indicator values for numerous design alternatives. The backgrounds of MOOs and MLPNNs are respectively reviewed in sections 3.4 and 3.5 of chapter 3, and the related applications in CDIA are respectively elaborated in sections 4.3.1 and 4.3.3 of chapter 4. The effects of MOOs and MLPNNs in the conceptual design of indoor arenas are verified in the case studies of two design examples in section 5.4.1 and section 5.4.3 of chapter 5.

For geometries of numerous design alternatives, it is unpractical for designers to study one by one. SOM clustering is used to group design alternatives into a small number of clusters according to geometry feature, therefore, support designers in exploring design alternatives based on geometry typology. The background of SOM clustering is reviewed in section 3.6 of chapter 3, and the application in CDIA is elaborated in section 4.3.2 and section 4.3.3 of chapter 4. The effects of SOM clustering to support the exploration based on geometry typology is verified in the case studies section 5.4.2 and section 5.4.3 of chapter 5.

Using three workflows to define promising designs with considerations of different emphases on numeric assessment and visual investigations

To address the third and fourth questions, in section 2.3 of chapter 2, based on the reviews and discussions about architectural conceptual design, the numeric assessments related to quantitative design requirements and the visual investigations related to qualitative design requirements for various design alternatives during design exploration are discussed and highlighted. Furthermore, three design scenarios are formulated based on three different emphases on numeric assessments and visual investigations. Correspondingly, three workflows in CDIA based on the different combinations of MOOs, MLPNNs, and SOMs are proposed for the three design scenarios.

The first workflow is based on MOOs which search for well-performing design alternatives according to numeric assessment criteria. Designers can explore these alternatives and select the final ones based on visual investigations. This workflow is used to support the design scenario in which designers intend to prioritize quantitative design requirements over qualitative ones.

The second workflow is based on the combination of SOM clustering and MOOs. This workflow, based on SOM clustering, first allows designers to visually investigate design alternatives according to geometry typology and select the types according to their knowledge and experience about qualitative design requirements. Among the selected types of design alternatives, a MOO is used to search for 'well-performing' ones according to numeric assessment criteria. This workflow is used to support the design scenario in which designers intend to prioritize qualitative design requirements over quantitative ones.

The third workflow is based on the SOM-MLPNN, which allows designers to explore design alternatives based on both numeric assessments and visual investigations, simultaneously. This workflow is used to support the design scenario in which equal emphases are placed on the quantitative and qualitative design requirements.

The workflows are elaborated in section 4.3 of chapter 4, and the effects are verified, and the limitations are discussed based on the case studies in chapter 5. According to the results of the case studies (which are discussed in section 5.5 of chapter 5), in general, the method of CDIA can satisfy the three basic demands of the conceptual of indoor arenas (which are formulated in chapter 2). Specifically, the three workflows in CDIA can satisfy the different emphases placed on numeric assessments and visual investigations about design alternatives, although there are still limitations for each of them.

6.1.2 Practical guidelines of CDIA

CDIA is proposed for the conceptual design of indoor arenas focusing on the integration of multi-functional space and long-span roof structure. It can be used for design practice, in which designers intend to explore various design alternatives according to both quantitative and qualitative design requirements rather than focusing on several fixed design alternatives. It can also be used for researchers and designers to study the relationships between the building geometries and numeric indicators related to spectator view, acoustics, and structural performance, which supports the acquisition of new knowledge.

It is worth noting that the application of CDIA is not a full automatic design process which replaces human designers. Instead, it intends to improve the conceptual design by providing various information about geometries and numeric indicators of diverse possible design alternatives for designers, therefore, to aid them to deeply think about the design problems and make decisions based on full investigations of various possibilities. For IAG, as mentioned, diverse design alternatives with three types of structure can be generated. The application of IAG requires to define design variables among design parameters, which is a process for designers to think about possible geometries during design exploration. In this process, according to the provided parameter list (table 4.1), designers should define which parameters are fixed according to the decisions made before conceptual design and which parameters should be changeable for the exploration to search for proper solutions. By using framework-NAIA to define numeric assessment criteria, designers also need to consider which indicators should be used to formulate the criteria to assess the design alternatives, according to the quantitative design requirements under specific conditions in practice.

For the three workflows of CDIA which are proposed for different design scenarios, designers need to make choices according to their emphases on numeric assessments related to quantitative design requirements or visual investigations related to qualitative design requirements. As the discussions in section 5.5 of chapter 5, the workflow three based on SOM-MLPNN can provide more information about geometries and quantitative indicators for various design alternatives, comparing to the other two workflows. However, there are uncertainties in using MLPNN to predict indicator values of design alternatives, which can be overcome but requires advanced techniques and professional knowledge and experience about MLPNNs. Hence, there is a trade-off in the selection of the workflow, which also requires designers to make a decision.

Based on the information provided by using CDIA about the geometries and quantitative indicators of various design indicators, designers still need to make a decision to select the final design(s) for the following design processes.

6.2 Conclusions

The main contribution of this thesis is the CDIA. CDIA uses computational techniques to effectively and efficiently support the conceptual design of indoor arenas with a focus on the integration of multi-functional space and long-span roof structure, based on design explorations emphasizing both numeric assessments related to quantitative design requirements and visual investigations related to qualitative design requirements.

Within the overall framework of CDIA, the proposed components and workflows also make contributions to both academic research and design practice. The IAG includes various types of geometries of multi-functional space and three types of long-span roof structures with various geometries, which can provide diverse types of design alternatives for both research and design. Besides being used in CDIA, it can also be used for other tasks in various fields.

The three workflows based on MOOs, MLPNNs, and SOM clustering provides different ways to support design explorations for architectural conceptual designs. The workflows can also be used to support academic research to further discover the interrelationships between building geometries and multiple kinds of performance. The overall process of the first workflow based on MOOs has been widely used in the research and designs of various types of buildings, but based on the wide design spaces provided by IAG, the MOOs in the proposed workflow can search for well-performing design alternatives in broader design spaces and provide quite different types of design alternatives in the Pareto sets. The proposed workflow improves the efficiency and effects of the design optimizations of buildings. The second and third workflows based on the combination of SOM clustering and of MOOs and SOM-MLPNN, respectively, are new methods for design explorations. The design scenarios, which are supported by these two workflows, are also crucial for design practice but are not efficiently supported by the existing computational design methods.

Besides, CDIA can also be used as the platform to study the relationships between the overall building geometries and the quantitative indicators (related to multi-functionality and structural performance), which is crucial for academic research and integrated designs as well as the cooperation between architects and structural engineers. Moreover, the method of CDIA is developable, therefore, more quantitative aspects (e.g. thermal, energy, daylighting, ventilation) can be considered, and the method can also be developed to use for the designs of other building types.

6.3 Recommendations

Currently, CDIA is still limited that it can only be used for the conceptual design of indoor arenas, since the parametric model (IAG) and the quantitative indicators included in framework-NAIA are only related to indoor arenas without considerations of other building types. Although it is possible for designers to introduce their own parametric model of other types of buildings into the method, it is difficult to guarantee the flexibility of the parametric model (which is crucial for the effect of this method).

For the quantitative design requirements, so far, only the aspects related to spectator view, acoustics, and structural performance are taken into account. For the data approximations based on MLPNN in the third workflow, there are still uncertainties which can lead to large errors.

To overcome these limitations, future work should focus on:

- developing flexible parametric models for other types of buildings which can be used for the proposed method;
- adding more indicators related to other aspects (e.g. thermal, daylighting, energy consumption) into the proposed method;
- introduce advanced techniques to quantify and limit the uncertainties of the data approximation based on MLPNN.

Besides, other developing directions can also be considered for the proposed method. One of the directions can be the integrated design of sports buildings with consideration of the urban contexts. The reason is that the geometries and layouts of sports arenas or stadia can largely influence the environments (thermal, ventilation,

and daylighting, etc.) in urban spaces, and the environments can also influence the performance of the buildings. Moreover, the qualitative aspects of sports buildings (which are mainly determined by the overall geometries and related to aesthetics, culture, psychology, etc.) are usually highlighted in the field of urbanism. Therefore, how to define the overall geometries of a sports building to meet the requirements of the urban environments, building performance, and qualitative aspects by using computation methods can be a new research focus for the application of CDIA.

Another direction can be using computational methods to aid designers to assess the aspects related to qualitative design requirements. As mentioned in chapter 1 and chapter 2, so far, the effective assessments of the qualitative design requirements for design alternatives still require the visual investigations of human designers according to their knowledge and experience. Nevertheless, with the development of computation technology, some techniques can potentially be developed to support the assessments of qualitative design requirements by learning the assessment patterns from the knowledge and experience of human designers. Such research can not only improve the design explorations in practice but also study how designers judge and consider when they assess designs according to qualitative design requirements.

Appendix

In this annex, 129 sport arenas all over the world are selected as practical cases for review. These arenas are:

- Arenas for Olympic games (including summer and winter games from 2004 to 2020) Arenas for NBA (National Basketball Association) or NHL (National Hockey League) (listed by Wikipedia)
- Top 15 arenas of the busiest arenas in 2016 according to the tickets selling for concerts (ranked by Pollstar).
- Top 10 arenas of the largest arenas in capacity (ranked by Wikipedia)

Olympics is the most important international sports events and the arenas satisfying the strict requirements are typical cases for study. Furthermore, most of the legacies transferred to important local sports arenas for events, which is also valuable for research. The arenas for NBA and NHL in America or Canada are also selected. Because, for the league match of indoor sports, this two are the most important, and the arenas are typical for holding daily sports events. The top 10 in the list of the busiest arenas provided by POLLSTAR (a trade industry journal) are selected, since they are typical sports arenas for concerts. Finally, ten largest arenas (in capacity) in the world are selected, because of their huge volume, expand span and daily operation modes.

Theses arenas are investigated in terms of capacity (for basketball competition), pitch shape, outline of the multi-functional space (the hall), roof geometry, typology and material of roof structure.

No.001 Athens Olympic Velodrome

Capacity: 5,250	Roof geometry: surface with Positive Gaussian curvature
Pitch: oval	Structural type: hybrid
Boundary of the seating bowl: oval (symmetric along the long- and short-axes of the pitch)	Structural material: steel

Images:

<https://cubusengineering.gr/en/projects/sport-facilities/olympic-velodrome-oaka-athens/>

https://en.wikipedia.org/wiki/Athens_Olympic_Velodrome

No.002 Nikos Galis Olympic Indoor Hall (OACA)

Capacity: 18,500	Roof geometry: flat
Pitch: rectangle	Structural type: space frame
Boundary of the seating bowl: rectangle (symmetric along the long- and short-axes of the pitch)	Structural material: steel

Images:

http://www.worldstadiums.com/stadium_pictures/europe/greece/athens_olympic.shtml

http://www.worldstadiums.com/stadium_pictures/europe/greece/athens_olympic.shtml

No.003 Hellinikon Olympic Arena

Capacity: 15,000	Roof geometry: flat
Pitch: rectangle	Structural type: truss beam
Boundary of the seating bowl: rectangle (symmetric along the long- and short-axes of the pitch)	Structural material: steel

Images:

<https://www.sdna.gr/mpasket/basket-league/article/549316/olympiako-gymnastirio-ano-liosion-ayto-einai-kastro-poy-thelei>

http://www.worldstadiums.com/stadium_pictures/europe/greece/athens_helliniko.shtml

No.004 Peace and Friendship Stadium

Capacity: 12,000	Roof geometry: surface with negative Gaussian curvature
Pitch: oval	Structural type: cable tension
Boundary of the seating bowl: oval (symmetric along the long- and short-axes of the pitch)	Structural material: steel

Images:

http://www.apada.com/2004/map_files/Volleyball.html

https://en.wikipedia.org/wiki/Peace_and_Friendship_Stadium#/media/File:Peace_and_Friendship_stadium_2014.JPG

No.005 Faliro Sports Pavilion Arena	
Capacity: 8,536	Roof geometry: surface with negative Gaussian curvature
Pitch: rectangle	Structural type: space frame
Boundary of the seating bowl: round (symmetric along the long- and short-axes of pitch)	Structural material: steel
Images: http://www.tpa.gr/index.php/activities/view/18/130 https://en.wikipedia.org/wiki/Faliro_Sports_Pavilion_Arena#/media/File:Faliro_Sport_Pavillion.jpg	

No.006 Galatsi Olympic Hall	
Capacity: 6,200	Roof geometry: surface with zero Gaussian curvature
Pitch: rectangle	Structural type: truss beam
Boundary of the seating bowl: rectangle (symmetric along the long- and short-axes of the pitch)	Structural material: steel
http://www.stadia.gr/galatsi/galatsi.html https://cuitandokter.com/galatsi-olympic-hall-athens-world-company-sports-games-2020/	

No.007 Beijing National Aquatics Centre	
Capacity: 17,000	Roof geometry: flat
Pitch: rectangle	Structural type: space frame
Boundary of the seating bowl: rectangle (symmetric along the long- and short-axes of the pitch)	Structural material: steel
Images: https://www.arup.com/projects/chinese-national-aquatics-center https://architizer.com/idea/359362/	

No.008 Beijing National Indoor Stadium	
Capacity: 20,000	Roof geometry: surface with zero Gaussian curvature
Pitch: rectangle	Structural type: space frame
Boundary of the seating bowl: rectangle (symmetric along the long- and short-axes of the pitch)	Structural material: steel
Images: https://www.skyscrapercity.com/threads/beijing-national-indoor-stadium-18-000.664660/ https://www.beijing2022.cn/a/20160729/038779.htm	

No.009 Beijing Science and Technology University Gymnasium

Capacity: 8,000	Roof geometry: flat
Pitch: rectangle	Structural type: space frame
Boundary of the seating bowl: drum-shape (symmetric along the long- and short-axes of the pitch)	Structural material: steel
Images: http://www.nipic.com/show/4/79/5018184k6ecad3a5.html https://lt.cjdbj.net/thread-2495794-1-1.html	

No.010 Beijing University of Technology Gymnasium

Capacity: 7,500	Roof geometry: surface with positive Gaussian curvature
Pitch: rectangle	Structural type: tension cable supported grid shell
Boundary of the seating bowl: round (symmetric along the long- and short-axes of the pitch)	Structural material: steel
Images: https://m.dahepiao.com/venue/venue_113041.html https://www.t248.com/picture/25943.html	

No.011 China Agricultural University Gymnasium

Capacity: 6,000	Roof geometry: discrete roof
Pitch: rectangle	Structural type: truss beam
Boundary of the seating bowl: rectangle (symmetric along the long- and short-axes of the pitch)	Structural material: steel
Images: http://www.piaocn.com/changguan/463.html http://news.sohu.com/20080725/n258376460_6.shtml	

No.012 Peking University Gymnasium

Capacity: 8,000	Roof geometry: complex shape
Pitch: rectangle	Structural type: space frame
Boundary of the seating bowl: rectangle (symmetric along the long- and short-axes of the pitch)	Structural material: steel
Images: http://www.ce.cn/cyssc/ztpd/08/bj2008/bjdxtyg/200807/09/t20080709_16101339.shtml https://kknews.cc/zh-my/sports/gjxp9ee.html	

No.013 Beihang University Gymnasium	
Capacity: 5,400	Roof geometry: flat
Pitch: rectangle	Structural type: space frame
Boundary of the seating bowl: rectangle (asymmetric along the short-axis of the pitch)	Structural material: steel
Images: http://2008.sina.com.cn/hd/other/p/2008-07-22/2217118695.shtml http://news.sohu.com/20080725/n258376460_7.shtml	

No.014 Beijing Institute of Technology Gymnasium	
Capacity: 5,000	Roof geometry: surface with negative Gaussian curvature
Pitch: rectangle	Structural type: hybrid (arch supported space frame)
Boundary of the seating bowl: drum-shape (symmetric along the long- and short-axes of the pitch)	Structural material: steel
Images: http://www.zizs.com/c/201307/2209.html http://www.blghk.com/m/view.php?aid=8	

No.015 Laoshan Velodrome	
Capacity: 6,000	Roof geometry: surface with positive Gaussian curvature
Pitch: oval	Structural type: space frame
Boundary of the seating bowl: oval (symmetric along the long- and short-axes of the pitch)	Structural material: steel
Images: http://2008.sina.com.cn/jz/cy/p/2007-10-28/231431315.shtml https://bkso.baidu.com/item/老山自行车馆/6511709?fromtitle=老山山地自行车场&fromid=6524284	

No.016 Wukesong Indoor Stadium (LeSports center)	
Capacity: 18,000	Roof geometry: flat
Pitch: rectangle	Structural type: space frame
Boundary of the seating bowl: rectangle (symmetric along the long- and short-axes of the pitch)	Structural material: steel
Images: http://h5.piao88.com/ticket/3255.html http://news.sohu.com/20080725/n258376460_2.shtml	

No.017 Beijing Capital Indoor Stadium

Capacity: 17,500	Roof geometry: flat
Pitch: rectangle	Structural type: space frame
Boundary of the seating bowl: rectangle (symmetric along the long- and short-axes of the pitch)	Structural material: steel
Images: http://www.piaocn.com/changguan/45.html http://2008.sina.com.cn/jz/other/p/2007-12-11/153236838.shtml	

No.018 Beijing Olympic Sports Centre Gymnasium

Capacity: 7,000	Roof geometry: surface with zero Gaussian curvature
Pitch: rectangle	Structural type: hybrid (cable supported space frame)
Boundary of the seating bowl: rectangle (symmetric along the long- and short-axes of the pitch)	Structural material: steel
Images: http://2008.people.com.cn/GB/22180/22196/96613/6517715.html http://www.zhxxw.net/zhnews4022/2008ay/cgjs/20080714172128.htm	

No.019 Workers Indoor Arena

Capacity: 13,000	Roof geometry: flat
Pitch: rectangle	Structural type: tension cable
Boundary of the seating bowl: round (symmetric along the long- and short-axes of the pitch)	Structural material: steel
Images: http://www.yaokaihui.com/3-d-129537.html http://www.easyjobmaterials.com/cases/detail/id/70.html	

No.020 North Greenwich arena (O2 arena)

Capacity: 20,000	Roof geometry: flat
Pitch: rectangle	Structural type: space frame
Boundary of the seating bowl: rectangle (asymmetric along the long-axis of the pitch)	Structural material: steel
Images: http://www.mapaplan.com/seating-plan/the-o2-arena-london/the-o2-arena-london-seating-plan.htm http://www.newsteelconstruction.com/wp/ssda-2008-the-o2-arena-north-greenwich/	

No.021 London aquatic centre

Capacity: 2,500	Roof geometry: surface with negative Gaussian curvature
Pitch: rectangle	Structural type: space frame
Boundary of the seating bowl: oval (asymmetric along the long-axis of the pitch)	Structural material: steel

Images:

<https://architectureofthegames.net/2012-london/london-2012-aquatics-centre-diagrams-and-drawings/>

<https://www.timeout.com/london/sport-fitness/the-london-aquatics-centre>

No.022 London velodrome

Capacity: 6,750	Roof geometry: surface with negative Gaussian curvature
Pitch: oval	Structural type: cable tension
Boundary of the seating bowl: oval (symmetric along the long- and short-axes of the pitch)	Structural material: steel

Images:

<https://miesarch.com/work/2586>

<https://www.bbc.com/news/uk-england-london-14595015>

No.023 London Basketball Arena

Capacity: 12,000	Roof geometry: surface with zero Gaussian curvature
Pitch: rectangle	Structural type: space frame
Boundary of the seating bowl: rectangle (symmetric along the long- and short-axes of the pitch)	Structural material: steel

Images:

<https://www.archdaily.com/255557/london-2012-basketball-arena-wilkinson-eyre-architects/5031a99028ba0d183000bca-london-2012-basketball-arena-wilkinson-eyre-architects-plan-01>

[https://en.wikipedia.org/wiki/Basketball_Arena_\(London\)](https://en.wikipedia.org/wiki/Basketball_Arena_(London))

No.024 Copper Box

Capacity: 7,500	Roof geometry: flat
Pitch: rectangle	Structural type: space frame
Boundary of the seating bowl: rectangle (symmetric along the long- and short-axes of the pitch)	Structural material: steel

Images:

https://www.bettervenues.org.uk/docs/default-source/venuebrochures/gll_pcr_copperbox_venueguide_a4_2015_fv_web.pdf?sfvrsn=4

http://www.londontown.com/LondonStreets/east_cross_centre_5ec.html/imagesPage/42081

No.025, 26, 27 Carioca arena 1, 2, 3

Capacity: 16,000, 10,000, 10,000	Roof geometry: flat
Pitch: rectangles	Structural type: space frame
Boundary of the seating bowl: rectangles (symmetric along the long- and short-axes of the pitch)	Structural material: steel

Images:

<https://www.dezeen.com/2016/08/11/wilkinson-eyre-arenas-cariocas-largest-venue-rio-2016-barra-olympic-park/>
https://en.wikipedia.org/wiki/Carioca_Arena_3

No.028 Rio Olympic Velodrome

Capacity: 5,000	Roof geometry: surface with zero Gaussian curvature
Pitch: oval	Structural type: space frame
Boundary of the seating bowl: oval (symmetric along the long- and short-axes of the pitch)	Structural material: steel

Images:

http://www.ecowebtown.it/n_1/en/angrilli_en.html
https://en.wikipedia.org/wiki/Rio_Olympic_Velodrome

No.029 Youth Arena

Capacity: 5,000	Roof geometry: flat
Pitch: rectangle	Structural type: truss beam
Boundary of the seating bowl: rectangle (symmetric along the long- and short-axes of the pitch)	Structural material: steel

Images:

<https://www.archdaily.com/787298/olympic-youth-arena-vigliecca-and-associados/57338115e58ecee808000001-youth-arena-vigliecca-and-associados-diagram>
<https://divisare.com/projects/320039-vigliecca-associados-leonardo-finotti-youth-arena>

No.030 Olympic Aquatics Stadium

Capacity: 15,000	Roof geometry: flat
Pitch: rectangle	Structural type: space frame
Boundary of the seating bowl: rectangle (symmetric along the long- and short-axes of the pitch)	Structural material: steel

Images:

No.031 Rio Olympic arena (HSBC)	
Capacity:12,000	Roof geometry: flat
Pitch: rectangle	Structural type: truss beam
Boundary of the seating bowl: rectangle (asymmetric along the long-axis of the pitch)	Structural material: steel
Images: https://www.gamesbids.com/forums/topic/23671-rio-2016-tickets/page/22/ https://in.pinterest.com/pin/705446729117357358/	

No.032 Future Arena	
Capacity: 12,000	Roof geometry: flat
Pitch: rectangle	Structural type: space frame
Boundary of the seating bowl: rectangle (symmetric along the long- and short-axes of the pitch)	Structural material: steel
Images: https://www.bloomberg.com/news/articles/2016-08-16/rio-plans-to-transform-its-arenas-into-schools-community-pools-and-public-parks https://globoesporte.globo.com/olimpiadas/noticia/prefeitura-e-ministerio-firmam-acordo-para-transformar-arena-do-futuro-em-4-escolas.ghtml	

No.033 Tokyo Metropolitan Gymnasium	
Capacity: 10,000	Roof geometry: discrete roof
Pitch: oval	Structural type: hybrid
Boundary of the seating bowl: round (symmetric along the long- and short-axes of the pitch)	Structural material: steel
Images: https://www.livehis.com/seat/seat2_t-taiiku.html https://en.wikipedia.org/wiki/Tokyo_Metropolitan_Gymnasium#/media/File:Tōkyō_Taiikukan_Japan.jpg	

No.034 Yoyogi National Stadium	
Capacity: 13,291	Roof geometry: surface with negative Gaussian curvature
Pitch: rectangle	Structural type: hybrid (tension supported truss beams)
Boundary of the seating bowl: round (symmetric along the long- and short-axes of the pitch)	Structural material: steel
Images: https://www.archdaily.com/109138/ad-classics-yoyogi-national-gymnasium-kenzo-tange/5038005628ba0d599b000852-ad-classics-yoyogi-national-gymnasium-kenzo-tange-axon-02 https://www.gotokyo.org/en/spot/346/index.html	

No.035 Ariake Arena	
Capacity: 10,000	Roof geometry: surface with zero Gaussian curvature
Pitch: rectangle	Structural type: truss beam
Boundary of the seating bowl: rectangle (symmetric along the long- and short-axes of the pitch)	Structural material: steel
Images: https://www.skyscrapercity.com/threads/tokyo-東京-tokyo-olympics-venues-東京オリンピック-競技会場.1729594/page-5#post-130068747 https://www.volleyball.world/en/beachvolleyball/worldtour/2019/news/ariake-arena-unveiled-as-volleyball-prepares-for?id=90466	

No.036 Olympic Gymnastic Centre	
Capacity: 12,000	Roof geometry: surface with negative Gaussian curvature
Pitch: rectangle	Structural type: arch beam
Boundary of the seating bowl: rectangle (symmetric along the long- and short-axes of the pitch)	Structural material: timber
Images: https://www.insidethegames.biz/articles/1086440/tokyo-2020-ariake-gymnastics-centre https://www.insidethegames.biz/articles/1035701/tokyo-2020-gymnastic-centre-will-no-longer-be-temporary-venue	

No.037 Olympic Aquatics Centre	
Capacity: 20,000	Roof geometry: flat
Pitch: rectangle	Structural type: space frame
Boundary of the seating bowl: rectangle (asymmetric along the long-axes of the pitch)	Structural material: steel
Images: https://www.2020games.metro.tokyo.lg.jp/7006817e788fa17d621baff8d8e6efa4.pdf https://nl.wikipedia.org/wiki/Tokyo_Aquatics_Centre	

No.038 Tatsumi International Swimming Centre	
Capacity: 3,635	Roof geometry: discrete roof
Pitch: rectangle	Structural type: space frame
Boundary of the seating bowl: semicircle (asymmetric along the short-axes of the pitch)	Structural material: steel
Images: https://japantravel.navitime.com/en/area/jp/spot/02301-1405002/ https://www.rethinktokyo.com/2020-olympic-designs-architecture	

No.039 Saitama Super Arena

Capacity: 36,500	Roof geometry: flat
Pitch: rectangle	Structural type: space frame
Boundary of the seating bowl: round/oval (symmetric along the long- and short-axes of the pitch)	Structural material: steel

Images:

<https://www.saitama-arena.co.jp/e/facility/>

<https://tokyo2020.org/en/news/oly-venue-description-saitama-super-arena>

No.040 Izu Velodrome

Capacity: 3,000	Roof geometry: surface with positive Gaussian curvature
Pitch: oval	Structural type: space frame
Boundary of the seating bowl: round (symmetric along the long- and short-axes of the pitch)	Structural material: steel

Images:

[https://commons.wikimedia.org/wiki/File:Izu_Velodrome_2017-01-07_\(31864516610\).jpg](https://commons.wikimedia.org/wiki/File:Izu_Velodrome_2017-01-07_(31864516610).jpg)

<https://www.insidethegames.biz/articles/1032374/cycling-events-at-tokyo-2020-to-take-place-outside-of-city-ioc-confirm>

No.041 Utah Olympic Oval

Capacity: 3,000	Roof geometry: surface with zero Gaussian curvature
Pitch: rectangle	Structural type: hybrid (tension supported truss beam)
Boundary of the seating bowl: rectangle (symmetric along the long- and short-axes of the pitch)	Structural material: steel

Images:

<https://www.insidethegames.biz/articles/1012833/utah-olympic-oval-to-host-us-speed-skating-sochi-2014-olympic-trials>

<https://www.insidethegames.biz/articles/1012833/utah-olympic-oval-to-host-us-speed-skating-sochi-2014-olympic-trials>

No.042 Oval Lingotto

Capacity: 8,500	Roof geometry: surface with zero Gaussian curvature
Pitch: oval	Structural type: space frame
Boundary of the seating bowl: rectangle (symmetric along the long- and short-axes of the pitch)	Structural material: steel

Images:

<https://www.gettyimages.nl/detail/nieuwsfoto's/general-view-of-the-oval-lingotto-during-the-essent-isu-nieuwsfotos/56415408>

<https://www.lingottofiere.it/space/uk-29/oval>

No.043 Torino Palavela

Capacity: 12,000	Roof geometry: surface with negative Gaussian curvature
Pitch: rectangle	Structural type: thin shell
Boundary of the seating bowl: irregular polygon (asymmetric along the short-axis of the pitch)	Structural material: reinforced concrete

Images:

https://www.accademiasanluca.eu/it/collezioni_online/architettura/archive/cat_id/803/id/675/gae-aulenti

<https://www.goalzz.com/?showstadiums=1&stadium=5647>

No.044 Palasport Olimpico

Capacity: 18,500	Roof geometry: flat
Pitch: rectangle	Structural type: space frame
Boundary of the seating bowl: rectangle (symmetric along the long- and short-axes of the pitch)	Structural material: steel

Images:

<https://trends.archiexpo.com/ceta-spa/project-152963-240268.html>

<https://www.arup.com/projects/turin-2006-olympics-ice-hockey-stadium>

No.045 Torino Esposizioni

Capacity: 6,165	Roof geometry: surface with zero Gaussian curvature
Pitch: rectangle	Structural type: truss beam
Boundary of the seating bowl: rectangle (symmetric along the long- and short-axes of the pitch)	Structural material: reinforced concrete

Images:

<http://www.leolimpiadiditalia.it/torino-esposizioni.html>

<http://quartieresansalvario.altervista.org/torino-esposizioni-i-recenti-progetti-di-recupero/>

No.046 Canada Hockey Place

Capacity: 18,630	Roof geometry: surface with positive Gaussian curvature
Pitch: rectangle	Structural type: space frame
Boundary of the seating bowl: rectangle (symmetric along the long- and short-axes of the pitch)	Structural material: steel

Images:

<https://sportfacilities.ubc.ca/bigimage03/>

<https://www.flickr.com/photos/jazzlawyer/4366057851/>

No.047 Pacific Coliseum

Capacity: 17,713	Roof geometry: flat
Pitch: rectangle	Structural type: space frame
Boundary of the seating bowl: round (symmetric along the long- and short-axes of the pitch)	Structural material: steel

Images:

<https://ar.pinterest.com/pin/234398355590998977/>

<https://searcharchives.vancouver.ca/pacific-coliseum-aerial-view-of-partially-completed-construction-of-pacific-coliseum>

No.048 Richmond Olympic Oval

Capacity: 8,000	Roof geometry: surface with zero Gaussian curvature
Pitch: oval	Structural type: arch beam
Boundary of the seating bowl: rectangle (symmetric along the long- and short-axes of the pitch)	Structural material: timber

Images:

<http://www.calgaryherald.com/sports/>

<http://www.calgaryherald.com/sports/Richmond+Olympic+Oval+state+speed+skating+facility+expect+many+records+2010+Games/1397502/story.html>

<https://www.allnationsstampandcoin.com/newsletters/news157.html>

No.049 Bolshoy Ice Dome

Capacity: 12,000	Roof geometry: surface with positive Gaussian curvature
Pitch: rectangle	Structural type: space frame
Boundary of the seating bowl: oval (symmetric along the long- and short-axes of the pitch)	Structural material: steel

Images:

<https://www.archdaily.com/359999/ice-dome-bolshoy-sic-mostovik/516c6dc3b3fc4bdb4e0000c0-ice-dome-bolshoy-sic-mostovik-level-00-plan>

<https://www.hauteresidence.com/bolshoy-ice-dome-sochi-sic-mostovik/>

No.050 Shayba Arena

Capacity: 7,000	Roof geometry: flat
Pitch: rectangle	Structural type: space frame
Boundary of the seating bowl: oval (symmetric along the long- and short-axes of the pitch)	Structural material: steel

Images:

<https://www.sportsandeventstickets.com/venues/sochi/shayba-arena-tickets.aspx>

https://supersmashbrosbowl.fandom.com/wiki/Shayba_Arena

No.051 Adler Arena Skating Center

Capacity: 8,000	Roof geometry: flat
Pitch: oval	Structural type: space frame
Boundary of the seating bowl: rectangle (symmetric along the long- and short-axes of the pitch)	Structural material: steel
Images: http://www.creativebuilding.eu/Adler-ice-skating-arena/detail https://en.wikipedia.org/wiki/Adler_Arena_Skating_Center	

No.052 Iceberg Skating Palace

Capacity: 12,000	Roof geometry: flat
Pitch: rectangle	Structural type: space frame
Boundary of the seating bowl: rectangle (symmetric along the long- and short-axes of the pitch)	Structural material: steel
Images: https://www.raitasport.com/references/2012-iceberg-skating-palace-sochi-russia/ https://en.wikipedia.org/wiki/Iceberg_Skating_Palace	

No.053 Gangneung Hockey Centre

Capacity: 10,000	Roof geometry: surface with positive Gaussian curvature
Pitch: rectangle	Structural type: space frame
Boundary of the seating bowl: octagon (symmetric along the long- and short-axes of the pitch)	Structural material: steel
Images: https://www.skyscrapercity.com/threads/pyeongchang-2018-winter-olympics-xxii-olympic-winter-games-%E2%80%8E.1413262/page-10 https://www.skyscrapercity.com/threads/pyeongchang-2018-winter-olympics-xxii-olympic-winter-games-%E2%80%8E.1413262/page-10	

No.054 Gangneung oval

Capacity: 8,000	Roof geometry: surface with zero Gaussian curvature
Pitch: oval	Structural type: space frame
Boundary of the seating bowl: rectangle (symmetric along the long- and short-axes of the pitch)	Structural material: steel
Images: https://www.dearchitect.nl/projecten/os2018-pyeongchang-gangneung-oval-idea-image-institute-architects-iiia https://www.koreaboo.com/lists/south-korea-spent-1-billion-winter-olympics-venues/	

No.055 Gangneung Ice Arena	
Capacity: 12,000	Roof geometry: surface with positive Gaussian curvature
Pitch: rectangle	Structural type: truss beam
Boundary of the seating bowl: rectangle (symmetric along the long- and short-axes of the pitch)	Structural material: steel
Images: http://www.zimbio.com/photos/Gangneung+Ice+Arena/ISU+Four+Continents+Figure+Skating+Championships/IXQk30c6ryp https://edrmadeso.com/the-olympic-gangneung-ice-arena-beautiful-sports-structure-built-with-tekla-bim-technology-by-trimble/	
No.056 Kwandong Hockey Centre	
Capacity: 10,000	Roof geometry: surface with positive Gaussian curvature
Pitch: rectangle	Structural type: space frame
Boundary of the seating bowl: rectangle (symmetric along the long- and short-axes of the pitch)	Structural material: steel
Images: http://www.globaltimes.cn/content/1085446.shtml https://www.gn.go.kr/eng/contents.do?key=1359	

No.057 Air Canada Centre	
Capacity: 19,800	Roof geometry: surface with zero Gaussian curvature
Pitch: rectangle	Structural type: space frame
Boundary of the seating bowl: rectangle (symmetric along the long- and short-axes of the pitch)	Structural material: steel
Images: http://www.mapaplan.com/seating-plan/toronto-air-canada-centre-detailed-numbers-rows-floor-chart/high-resolution/toronto-air-canada-centre-seating-chart-04-NHL-Toronto-Maple-Leafs-hockey-individual-seat-row-numbers-gate-entrances-Ticketmaster-map-high-resolution.htm https://en.wikipedia.org/wiki/Maple_Leaf_Sports_%26_Entertainment	

No.058 Amalie Arena	
Capacity: 20,500	Roof geometry: surface with zero Gaussian curvature
Pitch: rectangle	Structural type: space frame
Boundary of the seating bowl: rectangle (symmetric along the long- and short-axes of the pitch)	Structural material: steel
Images: http://alvin-almazov.com/stadiums/amalie-arena-tampa-fl/ https://tabonix.wixsite.com/titancompositesllc/projects?lightbox=dataItem-ivr7kixk	
No.059 American Airlines Arena	
Capacity: 21,000	Roof geometry: surface with positive Gaussian curvature
Pitch: rectangle	Structural type: space frame
Boundary of the seating bowl: round (symmetric along the long- and short-axes of the pitch)	Structural material: steel
Images: http://www.mapaplan.com/seating-plan/dallas-american-airlines-center-arena-detailed-row-numbers-chart/high-resolution/american-airlines-center-dallas-seating-chart-01-detailed-seat-row-number-mavericks-basketball-plan-lower-platinum-terrace-layout-high-resolution.htm https://www.langan.com/portfolio/american-airlines-arena	

No.060 American Airlines Center	
Capacity: 20,000	Roof geometry: surface with positive Gaussian curvature
Pitch: rectangle	Structural type: space frame
Boundary of the seating bowl: oval (symmetric along the long- and short-axes of the pitch)	Structural material: steel
Images: http://www.mapaplan.com/seating-plan/dallas-american-airlines-center-arena-detailed-row-numbers-chart/high-resolution/american-airlines-center-dallas-seating-chart-01-detailed-seat-row-number-mavericks-basketball-plan-lower-platinum-terrace-layout-high-resolution.htm https://en.wikipedia.org/wiki/American_Airlines_Center	
No.061 Amway Center	
Capacity: 18,846	Roof geometry: surface with positive Gaussian curvature
Pitch: oval	Structural type: space frame
Boundary of the seating bowl: oval (symmetric along the long- and short-axes of the pitch)	Structural material: steel
Images: https://www.amwaycenter.com/tickets-and-seating/mvp-tables https://primesource.net/2018/04/30/amway-center-aerial-view/	

No.062 AT&T Center

Capacity: 18,418	Roof geometry: surface with zero Gaussian curvature
Pitch: octagon	Structural type: space frame
Boundary of the seating bowl: octagon (asymmetric along the long-axis of the pitch)	Structural material: steel

Images:

<https://blog.ticketiq.com/blog/att-center-seating-chart-rows-seats-and-club-seats>

<http://basketball.ballparks.com/NBA/SanAntonioSpurs/newindex.htm>

No.063 BB&T Center

Capacity: 19,250	Roof geometry: surface with zero Gaussian curvature
Pitch: rectangle	Structural type: space frame
Boundary of the seating bowl: oval (symmetric along the long- and short-axes of the pitch)	Structural material: steel

Images:

<https://www.thebbtcenter.com/events/seating-charts>

https://pt.wikipedia.org/wiki/BB%26T_Center

No.064 Bankers Life Fieldhouse

Capacity: 17,923	Roof geometry: surface with zero Gaussian curvature
Pitch: rectangle	Structural type: truss beam
Boundary of the seating bowl: octagon (symmetric along the long- and short-axes of the pitch)	Structural material: steel

Images:

<https://www.bankerslifefieldhouse.com/arena-information/concessions/>

<https://usa.sika.com/sarnafil/en/sika-at-work/arenas-recreational-facilities/bankers-life-fieldhouse.html>

No.065 Barclays Center

Capacity: 18,732	Roof geometry: surface with zero Gaussian curvature
Pitch: rectangle	Structural type: space frame
Boundary of the seating bowl: octagon (symmetric along the long- and short-axes of the pitch)	Structural material: steel

Images:

<https://archive.nytimes.com/www.nytimes.com/interactive/2012/09/28/nyregion/barclays-center-an-arena-with-many-faces.html?ref=nyregion>

<https://libn.com/2019/08/16/brooklyn-nets-barclays-center-sold-to-tsai/>

No.066 Bradley Center

Capacity: 18,7171	Roof geometry: surface with positive Gaussian curvature
Pitch: rectangle	Structural type: space frame
Boundary of the seating bowl: octagon (symmetric along the long- and short-axes of the pitch)	Structural material: steel

Images:

https://gomarquette.com/news/1999/6/21/Bradley_Center_Seating_Chart.aspx

<https://urbanmilwaukee.com/2016/06/10/op-ed-bucks-will-privatize-a-public-space/>

No.067 Bell Centre

Capacity: 21,288	Roof geometry: flat
Pitch: rectangle	Structural type: space frame
Boundary of the seating bowl: oval (symmetric along the long- and short-axes of the pitch)	Structural material: steel

Images:

<https://www.sportsevents365.com/event/?q=eq,270794>

https://nl.wikipedia.org/wiki/Bell_Centre#/media/Bestand:CentreBell.jpg

No.068 Bell MTS Place

Capacity: 15,294	Roof geometry: surface with zero Gaussian curvature
Pitch: rectangle	Structural type: space frame
Boundary of the seating bowl: oval (symmetric along the long- and short-axes of the pitch)	Structural material: steel

Images:

<https://tickets.ca/Tickets/Winnipeg-Jets-Tickets>

<https://seatingchartview.com/bell-mts-place/>

No.069 Bridgestone Arena

Capacity: 17,113	Roof geometry: surface with zero Gaussian curvature
Pitch: rectangle	Structural type: space frame
Boundary of the seating bowl: oval (asymmetric along the long-axis of the pitch)	Structural material: steel

Images:

<http://alvin-almazov.com/stadiums/bridgestone-arena-nashville-tennessee/>

<https://www.nhl.com/news/nashville-predators-to-raise-awareness-for-those-affected-by-tornado/c-315804148>

No.070 Canadian Tire Cent

Capacity: 18,572	Roof geometry: flat
Pitch: rectangle	Structural type: space frame
Boundary of the seating bowl: oval (symmetric along the long- and short-axes of the pitch)	Structural material: steel

Images:

<http://www.canadiantirecentre.com/plan-your-visit/arena-map/>

<https://www.sporcle.com/games/Turtleman5/nhl-arenas>

No.071 Chesapeake Energy Arena

Capacity: 8,203	Roof geometry: surface with zero Gaussian curvature
Pitch: rectangle	Structural type: space frame
Boundary of the seating bowl: oval (symmetric along the long- and short-axes of the pitch)	Structural material: steel

Images:

<https://www.rateyourseats.com/questions/ford-center-nba/where-is-loud-city-section-at-chesapeake-energy-arena>

<https://seatingchartview.com/chesapeake-energy-arena/>

No.072 FedEx Forum

Capacity: 18,119	Roof geometry: surface with positive Gaussian curvature
Pitch: rectangle	Structural type: space frame
Boundary of the seating bowl: round (symmetric along the long- and short-axes of the pitch)	Structural material: steel

Images:

<http://www.mapaplan.com/seating-plan/memphis-fedexforum-arena-detailed-row-numbers-chart-map/high-resolution/fedexforum-memphis-seating-chart-05-general-admission-floor-concert-capacity-plan-stage-floor-section-best-seat-virtual-interactive-map-row-high-resolution.htm>

<https://www.mortenson.com/sports/projects/fedex-forum>

No.073 Gila River Arena

Capacity: 19,000	Roof geometry: flat
Pitch: rectangle	Structural type: space frame
Boundary of the seating bowl: oval (symmetric along the long- and short-axes of the pitch)	Structural material: steel

Images:

<http://www.mapaplan.com/seating-plan/glendale-gila-river-arena-detailed-row-numbers-chart-map/high-resolution/gila-river-arena-glendale-seating-chart-10-disney-ice-live-best-seat-finder-interactive-virtual-detailed-row-map-lower-club-upper-seating-high-resolution.htm>
<http://hockey.ballparks.com/NHL/PhoenixCoyotes/newindex.htm>

No.074 Golden 1 Center

Capacity: 17,608	Roof geometry: surface with zero Gaussian curvature
Pitch: rectangle	Structural type: space frame
Boundary of the seating bowl: octagon (symmetric along the long- and short-axes of the pitch)	Structural material: steel

Images:

<https://www.sacbee.com/news/local/city-arena/article84530092.html>
<https://bitcoinnoddschecker.com/stadiums/golden-1-center/>

No.075 Honda Center

Capacity: 17,174	Roof geometry: surface with positive Gaussian curvature
Pitch: rectangle	Structural type: space frame
Boundary of the seating bowl: oval (symmetric along the long- and short-axes of the pitch)	Structural material: steel

Images:

<http://www.mapaplan.com/seating-plan/anaheim-honda-center-arena-detailed-row-numbers-chart/high-resolution/honda-center-anaheim-seating-chart-10-marvel-universe-live-printable-virtual-information-guide-full-exact-row-letters-plan-row-high-resolution.htm>
<https://www.pinterest.ch/pin/425449496017800020/>

No.076 KeyBank Center

Capacity: 19,070	Roof geometry: surface with positive Gaussian curvature
Pitch: rectangle	Structural type: space frame
Boundary of the seating bowl: oval (symmetric along the long- and short-axes of the pitch)	Structural material: steel

Images:

<https://seatgeek.com/venues/keybank-center/seating-chart/buffalo-sabres-4558>
<https://www.sporcle.com/games/Turtleman5/nhl-arenas>

No.077 Little Caesars Arena

Capacity: 20,000	Roof geometry: surface with positive Gaussian curvature
Pitch: rectangle	Structural type: space frame
Boundary of the seating bowl: oval (symmetric along the long- and short-axes of the pitch)	Structural material: steel

Images:

<https://www.bizarrecreations.com/little-caesars-arena-seating-chart/>

<http://dmcorthopaedics.com/life-in-detroit/>

No.078 Madison Square Garden

Capacity: 19,812	Roof geometry: flat
Pitch: rectangle	Structural type: tension cable
Boundary of the seating bowl: round (symmetric along the long- and short-axes of the pitch)	Structural material: steel

Images:

<http://thelifeisdream.blogspot.com/1984/05/msg-interactive-seating-chart-rangers.html>

https://www.reddit.com/r/tiltshift/comments/96yivx/the_construction_of_madison_square_gardens_1968/

No.079 Moda Center

Capacity: 19,980	Roof geometry: surface with zero Gaussian curvature
Pitch: rectangle	Structural type: space frame
Boundary of the seating bowl: rectangle (symmetric along the long- and short-axes of the pitch)	Structural material: steel

Images:

<https://seatgeek.com/venues/moda-center/views/section-104>

<https://rosequarter.com/about-us/tours/rq/>

No.080 Nationwide Arena

Capacity: 18,144	Roof geometry: surface with zero Gaussian curvature
Pitch: rectangle	Structural type: truss beam
Boundary of the seating bowl: oval (symmetric along the long- and short-axes of the pitch)	Structural material: steel

Images:

<https://www.bizarrecreations.com/nationwide-arena-seating-chart/>

<https://sportsmatik.com/sports-corner/sports-venue/nationwide-arena>

No.081 Oracle Arena

Capacity: 19,596	Roof geometry: flat
Pitch: rectangle	Structural type: tension cable
Boundary of the seating bowl: round (symmetric along the long- and short-axes of the pitch)	Structural material: steel

Images:

<https://www.ticketinventory.com/concert/spookfest-tickets/oracle-arena.php>

<https://www.visitoakland.com/listing/oakland-arena/513/>

No.082 Pepsi Center

Capacity: 19,155	Roof geometry: surface with positive Gaussian curvature
Pitch: rectangle	Structural type: space frame
Boundary of the seating bowl: round (symmetric along the long- and short-axes of the pitch)	Structural material: steel

Images:

<https://www.pngguru.com/free-transparent-background-png-clipart-tnjej>

<https://www.uncovercolorado.com/landmarks/pepsi-center/>

No.083 Philips Arena

Capacity: 18,118	Roof geometry: surface with zero Gaussian curvature
Pitch: rectangle	Structural type: space frame
Boundary of the seating bowl: oval (asymmetric along the short-axis of the pitch)	Structural material: steel

Images:

<https://www.pinterest.cl/pin/625437466986475104/>

<http://www.georgiahockeymuseum.com/thrashers.html>

No.084 PNC Arena

Capacity: 18,680	Roof geometry: flat
Pitch: rectangle	Structural type: space frame
Boundary of the seating bowl: oval (symmetric along the long- and short-axes of the pitch)	Structural material: steel

Images:

<https://www.pncarena.com/events/detail/paul-mccartney>

<https://www.bizjournals.com/triangle/news/2019/11/22/biz-pnc-arena-landlord-charts-timeline-for.html>

No.085 PPG Paints Arena

Capacity: 18,387	Roof geometry: surface with zero Gaussian curvature
Pitch: rectangle	Structural type: space frame
Boundary of the seating bowl: oval (symmetric along the long- and short-axes of the pitch)	Structural material: steel

Images:

<http://www.ppgpaintsarena.com/ppg-paints-arena/entrance-gates>

<https://seatingchartview.com/ppg-paints-arena/>

No.086 Prudential Center

Capacity: 17,625	Roof geometry: surface with zero Gaussian curvature
Pitch: rectangle	Structural type: space frame
Boundary of the seating bowl: oval (symmetric along the long- and short-axes of the pitch)	Structural material: steel

Images:

<http://www.americanairlinescenter.com/events-tickets/seating-maps>

https://www.nj.com/news/2010/05/prudential_center_nj_devils_wo.html

No.087 Quicken Loans Arena

Capacity: 20,562	Roof geometry: surface with zero Gaussian curvature
Pitch: rectangle	Structural type: space frame
Boundary of the seating bowl: oval (symmetric along the long- and short-axes of the pitch)	Structural material: steel

Images:

<https://www.rocketmortgagefieldhouse.com/events/seating-charts>

[https://commons.wikimedia.org/wiki/File:Rocket_Mortgage_FieldHouse_\(2\).jpg](https://commons.wikimedia.org/wiki/File:Rocket_Mortgage_FieldHouse_(2).jpg)

No.088 Rogers Arena

Capacity: 18,910	Roof geometry: surface with positive Gaussian curvature
Pitch: rectangle	Structural type: space frame
Boundary of the seating bowl: oval (symmetric along the long- and short-axes of the pitch)	Structural material: steel

Images:

<https://www.ticketroute.com/venues/rogers-arena/>

<https://www.nhl.com/canucks/news/vancouver-giants-at-rogers-arena/c-308618088>

No.089 Rogers Place

Capacity: 18,641	Roof geometry: flat
Pitch: rectangle	Structural type: space frame
Boundary of the seating bowl: oval (symmetric along the long- and short-axes of the pitch)	Structural material: steel
Images: https://i.imgur.com/0WvkYQl.jpg https://www.kiss917.com/2016/08/27/rogers/	

No.090 SAP Center

Capacity: 17,562	Roof geometry: flat
Pitch: rectangle	Structural type: space frame
Boundary of the seating bowl: oval (symmetric along the long- and short-axes of the pitch)	Structural material: steel
Images: https://www.barrystickets.com/venue/sapcenter.php https://www.alliancerroofingcal.com/portfolio	

No.091 Scotiabank Saddledome

Capacity: 19,289	Roof geometry: surface with negative Gaussian curvature
Pitch: rectangle	Structural type: tension cable
Boundary of the seating bowl: oval (symmetric along the long- and short-axes of the pitch)	Structural material: steel
Images: http://www.arcaro.org/tension/album/saddledome.htm https://www.flickr.com/photos/140712914@N07/48932845387	

No.092 Scottrade Center

Capacity: 19,150	Roof geometry: surface with positive Gaussian curvature
Pitch: rectangle	Structural type: space frame
Boundary of the seating bowl: oval (symmetric along the long- and short-axes of the pitch)	Structural material: steel
Images: https://www.reddit.com/r/stlouisblues/comments/6muk23/new_seating_layout_for_scottrade_center_next/ https://www.bistateroof.com/sports-and-recreational-facilities.html	

No.093 Smoothie King Center

Capacity: 16,867	Roof geometry: surface with positive Gaussian curvature
Pitch: rectangle	Structural type: space frame
Boundary of the seating bowl: oval (symmetric along the long- and short-axes of the pitch)	Structural material: steel

Images:

<http://www.smoothiekingcenter.com/plan-your-visit/seating-charts>

<https://thestadiumreviews.com/parking/smoothie-king-center/>

No.094 Spectrum Center

Capacity: 19,077	Roof geometry: surface with zero Gaussian curvature
Pitch: rectangle	Structural type: space frame
Boundary of the seating bowl: oval (symmetric along the long- and short-axes of the pitch)	Structural material: steel

Images:

<https://www.bizarrecreations.com/spectrum-center-seating-chart/>

<https://www.gettyimages.nl/video/spectrum-center?phrase=spectrum%20center&sort=mostpopular>

No.095 Staples Center

Capacity: 18,997	Roof geometry: flat
Pitch: rectangle	Structural type: space frame
Boundary of the seating bowl: oval (symmetric along the long- and short-axes of the pitch)	Structural material: steel

Images:

<http://www.mapaplan.com/seating-plan/staples-center-seat-numbers-detailed-chart/high-resolution/staples-center-seating-chart-01-Lakers-detailed-seat-numbers-chart-with-rows-premier-sections-layout-high-resolution.htm>

<https://www.bizjournals.com/losangeles/news/2019/10/30/staples-center-looks-to-the-future-with-ambitious.html>

No.096 Talking Stick Resort Arena

Capacity: 18,422	Roof geometry: surface with positive Gaussian curvature
Pitch: rectangle	Structural type: space frame
Boundary of the seating bowl: octagon (symmetric along the long- and short-axes of the pitch)	Structural material: steel

Images:

<https://www.suiteexperiencegroup.com/all-suites/talking-stick-resort-arena/>

<http://basketball.ballparks.com/NBA/PhoenixSuns/index.htm>

No.097 Target Center

Capacity: 19,356	Roof geometry: flat
Pitch: rectangle	Structural type: space frame
Boundary of the seating bowl: octagon (symmetric along the long- and short-axes of the pitch)	Structural material: steel
Images: https://seatingchartview.com/target-center/ https://seatingchartview.com/target-center/	

No.098 TD Garden

Capacity: 18,624	Roof geometry: surface with zero Gaussian curvature
Pitch: rectangle	Structural type: space frame
Boundary of the seating bowl: oval (symmetric along the long- and short-axes of the pitch)	Structural material: steel
Images: http://www.mapaplan.com/seating-plan/boston-td-garden-arena-detailed-row-numbers-chart/high-resolution/td-garden-boston-seating-chart-05-boston-celtics-nba-basketball-court-best-seat-finder-chart-sports-deck-precise-aisle-seat-numbering-high-resolution.htm https://www.kone.com/en/references/td-garden.aspx	

No.099 T-Mobile Arena

Capacity: 17,368	Roof geometry: surface with positive Gaussian curvature
Pitch: rectangle	Structural type: space frame
Boundary of the seating bowl: oval (symmetric along the long- and short-axes of the pitch)	Structural material: steel
Images: https://www.reviewjournal.com/local/the-strip/heres-who-we-think-could-sell-out-t-mobile-arena/ https://www.reviewjournal.com/business/t-mobile-arena-filled-with-head-turning-features-photos/	

No. 100 Toyota Center

Capacity: 18,055	Roof geometry: surface with positive Gaussian curvature
Pitch: rectangle	Structural type: space frame
Boundary of the seating bowl: oval (symmetric along the long- and short-axes of the pitch)	Structural material: steel
Images: https://seatgeek.com/venues/toyota-center/seating-chart/concert https://www.face-off.nl/2017/11/16/mogelijke-uitbreiding-nhl-aantocht/toyota-center/	

No. 101 United Center

Capacity: 20,017	Roof geometry: surface with positive Gaussian curvature
Pitch: rectangle	Structural type: space frame
Boundary of the seating bowl: oval (symmetric along the long- and short-axes of the pitch)	Structural material: steel

Images:

<https://www.suiteexperiencegroup.com/all-suites/nba/chicago-bulls/>

<https://fineartamerica.com/featured/chicago-bulls-united-center-thomas-woolworth.html>

No. 102 Verizon Center

Capacity: 20,356	Roof geometry: surface with zero Gaussian curvature
Pitch: rectangle	Structural type: space frame
Boundary of the seating bowl: oval (symmetric along the long- and short-axes of the pitch)	Structural material: steel

Images:

<http://www.mapaplan.com/seating-plan/washington-verizon-center-arena-detailed-row-numbers-chart/high-resolution/verizon-center-washington-seating-chart-03-wizards-nba-gergetown-hoyas-mystics-basketball-exact-venue-map-individual-find-seat-courtside-high-resolution.htm>

<https://parkingaccess.com/blog/verizon-center-parking/>

No. 103 Vivint Smart Home Arena

Capacity: 19,596	Roof geometry: flat
Pitch: rectangle	Structural type: space frame
Boundary of the seating bowl: rectangle (symmetric along the long- and short-axes of the pitch)	Structural material: steel

Images:

<https://olayshowerdiscount.blogspot.com/2005/06/color-changing-by-pmc-lighting-at.html>

<https://www.caaicon.com/portfolio/vivint-smarhome-arena-renovation>

No. 104 Wells Fargo Centre

Capacity: 19,596	Roof geometry: surface with zero Gaussian curvature
Pitch: rectangle	Structural type: space frame
Boundary of the seating bowl: oval (symmetric along the long- and short-axes of the pitch)	Structural material: steel

Images:

<https://yeahthatskosher.com/2016/02/philly-wells-fargo-center-kosher-concessions-76ers-flyers-concerts/>

<https://yeahthatskosher.com/2016/02/philly-wells-fargo-center-kosher-concessions-76ers-flyers-concerts/>

No. 105 Xcel Energy Centre	
Capacity: 19,596	Roof geometry: surface with zero Gaussian curvature
Pitch: rectangle	Structural type: space frame
Boundary of the seating bowl: oval (symmetric along the long- and short-axes of the pitch)	Structural material: steel
Images: https://www.xcelenergycenter.com/events/seating https://www.twincities.com/2015/07/26/radisson-red-planned-for-site-across-from-xcel-energy-center/	

No. 106 AccorHotels Arena	
Capacity: 20,300	Roof geometry: surface with zero Gaussian curvature
Pitch: rectangle	Structural type: space frame
Boundary of the seating bowl: octagon (symmetric along the long- and short-axes of the pitch)	Structural material: steel
Images: https://www.leclercbilletterie.com/en/manifestation/tryo-ticket/idmanif/462702 https://www.leparisien.fr/sports/ile-de-france/omnisports-la-future-arena-bercy-2-sera-t-elle-deplacee-17-10-2017-7336530.ph	

No. 107 Manchester Arena	
Capacity: 21,000	Roof geometry: surface with zero Gaussian curvature
Pitch: rectangle	Structural type: space frame
Boundary of the seating bowl: oval (symmetric along the long- and short-axes of the pitch)	Structural material: steel
Images: https://www.eventtravel.com/manchester-evening-news-arena-roger-waters https://www.ibtimes.co.uk/salman-abedi-named-suspected-manchester-arena-bomber-by-us-officials-1623018	

No. 108 Arena ciudad de Mexico	
Capacity: 22,300	Roof geometry: flat
Pitch: rectangle	Structural type: truss beam
Boundary of the seating bowl: oval (symmetric along the long- and short-axes of the pitch)	Structural material: steel
Images: https://www.stubpass.com/venue/arena-ciudad-de-mexico/ http://www.avalanz.com/en/empresa/arena-ciudad-de-mexico/	

No. 109 Lenxess arena

Capacity: 19,596	Roof geometry: surface with positive Gaussian curvature
Pitch: rectangle	Structural type: hybrid (arch suspending truss beam)
Boundary of the seating bowl: oval (asymmetric along the long-axis of the pitch)	Structural material: steel

Images:

<https://www.seatingplan.net/lanxess-arena/standing>

https://nl.m.wikipedia.org/wiki/Bestand:Lanxess_Arena_Flight_over_Cologne.jpg

No. 110 Ziggo Dome

Capacity: 17,000	Roof geometry: surface with zero Gaussian curvature
Pitch: rectangle	Structural type: space frame
Boundary of the seating bowl: rectangle (asymmetric along the long-axis of the pitch)	Structural material: steel

Images:

<https://architectenweb.nl/nieuws/artikel.aspx?ID=20256>

<https://proteciustrialdoors.nl/projecten/de-ziggo-dome-amsterdam/>

No. 111 the SSE hydro

Capacity: 19,596	Roof geometry: surface with positive Gaussian curvature
Pitch: round	Structural type: space frame
Boundary of the seating bowl: round (asymmetric along the long-axis of the pitch)	Structural material: steel

Images:

<https://www.seetickets.com/event/david-gray/sec-the-sse-hydro/1444399?lang=nl-NL>

<https://www.kalzip.com/en/reference/the-sse-hydro-glasgow/>

No. 112 Barclaycard Arena Hamburg

Capacity: 16,000	Roof geometry: surface with positive Gaussian curvature
Pitch: rectangle	Structural type: space frame
Boundary of the seating bowl: oval (symmetric along the long- and short-axes of the pitch)	Structural material: steel

Images:

https://www.sitzplan.net/wiki/O2_World_Hamburg

[https://nl.wikipedia.org/wiki/Barclaycard_Arena_\(Hamburg\)](https://nl.wikipedia.org/wiki/Barclaycard_Arena_(Hamburg))

No. 113 Hallenstadion Zurich

Capacity: 15,000	Roof geometry: surface with positive Gaussian curvature
Pitch: rectangle	Structural type: truss beam
Boundary of the seating bowl: octagon (symmetric along the long- and short-axes of the pitch)	Structural material: steel

Images:

<https://hallenstadion.ch/business/veranstalter-info/raeume-layouts>

<https://hallenstadion.ch/das-hallenstadion/geschichte>

No. 114 Arena Monterrey

Capacity: 17,599	Roof geometry: surface with zero Gaussian curvature
Pitch: octagon	Structural type: truss beam
Boundary of the seating bowl: octagon (symmetric along the long- and short-axes of the pitch)	Structural material: steel

Images:

<http://sensation.idtprod.jibecompany.com/mexico/en/news/index/1015/>

<https://www.airheads.com.mx/#/grill-master-2915/>

No. 115 Sprint Centre

Capacity: 17,297	Roof geometry: flat
Pitch: rectangle	Structural type: space frame
Boundary of the seating bowl: oval (symmetric along the long- and short-axes of the pitch)	Structural material: steel

Images:

<https://www.bizarrecreations.com/sprint-center-seating-chart/>

<https://www.bizjournals.com/kansascity/news/2019/08/02/cover-story-sprint-tmobile-merger-naming-rights.html>

No. 116 3Arena

Capacity: 13,000	Roof geometry: flat
Pitch: semi-circle	Structural type: truss beam
Boundary of the seating bowl: fan-shaped (symmetric along the long-axis of the pitch)	Structural material: steel

Images:

<https://www.eventtravel.com/3arena-dublin-seated>

http://www.worldstadiums.com/stadium_pictures/europe/ireland/dublin_02.shtml

No. 117 Lotto Arena

Capacity: 18,400	Roof geometry: surface with positive Gaussian curvature
Pitch: oval	Structural type: truss beam
Boundary of the seating bowl: oval (asymmetric along the long-axis of the pitch)	Structural material: steel

Images:

<https://www.eventtravel.com/lotto-arena-antwerp>

<https://en.wikipedia.org/wiki/Sportpaleis>

No. 118 Philippines arena

Capacity: 52,000	Roof geometry: surface with positive Gaussian curvature
Pitch: rectangle	Structural type: space frame
Boundary of the seating bowl: oval (symmetric along the short-axis of the pitch)	Structural material: steel

Images:

<https://gistph.com/2017/06/28/how-much-are-purpose-tour-mnl-tickets/>

<https://www.goodnewspilipinas.com/worlds-largest-indoor-arena-in-bulacan-converted-to-covid-19-center-now-open/>

No. 119 SC Olimpiyskiy

Capacity: 22,0000	Roof geometry: flat
Pitch: rectangle	Structural type: tension cable
Boundary of the seating bowl: round (symmetric along the long- and short-axes of the pitch)	Structural material: steel

Images:

<https://spb.kassir.ru/sportivnye-kompleksy/sk-yubileynyiy#scheme>

https://www.triposo.com/poi/Olympic_Stadium_28Moscow29

No. 120 Gwangmyeong Velodrome

Capacity: 10,863	Roof geometry: surface with positive Gaussian curvature
Pitch: oval	Structural type: space frame
Boundary of the seating bowl: oval (symmetric along the long- and short-axes of the pitch)	Structural material: steel

Images:

<http://www.gm.go.kr/tr/jp/jpBt/TRJP0006.jsp>

<https://www.skyscrapercity.com/threads/indoor-velodromes.1555342/>

No. 121 Mineirinho Arena

Capacity: 35,000	Roof geometry: flat
Pitch: round	Structural type: tension cable
Boundary of the seating bowl: round (symmetric along the long- and short-axes of the pitch)	Structural material: steel

Images:

<https://www.skyscrapercity.com/threads/belo-horizonte-estádio-jornalista-felipe-drumond-mineirinho-24-482.1544051/>
<http://www.fim-live.com/en/article/le-superenduro-do-brazil/>

No. 122 Smart Araneta Coliseum

Capacity: 30,000	Roof geometry: surface with positive Gaussian curvature
Pitch: round	Structural type: truss beam
Boundary of the seating bowl: round (symmetric along the long- and short-axes of the pitch)	Structural material: steel

Images:

<https://www.smartaranetacoliseum.com/seat-map>
https://en.wikipedia.org/wiki/Smart_Araneta_Coliseum

No. 123 Rupp Arena

Capacity: 28,000	Roof geometry: flat
Pitch: rectangle	Structural type: space frame
Boundary of the seating bowl: octagon (symmetric along the long- and short-axes of the pitch)	Structural material: steel

Images:

<https://www.derbybox.com/ListEventTickets.php?eventid=1777445&x=Auburn%20Tigers%20at%20Kentucky%20Wildcats%20Basketball&venue=Rupp%20Arena&date=2020-02-29T15:45:00Z&city=Lexington,%20KY>
<http://www.nbbj.com/work/lexington-center-renovation-and-expansion/>

No. 124 Greensboro Coliseum

Capacity: 25,000	Roof geometry: surface with positive Gaussian curvature
Pitch: rectangle	Structural type: space frame
Boundary of the seating bowl: rectangle (symmetric along the long- and short-axes of the pitch)	Structural material: steel

Images:

<https://www.greensborocoliseum.com/events-tickets/seating-chart>
<https://venuesnow.com/wfu-contracts-with-greensboro-coliseum/>

No. 125 The Palace of Auburn Hills	
Capacity: 22,076	Roof geometry: flat
Pitch: oval	Structural type: space frame
Boundary of the seating bowl: oval (symmetric along the long- and short-axes of the pitch)	Structural material: steel
Images: https://www.313presents.com/events/detail/oprahs-the-life-you-want-weekend https://www.fox2detroit.com/news/pistons-owner-announces-deal-to-redevelp-palace-of-auburn-hills	

No. 126 KFC Yum! Centre	
Capacity: 22,000	Roof geometry: surface with zero Gaussian curvature
Pitch: rectangle	Structural type: space frame
Boundary of the seating bowl: dodecagon (symmetric along the long- and short-axes of the pitch)	Structural material: steel
Images: http://www.mapaplan.com/seating-plan/louisville-kfc-yum-center-arena-detailed-row-numbers-chart/high-resolution/kfc-yum-center-louisville-seating-chart-01-detailed-seat-row-number-endstage-concert-section-floor-plan-map-arena-lower-upper-level-layout-high-resolution.htm https://www.grandfunkrailroad.com/OOTR2018.html	

No. 127 Dean Smith Centre	
Capacity: 21,750	Roof geometry: surface with positive Gaussian curvature
Pitch: rectangle	Structural type: space frame
Boundary of the seating bowl: octagon (symmetric along the long- and short-axes of the pitch)	Structural material: steel
Images: https://seatgeek.com/venues/dean-e-smith-center/seating-chart https://www.rexhealth.com/rh/hospitals-locations/profile/?id=886	

No. 128 Thompson–Boling Arena	
Capacity: 21,678	Roof geometry: flat
Pitch: rectangle	Structural type: space frame
Boundary of the seating bowl: octagon (symmetric along the long- and short-axes of the pitch)	Structural material: steel
Images: http://www.arenafanatic.com/thompson-boling-arena-university-of-tennessee--knoxvilletennessee.html https://www.tbarena.com/info/	

No. 129 Ethias Arena

Capacity: 21,600	Roof geometry: surface with zero Gaussian curvature
Pitch: rectangle	Structural type: truss beam
Boundary of the seating bowl: no fixed seating bowl	Structural material: steel

Images:

<https://explosief.jimdofree.com/ethias-theater-hasselt-almaar-populairder/>

http://www.vanlut.be/dwplus/les03/les03_01/03/03.html

Computational Design of Indoor Arenas (CDIA)

Integrating multi-functional spaces and long-span roof structures

Wang Pan

Indoor arenas are important public buildings catering for various activities (e.g., sports events, stage performances, assemblies, exhibitions, and daily sports for the public) and serving as landmarks in urban contexts. The multi-functional space and long-span roof structure of an indoor arena are highly interrelated, which impact the multi-functionality and structural performance and mainly define the overall form of the building. Therefore, it is crucial to integrate the multi-functional space and long-span roof structure to formulate proper forms for indoor arenas, in order to satisfy various design requirements during the conceptual design.

This thesis aims at formulating a computational design method, 'Computational Design of Indoor Arena (CDIA)', to support the conceptual design of indoor arenas by using the computational techniques of parametric modelling, Building Performance Simulations (BPSs), Multi-Objective Optimizations (MOOs), surrogate models based on Multi-Layer Perceptron Neural Network (MLPNN), and clustering based on Self-Organizing Map (SOM clustering). In the formulation of CDIA, these techniques are modified, improved and organized into five components and three workflows, to satisfy the demands of the conceptual design of indoor arenas.

A+BE | Architecture and the Built Environment | TU Delft BK